AD-A046 091 GENERAL ELECTRIC CO SYRACUSE N Y ELECTRONICS LAB F/G 9/5
MULTIMODE FILTERS.(U)
OCT 77 S WANUGA, C M STEARNS, A L KACHELMYER DAAB07-76-C-1337
UNCLASSIFIED ECOM-76-1337-F NL

1 OF 3
ADA046091

12

Research and Development Technical Report

ECOM-76-1337-F

MULTIMODE FILTERS

S. Wanuga
C.M. Stearns
A.L. Kachelmyer
S.W. Tehon
GENERAL ELECTRIC COMPANY
Electronics Laboratory
Syracuse, N.Y. 13221

October 1977

DISTRIBUTION STATEMENT

Approved for public release; distribution unlimited.

ECOM

US ARMY ELECTRONICS COMMAND FORT MONMOUTH, NEW JERSEY 07703

NOTICES

Disclaimers

The findings in this report are not to be construed as an *official Department of the Army* position, unless so designated by other authorized documents.

The citation of trade names and names of manufacturers in this report is not to be construed as official Government indorsement or approval of commercial products or services referenced herein.

Disposition

Destroy this report when it is no longer needed. Do not return it to the originator.

UNCLASSIFIED

SECURITY CLASSIFICATION OF THIS PAGE (When Data Entered)

REPORT DOCUMENTATION PAGE

READ INSTRUCTIONS BEFORE COMPLETING FORM

1. REPORT NUMBER 19

18 ECOM-76-1337-F ✓

2. GOVT ACCESSION NO.

3. RECIPIENT'S CATALOG NUMBER

4. TITLE (and Subtitle)

6 MULTIMODE FILTERS,

5. TYPE OF REPORT & PERIOD COVERED

9 Final Technical Repo[redacted]t,
1 Jun[redacted] 76 [redacted]-28 Feb[redacted] 77,

6. PERFORMING ORG. REPORT NUMBER

7. AUTHOR(s)

10 S. Wanuga, C. M. Stearns, A. A. Kachelmyer and S. W. Tehon

8. CONTRACT OR GRANT NUMBER(s)

15 DAAB07-76-C-1337 new

9. PERFORMING ORGANIZATION NAME AND ADDRESS

General Electric Company
Electronics Park
Syracuse, NY 13201

10. PROGRAM ELEMENT, PROJECT, TASK AREA & WORK UNIT NUMBERS

16 6.27.05.A
1L7-62705-A H94 F101 17 F1
~~015~~

11. CONTROLLING OFFICE NAME AND ADDRESS

US Army Electronics Command
ATTN: DRSEL-TL-ML
Fort Monmouth, NJ 07703

12. REPORT DATE

11 Oct[redacted] [redacted]977

13. NUMBER OF PAGES

~~208~~ 12 210 p.

14. MONITORING AGENCY NAME & ADDRESS (if different from Controlling Office)

15. SECURITY CLASS. (of this report)

UNCLASSIFIED

15a. DECLASSIFICATION/DOWNGRADING SCHEDULE

16. DISTRIBUTION STATEMENT (of this Report)

Statement A.
Approved for public release; distribution unlimited.

17. DISTRIBUTION STATEMENT (of the abstract entered in Block 20, if different from Report)

18. SUPPLEMENTARY NOTES

19. KEY WORDS (Continue on reverse side if necessary and identify by block number)

		Transducers
Piezoelectric vibrators	Frequency selection	Crystal Filters
Piezoelectric resonators	Frequency control	Filters
Electromechanical filters	Crystal resonators	Bandwidth
Electromechanical transducers	Bandpass filters	Equivalent Circuits

20. ABSTRACT (Continue on reverse side if necessary and identify by block number)

This report describes work on Multi Mode Filters performed from 1 June 1976 to 28 February 1977. The objective of this program is to develop design criteria and establish tradeoffs for the transduction of acoustic bulk waves in crystal stacks, for use in filtering applications. A primary goal of the program is to explore methods of obtaining miniature low-loss acoustic filters using interactions among the three modes in each crystal layer, which depend on the thickness coordinate.

(continued)

DD FORM 1 JAN 73 1473 EDITION OF 1 NOV 65 IS OBSOLETE

149568

SECURITY CLASSIFICATION OF THIS PAGE (When Data Entered)

20. ABSTRACT (continued)

This report is concerned with Phase I of this overall Multi Mode Stacked Crystal Filter Program: The detailed requirements of this phase were to consider:

a. Number of crystal plates in the stack. Emphasis is placed on two- and three-plate stacks, exclusive of bonding or coupling layers, relative thicknesses of the plates, and bonds or coupling layers.

b. Materials comprising each crystal plate, bond, or coupling layer. Emphasis is placed on quartz and highly piezoelectric materials, such as lithium niobate. The material parameters used in all of the stacked filter programs are arbitrary; however, most results are illustrated using the material parameters of AT-cut quartz or are illustrated using the material parameters of AT-cut quartz or multiples of them. Results for berlinite are included (Section 2).

c. Number of thickness modes coupled piezoelectrically, in a given plate, to the electrode system. Number of thickness modes, coupled mechanically at the interfaces, for achieving the filter response. Emphasis is placed on one- and two-shear or quasi-shear modes.

d. Crystallographic orientation of each plate. Emphasis is placed on rotated Y-cuts of quartz and lithium niobate and relative rotation, about the common thickness axis, of the various plates with respect to each other.

e. Bonding materials for attaching resonator plates together. Techniques for accomplishing bonding so that welded interface boundary conditions are approached as closely as possible, and effects of finite thickness of bonds and bond viscosity are considered.

Bond effects for the single mode case are illustrated (Section 2) for bonds of various thicknesses and size relative to the crystal plate sizes. The effects of bond viscosity (Q) are also illustrated.

f. Various electroding arrangements, and interconnections between layers. Time did not permit an evaluation of this aspect of the stacked filter. When dealing with two plates, only a 180 degree phase reversal between the input and output electrodes of the stack is possible. An augmentation of the actual plate coordinate equivalent circuit (Section 3) is discussed in Section 5. This is appropriate to this problem and allows for arbitrary electrical interconnections between plate electrodes of the plates in a stack of more than two elements.

While additional design criteria would be desirable, most of the specific requirements of Phase I of this Multi Mode stacked crystal filter program have been accomplished.

TABLE OF CONTENTS

1. INTRODUCTION

This report describes work on Multi Mode Filters performed from June 1, 1976 to February 28, 1977 under Contract No. DAAB07-76-C-1337.

The objective of this program is to develop design criteria and establish tradeoffs for the transduction of acoustic bulk waves in crystal stacks, for use in filtering applications. A primary goal of the program is to explore methods of obtaining miniature low-loss acoustic filters using interactions among the three modes in each crystal layer, which depend on the thickness coordinate.

This report is concerned with Phase I of this overall Multi Mode Stacked Crystal Filter Program: the detailed requirements of this phase were to consider:

1. Number of crystal plates in the stack. Emphasis is placed on two and three-plate stacks, exclusive of bonding or coupling layers, relative thicknesses of the plates, and bonds or coupling layers.

   The MØDE programs (Section 3) handle only two plates in a stack with intimate contact between the plates. These plates are allowed independent thicknesses and material properties. The single mode programs (Section 2) allow for two and three plates in the stacked crystal filter, with bonds between the layers. These programs assume that the plates are made of identical material but are allowed to be of different thicknesses. The bonds in these single mode programs are all assumed to be identical in a single stack.

   Possible procedures for including arbitrary bonds in the MØDE programs and for including additional plates in the stacks of these programs are also described (Section 5).

2. Materials comprising each crystal plate, bond, or coupling layer. Emphasis is placed on quartz and highly piezoelectric materials, such as lithium niobate. The material parameters used in all of the stacked filter programs are arbitrary; however, most results are illustrated using the material parameters of AT-cut quartz or multiples of them. Results for berlinite are included (Section 2).

3. Number of thickness modes coupled piezoelectrically, in a given plate, to the electrode system. Number of thickness modes, coupled mechanically at the interfaces, for achieving the filter response. Emphasis is placed on one- and two-shear or quasi-shear modes. The various MØDE programs (Section 3) allow for from one to three piezoelectrically coupled modes in each plate. This number can vary between plates in a stack. These programs also allow for from one to three mechanically coupled modes at the boundaries of the plates.

4. <u>Crystallographic orientation of each plate</u>. Emphasis is placed on rotated Y-cuts of quartz and lithium niobate and relative rotation, about the common thickness axis, of the various plates with respect to each other.

   The programs CRØT, SYMEIG and VCØUP (Section 3) allow for calculation of the required input parameters for the MØDE programs using any arbitrary orientation of the plates with respect to the standard X, Y, Z axes. Operation of these programs is illustrated for AT-cut, which is a rotated Y-cut of quartz. The MØDE2 and MØDE3 programs allow for an arbitrary angle of rotation about the common thickness axis between the plates in the stack.

5. <u>Bonding Materials for attaching resonator plates together</u>. Techniques for accomplishing bonding so that welded interface boundary conditions are approached as closely as possible, and effects of finite thickness of bonds and bond viscosity are considered.

   Bond effects for the single mode case are illustrated (Section 2) for bonds of various thicknesses and size relative to the crystal plate sizes. The effects of bond viscosity (Q) are also illustrated.

   Techniques for including bonds in the MØDE programs are also discussed (Section 5).

   Information relative to bonding materials and techniques for accomplishing bonding is described (Section 4).

6. <u>Various electroding arrangements, and interconnections between layers</u>. Time did not permit an evaluation of this aspect of the stacked filter. When dealing with two plates only a 180° phase reversal between the input and output electrodes of the stack is possible. An augmentation of the actual plate coordinate equivalent circuit (Section 3) is discussed in Section 5. This is appropriate to this problem and allows for arbitrary electrical interconnections between plate electrodes of the plates in a stack of more than two elements.

While additional design criteria would be desirable it appears that most of the specific requirements of Phase I of this Multi Mode stacked crystal filter program have been accomplished.

2. SINGLE MODE BOND STUDIES

In this section Mason's equivalent circuit for piezoelectric transducers with constant flux density (in-line field model) is used to investigate the effects of bond parameters on multimode stacked filters. This model is shown in Figure 2.1. This same circuit can also be used to represent the bond between elements in the stack by eliminating the electromechanical transformer and associated electrical input network.

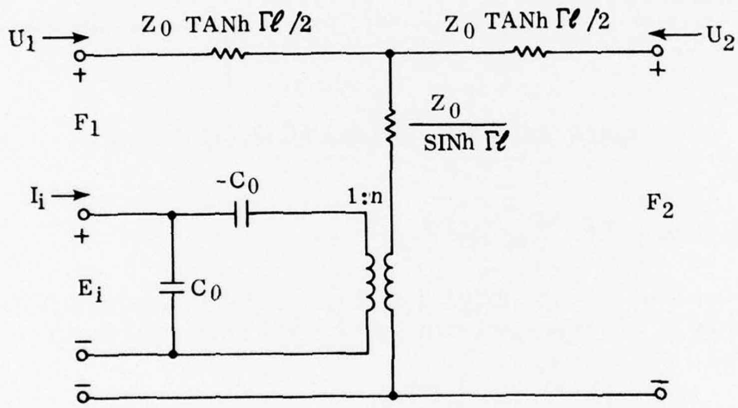

Figure 2.1. Mason's Equivalent Circuit of Single Mode Transducer with Constant Flux Density D (In-Line Field Model).

A. TWO-CRYSTAL SINGLE MODE FILTERS

Mason's equivalent circuit for piezoelectric transducers can be used to devise an equivalent electrical circuit that represents bonded crystals operating in a single shear mode. An equivalent circuit for two bonded crystals of the same dimensions is given in Figure 2.2. The impedances are found from Mason's equivalent circuit to be

$$Z_1 = Z_{OT}/\sinh(\Gamma_T \ell_T) \qquad 2.1$$

$$Z_2 = Z_{OT}/\tanh(\Gamma_T \ell_T/2) \qquad 2.2$$

$$Z_3 = Z_{OB}/\tanh(\Gamma_B \ell_B/2) \qquad 2.3$$

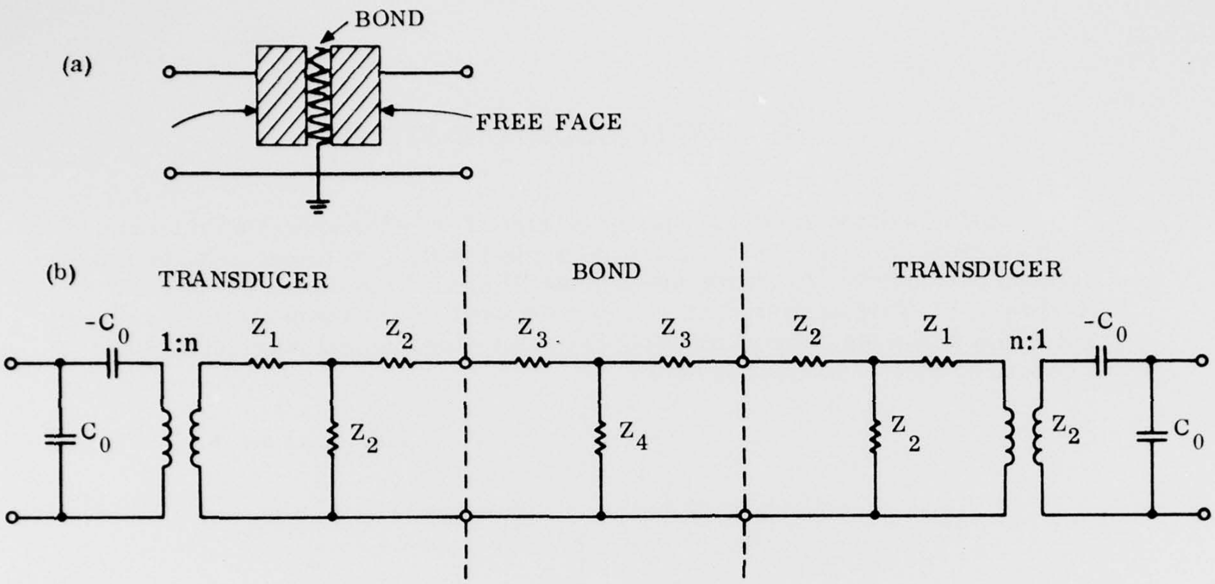

Figure 2.2. Two Bonded Identical Crystals.

$$Z_4 = Z_{OB}/\sinh(\Gamma_B \ell_B) \qquad 2.4$$

where Z_{OT}, Γ_T and Z_{OB}, Γ_B, ℓ_B are the characteristic impedance, complex propagation constant, and thickness for the transducer and bond, respectively.

C_o and n are clamped capacitance and electromechanical transformer turns ratio for the transducers.

The complex propagation constant, Γ, is given by

$$\Gamma = \frac{\omega}{c}\left(1 + \frac{j}{2Q}\right), \qquad 2.5$$

where ω is the angular frequency,

c is the velocity of propagation, and

Q is the mechanical Q of the material.

The capacitance C_o and electromechanical transformer turns ratio n are given by

$$C_o = \epsilon^S A/\ell = \epsilon^T (1 - k^2) A/\ell \qquad 2.6$$

$$n = k\sqrt{2f_o C_o Z_{OT}}, \qquad 2.7$$

where ϵ^S is the dielectric constant for the transducer crystal

k is the coefficient of electromechanical coupling

A is the transducer active area

ℓ is the transducer thickness

f_o is the fundamental resonant frequency, and

Z_{OT} is the transducer impedance

The transducer crystal thickness, ℓ, is chosen to be one-half wavelength at the frequency of mechanical resonance and electrical antiresonance, f_o

$$\ell = c/2f_o \tag{2.8}$$

The impedance, Z_o, of an arbitrary transducer or bond material is given by

$$Z_o = A\rho c\ , \tag{2.9}$$

where A is the cross-sectional area,

ρ is the material density and

c is the velocity of propagation in the material.

Note that from the Mason's equivalent circuit of Figure 2.1, the free faces of the crystals are assumed to have zero force. Hence, the terminals representing the free faces are connected to ground in the equivalent circuit. It is convenient to reduce the equivalent circuit of Figure 2.1 to the equivalent form shown in Figure 2.3 to avoid dealing with the simultaneous occurrence of poles in the branch impedance functions at resonance. The modified impedances are:

$$Z_1' = 2Z_{OT}/\tanh(\Gamma_T \ell_T/2) \tag{2.10}$$

$$Z_2' = 2Z_{OT} \tanh(\Gamma_T \ell_T/2) \tag{2.11}$$

A FØRTRAN computer program, MMPLOT, was written for two bonded crystal of arbitrary dimensions, and material types using the equivalent circuit

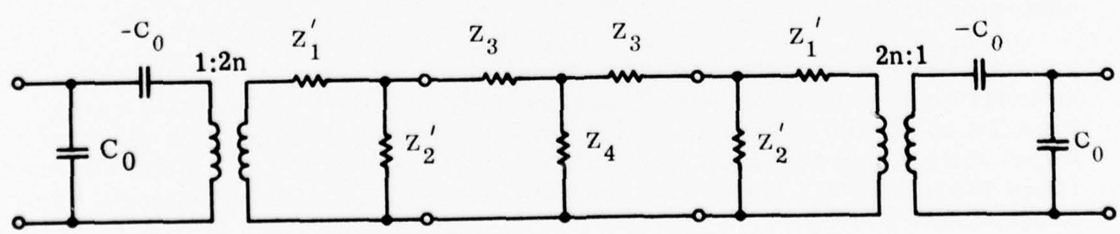

Figure 2.3. Equivalent Circuit of Two Bonded Identical Crystals.

form of Figure 2.3. A listing of MMPLOT is shown in Table 2.1 along with an equivalent circuit indicating the nomenclature employed.

A multimode filter, consisting of two epoxy bonded identical AT-cut quartz crystals operating in the pure thickness shear modes, was analyzed.

For AT cut quartz the material constants are

$$\rho = 2.65 \times 10^3 \text{ kg/m}^3$$

$$c = 3.32 \times 10^3 \text{ m/s}$$

$$Q > 10000$$

$$\epsilon = 4.58$$

$$k = 0.088$$

For a general epoxy bonding material the constants are:

$$\rho = 1.7 \times 10^3 \text{ kg/m}^3$$

$$c = 2.848 \times 10^3 \text{ m/s}$$

$$Q \cong 10$$

The crystals are one-half wavelength thick at 10 MHz. Electrical mismatch loss (power input to the crystal stack compared to the maximum available power) and Power out/Power in versus frequency are plotted in Figures 2.4 and 2.5, respectively, over the range of 1-50 MHz assuming a .01 mil thick epoxy bond and 50 ohm generator and load impedances. The mismatch curve of Figure 2.4 approaches the type of response expected for two crystals in intimate contact with zero bond thickness. The resonances at 5, 10 and 15 MHz correspond to the 1st, 2nd and 3rd harmonics, where the two-crystal thickness corresponds to one-half wavelength. A null occurs at 20 MHz, where both crystals are one wavelength thick.

An expanded view of the mismatch response at 5 MHz is given in Figure 2.6. The percent bandwidth is very small at .043% when using 50 ohm terminations. The bandwidth is increased to .34% by matching the filter with 1600 ohm terminations.

Since the mechanical Q's of most bond materials are virtually unknown, mismatch loss versus frequency was plotted in Figure 2.7 for assumed epoxy bond Q's of 10, 100 and 1000. The higher Q decreases the bandwidth and gives higher mismatch loss. Inaccurate values of Q will not have much effect in the range 100 to 1000 and higher, but accurate values of Q for low Q materials are important.

B. BOND PARAMETERS

The bond material, bond thickness, and bond area relative to the transducer active area are the important parameters for controlling the 3 dB bandwidth, insertion loss*, and passband ripple of the bonded crystal filter.

---

* Insertion loss includes mismatch loss plus the losses in the bond and crystals.

TABLE 2.1

A. EQUIVALENT CIRCUIT FOR TWO BONDED QUARTZ CRYSTALS OF ARBITRARY DIMENSIONS AND BOND MATERIAL TYPE (SINGLE THICKNESS SHEAR MODES)

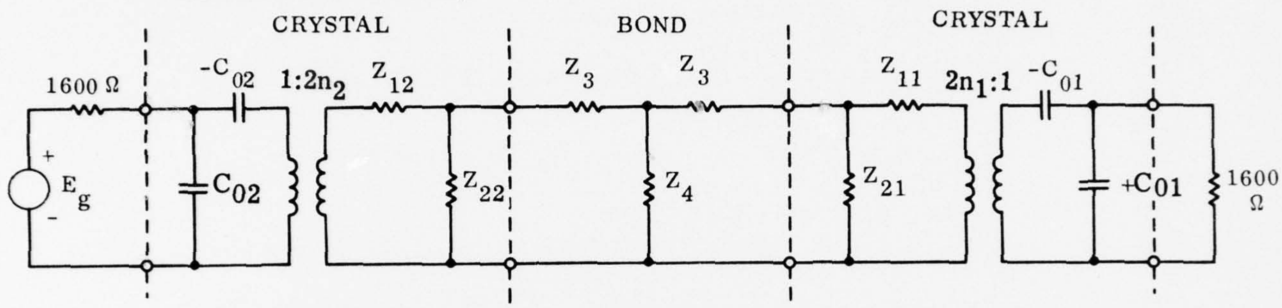

$$Z_{11} = 2Z_{OT}/\tanh(\Gamma_T \ell_{T1}/2)$$

$$Z_{21} = 2Z_{OT} \tanh(\Gamma_T \ell_{T1}/2)$$

$$Z_{12} = 2Z_{OT}/\tanh(\Gamma_T \ell_{T2}/2)$$

$$Z_{22} = 2Z_{OT} \tanh(\Gamma_T \ell_{T2}/2)$$

$$Z_3 = Z_{OB} \tanh(\Gamma_B \ell_B/2)$$

$$Z_4 = Z_{OB}/\sinh(\Gamma_B \ell_B)$$

The 1600-ohm load and generator impedances were chosen to maximize the bandwidth when using the AT-cut quartz transducers.

TABLE 2.1 (CONT'D)

B. COMPUTER PROGRAM, MMPLOT

```
10$:IDENT:865400-276-1265,ALK EP-3 135
20$:LIMITS:10,,,5000
30$:OPTION:FORTRAN
40$:FORTY:NLNO,NFORM
50$:LIMITS:03,26K
60$:REMOTE:$$,E1
70$:REMOTE:P*,E1
80          PARAMETER NPTS=1000,NPLTS=1
90          COMPLEX E,AMP,EO,EG
100          COMPLEX Z11,Z21,Z12,Z22,Z3,Z4,ZC1,ZC2,ZI
110          COMPLEX GT1,GT2,GB,GB2
120          COMPLEX SINH,TANHX
130          DIMENSION K1(NPLTS),PMIS(1000),PILOS(1000)
140          DIMENSION IX(10),IY(10),ID(10),BUF(1000)
150          CHARACTER DA*1(NPLTS)/"*"/
160          DATA IY(1),IY(2)/19,19HINSERTION LOSS (DB)/
170          DATA IX(1),IX(2)/15,15HFREQUENCY (KHZ)/
180          DATA ID(1),ID(2)/23,23HAL KACHELMYER  EP-3 135/
190          PI=3.14159
200          YINCH=8.
210          XINCH=10.
230          FO=1.E7
231          IND=1
232          I1=100
233          I2=700
234          N1=4
235          N2=4
236 502      IF(IND.EQ.1)GO TO 501
238          I1=400
239          I2=400
240          N1=1
242          N2=10
243 501      CONTINUE
244          IPLOT=1
245          D=10.E-3
250          AREA=PI*D*D/4.
260C          TRANSDUCER CONSTANTS
270          XK=.088
280          CT=3.32E3
290          DT=2.65E3
300          ZOT=AREA*CT*DT
310          QT=10000.
320C          BOND CONSTANTS
330          CB=1.2E3
340          DB=19.333E3
345          DO 5 IRATIO=I1,I2,100
346          RATIO=FLOAT(IRATIO)
347          IF(IRATIO.EQ.700)RATIO=50.
350          ZOB=AREA*CB*DB/RATIO
360          QB=100.
370C          TRANSDUCER DIMENSIONS
380          TL1=CT/(2.*FO)
390          TL2=TL1
```

TABLE 2.1 (CONT'D)

```
C        BOND THICKNESS
        DO 5 N=N1,N2
        BL=FLOAT(N)*2.54E-6
C        CAPACITANCE CO
        EP=4.58*8.85E-12
        CO1=EP*(1.-XK*XK)*AREA/TL1
        CO2=EP*(1.-XK*XK)*AREA/TL2
C        COUPLING COEFFICIENT PHI
        PH1=XK*SQRT(2.*FO*CO1*ZOT)
        PH2=XK*SQRT(2.*FO*CO2*ZOT)
        WRITE(6,11)CO1,CO2,PH1,PH2
   11   FORMAT(3X,"CO1=",E12.4,"  CO2=",E12.4,"  PH1=",F9.5,
      &"  PH2=",F9.5)
        PH1=2.*PH1
        PH2=2.*PH2
        IFS=99500
        IFE=102000
        INC=5
        K=0
C        LOOP THRU FREQUENCY
        DO 1 I=IFS,IFE,INC
        K=K+1
        FREQ=FLOAT(I)*1.E2
C        PROPAGATION CONSTANTS
        BT=2.*PI*FREQ/CT
        BB=2.*PI*FREQ/CB
        AT=BT/(2.*QT)
        AB=BB/(2.*QB)
        GT1=TL1*CMPLX(AT,BT)/2.
        GT2=TL2*CMPLX(AT,BT)/2.
        GB=BL*CMPLX(AB,BB)
        GB2=GB/2.
C        COMPLEX IMPEDANCES
        Z11=2.*ZOT/TANHX(GT1)
        Z21=2.*ZOT*TANHX(GT1)
        Z12=2.*ZOT/TANHX(GT2)
        Z22=2.*ZOT*TANHX(GT2)
        Z3=ZOB*TANHX(GB2)
        Z4=ZOB/SINH(GB)
        ZC1=CMPLX(0.,-1./(2.*PI*FREQ*CO1))
        ZC2=CMPLX(0.,-1./(2.*PI*FREQ*CO2))
C        CIRCUIT NETWORK EQUATIONS
        SCLF=6.25E-4
        EO=CMPLX(1.,0.)
        AMP=EO/ZC1+SCLF*CMPLX(1.,0.)
        E=(EO-AMP*ZC1)*PH1
        AMP=AMP/PH1
        E=E+AMP*Z11
        AMP=AMP+E/Z21
        E=E+AMP*Z3
        AMP=AMP+E/Z4
        E=E+AMP*Z3
        AMP=AMP+E/Z22
        E=(E+AMP*Z12)/PH2
        AMP=AMP*PH2
```

TABLE 2.1 (CONT'D)

```
      E=E-AMP*ZC2
      AMP=AMP+E/ZC2
      EIM=20.*ALOG10(CABS(E))
      ARGEI=ATAN(AIMAG(E)/REAL(E))
      ZI=E/AMP
      EG=AMP*1600.+E
C      POWER AND VOLTAGE RATIOS
       P50=((CABS(EG)/2.)**2)/1600.
       P=REAL(E*CONJG(AMP))
       PMIS(K)=10.*ALOG10(P/P50)
      PO=SCLF
      PILOS(K)=10.*ALOG10(PO/P50)
 1     CONTINUE
       WRITE(6,10)(PMIS(J),J=1,K)
      WRITE(6,10)(PILOS(J),J=1,K)
       FE=FLOAT(IFE)/10.
       DEL=FLOAT(INC)
       FS=FLOAT(IFS)/10.
       YMAX=0.
       YMIN=-24.
       DO 100 J=1,K
      IF(PILOS(J).LT.YMIN)PILOS(J)=YMIN
 100   CONTINUE
       IF(IPLOT.NE.1)GO TO 503
       CALL CPLOT0(PILOS,K,YMIN,YMAX,YINCH,FS,FE,XINCH,IY,IX,ID,BUF)
       GO TO 504
 503   CALL REPLOT(PILOS)
 504   IPLOT=IPLOT+1
 5     CONTINUE
       IND=IND+1
       IF(IND.EQ.2)GO TO 502
       CALL PLOT(0.,0.,999)
       STOP
 10    FORMAT(V)
       END
       COMPLEX FUNCTION SINH(Z)
       COMPLEX Z
       SINH=(CEXP(Z)-CEXP(-Z))/2.
       RETURN
       END
       COMPLEX FUNCTION TANHX(Y)
       COMPLEX Y
       TANHX=CEXP(Y)-CEXP(-Y)
       TANHX=TANHX/(CEXP(Y)+CEXP(-Y))
       RETURN
       END
$:LIBRARY:L1
$:EXECUTE
$:REMOTE:$$,E1
$:REMOTE:P*,E1
$:LIMITS:10,,,5000
$:PRMFL:L1,R,S,ADEUSERS/ADELIB
$:TAPE:17,X17DD,,E7098,,CALCOMP-1265
$:ENDJOB
```

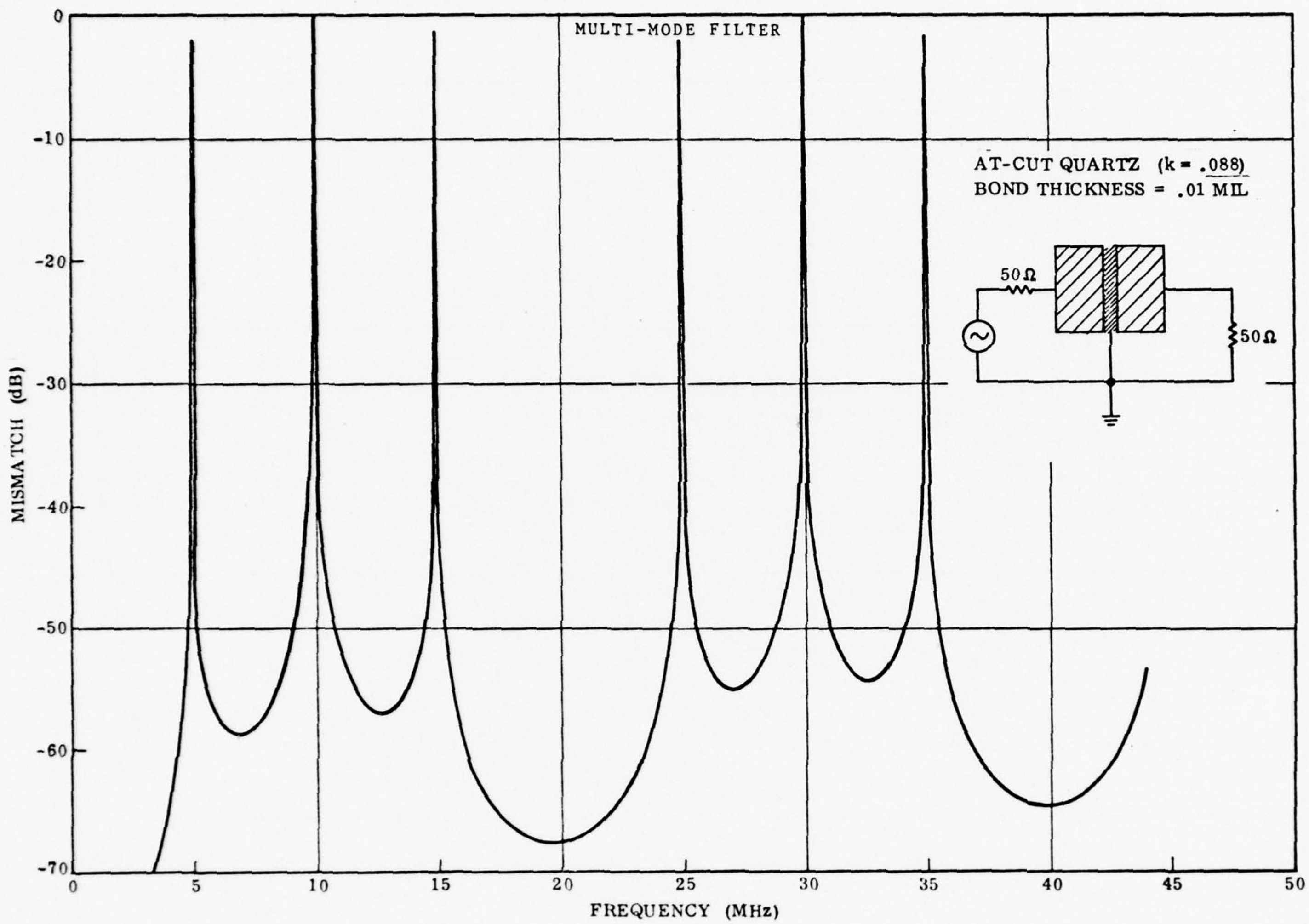

Figure 2.4. Mismatch Versus Frequency.

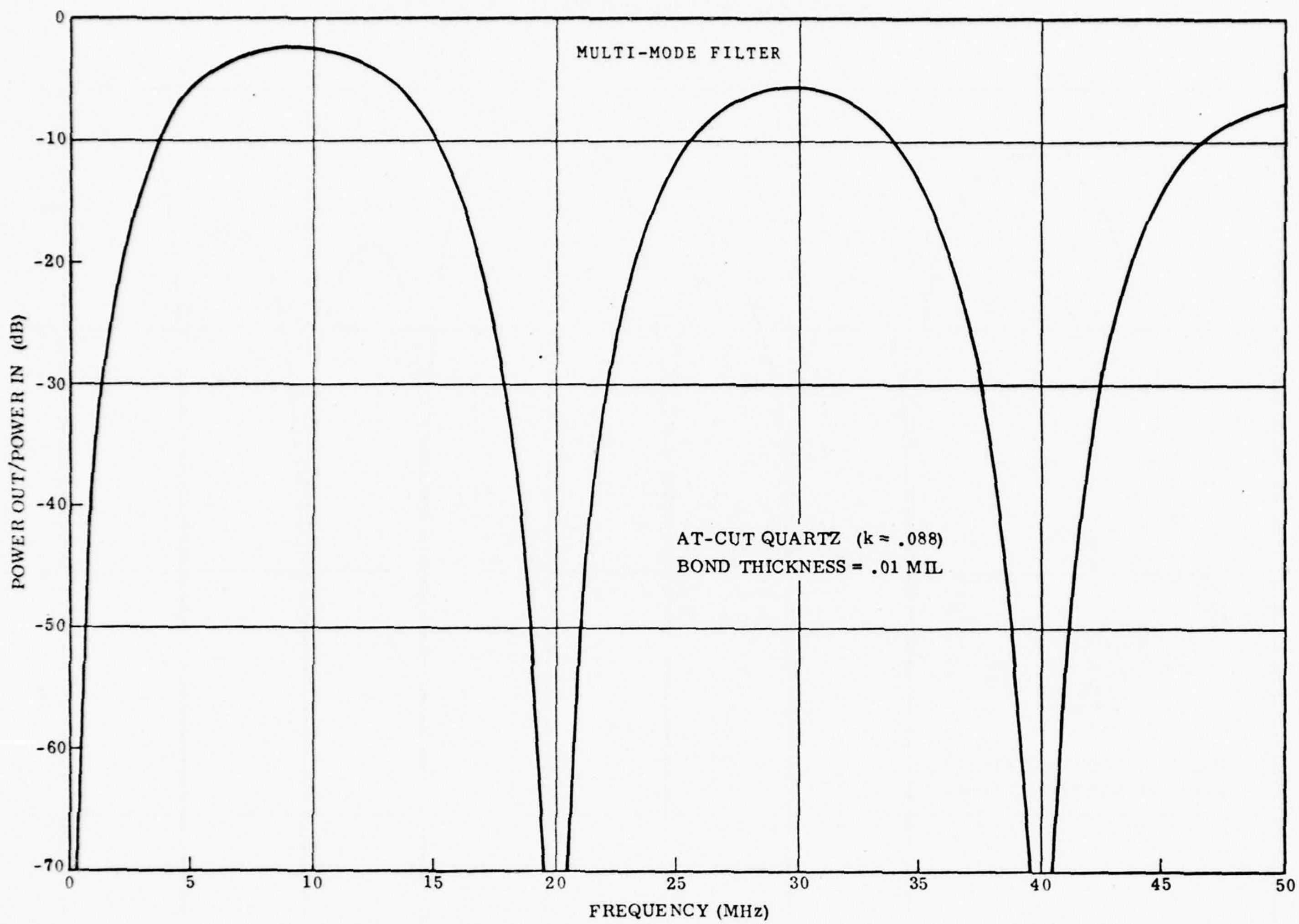

Figure 2.5. Power Out/Power In Versus Frequency.

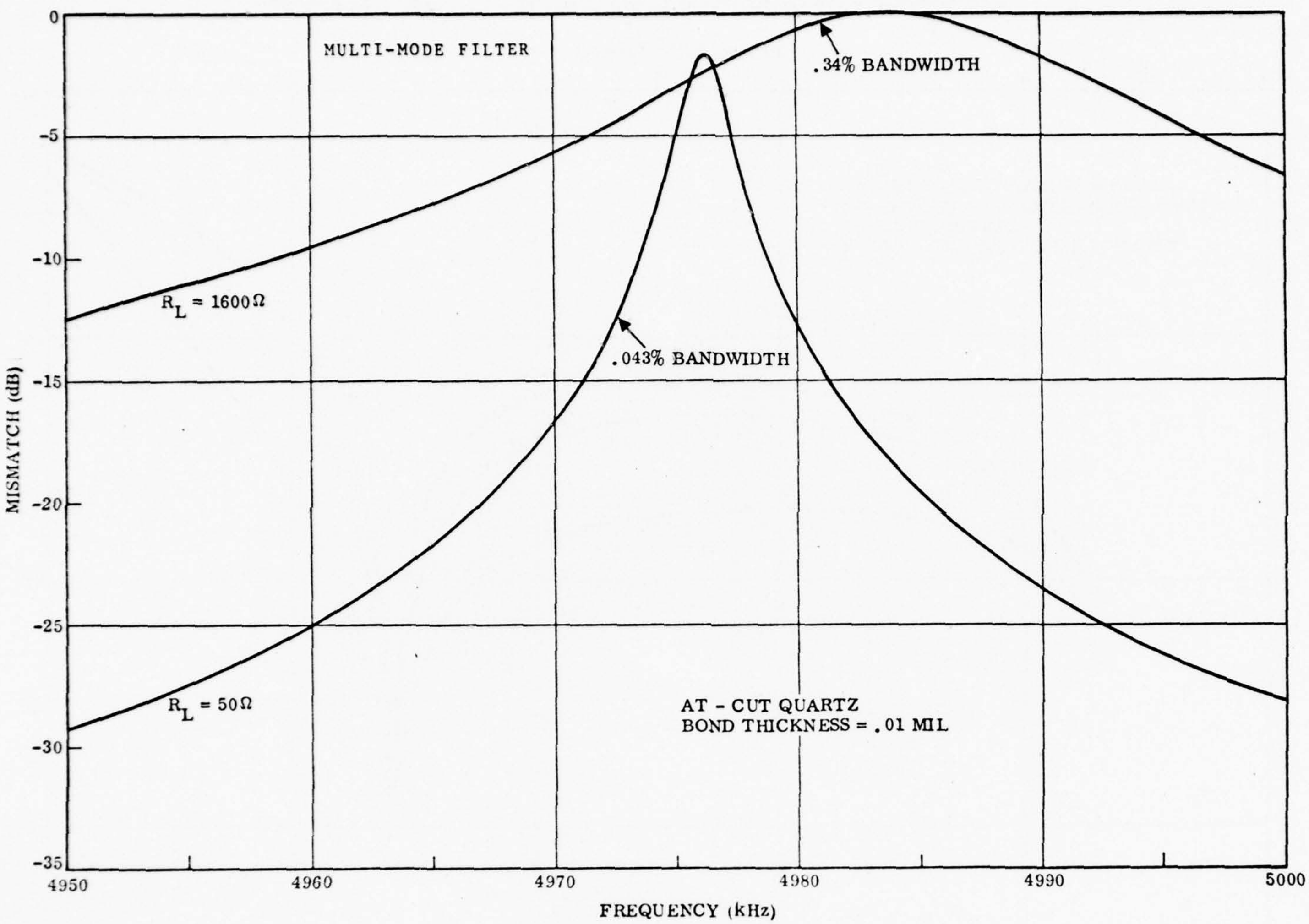

Figure 2.6. Mismatch Versus Frequency.

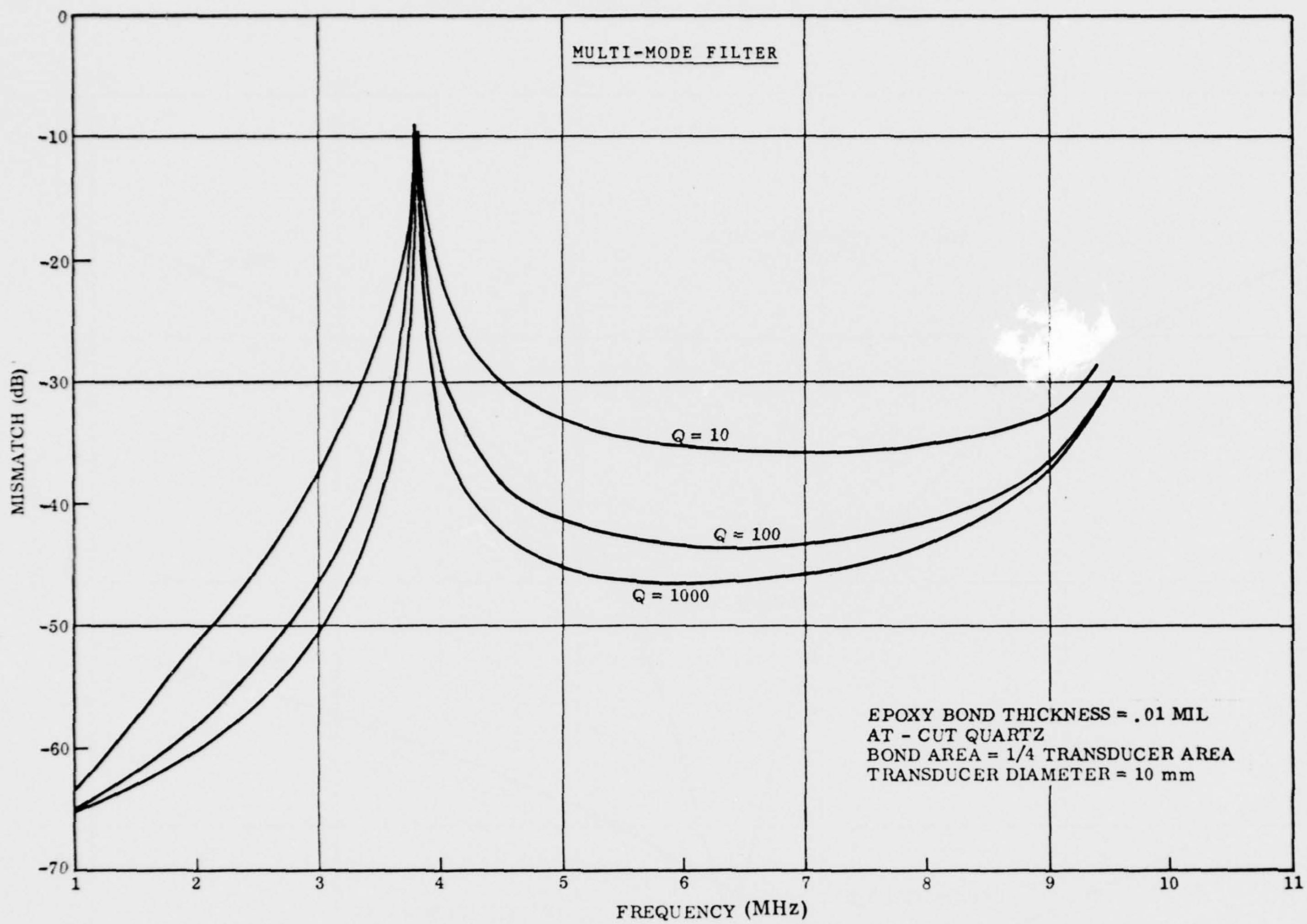

Figure 2.7. Effect of Bond Q On Mismatch Versus Frequency.

For a gold bond the appropriate material constants are:

$$\rho = 19.333 \times 10^3 \text{ kg/m}^3$$

$$c = 1.2 \times 10^3 \text{ m/s}$$

$$Q \geq 100$$

(1) Bond Material and Thickness

Insertion loss versus frequency over the passband at 10 MHz for the two crystal AT-cut quartz filter is plotted in Figures 2.8 and 2.9 using epoxy and gold bonds, respectively, for a series of bond thicknesses from .1 mil to 1 mil in steps of .1 mil. The bond area to active transducer area ratio was held constant at 1/400. The generator and load impedances are 1600 ohms in order to give a maximum bandwidth. Allowing 3 dB passband ripple, the epoxy bond gives a .65% bandwidth while the gold bond gives a .75% bandwidth. This corresponds to a 15% increase in bandwidth due to the better impedance match of the gold bond.

The family of curves clearly indicate the effect of bond thickness on the frequency response. As the bond thickness decreases, the crystals become more coupled, thus separating the peaks and giving a larger passband ripple.

(2) Bond Area to Transducer Area Ratio

Insertion loss versus frequency over the passband at 10 MHz for the two crystal AT-cut quartz filter is plotted in Figures 2.10 and 2.11 for a series of bond area to transducer active area ratios from 1/50 to 1/600. The bond thickness was held constant at .4 mil. The curves indicate that the area ratio plays the same role as that of the bond thickness. As the bond area to transducer area ratio becomes larger, the transducer crystals become more coupled with the same effect of separating the peaks with larger passband ripple.

The bond tends to act as a capacitive coupling ($c = \epsilon A/d$), where A corresponds to the area ratio and d corresponds to the bond thickness. Area ratio and bond thickness can be traded off to yield the desired passband response.

C. TRANSDUCER MATERIAL

AT-cut quartz was chosen for the stacked crystal (multi-mode) filter because of its pure mode characteristics. However, its low coupling coefficient, $k = .088$, limits the amount of bandwidth that can be obtainable.

A new material, berlinite, has the same pure thickness shear mode characteristics of AT-cut quartz but with a higher coupling coefficient of $k = .143$. The velocity of propagation, c, and density, ρ, for berlinite are:

$$c = 2.87 \times 10^3 \text{ m/s}$$

$$\rho = 2.62 \times 10^3 \text{ kg/m}^3$$

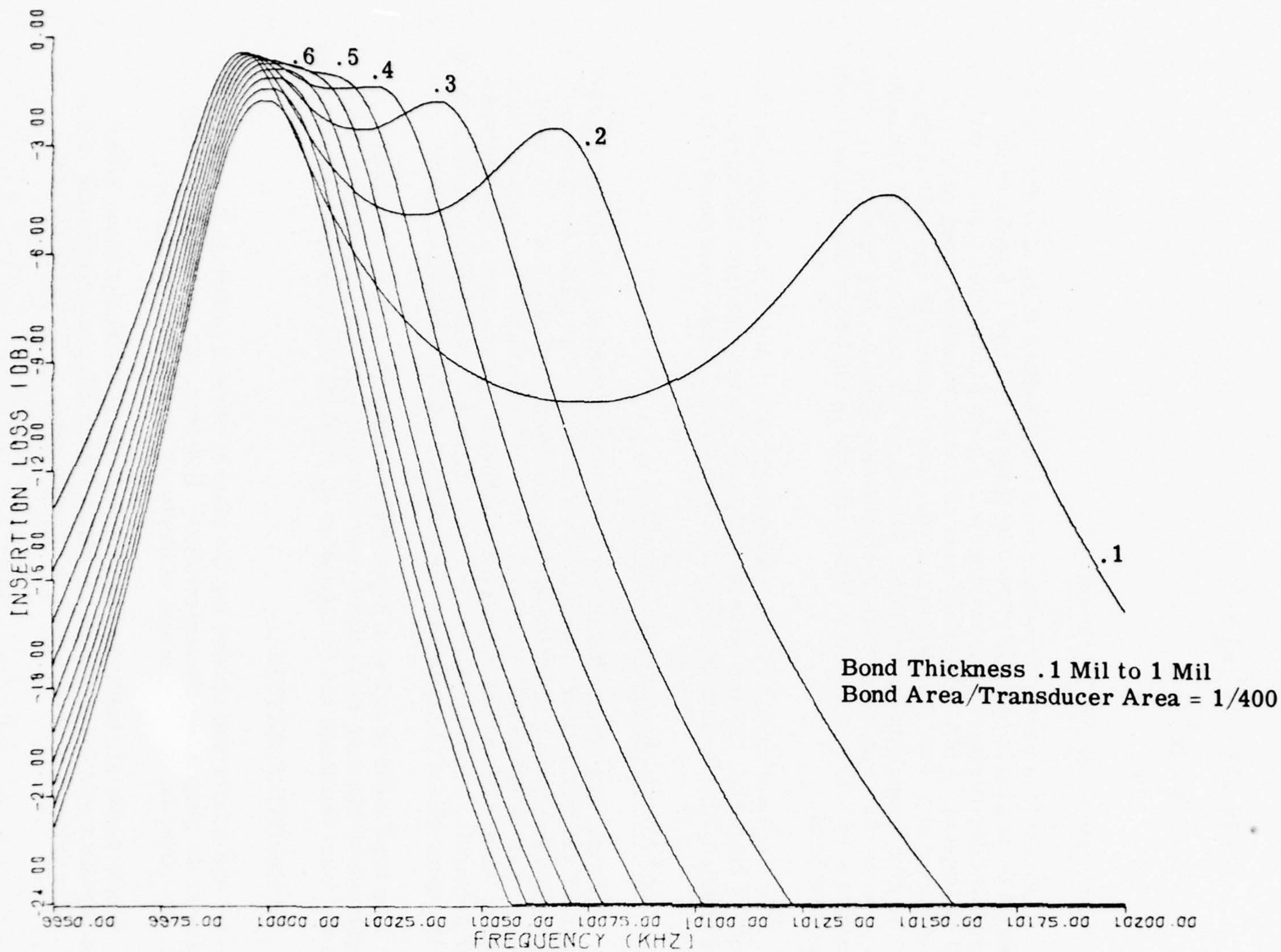

Figure 2.8. Insertion Loss Versus Frequency for Epoxy Bonded Two Crystal AT-Cut Quartz Filter.

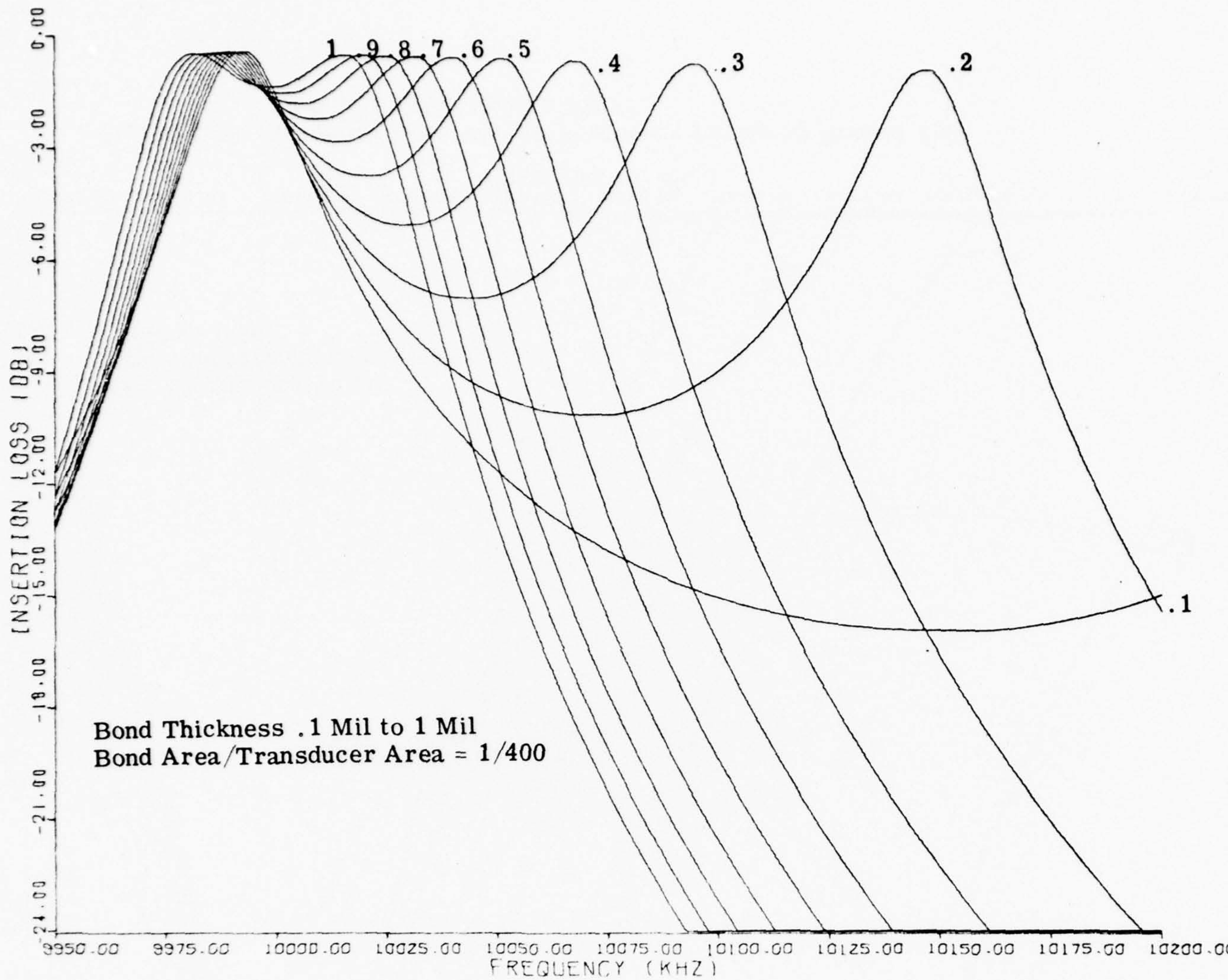

Figure 2.9. Insertion Loss Versus Frequency for Gold Bonded Two Crystal AT-Cut Quartz Filter.

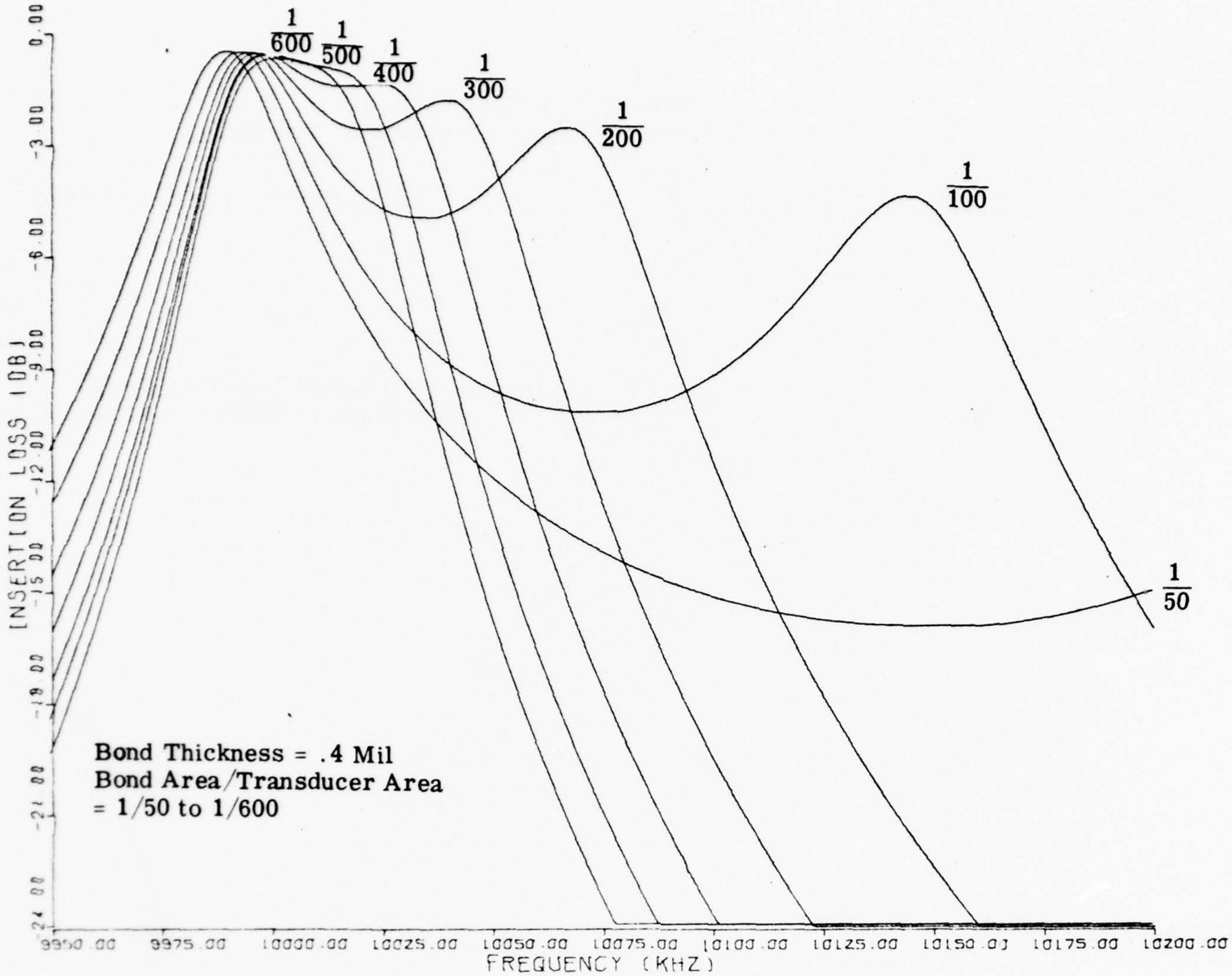

Figure 2.10. Insertion Loss Versus Frequency for Epoxy Bonded Two Crystal AT-Cut Quartz Filter.

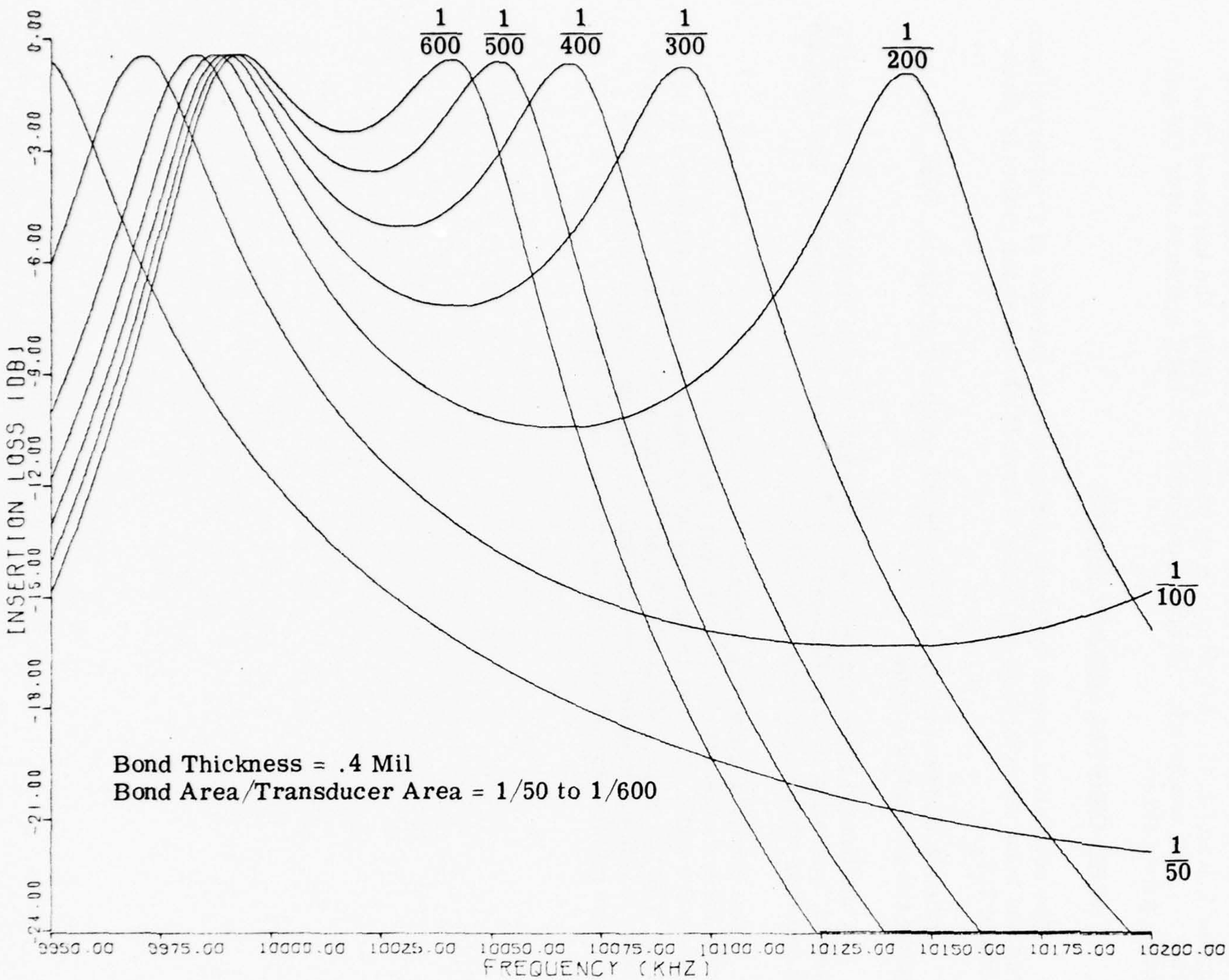

Figure 2.11. *Insertion Loss Versus Frequency for Gold Bonded Two Crystal AT-Cut Quartz Filter.*

The family of curves in Figures 2.12 and 2.13 for the gold-bonded two crystal berlinite filter can be compared to their quartz filter counterparts in Figures 2.9 and 2.11. Allowing a 3 dB passband ripple, the berlinite filter yields a 1.98% bandwidth. This corresponds to a 164% increase over the gold-bonded quartz filter.

D. THREE-CRYSTAL QUARTZ FILTER

The equivalent circuit for three bonded quartz crystals of arbitrary dimensions and bond material type operating in pure thickness shear modes is given in Table 2.2.

Table 2.2 also contains a listing of the computer program, 3CB, used to analyze the equivalent circuit.

A multimode filter consisting of three gold-bonded identical AT-cut quartz crystals, operating in pure thickness shear modes, was proposed. The crystals are one-half wavelength thick at 10 MHz.

The family of curves in Figures 2.14 and 2.15 for the three crystal quartz filter can be compared to the corresponding two crystal curves of Figures 2.9 and 2.11. The three-crystal curves are shifted downward in frequency with the same 3 dB bandwidth as the two-crystal filter. There appears to be no advantage in using three crystals in this particular configuration where the middle crystal only serves as a coupling layer.

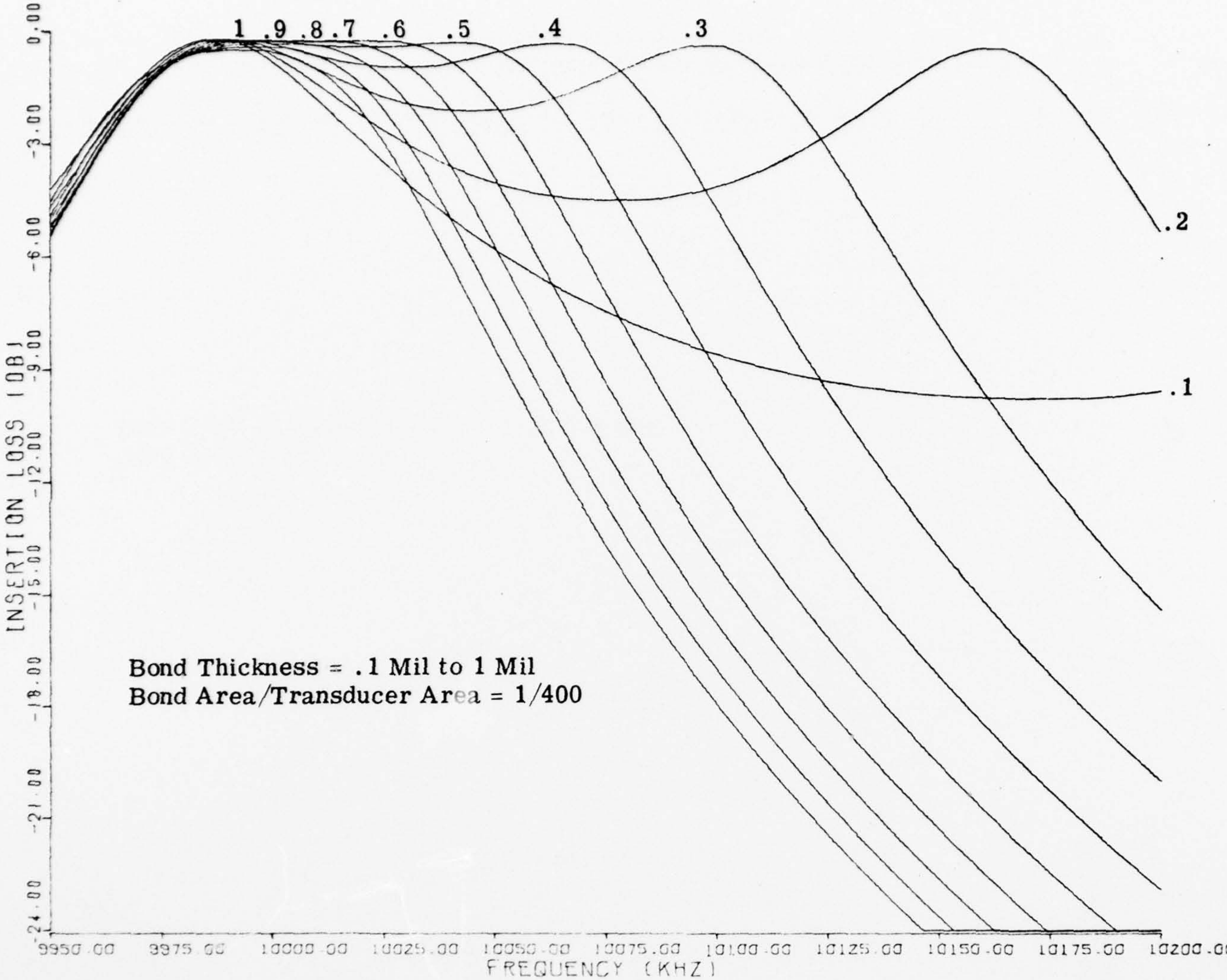

Figure 2.12. Insertion Loss Versus Frequency for Gold Bonded Two Crystal Berlinite Filter.

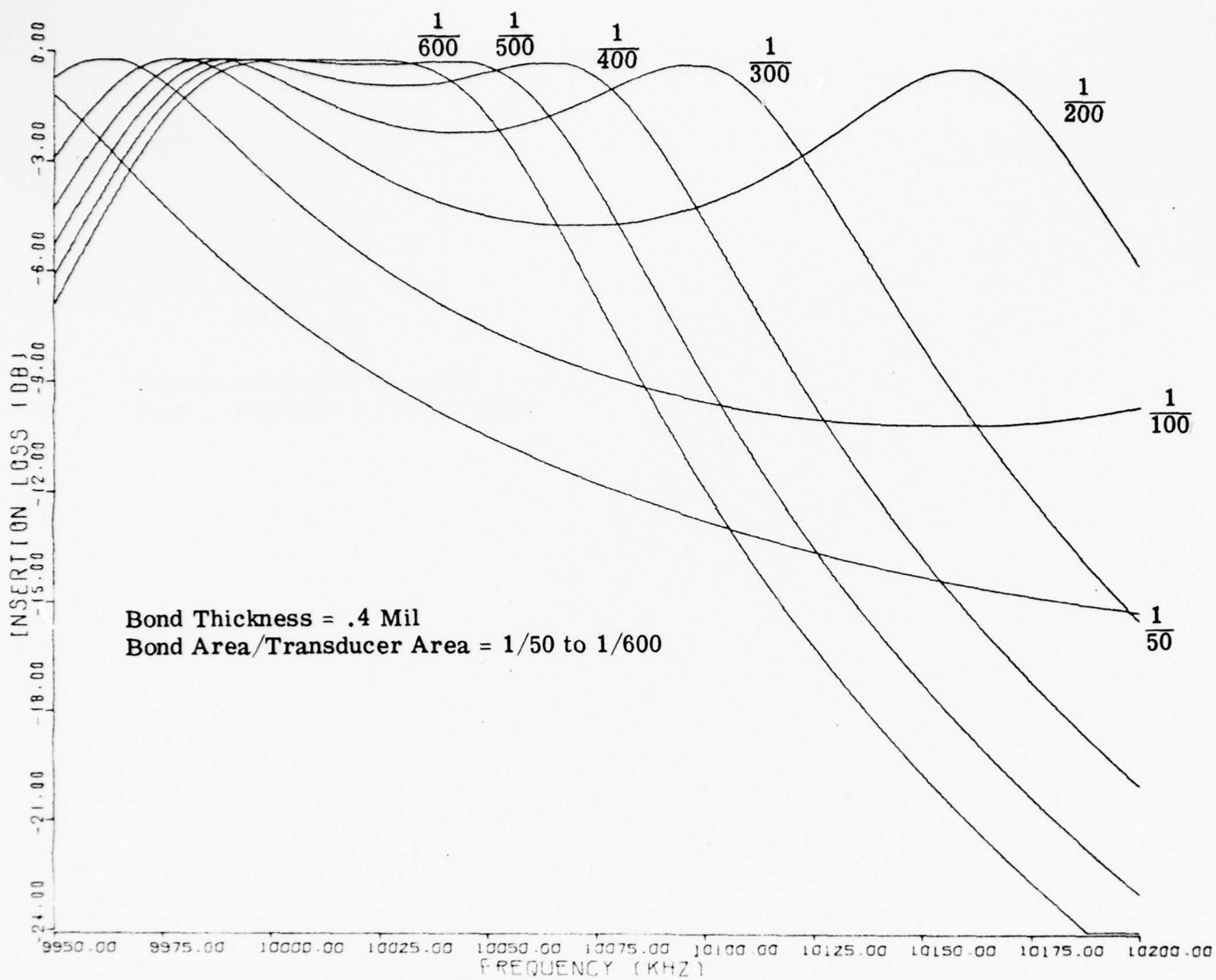

Figure 2.13. Insertion Loss Versus Frequency for Gold Bonded Two Crystal Berlinite Filter.

TABLE 2.2

A. EQUIVALENT CIRCUIT FOR THREE BONDED QUARTZ CRYSTALS OF ARBITRARY DIMENSIONS AND BOND MATERIAL TYPE (SINGLE THICKNESS SHEAR MODES)

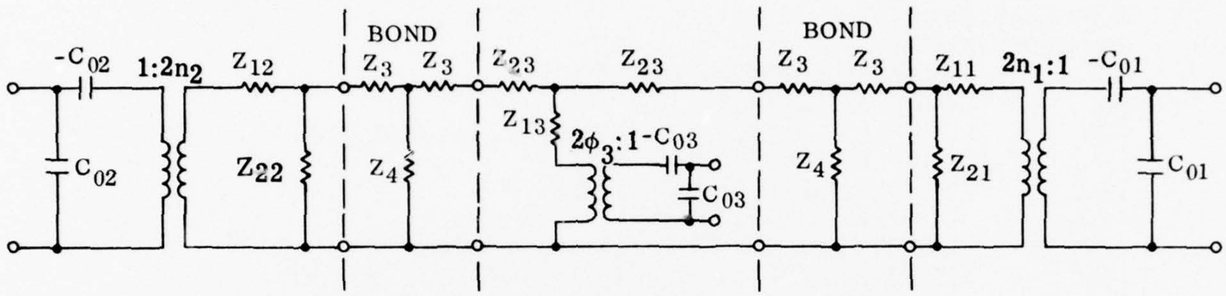

$$Z_{11} = 2Z_{OT}/\tanh(\Gamma_T \ell_{T1}/2)$$

$$Z_{21} = 2Z_{OT}\tanh(\Gamma_T \ell_{T1}/2)$$

$$Z_{12} = 2Z_{OT}/\tanh(\Gamma_T \ell_{T2}/2)$$

$$Z_{22} = 2Z_{OT}\tanh(\Gamma_T \ell_{T2}/2)$$

$$Z_{13} = Z_{OT}/\sinh(\Gamma_T \ell_{T3})$$

$$Z_{23} = Z_{OT}\tanh(\Gamma_T \ell_{T3}/2)$$

$$Z_3 = Z_{OB}\tanh(\Gamma_B \ell_B/2)$$

$$Z_4 = Z_{OB}/\sinh(\Gamma_B \ell_B)$$

TABLE 2.2 (CONT'D)

B. COMPUTER PROGRAM, 3CB

```
10$:IDENT:888400-276-1265,ALK EP-3 135
20$:LIMITS:10,,,5000
30$:OPTION:FORTRAN
40$:FORTY:NLNO,NFORM
50$:LIMITS:03,26K
60$:REMOTE:$$,E1
70$:REMOTE:P*,E1
80        PARAMETER NPTS=1000,NPLTS=1
90        COMPLEX E,AMP,E0,EG
100        COMPLEX Z11,Z21,Z12,Z22,Z3,Z4,ZC1,ZC2,ZI
105        COMPLEX Z13,Z23
110        COMPLEX GT1,GT2,GB,GB2
120        COMPLEX SINH,TANHX
130        DIMENSION KI(NPLTS),PMIS(1000),PILOS(1000)
140        DIMENSION IX(10),IY(10),ID(10),BUF(1000)
150        CHARACTER DA*1(NPLTS)/"*"/
160        DATA IY(1),IY(2)/19,19HINSERTION LOSS (DB)/
170        DATA IX(1),IX(2)/15,15HFREQUENCY (KHZ)/
180        DATA ID(1),ID(2)/23,23HAL KACHELMYER  EP-3 135/
190        PI=3.14159
200        YINCH=8.
210        XINCH=10.
220        ISHORT=1
230        FO=1.E7
231        IND=1
232        I1=100
233        I2=700
234        N1=4
235        N2=4
236 502    IF(IND.EQ.1)GO TO 501
238        I1=400
239        I2=400
240        N1=1
242        N2=10
243 501    CONTINUE
244        IPLOT=1
245        D=10.E-3
250        AREA=PI*D*D/4.
260C        TRANSDUCER CONSTANTS
270        XK=.088
280        CT=3.32E3
290        DT=2.65E3
300        ZOT=AREA*CT*DT
310        QT=10000.
320C        BOND CONSTANTS
330        CB=1.2E3
340        DB=19.333E3
345        DO 5 IRATIO=I1,I2,100
346        RATIO=FLOAT(IRATIO)
347        IF(IRATIO.EQ.700)RATIO=50.
350        ZOB=AREA*CB*DB/RATIO
360        QB=100.
```

TABLE 2.2 (CONT'D)

```
C        TRANSDUCER DIMENSIONS
         TL1=CT/(2.*F0)
         TL2=TL1
         TL3=TL1
C        BOND THICKNESS
         DO 5 N=N1,N2
         BL=FLOAT(N)*2.54E-6
C        CAPACITANCE CO
         EP=4.58*8.85E-12
         CO1=EP*(1.-XK*XK)*AREA/TL1
         CO2=EP*(1.-XK*XK)*AREA/TL2
         CO3=EP*(1.-XK*XK)*AREA/TL3
C        COUPLING COEFFICIENT PHI
         PH1=XK*SQRT(2.*F0*CO1*ZOT)
         PH2=XK*SQRT(2.*F0*CO2*ZOT)
         PH3=XK*SQRT(2.*F0*CO3*ZOT)
         WRITE(6,11)CO1,CO2,PH1,PH2
   11    FORMAT(3X,"CO1=",E12.4,"  CO2=",E12.4,"  PH1=",F9.5,
        &"  PH2=",F9.5)
         PH1=2.*PH1
         PH2=2.*PH2
         IFS=99500
         IFE=102000
         INC=5
         K=0
C        LOOP THRU FREQUENCY
         DO 1 I=IFS,IFE,INC
         K=K+1
         FREQ=FLOAT(I)*1.E2
C        PROPAGATION CONSTANTS
         BT=2.*PI*FREQ/CT
         BB=2.*PI*FREQ/CB
         AT=BT/(2.*QT)
         AB=BB/(2.*QB)
         GT1=TL1*CMPLX(AT,BT)/2.
         GT2=TL2*CMPLX(AT,BT)/2.
         GT3=TL3*CMPLX(AT,BT)/2.
         GB=BL*CMPLX(AB,BB)
         GB2=GB/2.
C        COMPLEX IMPEDANCES
         Z11=2.*ZOT/TANHX(GT1)
         Z21=2.*ZOT*TANHX(GT1)
         Z12=2.*ZOT/TANHX(GT2)
         Z22=2.*ZOT*TANHX(GT2)
         Z13=ZOT/SINH(2.*GT3)
         IF(ISHORT.EQ.1)Z13=Z13+CMPLX(0.,PH3*PH3/(2.*PI*FREQ*CO3))
         Z23=ZOT*TANHX(GT3)
         Z3=ZOB*TANHX(GB2)
         Z4=ZOB/SINH(GB)
         ZC1=CMPLX(0.,-1./(2.*PI*FREQ*CO1))
         ZC2=CMPLX(0.,-1./(2.*PI*FREQ*CO2))
```

TABLE 2.2 (CONT'D)

```
C       CIRCUIT NETWORK EQUATIONS
        SCLF=6.25E-4
        E0=CMPLX(1.,0.)
        AMP=E0/ZC1+SCLF*CMPLX(1.,0.)
        E=(E0-AMP*ZC1)*PH1
        AMP=AMP/PH1
        E=E+AMP*Z11
        AMP=AMP+E/Z21
        E=E+AMP*Z3
        AMP=AMP+E/Z4
        E=E+AMP*(Z3+Z23)
        AMP=AMP+E/Z13
        E=E+AMP*(Z3+Z23)
        AMP=AMP+E/Z4
        E=E+AMP*Z3
        AMP=AMP+E/Z22
        E=(E+AMP*Z12)/PH2
        AMP=AMP*PH2
        E=E-AMP*ZC2
        AMP=AMP+E/ZC2
        EIM=20.*ALOG10(CABS(E))
        ARGEI=ATAN(AIMAG(E)/REAL(E))
        ZI=E/AMP
        EG=AMP*1600.+E
C        POWER AND VOLTAGE RATIOS
         P50=((CABS(EG)/2.)**2)/1600.
         P=REAL(E*CONJG(AMP))
         PMIS(K)=10.*ALOG10(P/P50)
        P0=SCLF
        PILOS(K)=10.*ALOG10(P0/P50)
    1    CONTINUE
         WRITE(6,10)(PMIS(J),J=1,K)
        WRITE(6,10)(PILOS(J),J=1,K)
         FE=FLOAT(IFE)/10.
         DEL=FLOAT(INC)
         FS=FLOAT(IFS)/10.
         YMAX=0.
         YMIN=-24.
         DO 100 J=1,K
        IF(PILOS(J).LT.YMIN)PILOS(J)=YMIN
  100    CONTINUE
         IF(IPLOT.NE.1)GO TO 503
         CALL CPLOT 0(PILOS,K,YMIN,YMAX,YINCH,FS,FE,XINCH,IY,IX,ID,BUF)
         GO TO 504
  503    CALL REPLOT(PILOS)
  504    IPLOT=IPLOT+1
    5    CONTINUE
         IND=IND+1
         IF(IND.EQ.2)GO TO 502
         CALL PLOT(0.,0.,999)
         STOP
   10    FORMAT(V)
         END
```

TABLE 2.2 (CONT'D)

```
1260       COMPLEX FUNCTION SINH(Z)
1270       COMPLEX Z
1280       SINH=(CEXP(Z)-CEXP(-Z))/2.
1290       RETURN
1300       END
1310       COMPLEX FUNCTION TANHX(Y)
1320       COMPLEX Y
1330       TANHX=CEXP(Y)-CEXP(-Y)
1340       TANHX=TANHX/(CEXP(Y)+CEXP(-Y))
1350       RETURN
1360       END
1380$:LIBRARY:L1
1390$:EXECUTE
1400$:REMOTE:$$,E1
1410$:REMOTE:P*,E1
1415$:LIMITS:10,,,5000
1420$:PRMFL:L1,R,S,ADEUSERS/ADELIB
1430$:TAPE:17,X17DD,,E7197,,CALCOMP-1265
1440$:ENDJOB
```

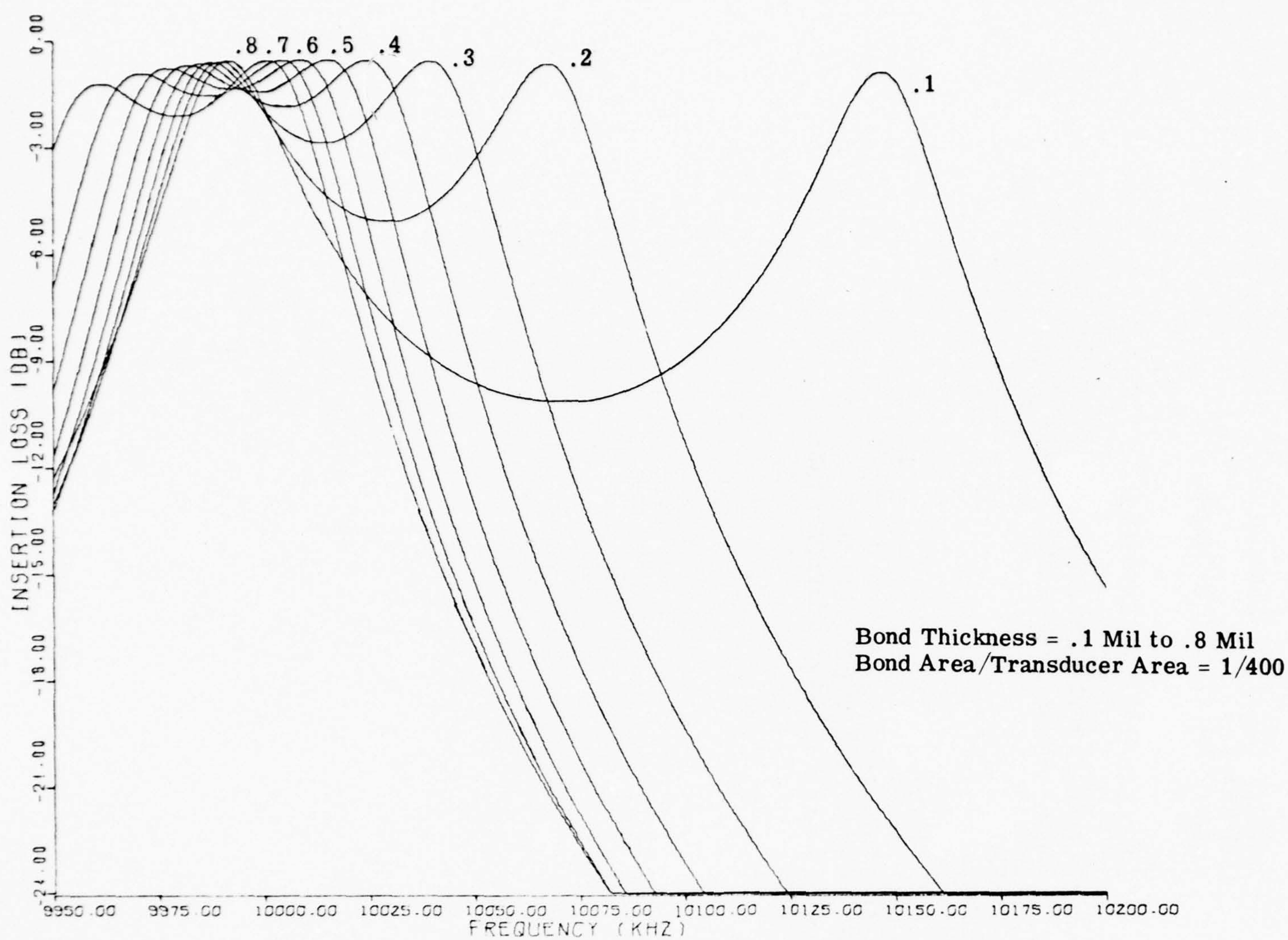

Figure 2.14. Insertion Loss Versus Frequency for Gold Bonded Three Crystal AT-Cut Quartz Filter.

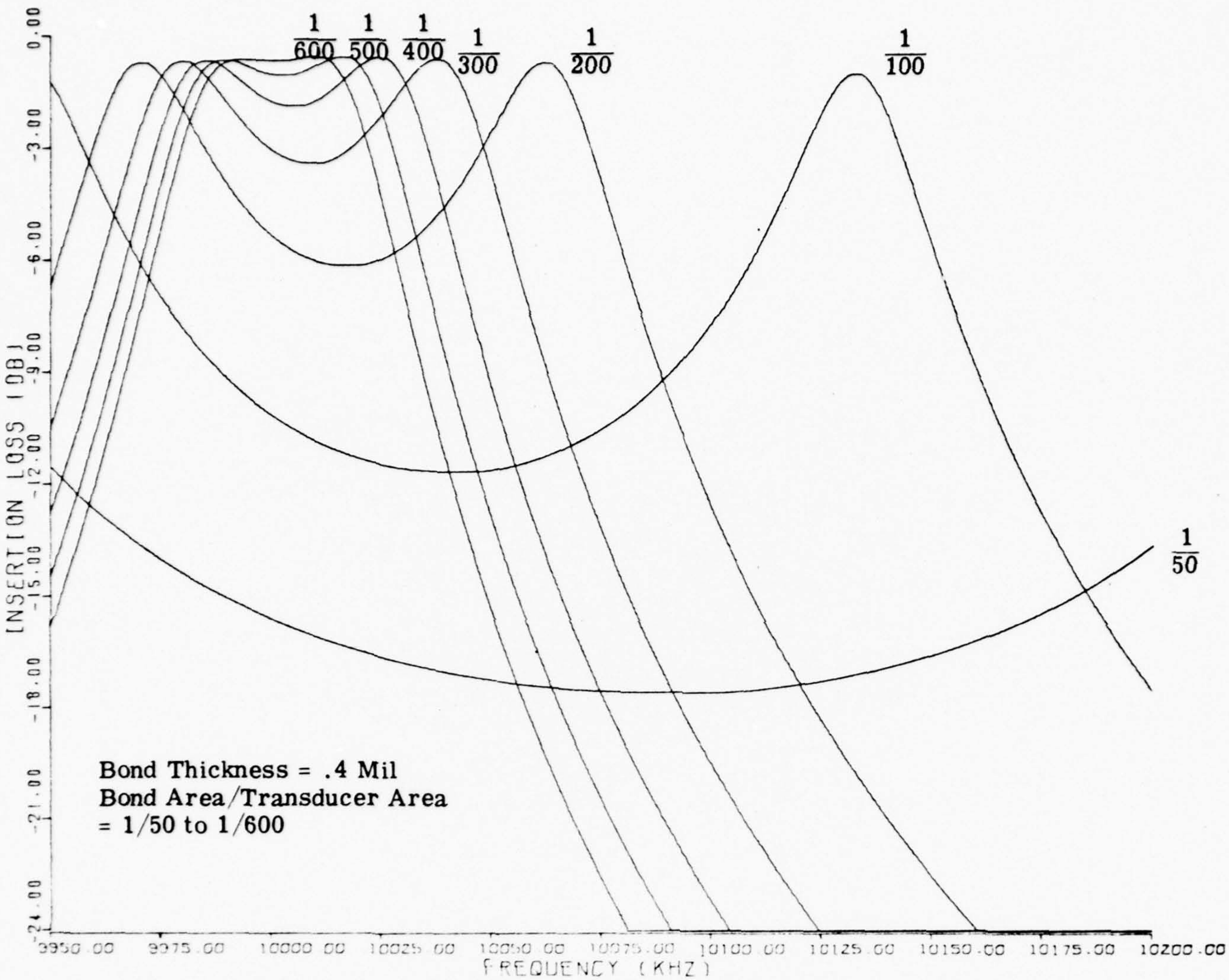

Figure 2.15. Insertion Loss Versus Frequency for Gold Bonded Three Crystal AT-Cut Quartz Filter.

3. THEORETICAL INVESTIGATIONS OF MULTIMODE STACKED FILTERS

The multimode stacked filter investigations in this section will make use of the transmission line model of a piezoelectric plate as developed by Dr. Ballato [1] instead of the Mason Equivalent circuit used previously.

A thorough derivation of this model is given in reference [1] ; however a brief discussion of its derivation will be included here as an aid to understanding the programs and results to be presented.

An attempt will also be made to present the ideas on a fairly elementary level so that the programs can be interpreted by those who are unfamiliar with crystal physics and tensor notation.

This derivation will be split into sections; the computer programs developed during the course of this contract will be presented at those points in the derivation where they are used.

In this presentation the following symbols and conventions will be used:

T_{ij} = stress (force per unit area)

(T_{ij} = component of force in the x_i direction transmitted across the face of the plate perpendicular to the x_j direction)

u_j = mechanical displacement

S_{ij} = strain

D_i = electric displacement

E_i = electric field

ρ = mass density

ϕ = electric potential

c^E_{ijkl} = elastic stiffness at constant electric field

e_{kij} = piezoelectric stress constant

ϵ^S_{ik} = dielectric permittivity at constant strain

Einstein summation convention (when a letter subscript occurs twice in the same term, summation with respect to that subscript is carried out)

$$a_i = \sum_{j=1}^{3} T_{ij} q_j = T_{ij} q_j$$

An index (subscript) preceded by a comma denotes differentiation with respect to the space coordinate represented by that index

$$u_{i,j} = \partial u_i / \partial x_j$$

A dot above a variable denotes differentiation with respect to time

$$\dot{u}_j = \frac{\partial u_j}{\partial t} \quad , \quad \ddot{u}_j = \frac{\partial^2 u_j}{\partial t^2}$$

All Latin indexes have the range 1, 2 and 3.

A. DEVELOPMENT OF THE SECULAR EQUATION AND PROGRAM CROT

The piezoelectric plate under consideration is assumed to be represented in an orthogonal right hand coordinate system x_i with one of the coordinates in the plate thickness direction.

The pertinent set of equations governing the behavior of this plate are: [2]

the stress equations of motion derived from Newton's second law

$$T_{ij,i} = \rho \ddot{u}_j \ , \qquad (1)$$

the equations defining mechanical strain,

$$S_{ij} = \frac{1}{2} (u_{i,j} + u_{j,i}) \ , \qquad (2)$$

the charge equation of electrostatics (the divergence relation from Maxwell's equations in the absence of free charge),

$$D_{i,i} = 0 \ , \qquad (3)$$

the electric field-electric potential relation for a quasi-static case,

$$E_k = -\phi_{,k} \qquad (4)$$

and the linear piezoelectric constitutive relations characterizing the medium,

$$T_{ij} = c^E_{ijkl} S_{kl} - e_{kij} E_k \tag{5}$$

and

$$D_i = e_{ikl} S_{kl} + \epsilon^S_{ik} E_k \quad . \tag{6}$$

Equation (5) is Hooke's law, extended to take into account piezoelectricity; Eq. (6) is the constitutive relation for a dielectric medium extended to include piezoelectricity.

Substituting Eqs. (2) and (4) into Eqs. (5) and (6) yields

$$T_{ij} = c^E_{ijlk} u_{l,k} + e_{kij} \phi_{,k} \tag{7}$$

$$D_i = e_{ilk} u_{l,k} - \epsilon^S_{ik} \phi_{,k} \;, \tag{8}$$

where use has been made of the following symmetry relations among the material constants [3], [4]:

$$c_{ijkl} = c_{ijlk} = c_{jikl} = c_{klij}$$

$$e_{ijk} = e_{ikj} \tag{9}$$

$$\epsilon_{ij} = \epsilon_{ji}$$

Equations (7) and (8) can be substituted in Eqs. (1) and (3) to yield

$$T_{ij,i} = c^E_{ijkl} u_{l,ki} + e_{kij} \phi_{,ki} = \rho \ddot{u}_j \tag{10}$$

$$D_{i,i} = e_{ilk} u_{l,ki} - \epsilon^S_{ik} \phi_{,ki} = 0 \tag{11}$$

Assuming a wave propagating in the i^{th} direction (the plate thickness direction) with electric potential applied in the same direction, and that there is no dependence on the other two directions, $q_{,j} = q_{,k} = 0$. Equation (11) can be solved for ϕ ;

$$\phi_{,ii} = \frac{e_{ili}}{\epsilon^S_{ii}} \quad u_{l,ii} \quad . \tag{12}$$

This equation can, in turn, be substituted into Eq. (10) to yield

$$\left\{ c^E_{ijli} + e_{iij} \left(\frac{e_{ili}}{\epsilon^S_{ii}} \right) \right\} \quad u_{l,ii} = \rho \ddot{u}_j \tag{13}$$

It is convenient to write this equation as

$$\bar{c}^{E}_{ijki}\, u_{k},_{ii} = \rho \ddot{u}_j , \tag{14}$$

where

$$\bar{c}^{E}_{ijki} = c^{E}_{ijli} + e_{iij} \left(\frac{e_{ili}}{\epsilon^{S}_{ii}} \right) \tag{15}$$

are the "piezoelectrically stiffened" elastic stiffnesses at constant normal electric displacement and constant tangential electric field.

If u_j takes the standard time factor form, $e^{j\omega t}$, and is only a function of the coordinate, x_i, in the thickness direction, then

$$u_j = u_j(x_i;t) = u_j(x_i)e^{j\omega t} , \tag{16}$$

and Eq. (14) becomes

$$\bar{c}^{E}_{ijki}\, u_k(x_i),_{ii} = -\rho\,\omega^2 u_j(x_i)$$

or (17)

$$\bar{c}^{E}_{ijki}\, u_k(x_i),_{ii} + \rho\,\omega^2 u_j(x_i) = 0 .$$

If it is further assumed that $u_k(x_i)$ represents plane waves traveling in the x_i direction with wave number, η, so that

$$u_j(x_i) = u_j(\hat{x}_j)e^{\pm j\eta x_i} , \tag{18}$$

where $\hat{x}_j$ indicates only that the direction of u_j is along the x_j direction, the equations in (17) are

$$\bar{c}^{E}_{ijki} \left(-\eta^2 u_k(\hat{x}_k) \right) + \rho\omega^2 u_j(\hat{x}_j) = 0 . \tag{19}$$

It is convenient at this point to define

$$c = \frac{\rho\omega^2}{\eta^2} ; \tag{20}$$

then Eq. (19) becomes Eq. (21) where the direction indicator, $\hat{x}_k$, has been dropped since it is now known that u_k lies in the x_k direction and that i must take on the value corresponding to the propagation direction x_i,

$$\bar{c}^{E}_{ijki}\, u_k - c u_j = 0 . \tag{21}$$

This expression can be written in a clearer form by introducing the Kronecker delta, defined by

$$\delta_{ij} = \begin{cases} 1 & (i = j) \\ 0 & (i \neq j) \end{cases} \quad . \tag{22}$$

Then Eq. (21) becomes

$$(\bar{c}^{E}_{ijki} - c\delta_{jk})\, u_k = 0 \quad . \tag{23}$$

Cramer's rule, applied to this set of equations for the u_k displacement proportionality constants, shows that non-trivial solutions can exist only if

$$\left| \bar{c}^{E}_{ijki} - c\,\delta_{jk} \right| = 0 \ . \tag{24}$$

Equation (24) is commonly referred to as the characteristic or secular equation for the allowed modes of vibration.

The whole purpose of this exercise is to show that the equations and results to be developed later are not dependent on any particular choice of the coordinate lying in the thickness direction of the piezoelectric plate. The form of the equations remain the same; only the constants change in value.

From now on only plates with x_3 lying in the thickness direction will be considered. For this case the equations in Eq. (23) become:

$$\begin{aligned}
(\bar{c}^{E}_{3113} - c)\, u_1 + \bar{c}^{E}_{3123}\, u_2 + \bar{c}^{E}_{3133}\, u_3 &= 0 \\
\bar{c}^{E}_{3213}\, u_1 + (\bar{c}^{E}_{3223} - c)\, u_2 + \bar{c}^{E}_{3233}\, u_3 &= 0 \\
\bar{c}^{E}_{3313}\, u_1 + \bar{c}^{E}_{3323}\, u_2 + (\bar{c}^{E}_{3333} - c)\, u_3 &= 0 \ ,
\end{aligned} \tag{25}$$

which can be simplified by using the symmetry relations in Eq. (9).

In order for non-trivial solutions of these equations to exist, it is necessary that the determinant of the coefficients of the u's be equal to zero, as shown in Eq. (24). Equation (24), or its explicit counterpart from Eq. (25), is a cubic equation in c, of the form,

$$c^3 + qc^2 + rc + s = 0 \ . \tag{26}$$

The first task in the quest for a multi-mode plate model is to solve Eq. (24). However, in deriving Eq. (24), a tacit assumption has been made. The derivation assumes that piezoelectric material constants are known values in the coordinate frame assigned to the plate. Unfortunately, this is not usually

the case. When measurements are made on piezoelectric crystals the tensor components of the material constants are specified in terms of a rectangular set of coordinate axes, which coincide with the crystallographic axes of the material, insofar as this is geometrically possible.

In crystallography, they talk about the a, b, c axes of the crystal; these axes are parallel to the edges of the unit cell, which is the parallelepiped out of which the crystal can be constructed. These a, b, c axes may or may not be mutually perpendicular. The IEEE[5] has established a standard for associating a rectangular set of X, Y, Z axes with the crystallographic a, b, c, axes, for each of the seven systems into which crystals are commonly classified, depending on their degree of symmetry. These seven systems are, in turn, divided into point groups or classes according to their symmetry, with respect to a point. There are thirty-two of these classes but only twenty of them exhibit piezoelectric properties. It is this system and class notation that determines which of the possible material constant components are non-zero.

The orientation of a crystal plate in terms of the rectangular X, Y, Z axes is specified in the IEEE standards by means of a rotational symbol of the form (A B a b c) $\Phi/\Theta/\Psi$, where

A is the initial direction of the plate thickness before rotation,

B is the direction of the plate length before rotation,

a = t, l, or w depending on which direction is the axis of first rotation,

b = t, l, or w depending on which edge is used for the second rotation, and

c = t, l, w according to the edge used for the third rotation.

Φ, Θ, Ψ indicate the corresponding rotation angles with sign where a positive angle is a rotation counterclockwise, looking toward the origin from the positive end of the axis of rotation. This positive end of the axis of rotation is the end that initially pointed in the positive directions of X, Y, Z. In this rotational symbol only as many specifications are used as are needed to completely specify the plate orientation. Unfortunately, people have a tendency (in the literature) to use names for various crystal cuts such as AC-cut quartz or AT-cut quartz, or they refer to them by names such as 35-1/4° rotated Y-cut, without supplying the rotational symbol. In this example AT-cut quartz and a 35-1/4° rotated Y-cut of quartz are the same, with a rotational symbol (YXl) 35-1/4°.

There are also left and right-hand crystals, which, in the case of quartz, leads to different numerical values for some of the material coefficients.

It is assumed now that we know the orientation of the plate under consideration in Eq. (25), relative to the standard X, Y, Z reference frame for the plate material; hence we are ready to obtain the required material coefficients. Now, another confusion factor presents itself. The usual way of listing material

coefficients is in a two-subscript (or less) notation rather than the tensor notation used to develop Eq. (25). The conversion to this two-subscript, or engineer notation, from the four subscript tensor notation is shown in Table 3-1[3]. Furthermore, the tensor symmetry relations shown in Eq. (9) reduce the 81 possible combinations for the elastic stiffness constants to a maximum of 21, the 27 possible combinations for the piezoelectric stress constants to 18, and the nine possible dielectric permittivities to a maximum of six. Tables 3-2 and 3-3, respectively, show the tensor coefficients and their engineering counterparts for the stiffness and piezoelectric stress constants. The tensor and engineer forms of the dielectric permittivity are identical; the only reduction taking place is that $\epsilon^S_{ij} = \epsilon^S_{ji}$.

TABLE 3-1. CONVERSION FROM TENSOR TO ENGINEERING NOTATION

$$C_{ijk\ell} = C_{pq}$$

$$e_{ik\ell} = e_{ip}$$

$$T_{ij} = T_p \; ; \; S_{ij} = S_p \text{ when } i = j, \; p = 1,2,3$$

$$2S_{ij} = S_p \text{ when } i \neq j, \; p = 4,5,6$$

$$i,j,k,\ell = 1,2,3$$

$$p,q = 1,2,3,4,5,6$$

ij or kℓ	p or q
11	1
22	2
33	3
23 or 32	4
31 or 13	5
12 or 21	6

This means that the matrices of the material coefficients of interest in this program will take the form shown in Figure 3-1a for the most general piezoelectric material. In this case there are 45 different non-zero coefficients. Figure 3-1b shows the same matrices for quartz, which was used in the theoretical investigations of this contract. In this case only 14 non-zero different coefficients are present and some of these differ only in sign.

Figure 3-2 shows a general form of the coordinate rotation problem about a common origin. We assume the material coefficients are known in the old x_1, x_2, x_3 (XYZ) system, and that the plate under consideration in Eq. (25) is oriented with the plate thickness direction in the x_3' direction of the new coordinate system, x_1', x_2', x_3'.

TABLE 3-2. RELATIONSHIP OF TENSOR STIFFNESS COEFFICIENTS TO ENGINEER COEFFICIENTS $C_{ijk\ell} = C_{ij\ell k} = C_{jik\ell} = C_{k\ell ij}$
$C_{pq} = C_{qp}$

C_{1111}	C_{1112}	C_{1113}	C_{1121}	C_{1122}	C_{1123}	C_{1131}	C_{1132}	C_{1133}
C_{11}	C_{16}	C_{15}	C_{16}	C_{12}	C_{14}	C_{15}	C_{14}	C_{13}
C_{1211}	C_{1212}	C_{1213}	C_{1221}	C_{1222}	C_{1223}	C_{1231}	C_{1232}	C_{1233}
C_{16}	C_{66}	C_{56}	C_{66}	C_{26}	C_{46}	C_{56}	C_{46}	C_{36}
C_{1311}	C_{1312}	C_{1313}	C_{1321}	C_{1322}	C_{1323}	C_{1331}	C_{1332}	C_{1333}
C_{15}	C_{56}	C_{55}	C_{56}	C_{25}	C_{45}	C_{55}	C_{45}	C_{35}
C_{2111}	C_{2112}	C_{2113}	C_{2121}	C_{2122}	C_{2123}	C_{2131}	C_{2132}	C_{2133}
C_{16}	C_{66}	C_{56}	C_{66}	C_{26}	C_{46}	C_{56}	C_{46}	C_{36}
C_{2211}	C_{2212}	C_{2213}	C_{2221}	C_{2222}	C_{2223}	C_{2231}	C_{2232}	C_{2233}
C_{12}	C_{26}	C_{25}	C_{26}	C_{22}	C_{24}	C_{25}	C_{24}	C_{23}
C_{2311}	C_{2312}	C_{2313}	C_{2321}	C_{2322}	C_{2323}	C_{2331}	C_{2332}	C_{2333}
C_{14}	C_{46}	C_{45}	C_{46}	C_{24}	C_{44}	C_{45}	C_{44}	C_{34}
C_{3111}	C_{3112}	C_{3113}	C_{3121}	C_{3122}	C_{3123}	C_{3131}	C_{3132}	C_{3133}
C_{15}	C_{56}	C_{55}	C_{56}	C_{25}	C_{45}	C_{55}	C_{45}	C_{35}
C_{3211}	C_{3212}	C_{3213}	C_{3221}	C_{3222}	C_{3223}	C_{3231}	C_{3232}	C_{3233}
C_{14}	C_{46}	C_{45}	C_{46}	C_{24}	C_{44}	C_{45}	C_{44}	C_{34}
C_{3311}	C_{3312}	C_{3313}	C_{3321}	C_{3322}	C_{3323}	C_{3331}	C_{3332}	C_{3333}
C_{13}	C_{36}	C_{35}	C_{36}	C_{23}	C_{34}	C_{35}	C_{34}	C_{33}

TABLE 3-3. RELATIONSHIP OF TENSOR PIEZOELECTRIC STRESS COEFFICIENTS TO ENGINEERING COEFFICIENTS $e_{ijk} = e_{ikj}$

e_{111}	e_{112}	e_{113}	e_{121}	e_{122}	e_{123}	e_{131}	e_{132}	e_{133}
e_{11}	e_{16}	e_{15}	e_{16}	e_{12}	e_{14}	e_{15}	e_{14}	e_{13}
e_{211}	e_{212}	e_{213}	e_{221}	e_{222}	e_{223}	e_{231}	e_{232}	e_{233}
e_{21}	e_{26}	e_{25}	e_{26}	e_{22}	e_{24}	e_{25}	e_{24}	e_{23}
e_{311}	e_{312}	e_{313}	e_{321}	e_{322}	e_{323}	e_{331}	e_{332}	e_{333}
e_{31}	e_{36}	e_{35}	e_{36}	e_{32}	e_{34}	e_{35}	e_{34}	e_{33}

By considering the scalar or dot product of the unit vectors i, j, k, in the old coordinate system with the unit vectors i', j', k' in the new coordinate system the following relationship can be determined.

The coordinates of any point, P, with respect to the new axes are given, in terms of the coordinates of P in the old axes, by the following relations:

$$x_1' = \cos\alpha_1 x_1 + \cos\beta_1 x_2 + \cos\gamma_1 x_3$$
$$x_2' = \cos\alpha_2 x_1 + \cos\beta_2 x_2 + \cos\gamma_2 x_3$$
$$x_3' = \cos\alpha_3 x_1 + \cos\beta_3 x_2 + \cos\gamma_3 x_3 \qquad (27)$$

It is more convenient to represent these direction cosines by the symbols l, m, and n where,

$$l_p = \cos\alpha_p$$
$$m_p = \cos\beta_p$$
$$n_p = \cos\gamma_p\ . \qquad (28)$$

A. Most General Crystal (Triclinic) Class 1

$$c^E_{pq} = \begin{bmatrix} c_{11} & c_{12} & c_{13} & c_{14} & c_{15} & c_{16} \\ c_{12} & c_{22} & c_{23} & c_{24} & c_{25} & c_{26} \\ c_{13} & c_{23} & c_{33} & c_{34} & c_{35} & c_{36} \\ c_{14} & c_{24} & c_{34} & c_{44} & c_{45} & c_{46} \\ c_{15} & c_{25} & c_{35} & c_{45} & c_{55} & c_{56} \\ c_{16} & c_{26} & c_{36} & c_{46} & c_{56} & c_{66} \end{bmatrix}$$

$$e_{ip} = \begin{bmatrix} e_{11} & e_{12} & e_{13} & e_{14} & e_{15} & e_{16} \\ e_{21} & e_{22} & e_{23} & e_{24} & e_{25} & e_{26} \\ e_{31} & e_{32} & e_{33} & e_{34} & e_{35} & e_{36} \end{bmatrix}$$

$$\epsilon^S_{ij} \begin{bmatrix} \epsilon_{11} & \epsilon_{12} & \epsilon_{13} \\ \epsilon_{12} & \epsilon_{22} & \epsilon_{23} \\ \epsilon_{13} & \epsilon_{23} & \epsilon_{33} \end{bmatrix}$$

B. Quartz Trigonal Class 32

$$c^E_{pq} = \begin{bmatrix} c_{11} & c_{12} & c_{13} & c_{14} & 0 & 0 \\ c_{12} & c_{11} & c_{13} & -c_{14} & 0 & 0 \\ c_{13} & c_{13} & c_{33} & 0 & 0 & 0 \\ c_{14} & -c_{14} & 0 & c_{44} & 0 & 0 \\ 0 & 0 & 0 & 0 & c_{44} & c_{14} \\ 0 & 0 & 0 & 0 & c_{14} & c_{66} \end{bmatrix} \qquad c_{66} = \frac{1}{2}(c_{11}-c_{12})$$

$$e_{ip} = \begin{bmatrix} e_{11} & -e_{11} & 0 & e_{14} & 0 & 0 \\ 0 & 0 & 0 & 0 & -e_{14} & -e_{11} \\ 0 & 0 & 0 & 0 & 0 & 0 \end{bmatrix}$$

$$\epsilon^S_{ij} = \begin{bmatrix} \epsilon_{11} & 0 & 0 \\ 0 & \epsilon_{11} & 0 \\ 0 & 0 & \epsilon_{33} \end{bmatrix}$$

Figure 3-1. Matrices for Coefficients of Piezoelectric Materials

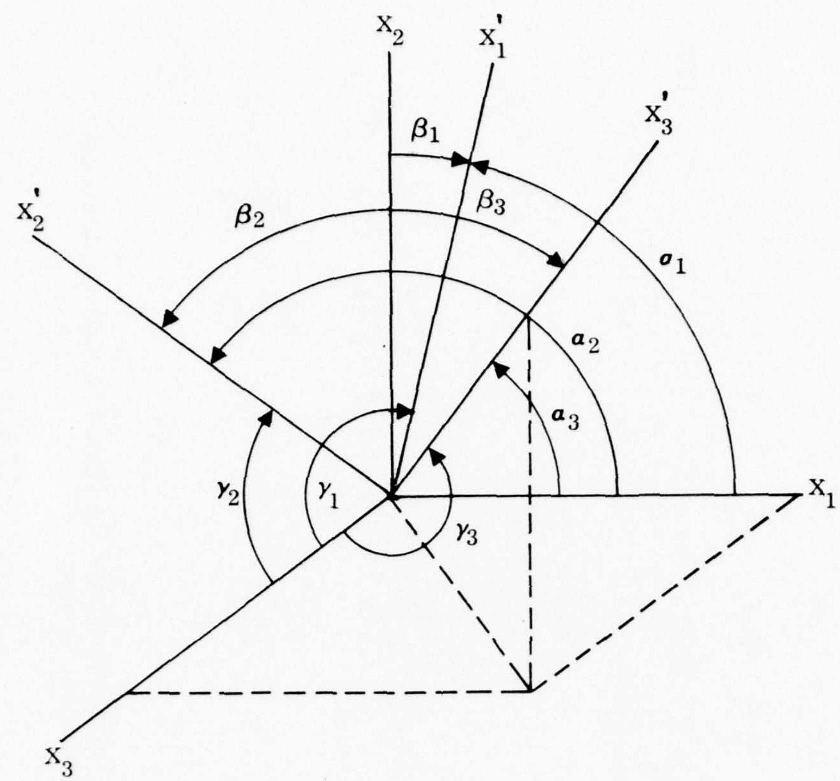

α_1, β_1, γ_1 = ANGLES BETWEEN NEW X_1' AXIS AND OLD X_1, X_2, X_3 AXES RESPECTIVELY

α_2, β_2, γ_2 = ANGLES BETWEEN NEW X_2' AXIS AND OLD X_1, X_2, X_3 AXES RESPECTIVELY

α_3, β_3, γ_3 = ANGLES BETWEEN NEW X_3' AXIS AND OLD X_1, X_2, X_3 AXES RESPECTIVELY

Figure 3-2. Rotation of Rectangular Axes About a Common Origin

Then

$$x'_1 = l_1 x_1 + m_1 x_2 + n_1 x_3$$
$$x'_2 = l_2 x_1 + m_2 x_2 + n_2 x_3$$
$$x'_3 = l_3 x_1 + m_3 x_2 + n_3 x_3 \quad , \tag{29}$$

while the coordinates of the point, P, with respect to the old axes are given in terms of the coordinates of P in the new axes by

$$x_1 = l_1 x'_1 + l_2 x'_2 + l_3 x'_3$$
$$x_2 = m_1 x'_1 + m_2 x'_2 + m_3 x'_3$$
$$x_3 = n_1 x'_1 + n_2 x'_2 + n_3 x'_3 \quad . \tag{30}$$

From these equations we obtain:

$$\frac{\partial x'_1}{\partial x_1} = \frac{\partial x_1}{\partial x'_1} = l_1 \qquad \frac{\partial x'_2}{\partial x_1} = \frac{\partial x_1}{\partial x'_2} = l_2 \qquad \frac{\partial x'_3}{\partial x_1} = \frac{\partial x_1}{\partial x'_3} = l_3$$

$$\frac{\partial x'_1}{\partial x_2} = \frac{\partial x_2}{\partial x'_1} = m_1 \qquad \frac{\partial x'_2}{\partial x_2} = \frac{\partial x_2}{\partial x'_2} = m_2 \qquad \frac{\partial x'_3}{\partial x_2} = \frac{\partial x_2}{\partial x'_3} = m_3$$

$$\frac{\partial x'_1}{\partial x_3} = \frac{\partial x_3}{\partial x'_1} = n_1 \qquad \frac{\partial x'_2}{\partial x_3} = \frac{\partial x_3}{\partial x'_2} = n_2 \qquad \frac{\partial x_3}{\partial x_3} = \frac{\partial x_3}{\partial x'_3} = n_3 \tag{31}$$

The general tensor transformation for a tensor of rank, n, from the x coordinates to the x' coordinates, is given by Mason [6] , as,

$$x'_{k1 \cdots kn} = \frac{\partial x'_{k1}}{\partial x_{j1}} \frac{\partial x'_{k2}}{\partial x_{j2}} \cdots \frac{\partial x'_{kn}}{\partial x_{jn}} x_{j1 \cdots jn} \tag{32}$$

In order to determine the material coefficients of concern in this program it is only necessary to deal with coefficients of the fourth rank and below.

If c'_{ijkl}, e'_{ijk} and ϵ'_{ij} represent the desired coefficients in the new reference frame (x'_1, x'_2, x'_3), and c_{mnop}, e_{lmn}, ϵ_{kl} represent the known coefficients in the old reference frame (x_1, x_2, x_3), Eq. (32) takes the form shown for each of the coefficients:

$$c'_{ijkl} = \frac{\partial x'_i}{\partial x_m} \frac{\partial x'_j}{\partial x_n} \frac{\partial x'_k}{\partial x_o} \frac{\partial x'_l}{\partial x_p} c_{mnop} \tag{33}$$

$$e'_{ijk} = \frac{\partial x'_i}{\partial x_l} \frac{\partial x'_j}{\partial x_m} \frac{\partial x'_k}{\partial x_n} e_{lmn}$$

$$\epsilon'_{ij} = \frac{\partial x'_i}{\partial x_k} \frac{\partial x'_j}{\partial x_l} \epsilon_{kl} \; .$$

It is more convenient to use the equivalent expression shown in Eq. (31) and to place these direction cosines in a matrix array A,

$$[a] = \begin{bmatrix} a_{11} & a_{12} & a_{13} \\ a_{21} & a_{22} & a_{23} \\ a_{31} & a_{32} & a_{33} \end{bmatrix} = \begin{bmatrix} l_1 & m_1 & n_1 \\ l_2 & m_2 & n_2 \\ l_3 & m_3 & n_3 \end{bmatrix} . \tag{34}$$

In this terminology Eqs. (29), (30), and (33) become, in tensor notation,

$$\begin{aligned} x'_i &= a_{ij}\, x_j \\ x_i &= a_{ji}\, x'_j \\ c'_{ijkl} &= a_{im} a_{jn} a_{ko} a_{lp} c_{mnop} \\ e'_{ijk} &= a_{il} a_{jm} a_{kn} e_{lmn} \\ \epsilon'_{ij} &= a_{ik} a_{jl} \epsilon_{kl} \; . \end{aligned} \tag{35}$$

The program for carrying out this transformation of the material coefficients, and for determining the piezoelectrically stiffened coefficients, $\bar{c}^E_{ijki}$, in the secular equation (Eq. 24) is listed in Table 3-4. This program was written for operation on the Honeywell Information Systems series 6000/600 computer, as installed at the General Electric ESD facility in Syracuse, in the Y FOR mode of time-sharing operation. However, most of the statements are standard Fortran IV and, hence, should be adaptable to any similar computing system.

An attempt was made to make the program self-explanatory but the following observations will help.

Line 10 is a first line run command and is not required. Lines 150 through 262 are the elastic stiffness constants, piezoelectric stress constants, and dielectric permittivities in the primary (unrotated or XYZ) reference frame. For the program illustrated they are Bechmann's [7] values for left-hand quartz. The order of input is that for the triclinic crystal shown in Figure 3-1. The

TABLE 3-4. LISTING OF PROGRAM CRØT FOR THE TRANSFORMATION OF PIEZOELECTRIC COEFFICIENTS AND GENERATION OF THE ELEMENTS IN THE SECULAR EQUATION

```
10*# RUNH-04=(CØRE=22)
100C PRØGRAM TØ TRANSFØRM THE CØEFFICIENTS ØF THE PIEZØELECTRIC
101C CØNSTITUTIVE EQUATIØNS FRØM ØNE SET ØF CØØRDINATES
102C TØ A RØTATED SET ØF CØØRDINATES
110 INTEGER Ø,P
120 DIMENSIØN G(21),GG(6,6),GGGG(3,3,3,3),IA(3,3)
130 DIMENSIØN C(21),CC(6,6),CCCC(3,3,3,3),A(3,3)
132 DIMENSIØN PS(18),PSI(3,3,3)
134 DIMENSIØN E(18),EEE(3,3,3)
136 DIMENSIØN DP(6),DPI(3,3)
138 DIMENSIØN EPS(6),EPSI(3,3)
139 DIMENSIØN CB(3,3)
140 DATA IA/1,6,5,6,2,4,5,4,3/
150C BECHMANN'S VALUES FØR LEFT HAND QUARTZ
159C THE ELASTIC STIFFNESS CØNSTANTS
160 G(1)=86.74E9
162 G(2)=6.99E9
164 G(3)=11.91E9
166 G(4)=-17.91E9
168 G(5)=0.
170 G(6)=0.
172 G(7)=86.74E9
174 G(8)=11.91E9
176 G(9)=17.91E9
178 G(10)=0.
180 G(11)=0.
182 G(12)=107.2E9
184 G(13)=0.
186 G(14)=0.
188 G(15)=0.
190 G(16)=57.94E9
192 G(17)=0.
194 G(18)=0.
196 G(19)=57.94E9
198 G(20)=-17.91E9
200 G(21)=39.88E9
210C THE PIEZØELECTRIC STRESS CØNSTANTS
212 PS(1)=0.171
214 PS(2)=-0.171
216 PS(3)=0.
218 PS(4)=-0.0406
220 PS(5)=0.
222 PS(6)=0.
224 PS(7)=0.
226 PS(8)=0.
228 PS(9)=0.
230 PS(10)=0.
232 PS(11)=0.0406
234 PS(12)=-0.171
236 PS(13)=0.
238 PS(14)=0.
240 PS(15)=0.
242 PS(16)=0.
244 PS(17)=0.
246 PS(18)=0.
```

TABLE 3-4 (Cont'd)

```
250C THE DIELECTRIC PERMITTIVITES
252 DP(1)=39.21E-12
254 DP(2)=0.
256 DP(3)=0.
258 DP(4)=39.21E-12
260 DP(5)=0.
262 DP(6)=41.03E-12
300C X3 IS IN THE THICKNESS DIRECTIØN
310C THIS IS AT CUT QUARTZ  (YXL)THETA
320 THETA=35.25
360 PI=3.1415926
369C THESE ARE DIRECTIØN CØSINES BETWEEN NEW AND ØLD AXES
370 RL1=1.
380 RM1=0.
390 RN1=0.
400 RL2=0.
410 RM2=SIN(THETA*PI/180.)
420 RN2=-CØS(THETA*PI/180.)
430 RL3=0.
440 RM3=-RN2
450 RN3=RM2
460 A(1,1)=RL1
470 A(1,2)=RM1
480 A(1,3)=RN1
490 A(2,1)=RL2
500 A(2,2)=RM2
510 A(2,3)=RN2
520 A(3,1)=RL3
530 A(3,2)=RM3
540 A(3,3)=RN3
600C CØNVERT THE 21 ELASTIC CØNSTANTS G(I) INTØ ENGINEERING
601C NØTATIØN GG(M,N)
610 N=0
620 DØ 10 I=1,6
630 DØ 10 J=I,6
640 N=N+1
650 GG(I,J)=G(N)
660 GG(J,I)=GG(I,J)
670 10 CØNTINUE
680C CØNVERT FRØM ENGINEERING NØTATIØN GG(M,N) INTØ
681C TENSØR NØTATIØN GGGG(I,J,K,L)
690 DØ 20 I=1,3
700 DØ 20 J=1,3
710 DØ 20 K=1,3
720 DØ 20 L=1,3
730 M=IA(I,J)
740 N=IA(K,L)
750 GGGG(I,J,K,L)=GG(M,N)
760 20 CØNTINUE
770C CØMPUTE THE CØMPØNENTS ØF THE RØTATED MATRIX
780 DØ 40 I=1,3
790 DØ 40 J=1,3
800 DØ 40 K=1,3
810 DØ 40 L=1,3
820 CCCC(I,J,K,L)=0.
830 DØ 30 M=1,3
840 DØ 30 N=1,3
850 DØ 30 Ø=1,3
```

TABLE 3-4 (Cont'd)

```
860 DØ 30 P=1,3
870 CCCC(I,J,K,L)=A(I,M)*A(J,N)*A(K,Ø)*A(L,P)*GGGG(M,N,Ø,P)
871& +CCCC(I,J,K,L)
880 30 CØNTINUE
890 M=IA(I,J)
900 N=IA(K,L)
910 CC(M,N)=CCCC(I,J,K,L)
920 40 CØNTINUE
970 PRINT 900
980 PRINT 910
990C CØNVERT BACK TØ ØBTAIN THE 21 RØTATED ELASTIC CØNSTANTS C(I)
1000 N=0
1010 DØ 50 I=1,6
1020 DØ 50 J=1,6
1030 N=N+1
1040 C(N)=CC(I,J)
1050 PRINT 920,N,G(N),C(N)
1060 50 CØNTINUE
1100C CØNVERT THE 18 PIEZØELECTRIC STRESS CØNSTANTS PS(M)
1101C INTØ TENSØR NØTATIØN PST(I,J,K)
1110 DØ 60 I=1,3
1120 DØ 60 J=1,3
1130 DØ 60 K=1,3
1140 M=IA(J,K)+(I-1)*6
1150 PST(I,J,K)=PS(M)
1160 60 CØNTINUE
1170C CØMPUTE THE CØMPØNENTS ØF THE RØTATED MATRIX
1180 DØ 80 I=1,3
1190 DØ 80 J=1,3
1200 DØ 80 K=1,3
1210 EEE(I,J,K)=0.
1220 DØ 70 L=1,3
1230 DØ 70 M=1,3
1240 DØ 70 N=1,3
1250 EEE(I,J,K)=A(I,L)*A(J,M)*A(K,N)*PST(L,M,N)+EEE(I,J,K)
1260 70 CØNTINUE
1270C CØNVERT BACK TØ ØBTAIN THE 18 RØTATED
1271C PIEZØELECTRIC STRESS CØNSTANTS E(I)
1280 M=IA(J,K)+(I-1)*6
1290 E(M)=EEE(I,J,K)
1300 80 CØNTINUE
1310 PRINT 930
1320 PRINT 910
1330 DØ 90 N=1,18
1340 PRINT 920, N, PS(N), E(N)
1350 90 CØNTINUE
1400C CØNVERT THE 6 DIELECTRIC PERMITTIVITIES DP(N)
1401C INTØ TENSØR NØTATIØN DPT(I,J)
1410 N=0
1420 DØ 100 I=1,3
1430 DØ 100 J=1,3
1440 N=N+1
1450 DPT(I,J)=DP(N)
1460 DPT(J,I)=DPT(I,J)
1470 100 CØNTINUE
1480C CØMPUTE THE CØMPØNENTS ØF THE RØTATED MATRIX
1490 DØ 120 I=1,3
1500 DØ 120 J=1,3
1510 EPST(I,J)=0.
```

TABLE 3-4 (Cont'd)

```
1520 DØ 110 K=1,3
1530 DØ 110 L=1,3
1540 EPST(I,J)=A(I,K)*A(J,L)*DPT(K,L)+EPST(I,J)
1550 110 CØNTINUE
1560 120 CØNTINUE
1570 PRINT 940
1580 PRINT 910
1590C CØNVERT BACK TØ ØBTAIN THE 6 RØTATED DIELECTRIC
1591C PERMITTIVITIES
1600 N=0
1610 DØ 130 I=1,3
1620 DØ 130 J=1,3
1630 N=N+1
1640 EPS(N)=EPST(I,J)
1650 PRINT 920, N, DP(N), EPS(N)
1660 130 CØNTINUE
1700 900 FØRMAT(14X,'THE ELASTIC STIFFNESS CØNSTANTS ARE',//)
1710 910 FØRMAT(11X,'N',4X,'BEFØRE RØTATIØN',7X,'AFTER RØTAIØN')
1720 920 FØRMAT(11X,I2,3X,E15.8,6X,E15.8)
1730 930 FØRMAT(/,12X,'THE PIEZØELECTRIC STRESS CØNSTANTS ARE',//)
1740 940 FØRMAT(/,15X,'THE DIELECTRIC PERMITTIVITIES ARE',//)
1810C THIS PART USES THE RØTATED VALUES TØ CALCULATE THE
1811C STIFFENED MATRIX ELEMENTS IN THE SECULAR EQUATIØN
1812C ØF THE FØRM CB(J,K)-DELTA(J,K)*C=0
1815C IN THE FØLLØWING I REPRESENTS THE CØØRDINATE IN
1816C THE THICKNESS DIRECTIØN. I.E. FØR X3 I=3
1820 I=3
1830 DØ 140 J=1,3
1840 DØ 140 K=1,3
1850 CB(J,K)=0.
1860 CB(J,K)=CCCC(I,J,K,I)+EEE(I,I,J)*EEE(I,I,K)/EPST(I,I)
1870 140 CØNTINUE
1880 PRINT 950,I
1890 PRINT 960
1900 PRINT 970,((CB(K,J),J=1,3),K=1,3)
1910 950 FØRMAT(/,'FØR X',I1,' IN THE THICKNESS DIRECTIØN')
1920 960 FØRMAT(/,10X,'THE ELEMENTS IN THE SECULAR EQUATIØN ARE')
1930 970 FØRMAT(/,3X,E15.8,6X,E15.8,6X,E15.8)
1950C THESE CB(I,J) VALUES IN TURN CAN BE USED TØ CALCULATE
1951CTHE CØEFFICIENTS ØF THE CUBIC EQUATIØN IN C
1955C IF C**3+Q*C**2+R*C+S=0 THEN IN TERMS ØF CB(I,J)
1960 Q=-(CB(1,1)+CB(2,2)+CB(3,3))
1970 R=CB(2,2)*(CB(3,3)+CB(1,1))+CB(1,1)*CB(3,3)
1980& -(CB(2,3)*CB(3,2)+CB(1,2)*CB(2,1)+CB(3,1)*CB(1,3))
1990 S=CB(2,1)*(CB(1,2)*CB(3,3)-CB(1,3)*CB(3,2))
2000& +CB(2,2)*(CB(1,3)*CB(3,1)-CB(1,1)*CB(3,3))
2010& +CB(2,3)*(CB(3,2)*CB(1,1)-CB(1,2)*CB(3,1))
2020 PRINT 980
2030 PRINT 990,Q
2040 PRINT 991,R
2050 PRINT 992,S
2060 980 FØRMAT(5X,'IN C**3 +Q*C**2 + R*C + S =0')
2070 990 FØRMAT(8X,'Q=',E15.8)
2080 991 FØRMAT(8X,'R=',E15.8)
2090 992 FØRMAT(8X,'S=',E15.8)
3000C FØR USE IN CALCULATING THE CØUPLING
3001C CØEFFICIENTS AND CAPACITANCE WE NEED
3002C THE FØLLØWING VALUES
```

TABLE 3-4 (Cont'd)

```
3010 PRINT 995
3020 PRINT 996, (EEE(1,I,J),J=1,3)
3030 PRINT 997
3040 PRINT 998,EPST(I,I)
3050 995 FØRMAT(/,2X,'THE APPRØPRIATE PIEZØELECTRIC ',
3051& 'STRESS CØNSTANTS ARE')
3060 996 FØRMAT(/,10X,'E(1) = ',E15.8,/,10X,
3061&    'E(2) = ',E15.8,/10X,'E(3) = ',E15.8,/)
3070 997 FØRMAT(/,2X,'THE APPRØPRIATE DIELECTRIC ',
3071&    'PERMITTIVITY IS')
3080 998 FØRMAT(/,10X,'EP = ',E15.8)
3090 STØP
4000 END
```

matrices are inputted by rows, and only elements that have not been previously defined are entered. This input data arrangement is shown in Table 3-5. Lines 300 through 430 specify the plate orientation in terms of the direction cosines in Eqs. (28), (29), and (34).

The transformation matrix,[8] lines 730 and 740, loaded as shown in line 140, follows Table 3-2. The input at line 1820 designates the coordinate that lies in the plate thickness direction; the appropriate coefficients in the secular equation are calculated as well as the appropriate piezoelectric stress constants and dielectric permittivity for this orientation of the plate.

A printout of the results of this program, using AT-cut quartz as the plate material with x_3 in the thickness direction, is shown in Table 3-6.

To switch material it is necessary to change statements 150 to 262. To change orientations it is necessary to change line 300 to 450, and line 1820. Table 3-7 shows these changes and a printout for AT-cut quartz with x_2 in the thickness direction. These particular values check with those given by Tiersten[3].

B. SOLUTION OF THE SECULAR EQUATION AND PROGRAM SYMEIG

As a result of the output of the CROT program we have numerical values for the $\bar{c}^E_{ijki}$ coefficients in Eqs. (23) and (24), in general, or in Eq. (25) for the plate thickness direction, restricted to lie in the x_3 direction. We also know the values of the coefficients of c in Eq. (26). Since the array of $\bar{c}^E_{ijki}$ coefficients is a symmetrical matrix array with real coefficients, the characteristic numbers or eigenvalues of the secular equation will be real. It also turns out that they will be positive since this is a positive definite matrix.

Thus, the solution of Eqs. (24) or (26) will yield three real, positive roots, $c^{(i)}$, from which three real wave numbers, $\eta^{(i)}$, can be obtained from Eq. (20) for a specified value of ω. If these values of $c^{(i)}$ are substituted into Eqs. (23) or (25), a set of ratios among the $u^{(i)}_k$ amplitudes can be determined for each value of $c^{(i)}$. These ratios can then be used to construct a new ref-

TABLE 3-5. INPUT DATA ARRANGEMENT

Elastic Stiffness Coefficients

Input Symbol (N)	Output Symbol (N)	Engineering Equivalents	Tensor Equivalents
G(1)	C(1)	C_{11}	C_{1111}
G(2)	C(2)	$C_{12} = C_{21}$	$C_{1122} = C_{2211}$
G(3)	C(3)	$C_{13} = C_{31}$	$C_{1133} = C_{3311}$
G(4)	C(4)	$C_{14} = C_{41}$	$C_{1123} = C_{1132} = C_{2311} = C_{3211}$
G(5)	C(5)	$C_{15} = C_{51}$	$C_{1113} = C_{1131} = C_{1311} = C_{3111}$
G(6)	C(6)	$C_{16} = C_{61}$	$C_{1112} = C_{1121} = C_{1211} = C_{2111}$
G(7)	C(7)	C_{22}	C_{2222}
G(8)	C(8)	$C_{23} = C_{32}$	$C_{2233} = C_{3322}$
G(9)	C(9)	$C_{24} = C_{42}$	$C_{2223} = C_{2232} = C_{2322} = C_{3222}$
G(10)	C(10)	$C_{25} = C_{52}$	$C_{2213} = C_{2231} = C_{1322} = C_{3122}$
G(11)	C(11)	$C_{26} = C_{62}$	$C_{2212} = C_{2221} = C_{1222} = C_{2122}$
G(12)	C(12)	C_{33}	C_{3333}
G(13)	C(13)	$C_{34} = C_{43}$	$C_{3323} = C_{3332} = C_{2333} = C_{3233}$
G(14)	C(14)	$C_{35} = C_{53}$	$C_{3313} = C_{3331} = C_{1333} = C_{3133}$
G(15)	C(15)	$C_{36} = C_{63}$	$C_{3312} = C_{3321} = C_{1233} = C_{2133}$
G(16)	C(16)	C_{44}	$C_{2323} = C_{2332} = C_{3223} = C_{3232}$
G(17)	C(17)	$C_{45} = C_{54}$	$C_{2313} = C_{2331} = C_{1323} = C_{3123}$
			$= C_{3213} = C_{3231} = C_{1332} = C_{3132}$
G(18)	C(18)	$C_{46} = C_{64}$	$C_{2312} = C_{2321} = C_{1223} = C_{1232}$
			$= C_{2123} = C_{2132} = C_{3212} = C_{3221}$
G(19)	C(19)	C_{55}	$C_{1331} = C_{1313} = C_{3113} = C_{3131}$
G(20)	C(20)	$C_{56} = C_{65}$	$C_{1312} = C_{1321} = C_{1213} = C_{1231}$
			$= C_{2113} = C_{2131} = C_{3112} = C_{3121}$
G(21)	C(21)	C_{66}	$C_{1212} = C_{1221} = C_{2112} = C_{2121}$

TABLE 3-5 (Cont'd)

Piezoelectric Stress Constants

Input Symbol (N)	Output Symbol (N)	Engineering Equivalents	Tensor Equivalents
PS(1)	E(1)	e_{11}	e_{111}
PS(2)	E(2)	e_{12}	e_{122}
PS(3)	E(3)	e_{13}	e_{133}
PS(4)	E(4)	e_{14}	$e_{123} = e_{132}$
PS(5)	E(5)	e_{15}	$e_{113} = e_{131}$
PS(6)	E(6)	e_{16}	$e_{112} = e_{121}$
PS(7)	E(7)	e_{21}	e_{211}
PS(8)	E(8)	e_{22}	e_{222}
PS(9)	E(9)	e_{23}	e_{233}
PS(10)	E(10)	e_{24}	$e_{223} = e_{232}$
PS(11)	E(11)	e_{25}	$e_{213} = e_{231}$
PS(12)	E(12)	e_{26}	$e_{212} = e_{221}$
PS(13)	E(13)	e_{31}	e_{311}
PS(14)	E(14)	e_{32}	e_{322}
PS(15)	E(15)	e_{33}	e_{333}
PS(16)	E(16)	e_{34}	$e_{323} = e_{332}$
PS(17)	E(17)	e_{35}	$e_{313} = e_{331}$
PS(18)	E(18)	e_{36}	$e_{312} = e_{321}$

TABLE 3-5 (Cont'd)

Dielectric Permittivities at Constant Strain

Input Symbol (N)	Output Symbol (N)	Engineering Equivalents	Tensor Equivalents
DP(1)	EPS(1)	ϵ^S_{11}	ϵ^S_{11}
DP(2)	EPS(2)	$\epsilon^S_{12} = \epsilon^S_{21}$	$\epsilon^S_{12} = \epsilon^S_{21}$
DP(3)	EPS(3)	$\epsilon^S_{13} = \epsilon^S_{31}$	$\epsilon^S_{13} = \epsilon^S_{31}$
DP(4)	EPS(4)	ϵ^S_{22}	ϵ^S_{22}
DP(5)	EPS(5)	$\epsilon^S_{23} = \epsilon^S_{32}$	$\epsilon^S_{23} = \epsilon^S_{32}$
DP(6)	EPS(6)	ϵ^S_{33}	ϵ^S_{33}

TABLE 3-6. RESULTS OF CRØT FOR AT CUT QUARTZ WITH X_3 IN THE THICKNESS DIRECTION

23511 02/23/77 12.359

THE ELASTIC STIFFNESS CONSTANTS ARE

N	BEFORE ROTATION	AFTER ROTATION
1	0.86740000E 11	0.86740000E 11
2	0.69900000E 10	0.27153374E 11
3	0.11910000E 11	-0.82534741E 10
4	-0.17910000E 11	0.36595334E 10
5	0.	0.
6	0.	0.
7	0.86740000E 11	0.19213551E 12
8	0.11910000E 11	-0.73134733E 10
9	0.17910000E 11	-0.99212797E 10
10	0.	0.
11	0.	0.
12	0.10720000E 12	0.12276634E 12
13	0.	-0.57084231E 10
14	0.	0.
15	0.	0.
16	0.57940000E 11	0.38511527E 11
17	0.	0.
18	0.	0.
19	0.57940000E 11	0.22012015E 11
20	-0.17910000E 11	-0.25335713E 10
21	0.39880000E 11	0.68306936E 11

THE PIEZOELECTRIC STRESS CONSTANTS ARE

N	BEFORE ROTATION	AFTER ROTATION
1	0.17100000E 00	0.17100000E 00
2	-0.17100000E 00	-0.13592357E-01
3	0.	-0.15231173E 00
4	-0.40600000E-01	-0.57043247E-01
5	0.	0.
6	0.	0.
7	0.	0.
8	0.	0.
9	0.	0.
10	0.	0.
11	0.40600000E-01	-0.57072126E-01
12	-0.17100000E 00	-0.75023134E-01
13	0.	0.
14	0.	0.
15	0.	0.
16	0.	0.
17	0.	-0.94938857E-01
18	0.	-0.10757213E 00

TABLE 3-6 (Cont'd)

```
          THE DIELECTRIC PERMITTIVITIES ARE

      N      BEFORE ROTATION          AFTER ROTATION
      1      0.39210000E-10           0.39210000E-10
      2      0.                       0.
      3      0.                       0.
      4      0.39210000E-10           0.40423765E-10
      5      0.                      -0.85730335E-12
      6      0.41030000E-10           0.39816236E-10

FOR X3 IN THE THICKNESS DIRECTION

        THE ELEMENTS IN THE SECULAR EQUATION ARE

  0.29239228E 11        0.                      0.

  0.                    0.33611527E 11        -0.57004245E 10

  0.                   -0.57004232E 10         0.12976634E 12
   IN C**3 +Q*C**2 + R*C + S =0
      Q=-0.19751709E 12
      R= 0.99012206E 22
      S=-0.14555234E 33

THE APPROPRIATE PIEZOELECTRIC STRESS CONSTANTS ARE

        E(1) = -0.94904867E-01
        E(2) =  0.
        E(3) =  0.

THE APPROPRIATE DIELECTRIC PERMITTIVITY IS

        EP =  0.39816236E-10
```

TABLE 3-7. AT-CUT QUARTZ WITH X_2 IN THE THICKNESS DIRECTION

a) Material Constants

```
150C BECHMANN'S VALUES FØR LEFT HAND QUARTZ
159C THE ELASTIC STIFFNESS CØNSTANTS
160 G(1)=86.74E9
162 G(2)=6.99E9
164 G(3)=11.91E9
166 G(4)=-17.91E9
168 G(5)=0.
170 G(6)=0.
172 G(7)=86.74E9
174 G(8)=11.91E9
176 G(9)=17.91E9
178 G(10)=0.
180 G(11)=0.
182 G(12)=107.2E9
184 G(13)=0.
186 G(14)=0.
188 G(15)=0.
190 G(16)=57.94E9
192 G(17)=0.
194 G(18)=0.
196 G(19)=57.94E9
198 G(20)=-17.91E9
200 G(21)=39.88E9
210C THE PIEZOELECTRIC STRESS CØNSTANTS
212 PS(1)=0.171
214 PS(2)=-0.171
216 PS(3)=0.
218 PS(4)=-0.0406
220 PS(5)=0.
222 PS(6)=0.
224 PS(7)=0.
226 PS(8)=0.
228 PS(9)=0.
230 PS(10)=0.
232 PS(11)=0.0406
234 PS(12)=-0.171
236 PS(13)=0.
238 PS(14)=0.
240 PS(15)=0.
242 PS(16)=0.
244 PS(17)=0.
246 PS(18)=0.
250C THE DIELECTRIC PERMITTIVITIES
252 DP(1)=39.21E-12
254 DP(2)=0.
256 DP(3)=0.
258 DP(4)=39.21E-12
260 DP(5)=0.
262 DP(6)=41.03E-12
```

TABLE 3-7. (Cont'd)

b) Plate Orientation

```
300C X2 IS IN THE THICKNESS DIRECTION
310C THIS IS AT CUT QUARTZ  (YXL)THETA
320 THETA=35.25
360 PI=3.1415926
369C THESE ARE DIRECTION COSINES BETWEEN NEW AND OLD AXES
370 RL1=1.
380 RM1=0.
390 RN1=0.
400 RL2=0.
410 RM2=COS(THETA*PI/180.)
420 RN2=SIN(THETA*PI/180.)
430 RL3=0.
440 RM3=-RN2
450 RN3=RM2

1810C THIS PART USES THE ROTATED VALUES TO CALCULATE THE
1811C STIFFENED MATRIX ELEMENTS IN THE SECULAR EQUATION
1812C OF THE FORM CB(J,K)-DELTA(J,K)*C=0
1815C IN THE FOLLOWING I REPRESENTS THE COORDINATE IN
1816C THE THICKNESS DIRECTION. I.E. FOR X3 I=3
1820 I=2
```

c) Results

```
25721     03/14/77     13.363

         THE ELASTIC STIFFNESS CONSTANTS ARE

 N     BEFORE ROTATION          AFTER ROTATION
 1      0.86740000E 11          0.86740000E 11
 2      0.69900000E 10         -0.82535741E 10
 3      0.11910000E 11          0.27153574E 11
 4     -0.17910000E 11         -0.36595352E 10
 5      0.                      0.
 6      0.                      0.
 7      0.86740000E 11          0.12976534E 12
 8      0.11910000E 11         -0.74164757E 10
 9      0.17910000E 11          0.57004240E 10
10      0.                      0.
11      0.                      0.
12      0.10720000E 12          0.10263051E 12
13      0.                      0.99212510E 10
14      0.                      0.
15      0.                      0.
16      0.57940000E 11          0.38011927E 11
17      0.                      0.
18      0.                      0.
19      0.57940000E 11          0.63606906E 11
20     -0.17910000E 11          0.25335716E 10
21      0.39850000E 11          0.29013015E 11
```

TABLE 3-7. (Cont'd)

THE PIEZOELECTRIC STRESS CONSTANTS ARE

N	BEFORE ROTATION	AFTER ROTATION
1	0.17100000E 00	0.17100000E 00
2	-0.17100000E 00	-0.15231173E 00
3	0.	-0.13688267E-01
4	-0.40600000E-01	0.67043287E-01
5	0.	0.
6	0.	0.
7	0.	0.
8	0.	0.
9	0.	0.
10	0.	0.
11	0.40600000E-01	0.10767213E 00
12	-0.17100000E 00	-0.94904867E-01
13	0.	0.
14	0.	0.
15	0.	0.
16	0.	0.
17	0.	-0.76095134E-01
18	0.	0.67072126E-01

THE DIELECTRIC PERMITTIVITIES ARE

N	BEFORE ROTATION	AFTER ROTATION
1	0.39210000E-10	0.39210000E-10
2	0.	0.
3	0.	0.
4	0.39210000E-10	0.39816236E-10
5	0.	0.85780385E-12
6	0.41030000E-10	0.40423765E-10

FOR X2 IN THE THICKNESS DIRECTION

THE ELEMENTS IN THE SECULAR EQUATION ARE

0.29239228E 11	0.	0.
0.	0.12976634E 12	0.57004240E 10
0.	0.57004246E 10	0.38611527E 11

IN C**3 +Q*C**2 + R*C + S =0
Q=-0.19761709E 12
R= 0.99012206E 22
S=-0.14555234E 33

THE APPROPRIATE PIEZOELECTRIC STRESS CONSTANTS ARE

E(1) = -0.94904867E-01
E(2) = 0.
E(3) = 0.

THE APPROPRIATE DIELECTRIC PERMITTIVITY IS

EP = 0.39816236E-10

erence system in which the modes of vibration are displayed mutually independent of each other*. This is the so-called normal coordinate reference system in which the allowed modes of operation are termed the normal modes. The directions of these normal coordinates are given by the characteristic vendors or eigenvectors associated with each $c^{(i)}$. This set of ratios among the $u_k^{(i)}$ amplitudes will be designated as the $\beta_k^{(i)}$ components of the i^{th} eigenvector associated with each $c^{(i)}$. For example $c^{(1)}$ is associated with the values $\beta_1^{(1)}$, $\beta_2^{(1)}$, $\beta_3^{(1)}$, which each $c^{(2)}$ is associated with the values $\beta_1^{(2)}$, $\beta_2^{(2)}$, $\beta_3^{(2)}$.

Furthermore, if the components for each (i) are normalized so that

$$\beta_k \beta_k = 1 \text{ or } \beta_1^{(i)} \beta_1^{(i)} + \beta_2^{(i)} \beta_2^{(i)} + \beta_3^{(i)} \beta_3^{(i)} = 1 , \tag{36}$$

then these $\beta_k^{(i)}$ are the direction cosines of the particle displacement for each of the three modes, (i), in relation to the plate coordinates. The vector set formed in this fashion is also orthonormal and has the properties,

$$\beta_j^{(i)} \beta_k^{(i)} = \beta_m^{(j)} \beta_m^{(k)} = \delta_{jk} \quad . \tag{37}$$

The general procedure, therefore, is to solve Eq. (26) for its roots or determine them from Eq. (24) and substitute into Eq. (23) for each root, to determine the u_k values appropriate to this root. Then normalize these to unity and construct the eigenvector for this root; then repeat the procedure for the next root, etc. If, working with Eq. (26), this cubic equation can be reduced to the form

$$d^3 + a d + b = 0 ,$$

where

$$c = d - (q/3) \tag{38}$$

$$a = \frac{1}{3} (3r - q^2)$$

$$b = \frac{1}{27} (2q^3 - 9qr + 27s) ,$$

then, letting $d = m \cos \Theta$, where $m = 2\sqrt{\frac{-a}{3}}$, $\cos 3\Theta = \frac{-4b}{m^3}$,

gives the roots [14] (39)

$$d_1 = m \cos \Theta_1 ,\ d_2 = m \cos (\Theta_1 + \frac{2\pi}{3}) ,\ d_3 = m \cos (\Theta_1 + \frac{4\pi}{3}) .$$

Here Θ_1 is the smallest value that satisfies $\cos 3\Theta = -\frac{4b}{m^3}$.

---

* In the general case the number of roots of c is $c^{(k)}$ and the normal coordinate reference system has k dimensions instead of three, as in our special case.

Instead of following this procedure and writing a program for it, the Honeywell Information Series 600/6000 Time-Sharing Systems has a program available that is in the ESD computers time-sharing library. This program solves the equation and computes the eigenvectors as well as giving the eigenvalues. This "canned" routine was used to solve Eq. (25) and to obtain the eigenvectors satisfying Eq. (40).

$$(\bar{c}^{E}_{3jk3} - c^{(i)}\delta_{jk})\,\beta^{(i)}_{k} = 0 \qquad \text{(no sum over } i \text{ is taken here)} \tag{40}$$

The instructions for this "canned program" called SYMEIG, together with a listing of it, are shown in Table 3-8. This program is written in Time-Sharing FORTRAN, but the conversion to a more conventional form is relatively obvious.

The output of this program is shown in Table 3-9 when the required results from CRØT in Table 3-6 were supplied. Both the Yes and No responses to the instruction question are shown.

Figure 3-3 uses these results for AT-cut quartz, with x_3 in the thickness direction, to clarify the previous discussion. It shows the construction of the eigenvectors for this simple 3-mode case, and the relationship of the 3-dimensional normal mode axes to the plate axes. For waves propagating along the x_3 plate axis we have one pure shear mode (particle displacement at right angles to the propagation direction), $\beta^{(1)}$, one *quasi-shear mode*, $\beta^{(2)}$, and one quasi-longitudinal mode, $\beta^{(3)}$. For waves propagating along the normal mode axis, 3, we have two pure shear modes, $\beta^{(1)}$ and $\beta^{(2)}$, and one pure longitudinal mode (particle displacement in the direction of propagation direction), $\beta^{(3)}$.

Another program for the purpose of debugging, was written at this time. Its purpose was an essential test of the results obtained up to this point.

The nine separate equations in Eq. (40) (three for each value of $c^{(i)}$ can be written as follows (where $CB_{jk} = \bar{c}^{E}_{3jk3}$ in matrix form):

$$\begin{bmatrix} CB_{11} & CB_{12} & CB_{13} \\ CB_{21} & CB_{22} & CB_{23} \\ CB_{31} & CB_{32} & CB_{33} \end{bmatrix} \begin{bmatrix} \beta_1^{(1)} & \beta_1^{(1)} & \beta_1^{(3)} \\ \beta_2^{(1)} & \beta_2^{(2)} & \beta_2^{(3)} \\ \beta_3^{(1)} & \beta_3^{(2)} & \beta_3^{(3)} \end{bmatrix} = \begin{bmatrix} \beta_1^{(1)} & \beta_1^{(2)} & \beta_1^{(3)} \\ \beta_2^{(1)} & \beta_2^{(2)} & \beta_2^{(3)} \\ \beta_3^{(1)} & \beta_3^{(2)} & \beta_3^{(3)} \end{bmatrix} \begin{bmatrix} c^{(1)} & 0 & 0 \\ 0 & c^{(2)} & 0 \\ 0 & 0 & c^{(3)} \end{bmatrix} \tag{41}$$

This matrix can be pre-multiplied on each side by β inverse $= [\beta]^{-1}$ to yield

$$[\beta]^{-1} \begin{bmatrix} CB_{11} & CB_{12} & CB_{13} \\ CB_{21} & CB_{22} & CB_{23} \\ CB_{31} & CB_{32} & CB_{33} \end{bmatrix} \begin{bmatrix} \beta_1^{(1)} & \beta_1^{(2)} & \beta_1^{(3)} \\ \beta_2^{(1)} & \beta_2^{(2)} & \beta_2^{(3)} \\ \beta_3^{(1)} & \beta_3^{(3)} & \beta_3^{(3)} \end{bmatrix} = \begin{bmatrix} c^{(1)} & 0 & 0 \\ 0 & c^{(2)} & 0 \\ 0 & 0 & c^{(3)} \end{bmatrix}, \tag{42}$$

TABLE 3-8. INSTRUCTIONS FOR SYMEIG AND THE PROGRAM LISTING OF SYMEIG FOR CALCULATING THE EIGENVALUES AND EIGENVECTORS

a) Instructions

This FORTRAN program calculates the eigenvectors and eigenvalues of a real, symmetrical matrix.

METHOD

The method used is Jacobi's method, which was adapted for computer use by von Neumann. The method consists of applying to the matrix a system of plane rotations given by orthogonal matrices designed to reduce the off-diagonal elements to zero. The eigenvalues are then the diagonal elements of the original matrix and, if the eigenvectors were desired, they are developed as the columns of the product of the orthogonal matrices.

INSTRUCTIONS

Enter data as requested. For further instructions run the program.

SAMPLE SOLUTION

```
SYMEIG


*RUN

DØ YØU WANT INSTRUCTIØNS?
= YES
INSTRUCTIØNS FØR SYMEIG
THIS PRØGRAM CALCULATES THE EIGENVECTØRS AND EIGENVALUES ØF A
REAL,SYMMETRICAL MATRIX.  THE METHØD USED IS JACØBI'S LITERATIØN
METHØD. THE METHØD CØNSISTS ØF APPPLYING TØ THE MATRIX A SYSTEM
ØF PLANE RØTATIØNS GIVEN BY ØRTHØGØNAL MATRICES MADE TØ REDUCE
THE ØFF-DIAGØNAL ELEMENTS TØ ZERØ.  THIS PRØGRAM USES FØUR
ARGUMENTS.  A IS THE NAME ØF A TWØ-DIMENSIØNAL ARRAY CØNTAINING
THE REAL,SYMMETRIC MATRIC IN ITS FIRST N RØWS AND CØLUMNS
R IS THE NAME ØF THE TWØ-DIMENSIØNAL ARRAY WHICH WILL CØNTAIN
THE EIGENVECTØRS IN ITS FIRST N CØLUMNS.
N IS AN INTEGER VARIABLE ØR CØNSTANT GIVING THE ØRDER
ØF THE MATRIX.
MV IS AN INTEGER VARIABLE ØR CØNSTANT WHICH MUST BE 0 ØR 1.
IF IT IS 0 BØTH EIGENVECTØRS AND EIGENVALUES ARE FØRMED.
IF IT IS ØNE ØNLY THE EIGENVALUES ARE FØUND.
ENTER THE ØRDER ØF MATRIX AND THE MATRIX SEPARATED BY CØMMAS.
= 3
= 1,1,.5
= 1,1,.25
= .5,.25,2
THE MATRIX IS
    1.0000000E+00    1.0000000E+00    5.0000000E-01
    1.0000000E+00    1.0000000E+00    2.5000000E-01
    5.0000000E-01    2.5000000E-01    2.0000000E+00
EACH EIGENVALUE FØLLØWED BY CØRRESPØNDING EIGENVECTØR
  -1.6647290E-02
  -7.2120713E-01    6.8634924E-01    9.3727956E-02
   1.4801212E+00
   4.4428103E-01    5.6210938E-01   -6.9760113E-01
   2.5365255E+00
   5.3148334E-01    4.6147330E-01    7.1032929E-01
```

TABLE 3-8. (Cont'd)

b) Program Listing

```
1* GE-600 LINE TIME SHARING LIBRARY PROGRAMS
2* SEE CPB-1694 FOR EXTERNAL DOCUMENTATION
4*
5*  REVISED NOVEMBER 12,1969
6*
7*  SYMEIG
8*
9      DIMENSION A(30,30),R(30,30)
10     ASCII YES,NO,ANS:YES="YES";NO="NO"
11     PRINT 99;PRINT:"SYMEIG";PRINT 99:99 FORMAT(/////)
14     PRINT:"DO YOU WANT INSTRUCTIONS?"
15   1 READ:ANS
16     IF(ANS.EQ.YES)GO TO 11
17     IF(ANS.EQ.NO)GO TO 3
18     PRINT:"ANSWER ONLY WITH YES OR NO."
19     GO TO 1
20  11 PRINT:"INSTRUCTIONS FOR SYMEIG"
21     PRINT:"THIS PROGRAM CALCULATES THE EIGENVECTORS AND EIGENVALUES OF A"
22     PRINT:"REAL,SYMMETRICAL MATRIX.  THE METHOD USED IS JACOBI'S ITERATION"
23     PRINT:"METHOD. THE METHOD CONSISTS OF APPPLYING TO THE MATRIX A SYSTEM"
24     PRINT:"OF PLANE ROTATIONS GIVEN BY ORTHOGONAL MATRICES MADE TO REDUCE"
25     PRINT:"THE OFF-DIAGONAL ELEMENTS TO ZERO.  THIS PROGRAM USES FOUR"
26     PRINT:"ARGUMENTS.  A IS THE NAME OF A TWO-DIMENSIONAL ARRAY CONTAINING"
27     PRINT:"THE REAL,SYMMETRIC MATRIC IN ITS FIRST N ROWS AND COLUMNS"
28     PRINT:"R IS THE NAME OF THE TWO-DIMENSIONAL ARRAY WHICH WILL CONTAIN"
29     PRINT:"THE EIGENVECTORS IN ITS FIRST N COLUMNS."
30     PRINT:"N IS AN INTEGER VARIABLE OR CONSTANT GIVING THE ORDER"
31     PRINT:"OF THE MATRIX."
32  PRINT:"MV IS AN INTEGER VARIABLE OR CONSTANT WHICH MUST BE 0 OR 1."
33     PRINT:"IF IT IS 0 BOTH EIGENVECTORS AND EIGENVALUES ARE FORMED."
34     PRINT:"IF IT IS ONE ONLY THE EIGENVALUES ARE FOUND."
35   3 PRINT:"ENTER THE ORDER OF MATRIX AND THE MATRIX SEPARATED BY COMMAS."
36     READ:N,((A(I,J),I=1,N),J=1,N)
37     PRINT:"THE MATRIX IS"
38     DO 10 I=1,N
40  10 PRINT:(A(I,J),J=1,N)
45     MV=0
50     CALL MATEIG(A,R,N,MV)
55     PRINT:"EACH EIGENVALUE FOLLOWED BY CORRESPONDING EIGENVECTOR"
60     DO 20 I=1,N
65     PRINT:""
70     PRINT:A(I, I)
75  20 PRINT:(R(J,I),J=1,N)
80     CONTINUE
85     STOP;END
110                  SUBROUTINE MATEIG(A,R,N,MV)
120          DIMENSION A(30,30),R(30,30)
130           IF(MV-1)10,25,10
140 10        DO 20 J=1,N
150           DO 20 I=1,N
160           R(I,J)=0.0
170 20        R(I,I)=1.0
180C                COMPUTE THE INITIAL AND FINAL NORMS
190 25        ANORM=0.0
200           DO 35 I=1,N
```

TABLE 3-8. (Cont'd)

```
        DO 35 J=1,N
        IF(I-J)30,35,30
 30     ANORM=ANORM+A(I,J)*A(I,J)
 35     CONTINUE
        IF(ANORM)165,165,40
 40     ANORM=SQRT(ANORM*2.)
        ANRMX=ANORM*1.0E-6/FLOAT(N)
C               INITIALIZE INDICATORS AND COMPUTE THRESHOLD
        IND=0
        THR=ANORM
 45     THR=THR/N
      N1=N-1
  50    DO 149 L=1,N1
       L1=L+1
      DO 149 M=L1,N
C               COMPUTE SINE AND COSINE
 62     IF(ABS(A(L,M))-THR)149,65,65
 65     IND=1
        X=0.5*(A(L,L)-A(M,M))
 68     Y=A(L,M)
        Z=SQRT(Y*Y+X*X)
        Y=-A(L,M)/Z
        IF(X)70,75,75
 70     Y=-Y
 75 SINX=Y/SQRT(2.0*(1.0+(SQRT(1.0+Y*Y))))
        SINX2=SINX*SINX
 78     COSX=SQRT(1.0-SINX2)
        COSX2=COSX*COSX
        SINCS=SINX*COSX
C               ROTATE L AND M COLUMNS
        DO 90 I=1,N
        IF(I-L)80,90,80
 80     IF(I-M)85,90,85
 85     X=A(I,L)*COSX-A(I,M)*SINX
        A(I,M)=A(I,L)*SINX+A(I,M)*COSX
        A(I,L)=X
 90     CONTINUE
        X=2.0*A(L,M)*SINCS
        Y=A(L,L)*COSX2+A(M,M)*SINX2-X
        X=A(L,L)*SINX2+A(M,M)*COSX2+X
        A(L,M)=(A(L,L)-A(M,M))*SINCS+A(L,M)*(COSX2-SINX2)
        A(L,L)=Y
        A(M,M)=X
        DO 100 I=1,N
        A(L,I)=A(I,L)
        A(M,I)=A(I,M)
        IF(MV-1)95,100,95
 95     X=R(I,L)*COSX-R(I,M)*SINX
        R(I,M)=R(I,L)*SINX+R(I,M)*COSX
        R(I,L)=X
 100    CONTINUE
 149    CONTINUE
 150    IF(IND-1)160,155,160
 155    IND=0
```

TABLE 3-8. (Cont'd)

```
            GO TO 50
      160   IF(THR-ABS(X))165,165,45
      165   DO 185 I=1,N
            DO 185 J=1,N
            IF(A(I,I)-A(J,J))170,185,185
      170   X=A(I,I)
            A(I,I)=A(J,J)
            A(J,J)=X
            IF(MV-1) 175, 190, 175
      175   DO 180 K=1,N
            X=R(K,I)
            R(K,I)=R(K,J)
      180   R(K,J)=X
      185   CONTINUE
      190   RETURN
         SYMEIG
            END
```

TABLE 3-9. OUTPUT OF SYMEIG FOR AT CUT QUARTZ WITH X_3 IN THICKNESS DIRECTION

```
SYMEIG



DO YOU WANT INSTRUCTIONS?
=YES
INSTRUCTIONS FOR SYMEIG
THIS PROGRAM CALCULATES THE EIGENVECTORS AND EIGENVALUES OF A
REAL,SYMMETRICAL MATRIX.  THE METHOD USED IS JACOBI'S LITERATION
METHOD. THE METHOD CONSISTS OF APPPLYING TO THE MATRIX A SYSTEM
OF PLANE ROTATIONS GIVEN BY ORTHOGONAL MATRICES MADE TO REDUCE
THE OFF-DIAGONAL ELEMENTS TO ZERO.  THIS PROGRAM USES FOUR
ARGUMENTS.  A IS THE NAME OF A TWO-DIMENSIONAL ARRAY CONTAINING
THE REAL,SYMMETRIC MATRIC IN ITS FIRST N ROWS AND COLUMNS
R IS THE NAME OF THE TWO-DIMENSIONAL ARRAY WHICH WILL CONTAIN
THE EIGENVECTORS IN ITS FIRST N COLUMNS.
N IS AN INTEGER VARIABLE OR CONSTANT GIVING THE ORDER
OF THE MATRIX.
MV IS AN INTEGER VARIABLE OR CONSTANT WHICH MUST BE 0 OR 1.
IF IT IS 0 BOTH EIGENVECTORS AND EIGENVALUES ARE FORMED.
IF IT IS ONE ONLY THE EIGENVALUES ARE FOUND.
ENTER THE ORDER OF MATRIX AND THE MATRIX SEPARATED BY COMMAS.
=3,0.29239228E11,0.,0.
=0.,0.33611527E11,-0.57004232E10
=0.,-0.57004245E10,0.12976634E12
THE MATRIX IS
  0.29239228E 11  0.              0.
  0.              0.33611527E 11 -0.57004245E 10
  0.             -0.57004232E 10  0.12976634E 12
EACH EIGENVALUE FOLLOWED BY CORRESPONDING EIGENVECTOR

  0.29239228E 11
  0.10000000E 01  0.              0.

  0.38256431E 11
  0.              0.99806542E 00  0.62172465E-01

  0.13012148E 12
  0.             -0.62172465E-01  0.99806542E 00
```

TABLE 3-9 (Cont'd)

```
SYMEIG


DO YOU WANT INSTRUCTIONS?
=NO
ENTER THE ORDER OF MATRIX AND THE MATRIX SEPARATED BY COMMAS.
=3,0.29239228E11,0.,0.
=0.,0.38611527E11,-0.57004232E10
=0.,-0.57004245E10,0.12976634E12
THE MATRIX IS
  0.29239228E 11  0.               0.
  0.              0.38611527E 11 -0.57004245E 10
  0.             -0.57004232E 10  0.12976634E 12
EACH EIGENVALUE FOLLOWED BY CORRESPONDING EIGENVECTOR

  0.29239228E 11
  0.10000000E 01  0.               0.

  0.38256431E 11
  0.              0.99806542E 00  0.62172465E-01

  0.13012144E 12
  0.             -0.62172465E-01  0.99806542E 00
```

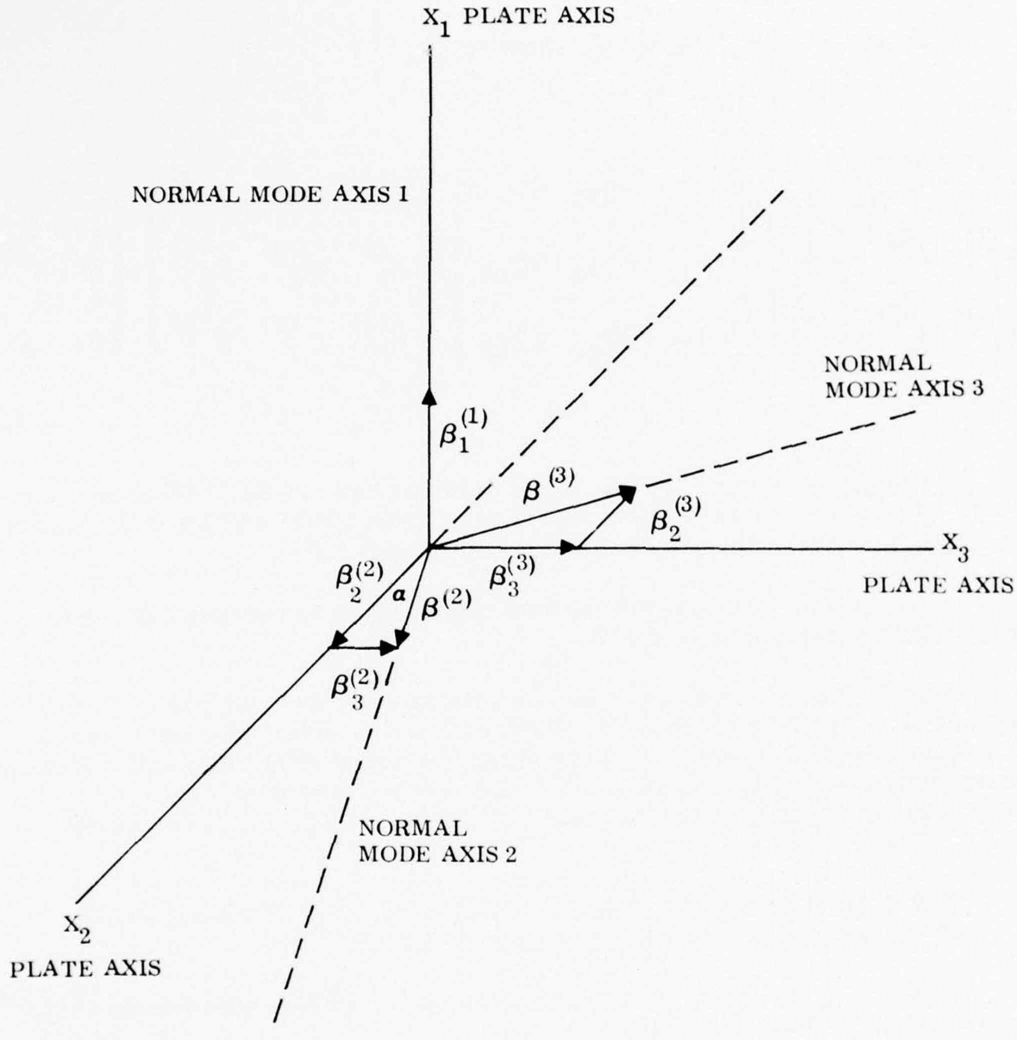

ANGLE BETWEEN NORMAL MODE AXIS 2 AND X_2 IS α

ANGLE BETWEEN NORMAL MODE AXIS 2 AND X_3 IS $90 - \alpha$

$$\cos \alpha = \frac{\beta_2^{(2)}}{\beta^{(2)}} = \beta_2^{(2)} \qquad \beta^{(2)} = 1 = \beta^{(1)} = \beta^{(3)}$$

$$\cos (90 - \alpha) = \sin \alpha = \frac{\beta_3^{(2)}}{\beta^{(2)}} = \beta_3^{(2)}$$

Figure 3-3. Relation of Normal Coordinate Axes to Plate Axes for AT-Cut Quartz with X_3 in the Thickness Direction

Since $[\beta]^{-1}\,[\beta] = 1$.

However if $[\beta]$ is an orthogonal matrix[9]

β transpose = $[\beta]^T$ should be equal to $[\beta]^{-1}$;

hence,

$$\begin{bmatrix} \beta_1^{(1)} & \beta_2^{(1)} & \beta_3^{(1)} \\ \beta_1^{(2)} & \beta_2^{(2)} & \beta_3^{(2)} \\ \beta_1^{(3)} & \beta_2^{(3)} & \beta_3^{(3)} \end{bmatrix} \begin{bmatrix} CB_{11} & CB_{12} & CB_{13} \\ CB_{21} & CB_{22} & CB_{23} \\ CB_{31} & CB_{32} & CB_{33} \end{bmatrix} \begin{bmatrix} \beta_1^{(1)} & \beta_1^{(2)} & \beta_1^{(3)} \\ \beta_2^{(1)} & \beta_2^{(2)} & \beta_2^{(3)} \\ \beta_3^{(1)} & \beta_3^{(2)} & \beta_3^{(3)} \end{bmatrix} = \begin{bmatrix} c^{(1)} & 0 & 0 \\ 0 & c^{(2)} & 0 \\ 0 & 0 & c^{(3)} \end{bmatrix} \tag{43}$$

The program Norm listed in Table 3-10 carries out Eq. (43) using, as inputs, the secular matrix coefficients, CB_{jk}, from CROT and the $\beta_k^{(i)}$ values from SYMEIG. It should return the correct values of $c^{(i)}$.

The direction of the plate thickness can be made to correspond to that used in CROT by changing line 120.

Table 3-11 shows the output of this program for the example in Tables 3-6 and 3-9. The output should be a diagonal matrix whose elements correspond to the eigenvalues in Table 3-9. Notice that the output is not diagonal. However a closer examination shows that the off-diagonal terms are errors in the last-listed digit, or beyond, of the diagonal terms and, hence, represent computer round-off errors.

C. TRANSFORMATION TO NORMAL COORDINATES, NORMAL MODE IMPEDANCE MATRIX AND PROGRAM VCOUP

At this point we carry out a transformation to normal coordinates [15],[16] by defining the following quantities.

$$T_{3j}^{o} = \beta_i^{(j)}\, T_{3i} \tag{44}$$

$$u_j^{o} = \beta_i^{(j)}\, u_i \tag{45}$$

$$e_{33j}^{o} = \beta_i^{(j)}\, e_{33i} \ . \tag{46}$$

TABLE 3-10. LISTING OF PROGRAM NØRM FOR DIAGONALIZATION OF THE SECULAR MATRIX COEFFICIENTS

```
C THIS PRØGRAM CØNVERTS THE CØEFFICIENTS IN THE SECULAR
C EQUATIØN TØ DIAGØNAL FØRM
DIMENSIØN CB(3,3),B(3,3),CN(3,3)
I=3
C THIS MATRIX STØRES THE ELEMENTS ØF THE SECULAR EQUATIØN
CB(1,1)=0.29239228E11
CB(1,2)=0.
CB(1,3)=0.
CB(2,1)=0.
CB(2,2)=0.38611527E11
CB(2,3)=-0.57004245E10
CB(3,1)=0.
CB(3,2)=-0.57004232E10
CB(3,3)=0.12976634E12
C THIS MATRIX STØRES THE EIGENVECTØRS ØF CB BY CØLUMNS
C THE CØMPØNENTS ØF THE EIGENVECTØRS ARE THE
C DIRECTIØN CØSINES BETWEEN THE NØRMAL MØDE
C AXES AND THE PLATE AXES(B(1,1)=CØSINE ØF
C ANGLE BETWEEN N1 AND X1,B(2,1) BETWEEN N1 AND X2,ETC)
B(1,1)=0.1E1
B(2,1)=0.
B(3,1)=0.
B(1,2)=0.
B(2,2)=0.99806542
B(3,2)=0.62172451E-1
B(1,3)=0.
B(2,3)=-0.62172451E-1
B(3,3)=0.99806542
C THIS MATRIX SHØULD CØNTAIN THE EIGENVALUES ØN
C THE MAIN DIAGØNAL. IT REPRESENTS BT*CB*B
C BT IS THE TRANSPØSE ØF B
DØ 10 L=1,3
DØ 10 M=1,3
DØ 10 J=1,3
DØ 10 K=1,3
CN(L,M)=B(J,L)*B(K,M)*CB(J,K)+CN(L,M)
10 CØNTINUE
PRINT 900,I
PRINT 910
PRINT 920,((CN(I,J),J=1,3),I=1,3)
STØP
900 FØRMAT(/,'FØR X',I1,' IN THE THICKNESS DIRECTIØN')
910 FØRMAT(/,5X,'THE ELEMENTS IN THE NØRMAL CØØRDINATE',
& ' EQUATIØN ARE')
920 FØRMAT(/,3X,E15.8,6X,E15.8,6X,E15.8)
END
```

TABLE 3-11. OUTPUT OF NØRM FOR AT CUT QUARTZ WITH X_3 IN THE THICKNESS DIRECTION

```
331[illegible]    02/28/77    15.592

[illegible] X3 IN THE THICKNESS DIRECTION

   THE ELEMENTS IN THE NORMAL COORDINATE EQUATION ARE

 0.2223[illegible] 11        0.                      0.

 0.                          0.[illegible]25643[illegible] 11     -0.124[illegible]

 0.                          0.31516[illegible] 02   0.1301214[illegible] 12
```

Furthermore, since the $\beta_i^{(j)}$ are orthonormal, the inverse transformations are

$$T_{3j} = \beta_j^{(i)} T_{3i}^o \tag{47}$$

$$u_j = \beta_j^{(i)} u_i^o \tag{48}$$

$$e_{33j} = \beta_j^{(i)} e_{33i}^o \; . \tag{49}$$

Equation (44) for example gives:

$$T_{31}^o = \beta_1^{(1)} T_{31} + \beta_2^{(1)} T_{32} + \beta_3^{(1)} T_{33} \; . \tag{50}$$

In terms of these new quantities Eq. (1) for i in the x_3 direction becomes

$$T_{3j},_3^o = -\rho\omega^2 u_j^o \; . \tag{51}$$

Returning to Eq. (12) for x_3 in the thickness direction (i.e. i = 3) we have,

$$\phi,_{33} = \left(e_{3k3}/\epsilon_{33}^s\right) u_k,_{33}, \tag{52}$$

which can be integrated to give,

$$\phi = \left(\frac{e_{3k3}}{\epsilon_{33}^s}\right) u_k + a_3 x_3 + b_3 \; . \tag{53}$$

This in turn can be substituted into Eq. (7) for i = 3, k = 3 to yield,

$$T_{3j} = c^E_{3jk3}\, u_{k',3} + e_{33j} \left(\frac{e_{3k3}}{\epsilon^S_{33}} \right) u_{k',3} + e_{33j}\, a_3 \; . \tag{54}$$

Multiplying Eq. (54) by $\beta_j^{(i)}$ and using Eq. (15) leads to,

$$T^o_{3i} = \beta_j^{(i)}\, T_{3j} = \bar{c}^E_{3jk3}\, \beta_j^{(i)}\, u_{k',3} + \beta_j^{(i)}\, e_{33j}\, a_3 \; ; \tag{55}$$

but from Eq. (40) or Eq. (25),

$$\bar{c}^E_{3jk3}\, \beta_j^{(i)} = c^{(i)} \delta_{kj}\, \beta_j^{(i)} \; , \qquad \text{(no sum over i)} \tag{56}$$

so that

$$T^o_{3i} = c^{(i)} \delta_{kj}\, \beta_j^{(i)}\, u_{k',3} + e^o_{33i}\, a_3 \qquad \text{(no sum over i)}$$

or $$T^o_{3i} = c^{(i)}\, \beta_j^{(i)}\, u_{j',3} + e^o_{33i}\, a_3 \quad \text{(no sum over i)} \; , \tag{57}$$

from which we obtain

$$T^o_{3i} = c^{(i)}\, u^o_{i',3} + e^o_{33i}\, a_3 \quad \text{(no sum over i)} \; . \tag{58}$$

This equation can be substituted into Eq. (51) to give

$$c^{(i)}\, u^o_{i',33} + \rho\,\omega^2\, u^o_i = 0 \qquad \text{(no sum over i)}$$

or

$$\begin{aligned} c^{(1)}\, u^o_{1',33} + \rho\,\omega^2\, u^o_1 &= 0 \\ c^{(2)}\, u^o_{2',33} + \rho\,\omega^2\, u^o_2 &= 0 \\ c^{(3)}\, u^o_{3',33} + \rho\,\omega^2\, u^o_3 &= 0 \; . \end{aligned} \tag{59}$$

This clearly shows that the normal coordinate motions, u^o_i, are uncoupled.

If use is made of the symmetry relations of Eq. (9), it is possible to write

$$e_{3k3} u_k = (\beta_k^{(i)} e^o_{3i3})(\beta_k^{(m)} u^o_m)$$

$$= \beta_k^{(i)} \beta_k^{(m)} e^o_{3i3} u^o_m \tag{60}$$

$$= \delta_{im} e^o_{3i3} u^o_m = e^o_{3i3} u^o_i ,$$

where the orthonormal properties of the $\beta_k^{(i)}$ in Eq. (37) are used.

This shows that

$$e_{3k3} u_k = e^o_{3k3} u^o_k \tag{61}$$

is invariant under the transformation.

Equation (53) for the potential then becomes

$$\phi = (e^o_{3k3}/\epsilon^s_{33}) u^o_k + a_3 x_3 + b_3 , \tag{62}$$

which shows that the x_3-directed component of an electric field, arising from particle displacement due to passage of a wave, reverses direction when the wave direction reverses.

It is now desirable to show that Eqs. (59) can be represented by transmission line equations. The standard lossless transmission line equations[17]

$$\frac{\partial V}{\partial z}(z;t) = -L \frac{\partial I}{\partial t}(z;t)$$

$$\frac{\partial I}{\partial z}(z;t) = -C \frac{\partial V}{\partial t}(z;t) , \tag{63}$$

where L and C represent the inductance and capacitance per unit length, can be put in the desired form by the following procedure.

Let $V(z;t)$ and $I(z;t)$ take the same form as $u_1(x_i;t)$ in Eqs. (16) and (18), so that

$$V(z;t) = Ve^{\pm j\eta z} e^{\pm j\omega t} = Ve^{j\omega(t - \frac{\eta}{\omega} z)} = Ve^{j\omega(t - \frac{z}{v})}$$

$$I(z;t) = Ie^{\pm j\eta z} e^{\pm j\omega t} = Ie^{j\omega(t - \frac{\eta}{\omega} z)} = Ie^{j\omega(t - \frac{z}{v})} \tag{64}$$

represent sinusoidal time functions propagating in the z direction with a velocity, v.

Eqs. (64) can be substituted into (63) to yield

$$-j\eta V = -j\omega LI$$

$$-j\eta I = -j\omega CV \text{ or } I = \frac{\omega C}{\eta} V . \qquad (65)$$

If the second equation of Eq. (65) is substituted into the first,

$$-j\eta V = -j\frac{\omega^2 LCV}{\eta} \quad \text{or} \quad \left(1 - \frac{\omega^2 LC}{\eta^2}\right) V = 0 . \qquad (66)$$

Equation (66) can be satisfied for arbitrary values of V only if

$$\eta = \omega \sqrt{LC} . \qquad (67)$$

The following identification between the velocity of propagation, v, and the wave number, η, must be made from the last form of Eq. (64):

$$v = \frac{\omega}{\eta} \quad \text{or} \quad \eta = \frac{\omega}{v} \quad v = \frac{1}{\sqrt{LC}} . \qquad (68)$$

If a transmission line characteristic impedance and admittance are defined as

$$Z_0 = \sqrt{\frac{L}{C}} = \frac{1}{Y_0} , \qquad (69)$$

then, for an arbitrary wavenumber $\eta^{(i)}$, Eqs. (63) can be put in the form,

$$V^{(i)}_{,3} = -j\omega \sqrt{\frac{L^{(i)}}{C^{(i)}}} \sqrt{L^{(i)} C^{(i)}}\, I^{(i)} = -j\eta^{(i)} Z_0^{(i)} I^{(i)} \qquad (70)$$

$$I^{(i)}_{,3} = -j\omega \sqrt{\frac{C^{(i)}}{L^{(i)}}} \sqrt{L^{(i)} C^{(i)}}\, V^{(i)} = -j\eta^{(i)} Y_0^{(i)} V^{(i)} ,$$

where it is assumed that the wave is propagating in the x_3 direction.

If the second of Eqs. (70) is differentiated with respect to x_3 and substituted into the first equation, $V^{(i)}$ can be eliminated, and vice versa, to yield

$$I^{(i)}_{,33} + \left(\eta^{(i)}\right)^2 I^{(i)} = 0 \qquad (71)$$

$$V^{(i)}_{,33} + \left(\eta^{(i)}\right)^2 V^{(i)} = 0 .$$

Both of these equations are identical to Eq. (59) when Eq. (20) is used, so it should be possible, at least, to determine that there is a correspondence between the normal mode displacements and the transmission line variables.

Also, note that by writing Eqs. (16) and (18) in the same form as the last of Eq. (64), the acoustic wave velocity for each $\eta^{(i)}$ is given by

$$v^{(i)} = \frac{\omega}{\eta^{(i)}} = \sqrt{c^{(i)}/\rho} \quad . \tag{72}$$

Since we are free to make corresponding wave numbers of the transmission line and elastic waves equal, Eq. (59) amounts to using three transmission lines (one for each i), and supporting a wave propagating with the velocity, $v^{(i)}$ from Eq. (72), if the other variables in the acoustic wave equations can be made consistent with Eq. (70).

Equations (51) and (58) represent a set relating T^o_{3i} and u^o_i, which are very similar to the first-order differential equations of Eq. (70). However, the $e^o_{33i}\ a_3$ term of Eq. (58) hinders this analogy. This term is piezoelectric in nature and a spatial constant; hence if T^o_{3i} is separated into two parts by defining

$$T^o_{3i} = \tilde{T}^o_{3i} + \overline{T}^o_{3i} \quad \text{with} \quad \overline{T}^o_{3i} = e^o_{33i}\, a_3 \ , \tag{73}$$

then, because $\overline{T}_{3i}$, is a constant,

$$\overline{T}_{3i},_3 = 0 \quad , \tag{74}$$

so that Eqs. (51) and (58) become

$$\begin{aligned} \tilde{T}^o_{3j},_3 &= -\rho\omega^2\, u^o_i \\ c^{(i)}\, u^o_{i,3} &= \tilde{T}^o_{3i} \ , \end{aligned} \tag{75}$$

which now has the structure of Eq. (70).

To complete the analogy between the acoustic waves and the transmission line it is necessary to pair corresponding quantities. For reasons, given in Ref. [1], the following choices are made:

$$V^{(i)} = A\, \tilde{T}_{3i}$$

$$I^{(i)} = -\dot{u}^o_i = -j\omega u^o_i$$

$$Z^{(i)}_0 = A\rho v^{(i)}$$

$$
\begin{aligned}
c^{(i)} &= \rho\left(v^{(i)}\right)^2 \\
Z_0^{(i)} &= 1/Y_0^{(i)} \qquad\qquad (76) \\
\eta^{(i)} &= \omega/v^{(i)}
\end{aligned}
$$

$I^{(i)}$ is the negative of the particle velocity in the normal coordinate system. The negative sign is a result of the convention for positive power flow in acoustics. If a positive tensile force is applied to an elastic body a positive outward particle velocity is produced but, under these conditions, power is said to produce a power flow into the body. Hence, the outward velocity associated with an inward power flow produces the negative sign.

The factor, A, in Eq. (76) is a portion of the area perpendicular to the wave propagation, i.e. normal to x_3.

Still following Dr. Ballato's presentation, we now turn to an examination of the thickness modes of an electroded, piezoelectric crystal plate with traction-free surfaces, driven by an electric field in the thickness direction, (since this is a clever way to incorporate the electrical circuit into the transmission line model). Figure 3-4 is a sketch of the situation to be analyzed. The plate is laterally

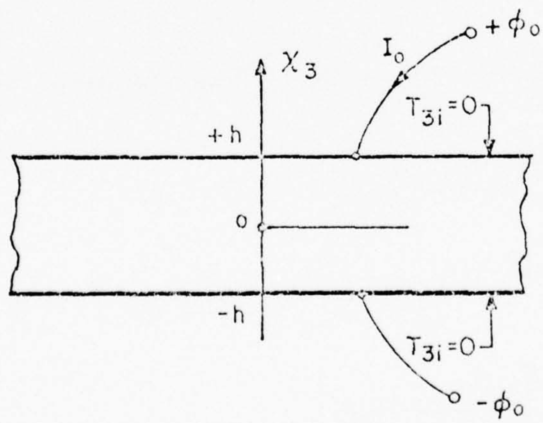

Figure 3-4. Unbounded, Traction-Free, Piezoelectric Plate. Thickness Excitation of Thickness Modes

unbounded, of thickness 2h, with upper and lower surfaces at $x_3 = +h$ and $-h$, respectively. These surfaces are also assumed to be maintained at potentials $+\phi_0$ and $-\phi_0$, respectively. Lateral coordinates are of no interest and the $e^{j\omega t}$ time factor is ignored.

At the plate boundaries the conditions to be satisfied are:

$$
\begin{aligned}
T_{3j} &= 0 \text{ at } x_3 = \pm h \qquad\qquad (77) \\
\phi &= \pm\phi_0 \text{ at } x_3 = \pm h
\end{aligned}
$$

If Cramer's rule is applied to Eqs. (47) it is seen that, if the untransformed stress, T_{3j}, vanishes at the surfaces, the transformed stress, T^o_{3j}, must also vanish since, to satisfy the orthogonality condition that the transpose of the β matrix is equal to its inverse, the determinant of the β's must be non-zero. Hence

$$T^o_{3i} = 0 \text{ at } x_3 = \pm h \ . \tag{78}$$

We seek a solution of Eq. (59) that satisfies Eqs. (77) and (78) when inserted into Eqs. (58) and (62). From now on until further notice the Einstein convention is dropped and no sum is to be taken unless it is specifically indicated. To this end we select

$$u^o_i = U_i \sin \eta^{(i)} x_3 \ , \tag{79}$$

so that

$$u^o_{i,3} = U_i \eta^{(i)} \cos \eta^{(i)} x_3 \text{ and } u^o_{i,33} = -U_i (\eta^i)^2 \sin \eta^{(i)} x_3 \ ,$$

which satisfies Eq. (59), provided

$$(\eta^{(i)})^2 = \frac{\rho \omega^2}{c^{(i)}} \quad , \tag{80}$$

which it does, from Eq. (20). If Eq. (79) is now placed into Eq. (58) and use is made of Eq. (78),

$$\begin{aligned} T^o_{3i} &= c^{(i)} u_{i,3} + e^o_{33i} a_3 \\ &= c^{(i)} \eta^{(i)} U_i \cos \eta^{(i)} x_3 + e^o_{33i} a_3 = 0 \text{ at } x_3 = \pm h \ . \end{aligned} \tag{81}$$

Hence,

$$U_i = \frac{-e^o_{33i} a_3}{c^{(i)} \eta^{(i)} \cos \eta^{(i)} h} \ . \tag{82}$$

Using Eq. (62) along with Eq. (79) yields:

$$\begin{aligned} \phi &= \left(\frac{e^o_{3k3}}{\epsilon^s_{33}} \right) u^o_k + a_3 x_3 + b_3 \quad \text{(sum over k)} \\ &= \frac{e^o_{313}}{\epsilon^s_{33}} U_1 \sin \eta^{(1)} x_3 + \frac{e^o_{323}}{\epsilon^s_{33}} U_2 \sin \eta^{(2)} x_3 \end{aligned} \tag{83}$$

$$+ \frac{e^{o}_{333}}{\epsilon^{s}_{33}} U_3 \sin \eta^{(3)} x_3 + a_3 x_3 \quad .$$

Substituting from Eq. (82) yields:

$$\phi = \frac{-e^{o}_{313}\, e^{o}_{331}\, a_3 \sin \eta^{(1)} x_3}{\epsilon^{s}_{33}\, c^{(1)}\, \eta^{(1)} \cos \eta^{(1)} h} - \frac{e^{o}_{323}\, e^{o}_{332}\, a_3 \sin \eta^{(2)} x_3}{\epsilon^{s}_{33}\, c^{(2)}\, \eta^{(2)} \cos \eta^{(2)} h}$$

$$- \frac{e^{o}_{333}\, e^{o}_{333}\, a_3 \sin \eta^{(3)} x_3}{\epsilon^{s}_{33}\, c^{(3)}\, \eta^{(3)} \cos \eta^{3} h} + a_3 x_3 + b_3 \qquad (84)$$

Letting $\phi = \pm \phi_0$ at $x_3 = \pm h$ leads to

$$\phi_0 + (-\phi_0) = 0 = 2b_3 \quad .$$

Thus

$$b_3 = 0 \qquad (85)$$

and

$$\phi_0 = a_3 h \left(1 - \frac{1}{h} \sum_{i=1}^{3} \left(\frac{e^{o}_{3i3}\, e^{o}_{33i}}{\epsilon^{s}_{33}\, c^{(i)}} \right) \frac{\tan \eta^{(i)} h}{\eta^{(i)}} \right) \quad . \qquad (86)$$

This leads to:

$$a_3 = \frac{\phi_0 / h}{\left\{ 1 - \sum_{i=1}^{3} \frac{e^{o}_{3i3}\, e^{o}_{33i}}{\epsilon^{s}_{33}\, c^{(i)}} \; \frac{\tan \eta^{(i)} h}{\eta^{(i)} h} \right\}}$$

Now we define:

$$(k^{(i)})^2 = \frac{e^{o}_{3i3}\, e^{o}_{33i}}{\epsilon^{s}_{33}\, c^{(i)}} \quad , \qquad (88)$$

where no sum over i is taken, so that

$$(k^{(1)})^2 = \frac{e^o_{313} e^o_{331}}{\epsilon^s_{33} c^{(1)}} = \frac{(e^o_{331})^2}{\epsilon^s_{33} c^{(1)}} \;,\; (k^{(2)})^2 = \frac{(e^o_{332})^2}{\epsilon^s_{33} c^{(2)}} \;,\; (k^{(3)})^2 = \frac{(e^o_{333})^2}{\epsilon^s_{33} c^{(3)}} \;,$$

when use is made of the symmetry relations for e^o_{ijk}. Here $k^{(i)}$ is the piezoelectric coupling coefficient for the i^{th} mode in the Thickness Excitation of Thickness Mode (TETM) case.

Putting Eq. (82) into Eq. (58) and Eq. (79) along with Eq. (87) leads to

$$T^o_{3i} = e^o_{333i}\, a_3 \left(1 - \frac{\cos \eta^{(i)} x_3}{\cos \eta^{(i)} h}\right) \tag{89}$$

$$u^0_i = \frac{-e^o_{33i} \sin \eta^{(i)} x_3}{hc^{(i)} \eta^{(i)} \cos \eta^{(i)} h} \left\{ \frac{\phi}{1 - \sum_{j=1}^{3} (k^{(j)})^2 \dfrac{\tan \eta^{(j)} h}{\eta^{(j)} h}} \right\} \tag{90}$$

Substituting Eq. (53) into Eq. (8), specialized to the 3-direction by letting $i = k = 3$, leads to:

$$D_3 = -\epsilon^s_{33} a_3 = \frac{-\epsilon^s_{33} \phi_0/h}{\left\{1 - \sum_{j=1}^{3} (k^{(j)})^2 \dfrac{\tan \eta^{(j)} h}{\eta^{(j)} h}\right\}} \tag{91}$$

Now, consider a portion of the plate having a lateral area, A, as introduced in connection with Eq. (76). The current I_0, intercepted by this area is equal to

$$I_0 = -A\dot{D}_3 = -j\omega A D_3 \;. \tag{92}$$

The minus sign is here because, at the positive (upper) electrode, the surface normal points in the direction of minus x_3 within the crystal.

Considering this plate to be an electrical network, one sees an admittance

$$Y_{in}(\text{TETM}) = I/E = I_0/2\phi_0 \;. \tag{93}$$

Defining a capacitance C_0 by

$$C_0 = A\,\epsilon^s_{33}/2h \;, \tag{94}$$

Equation (93) becomes

$$Y_{in}(TETM) = \frac{j\omega C_0}{\left\{1 - \sum_{p=1}^{3} (k^{(p)})^2 \frac{\tan \eta^{(p)} h}{\eta^{(p)} h}\right\}} , \tag{95}$$

by substituting Eqs. (86), (88), (91), (92) and (94).

We now assume $Y_{in}(TETM)$ can be represented by the configuration shown in Figure 3-5. Then

$$Y_{in}(TETM) = j\omega C_0 + \frac{(-j\omega C_0)Y_{(TL)}}{Y_{(TL)} - j\omega C_0} \tag{96}$$

$$= \frac{j\omega C_0}{\left(1 - \frac{Y(TL)}{j\omega C_0}\right)} .$$

Equations (95) and (96) are identical if

$$Y_{(TL)} = j\omega C_0 \left(\sum_{p=1}^{3} (k^{(p)})^2 \frac{\tan \eta^{(p)} h}{\eta^{(p)} h} \right) \left(\begin{array}{l} \text{only} \\ \text{indicated sum} \\ \text{over p} \end{array} \right) \tag{97}$$

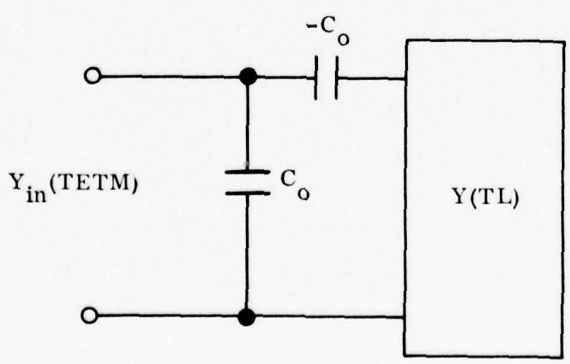

Figure 3-5. Assumed Input Admittance Network

This can be interpreted as the sum of three admittances in parallel, with each admittance containing one tangent function; i.e.,

$$Y_{(TL)} = \sum_{i=1}^{3} Y_{TL}^{(i)} , \tag{98}$$

where $$Y_{TL}^{(i)} = j\omega C_0 \left(\frac{e^o_{3i3}\, e^o_{33i}}{\epsilon^s_{33}\, c^{(i)}} \right) \frac{\tan \eta^{(i)} h}{\eta^{(i)} h} .$$

Using the variables defined in Eq. (76) this can be written as

$$Y_{TL}^{(i)} = \frac{jA}{2h^2} \frac{e^o_{3i3}\, e^o_{33i}}{\rho v^{(i)}} \tan \eta^{(i)} h = \frac{jA}{2h^2} e^o_{3i3} \frac{e^o_{33i} \tan \eta^{(i)} h}{Z_0}$$

$$= \frac{A^2}{4h^2} e^o_{3i3}\, e^o_{33i} \frac{2 \tan \eta^{(i)} h}{-jZ_0^{(i)}} = \frac{A^2}{4h^2} e^o_{3i3}\, e^o_{33i} \frac{1}{-j \frac{Z_0}{2} \cot \eta^{(i)} h} . \tag{99}$$

The input impedance of an open-circuited lossless transmission line of length, h, characteristic impedance, Z_0, and propagation constant, η, is

$$Z_{0c} = -jZ_0 \cot \eta h ; \tag{100}$$

and the impedance of two of these lines in parallel is $-j \frac{Z_0}{2} \cot \eta h$.

Hence, we are tempted to represent $Y_{TL}^{(i)}$ as shown in Figure 3-6. For this configuration

$$Y_{TL}^{(i)} = \frac{1}{Z_{TL}^{(i)}} = \frac{1}{\frac{1}{(n_i)^2} \left(-j \frac{Z_0^{(i)}}{2} \cot \eta^{(i)} h \right)} \tag{101}$$

Equation (101) will agree with Eq. (99) if

$$n_i = \frac{A \sqrt{e^o_{3i3}\, e^o_{33i}}}{2h} = \frac{A e^o_{33i}}{2h} . \tag{102}$$

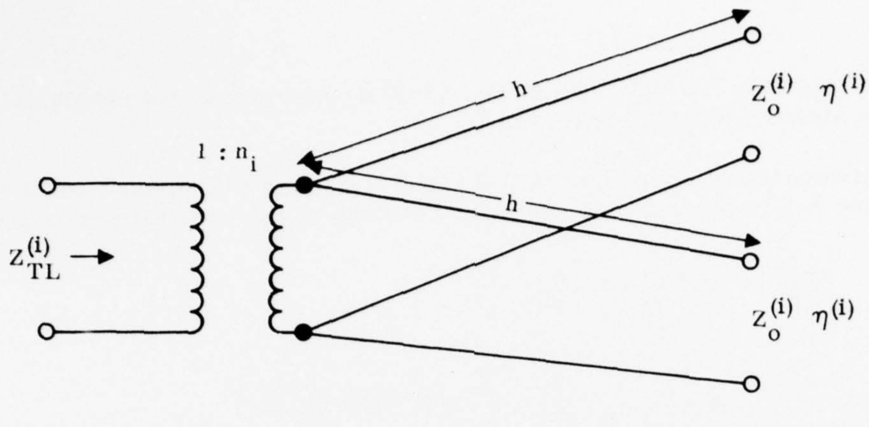

Figure 3-6. Assumed Configuration for $Y_{TL}^{(i)}$

Figure 3-6 can be redrawn as shown in Figure 3-7, since, in this circuit, no current will flow at the center of the transmission line so the wires in Figure 3-7 can be cut.

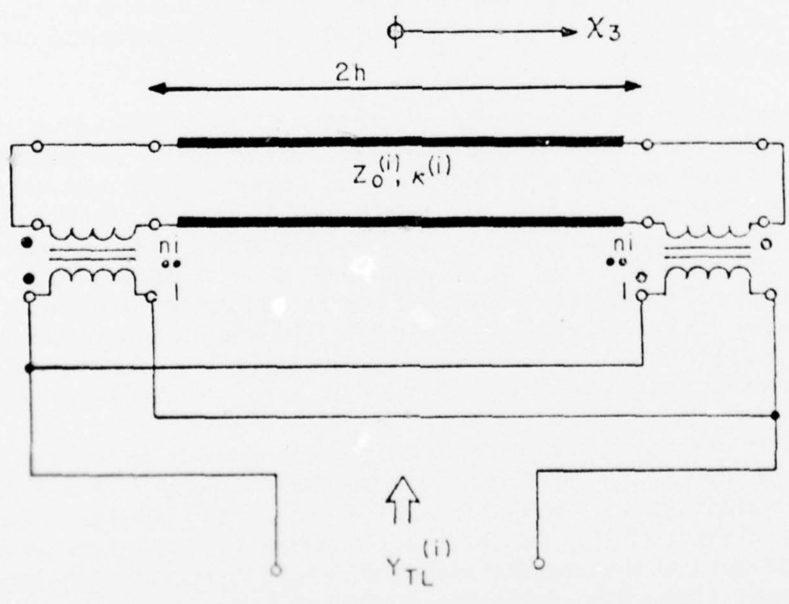

Figure 3-7. Traction-Free Plate. Representation of Single Thickness Mode, Electrical Input Circuit Omitted

In Figures 3-6 and 3-7 and Eq. (102) n_i represents the piezoelectric turns ratio in Mason's Equivalent Circuit.

In connection with Figures 3-6 and 3-7 it should be pointed out that, if $-C_0$ in Figure 3-5 is ignored, the secondary voltage of the transformer is given by:

$$
\begin{aligned}
E_s^{(i)} &= n_i 2\phi_0 = A e^o_{33i} \frac{\phi_0}{h} \\
&= A e^o_{33i} a_3 \left(1 - \sum_{j=1}^{3} k^{(j)} \frac{\tan \eta^{(j)} h}{\eta^{(j)} h} \right) .
\end{aligned}
\tag{103}
$$

Hence, $E_s^{(i)}$ is proportional to $A e^o_{33i} a_3$ but, by Eq. (73), $E_s^{(i)}$ is proportional to $A\bar{T}^o_{3i}$. Thus, while the voltage variables associated with the waves on the transmission lines are $A\tilde{T}^o_{3i}$, the electromechanical transformer's secondary voltages can be identified with $A\bar{T}^o_{3i}$, so that the circuit accounts for the total stress, AT^o_{3i}.

Dr. Ballato goes into several ramifications on drawing the network as shown in Figure 3-7; these will not be dealt with here. All that we emphasize here is that, if the transformers are placed at the ends, as shown, then the polarity dots must be as indicated, in order for this to be a valid representation of Figure 3-6. Figure 3-8 shows the complete 3-mode equivalent circuit for this traction-free case.

Figure 3-9 shows the resulting network with the traction-free condition removed so that the short circuits of Figure 3-8 are gone. Because it pertains to normal coordinates, the port variables are superscripted with the degree sign. The port variables are numbered so that the left side (bottom or -h side of the crystal plate) of the transmission line supporting mode (i) leads to port (i^o), while the right side (top or +h side of the crystal plate) leads to port $(i + 3)^o$. Ports 1^o to 6^o are mechanical ports and port 7^o is an electrical port. We also define V^o_π and I^o_π ($\pi = 1, 2 -- 7$) as the voltages and currents appropriate to port π, with the sign conventions shown in Figure 3-9. At present, no attempt is made to match these port variables with the stresses and displacements.

In order to obtain the impedance matrix appropriate to this network it is convenient to replace the distributed transmission lines in Figure 3-9 with their lumped equivalent form. The equivalent tee form of the lossless transmission line, shown in Figure 3-10, may be ascertained by evaluating its open circuit, short circuit and transfer impedances, and comparing them to the transmission line equations. Using this equivalence Figure 3-9 can be redrawn as shown in Figure 3-11.

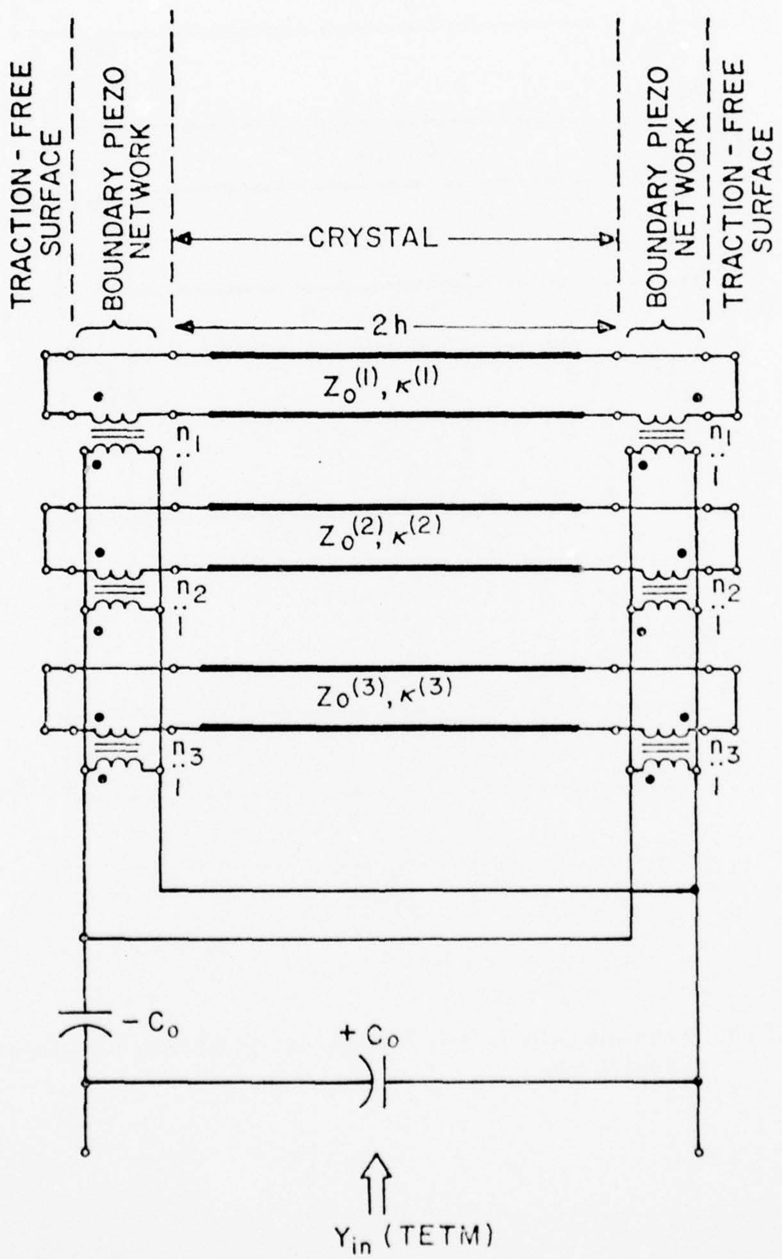

Figure 3-8. Equivalent Network Analog Representation of Traction-Free Plate, TETM

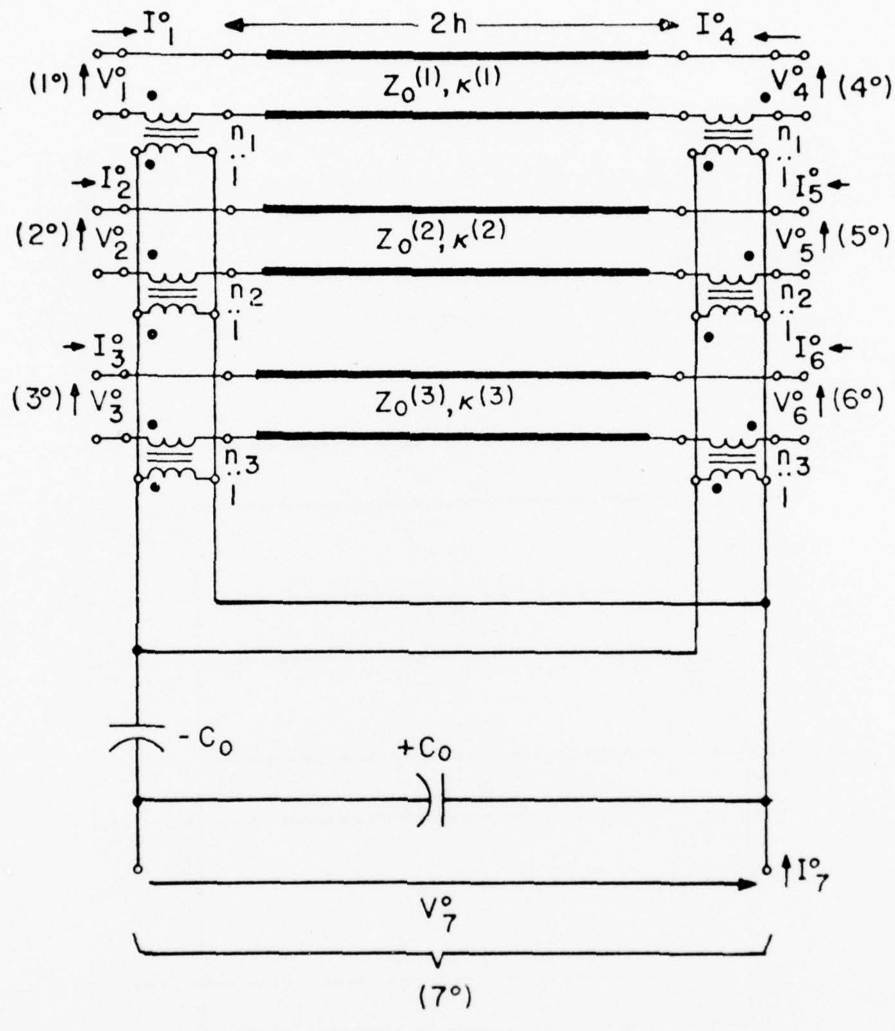

Figure 3-9. Possible Seven-Port Normal Mode Equivalent Circuit of a Crystal Plate

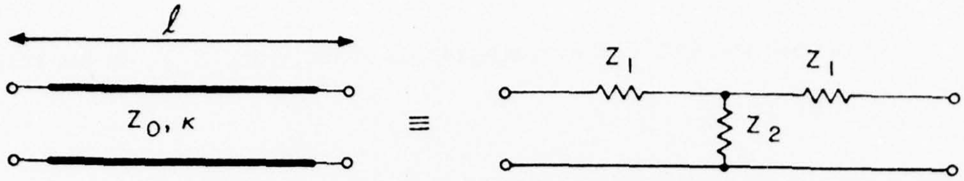

$$Z_1 = \frac{Z_0}{j \sin \theta} (\cos \theta - 1) = j Z_0 \tan(\theta/2)$$

$$Z_2 = \frac{Z_0}{j \sin \theta} \quad ; \quad \theta = \kappa \ell$$

Figure 3-10. Lumped, Tee, Form of a Transmission-Line Section

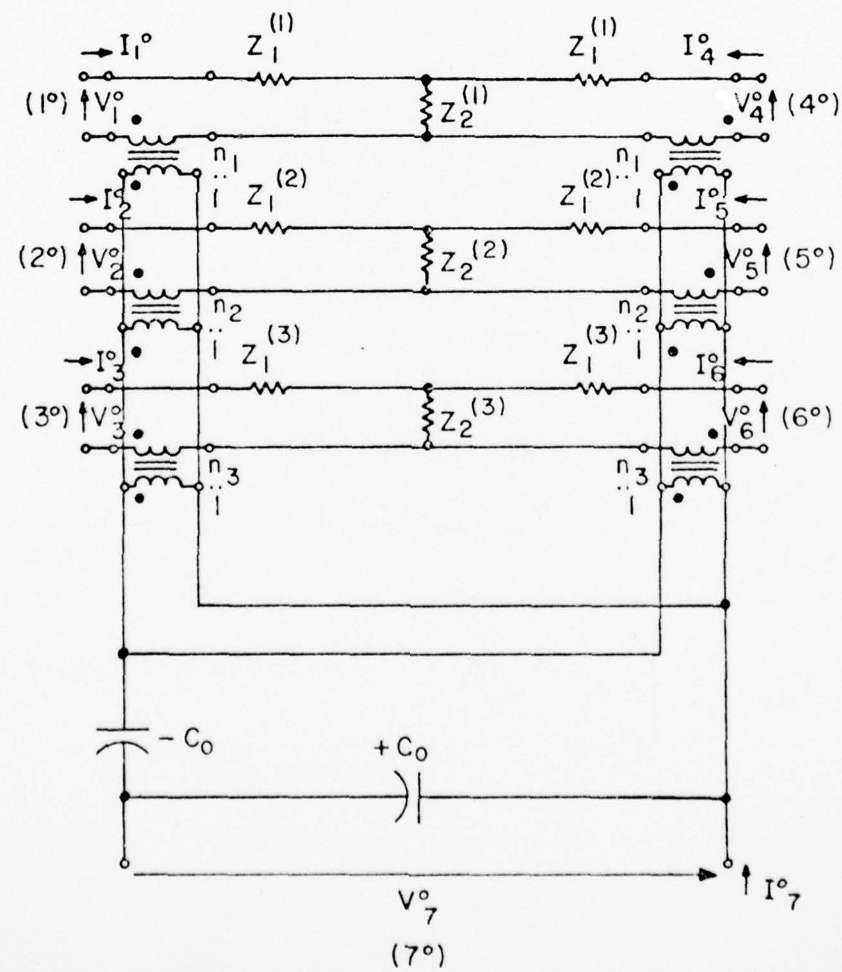

Figure 3-11. Lumped Circuit for Evaluating TETM Electro-Mechanical Impedance Matrix

It is now necessary to evaluate terms of the type, $Z^{o}_{\pi\xi}$, in the relation

$$V^{o}_{\pi} = Z^{o}_{\pi\xi} \; I^{o}_{\xi} \; , \qquad (104)$$

where the Greek indices range from 1 to 7. Because this is a lumped, linear, passive, bilateral network, and because of the sign convention for currents and voltage shown in Figure 3-11, the overall matrix will be symmetrical about its principal diagonal. Furthermore, all mechanical port-driving point impedances will be identical in form, differing only in the mode index number. The same will be true for all mechanical transfer impedances connecting ports on the same transmission line. Likewise all electromechanical transfer impedances will differ only in mode index number.

When the electrical port (7^{o}) is open-circuited so that $I^{o}_{7} = 0$, the two capacitances, $+C_0$ and $-C_0$, add together to produce shorts at the piezoelectric transformers. This completely decouples the transmission lines from each other.

Using this last effect means that:

$$Z^{o}_{\pi\xi} = \left. \frac{V^{o}_{\pi}}{I^{o}_{\xi}} \right|_{I^{o}_{\beta=0}} = 0 \qquad \begin{array}{l} I^{o}_{\beta} \text{ means all } I^{o}_{\beta} = 0 \text{ except } \beta = \xi \\ \xi = 1 \text{ to } 6 \text{ except } \xi \neq \pi \neq \pi \pm 3 \end{array} \quad . \qquad (105)$$

Hence

$$Z^{o}_{12} = Z^{o}_{13} = Z^{o}_{15} = Z^{o}_{16} = Z^{o}_{21} = Z^{o}_{23} = Z^{o}_{24} = Z^{o}_{26} = Z^{o}_{31} = Z^{o}_{32}$$

$$= Z^{o}_{34} = Z^{o}_{35} = Z^{o}_{42} = Z^{o}_{43} = Z^{o}_{45} = Z^{o}_{46} = Z^{o}_{51} = Z^{o}_{53}$$

$$= Z^{o}_{54} = Z^{o}_{56} = Z^{o}_{61} = Z^{o}_{62} = Z^{o}_{64} = Z^{o}_{65} = 0 \; .$$

The mechanical driving point impedances are

$$Z^{o}_{\pi\pi} = \left. \frac{V^{o}_{\pi}}{I^{o}_{\pi}} \right|_{I^{o}_{\beta} = 0} = Z_1^{(k)} + Z_2^{(k)} \qquad \begin{array}{l} I^{o}_{\beta} \text{ means all } I^{o}_{\beta} = 0 \text{ except } \beta = \pi \\ \\ k = \pi \text{ or } \pi - 3 \end{array}$$

(106)

$$Z^o_{11} = Z^o_{44} = \frac{Z^{(1)}_o}{j \tan \theta_1}$$

$$Z^o_{22} = Z^o_{55} = \frac{Z^{(2)}_o}{j \tan \theta_2} \qquad (106) \text{ (continued)}$$

$$Z^o_{33} = Z^o_{66} = \frac{Z^{(3)}_o}{j \tan \theta_3} ,$$

where $\theta_i = 2 h \eta^{(i)}$.

The mechanical transfer impedances between ports on the same line are:

$$Z^o_{\pi;\pi+3} = \left.\frac{V^o_\pi}{I^o_{\pi+3}}\right|_{I^o_\beta = 0} = Z^{(k)}_2$$

I^o_β means all $I^o_\beta = 0$ except $\beta = \pi + 3$

$\pi = 1$ to 3

$k = \pi$

$$Z^o_{\pi;\pi+3} = Z^o_{\pi+3;\pi}$$

$$Z^o_{14} = Z^o_{41} = \frac{Z^{(1)}_o}{j \sin \theta_1}$$

$$Z^o_{25} = Z^o_{52} = \frac{Z^{(2)}_o}{j \sin \theta_2} \qquad (107)$$

$$Z^o_{36} = Z^o_{63} = \frac{Z^{(3)}_o}{j \sin \theta_3} .$$

This accounts for all the impedances except those related to the electrical port.

With all the mechanical ports open-circuited all the electrical mechanical transformers are open-circuited, so that no current can flow through $-C_0$. Hence the electrical port driving point impedance is

$$Z^o_{77} = \left.\frac{V^o_7}{I^o_7}\right|_{I_{\beta=0,\, \beta\neq 7}} = \frac{1}{j \omega C_o} \qquad (108)$$

The electromechanical transfer impedances are

$$Z^o_{7;\pi} = \left.\frac{V^o_7}{I^o_\pi}\right|_{I^o_{\beta=0,\,\beta\neq\pi}} \quad \text{and} \quad Z^o_{\pi;7} = \left.\frac{V^o_\pi}{I^o_7}\right|_{I^o_\beta = 0,\,\beta\neq 7} . \tag{109}$$

With all the ports open-circuited except mechanical port π, the only current flowing is that at port π. This current must flow through the electromechanical transformer closest to port π with turns ratio 1 to n_π or 1 to $n_{\pi-3}$. This produces a primary current of $n_\pi I_\pi$ or $n_{\pi-3} I_\pi$ flowing out of the polarity dot terminal, since $I^o_7 = 0$. This current must flow through C_o and produce a voltage $\frac{n_\pi I_\pi}{j\omega C_o}$ or $\frac{n_{\pi-3} I_\pi}{j\omega C_o}$. A similar argument can be employed to determine $Z^o_{\pi,7}$ since I^o_7 must flow through C_o to produce a primary voltage, $-\frac{I^o_7}{j\omega C_o}$, or a secondary voltage, $\frac{-n_\pi I^o_7}{j\omega C_o}$ or $\frac{-n_{\pi-3} I^o_7}{j\omega C_o}$, in relation to the polarity dots of the transformers. This voltage appears at port π as a voltage, $V_\pi = \frac{n_\pi I^o_7}{j\omega C_o}$ or $\frac{n_{\pi-3} I^o_7}{j\omega C_o}$.

$$\begin{aligned}
Z^o_{17} = Z^o_{47} = Z^o_{71} = Z^o_{74} &= \frac{n_1}{j\omega C_o} \\
Z^o_{27} = Z^o_{57} = Z^o_{72} = Z^o_{75} &= \frac{n_2}{j\omega C_o} \\
Z^o_{37} = Z^o_{67} = Z^o_{73} = Z^o_{76} &= \frac{n_3}{j\omega C_o}
\end{aligned} \tag{110}$$

Now that all the terms in this matrix have been evaluated, it is necessary to show it represents the normal coordinate matrix for a piezoelectric plate.

Following the earlier analogy to a transmission line in Eq. (76), let

$$\begin{aligned}
V^o_\pi &= AT^o_{3i}(-h) \qquad (\pi = i = 1,2,3) \\
V^o_\pi &= AT^o_{3i}(+h) \qquad (\pi = i+3 = 4,5,6) \\
V^o_\pi &= V^o_7 \qquad (\pi = 7)
\end{aligned} \tag{111}$$

where $T^o_{3i}(\pm h)$ refers to the values of T^o_{3i} at the upper or top of the plate and the lower (bottom) surfaces of the plate, respectively. The choice of V's here pertains to the total stress, T^o_{3i}, and not simply the wavy portion, $\tilde{T}^o_{3i}$, as in Equation (76).

The currents are taken as

$$
\begin{aligned}
I_\xi^o &= -\dot{u}_i^o(-h) = -j\omega u_i^o(-h) \quad (\xi = i = 1,2,3) \\
I_\xi^o &= +u_i^o(+h) = +j\omega u_i^o(+h) \quad (\xi = i+3 = 4,5,6) \\
I_\xi^o &= I_7^o \quad (\xi = 7) \ ,
\end{aligned}
\tag{112}
$$

where $u_i^o(\pm h)$ again refers to values of u_i^o at $x_3 = \pm h$. The reason for the sign reversal in the equations for I_ξ^o, above, is that it is desirable to define the port currents as being directed into the positive voltage terminal of a port, while the transmission line equations (which Eq. (76) represents) do not allow the sense of the current to change with respect to the voltage, as the wave progresses down the line.

With these choices of variables the impedance matrix elements depend on quotients of stress components and components of displacement in the normal-coordinate system, and are given by,

$$Z_{\pi\xi}^o = V_\pi^o / I_\xi^o \quad , \tag{113}$$

with all currents equal to zero except for I_ξ^o.

With these definitions, when all the currents except I_7 are equal to zero we are forcing all the displacement components, at the top and bottom faces of the plate, in the normal coordinate framework, to be zero. This corresponds to completely clamping the plate at the top and bottom surfaces so that the plate cannot move. Therefore we do not expect Z_{77}^o to be the reciprocal of Y_{in} (TETM) in Eq. (95), since it was derived on the traction-free basis, where the stresses vanished in the normal coordinate system and, hence, for that case the plate was completely free to move.

Letting u_i^o $(i = 1,2,3)$ to be identically zero everywhere, satisfies Eq. (59) and reduces Eq. (62) to

$$\phi = a_3 x_3 + b_3 \ . \tag{114}$$

The boundary condition is that $\phi = \pm\phi_0$ at $x_3 = \pm h$ can only be satisfied if

$$
\begin{aligned}
b_3 &= 0 \\
a_3 &= \phi_o / h \ .
\end{aligned}
\tag{115}
$$

Specializing Eq. (8) to the 3-direction by letting i = k = 3 and then, substituting Eq. (53), yields

$$D_3 = -\epsilon_{33}^S a_3 \quad . \tag{116}$$

For this case, using Eq. (92),

$$\begin{aligned} I_7^o &= -j\omega A D_3 = \\ &= j\omega A\, \epsilon_{33}^S a_3 = j\omega \frac{A\, \epsilon_{33}^S}{h} \phi_o \quad , \end{aligned} \tag{117}$$

and

$$V_7^o = 2\phi_o \quad .$$

So Eq. (113) becomes

$$Z_{77}^o = \frac{2\phi_o}{j\,\frac{\omega A}{h}\,\epsilon_{33}^S \phi_o} = \frac{1}{j\omega C_o} \tag{118}$$

where Eq. (94) was employed.

The remaining impedances require one of the u_i^o to be finite and the other two to be zero. This obviously satisfies Eq. (59) for the two $u_i^o = 0$ components and makes four of the mechanical currents equal to zero. The fifth component of mechanical current can be made to vanish if the non-zero u_i^o is chosen to be zero at the appropriate surface ($\pm h$) and non-zero at the other ($\mp h$). This can be accomplished by choosing the non-zero u_i^o as

$$u_i^o = U_i \sin \eta^{(i)} (h \pm x_3) \quad . \tag{119}$$

However, we also require, for these impedances, that $I_7^o = 0$. Using Eqs. (92) and (116) this means that

$$I_7^o = -j\omega A D_3 = j\omega A\, \epsilon_{33}^S a_3 = 0 \quad ,$$

or $$a_3 = 0 \quad . \tag{120}$$

Substituting this requirement into Eq. (58) leads to

$$T^o_{3i} = c^{(i)} u^o_{i,3} \quad , \tag{121}$$

for the case under consideration.

Hence, the normal coordinate stresses corresponding to the zero components of normal coordinate displacements, u^o_i, of mode index, i, are zero and so are V^o_π, corresponding to these mode indexes from Eq. (111), and the corresponding $Z^o_{\pi\xi}$ of Eq. (113).

For example, take

$$u^o_2 = u^o_3 = 0 \tag{122}$$

$$u^o_1 = U_1 \sin \eta^{(1)} (h-x_3) ,$$

so that Eq. (112) gives $I^o_2 = I^o_3 = I^o_5 = I^o_6 = 0$, and let $I^o_7 = 0$. Eq. (121) requires that

$$T^o_{32} = T^o_{33} = 0 \; , \tag{123}$$

so that, from Eq. (111),

$$V^o_2 = V^o_3 = V^o_5 = V^o_6 = 0 \quad . \tag{124}$$

The choice for u^o_1 in Eq. (122) leads to

$$I^o_1 = -j\omega u^o_1(-h) = -j\omega U_1 \sin(2h\eta^{(1)}) = -j\omega U_1 \sin \Theta_1$$

$$I^o_4 = j\omega u^o(+h) = 0 \tag{125}$$

$$T^o_{31} = c^{(1)} u^o_{1,3} = -c^{(1)} U_1 \eta^{(1)} \cos \eta^{(1)} (h-x_3) \; .$$

Substituting this value of T^o_{31} into Eq. (111) gives

$$V^o_1 = A T^o_{31}(-h) = -c^{(1)} \eta^{(1)} A U_1 \cos(\eta^{(1)} 2h) = -\eta^{(1)} c^{(1)} A U_1 \cos \Theta_1$$

$$V^o_4 = A T^o_{31}(+h) = -c^{(1)} \eta^{(1)} U_1 A \; . \tag{126}$$

Then, from Eqs. (113) and (124),

$$Z^{o}_{21} = Z^{o}_{31} = Z^{o}_{51} = Z^{o}_{61} = 0 \,. \tag{127}$$

If, in place of u^{o}_{1} in Eq. (122), we had chosen u^{o}_{2} to be finite and let $u^{o}_{1} = 0$, then $V^{o}_{1} = V^{o}_{3} = V^{o}_{4} = V^{o}_{6} = 0$ in Eq. (124), while $I^{o}_{2} \neq 0$ and $I^{o}_{5} = 0$ in Eq. (125), so that

$$Z^{o}_{12} = Z^{o}_{32} = Z^{o}_{42} = Z^{o}_{62} = 0 \,. \tag{128}$$

Repeating the argument, with u^{o}_{3} finite, yields

$$Z^{o}_{13} = Z^{o}_{23} = Z^{o}_{43} = Z^{o}_{53} = 0 \,. \tag{129}$$

Returning, now, to the finite impedances resulting from the choice in Eq. (122), the values in Eqs. (125) and (126) lead to

$$Z^{o}_{11} = \frac{V^{o}_{1}}{I^{o}_{1}} = \frac{\eta^{(1)} c^{(1)} A \cos \Theta_1}{j\,\omega \sin \Theta_1} = \frac{Z_o^{(1)}}{j \tan \Theta_1} \tag{130}$$

$$Z^{o}_{41} = \frac{V^{o}_{4}}{I^{o}_{1}} = \frac{c^{(1)} \eta^{(1)} A}{j\,\omega \sin \Theta_1} = \frac{Z_o^{(1)}}{j \sin \Theta_1} \tag{131}$$

where definitions in Eq. (76) have been employed and $\Theta_i = 2h\,\eta^{(i)}$.

If the choice in (122) had been

$$u^{o}_{1} = U_1 \sin \eta^{(1)} (h + x_3) \tag{132}$$

the result would have been

$$I^{o}_{1} = -j\,\omega u^{o}_{1}(-h) = 0$$

$$I^{o}_{4} = j\omega u^{o}_{1}(+h) = j\omega U_1 \sin(\eta^{(1)} 2h) = j\omega U_1 \sin \Theta_1$$

$$T^{o}_{31} = c^{(1)} U_1 \eta^{(1)} \cos((h + x_3)\,\eta^{(1)}) \,. \tag{133}$$

This leads to

$$V_1^o = A\,T_{31}^o(-h) = c^{(1)}\eta^{(1)}U_1 A$$

$$V_4^o = A\,T_{31}^o(+h) = c^{(1)}\eta^{(1)}A\,U_1 \cos(\eta^{(1)}2h)\ . \qquad (134)$$

Substituting these values into Eq. (113) leads to

$$Z_{44}^o = \frac{V_4^o}{I_4^o} = \frac{Z_o^{(1)}}{j\tan\Theta_1} = Z_{11}^o$$

$$Z_{14} = \frac{V_1^o}{I_4^o} = \frac{Z_o^{(1)}}{j\sin\Theta_1} = Z_{41}^o\ , \qquad (135)$$

while the requirement that $u_2^o = u_3^o = 0$ still requires $V_2^o = V_3^o = V_5^o = V_6^o = 0$. Hence,

$$Z_{24}^o = Z_{34}^o = Z_{54}^o = Z_{64}^o = 0\ . \qquad (136)$$

It is now obvious that repeating this procedure, using u_2^o and u_3^o in place of u_1^o in Eqs. (122) and (132), and setting $u_1^o = 0$, will yield:

$$Z_{22}^o = Z_{55}^o = \frac{Z_o^{(2)}}{j\tan\theta_2}$$

$$Z_{25}^o = Z_{52}^o = \frac{Z_o^{(2)}}{j\sin\theta_2}$$

$$Z_{33}^o = Z_{66}^o = \frac{Z_o^{(3)}}{j\tan\theta_3} \qquad (137)$$

$$Z_{36}^o = Z_{63}^o = \frac{Z_o^{(3)}}{j\sin\theta_3}$$

$$Z_{15}^o = Z_{35}^o = Z_{45}^o = Z_{65}^o = Z_{16}^o = Z_{26}^o = Z_{46}^o = Z_{56}^o = 0\ .$$

Thus, all the elements except the electromechanical transfer impedances have been calculated.

These can be obtained by, again, requiring $I_7^o = 0$. Using Eqs. (92) and (116) leads to

$$I_7^o = -j\omega AD_3 = j\omega A\,\epsilon_{33}^s\, a_3 = 0 \tag{138}$$

so that

$$a_3 = 0 \ . \tag{139}$$

If this value is substituted into Eq. (62) it becomes

$$\phi = \left(\frac{e_{3k3}^o}{\epsilon_{33}^s} \right) u_k^o + b_3 \ , \tag{140}$$

where the sum over k is to be taken.

With the sign convention adopted in Figure 9,

$$V_7^o = \left[\phi_{(x_3=+h)} - \phi_{(x_3=-h)} \right] \ . \tag{141}$$

If the choice for mechanical displacements in Eq. (122) is made Eqs. (140) and (141) become

$$\phi = \frac{e_{313}^o}{\epsilon_{33}^s} u_1^o + b_1 \tag{142}$$

$$V_7^o = \left[\frac{e_{313}^o}{\epsilon_{33}^s} u_1^o(+h) - \frac{e_{313}^o}{\epsilon_{33}^s} u_1^o(-h) \right] \ ,$$

which, for this particular choice for the form of u_1^o, leads to

$$V_7^o = \frac{-e_{313}^o}{\epsilon_{33}^s} U_1 \sin(\eta^{(1)} 2h) \ . \tag{143}$$

When Eqs. (143) and (125) are substituted into Eq. (113),

$$Z_{71}^o = \frac{V_7^o}{I_1^o} = \frac{e_{313}^o}{j\omega\epsilon_{33}^s} = \frac{n_1}{j\omega C_o} \ , \tag{144}$$

where Eqs. (94) and (102) have been used.

AD-A046 091 GENERAL ELECTRIC CO SYRACUSE N Y ELECTRONICS LAB F/G 9/5
MULTIMODE FILTERS.(U)
OCT 77 S WANUGA, C M STEARNS, A L KACHELMYER DAAB07-76-C-1337
UNCLASSIFIED ECOM-76-1337-F NL

2 OF 3
ADA046091

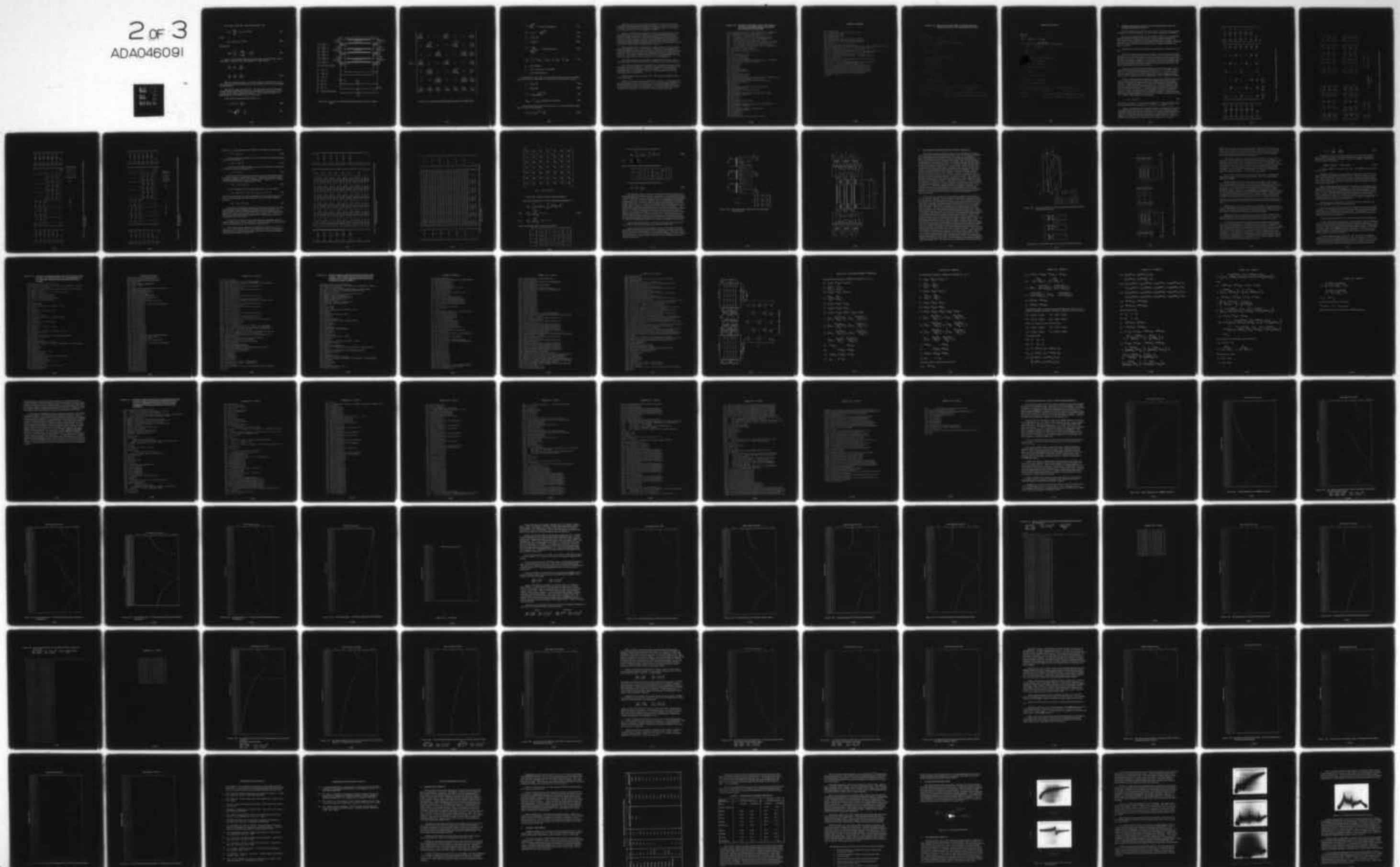

If the choice of u_1^o in Eq. (132) had been made, then

$$V_7^o = \frac{e_{313}^o}{\epsilon_{33}^s} U_1 \sin(\eta^{(1)} 2h) , \tag{145}$$

while

$$I_4^o = j\omega U_1 \sin(\eta^{(1)} 2h) . \tag{146}$$

This leads to

$$Z_{74}^o = \frac{V_7^o}{I_4^o} = \frac{e_{313}^o}{j\omega\epsilon_{33}^s} = \frac{n_1}{j\omega C_o} . \tag{147}$$

Again it is obvious that repeating this procedure, using u_2^o and u_3^o in place of u_1^o in Eqs. (122) and (132), and setting $u_1^o = 0$, will result in

$$Z_{72}^o = Z_{75}^o = \frac{n_2}{j\omega C_o}$$

$$Z_{73}^o = Z_{76}^o = \frac{n_3}{j\omega C_o} \tag{148}$$

While it should be possible, in a similar fashion, to show that $Z_{\xi 7} = Z_{7\xi}$, the requirement that this matrix must be symmetrical about the principal diagonal will be used here.

The goal has finally been achieved. The equivalent circuit of a thickness-excited thickness mode plate in the normal coordinate reference frame is shown in Figure 3-12 (which is identical to Figure 9). The Normal Coordinate Impedance Matrix of this plate is given in Figure 3-13.

In this matrix the parameters of interest are:

$$\theta_i = 2h\,\eta^{(1)} = \frac{2h\omega}{v^{(i)}} \tag{149}$$

$$\eta^{(i)} = \omega\sqrt{\frac{\rho}{c^{(i)}}} = \frac{\omega}{v^{(i)}} \tag{20}$$

$V_1^o = AT_{31}^o\,(-h)$

$V_2^o = AT_{32}^o\,(-h)$

$V_3^o = AT_{33}^o\,(-h)$

$V_4^o = AT_{31}^o\,(+h)$

$V_5^o = AT_{32}^o\,(+h)$

$V_6^o = AT_{33}^o\,(+h)$

V_7^o = Electrical Voltage

$I_1^o = -\dot{u}_1^o\,(-h)$

$I_2^o = -\dot{u}_2^o\,(-h)$

$I_3^o = -\dot{u}_3^o\,(-h)$

$I_4^o = \dot{u}_1^o\,(+h)$

$I_5^o = \dot{u}_2^o\,(+h)$

$I_6^o = \dot{u}_3^o\,(+h)$

I_7^o = Electrical Current

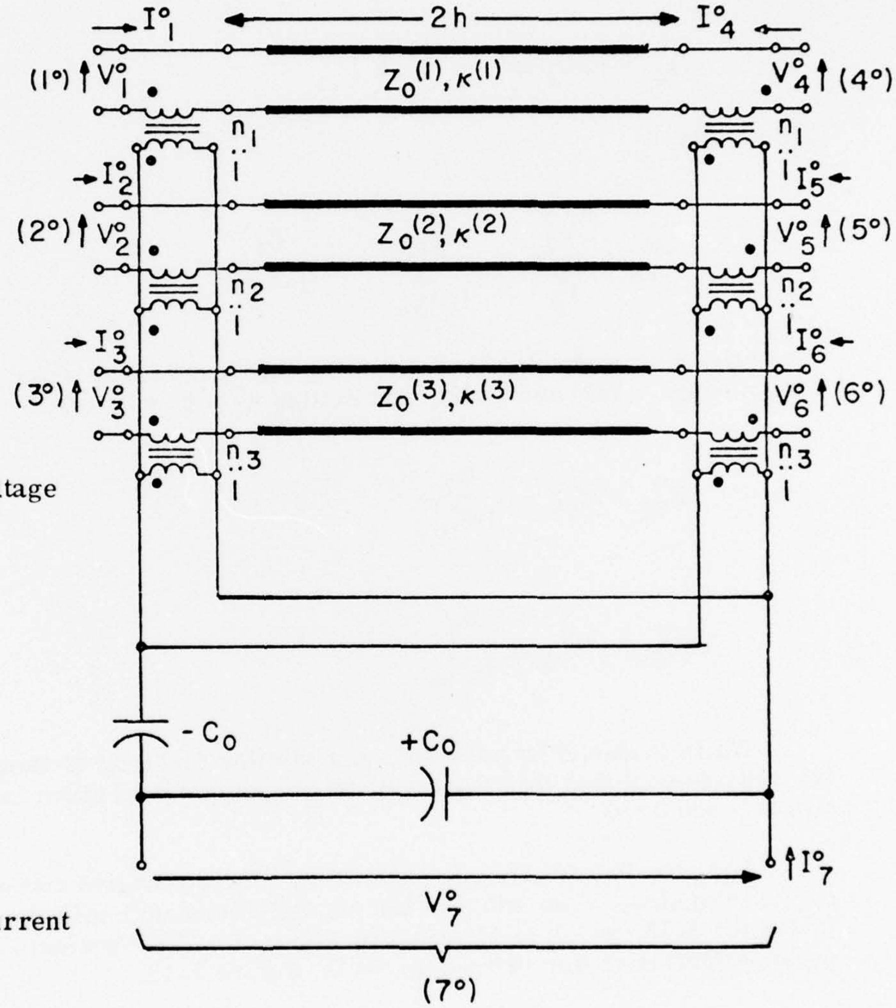

Figure 3-12. Seven-Port, Normal-Mode, Equivalent Circuit, for a TETM Plate

$$
[Z^{\circ}] = \begin{bmatrix}
\frac{Z_0^{(1)}}{j\tan\theta_1} & 0 & 0 & \frac{Z_0^{(1)}}{j\sin\theta_1} & 0 & 0 & \frac{n_1}{j\omega C_0} \\
0 & \frac{Z_0^{(2)}}{j\tan\theta_2} & 0 & 0 & \frac{Z_0^{(2)}}{j\sin\theta_2} & 0 & \frac{n_2}{j\omega C_0} \\
0 & 0 & \frac{Z_0^{(3)}}{j\tan\theta_3} & 0 & 0 & \frac{Z_0^{(3)}}{j\sin\theta_3} & \frac{n_3}{j\omega C_0} \\
\frac{Z_0^{(1)}}{j\sin\theta_1} & 0 & 0 & \frac{Z_0^{(1)}}{j\tan\theta_1} & 0 & 0 & \frac{n_1}{j\omega C_0} \\
0 & \frac{Z_0^{(2)}}{j\sin\theta_2} & 0 & 0 & \frac{Z_0^{(2)}}{j\tan\theta_2} & 0 & \frac{n_2}{j\omega C_0} \\
0 & 0 & \frac{Z_0^{(3)}}{j\sin\theta_3} & 0 & 0 & \frac{Z_0^{(3)}}{j\tan\theta_3} & \frac{n_3}{j\omega C_0} \\
\frac{n_1}{j\omega C_0} & \frac{n_2}{j\omega C_0} & \frac{n_3}{j\omega C_0} & \frac{n_1}{j\omega C_0} & \frac{n_2}{j\omega C_0} & \frac{n_3}{j\omega C_0} & \frac{1}{j\omega C_0}
\end{bmatrix}
$$

Figure 3-13. Normal Coordinate Impedance Matrix of a TETM Plate

$$v^{(i)} = \sqrt{\frac{c^{(i)}}{\rho}} = \text{velocity of propagation} \tag{72}$$

$$Z_o^{(i)} = A\rho v^{(i)} = A\sqrt{\rho c^{(i)}} \tag{76}$$

$$C_o = A\,\epsilon_{33}^{s}/2h \tag{94}$$

$$n_i = A\,e_{33i}^{o}/2h \tag{102}$$

$$k^{(i)} = \frac{e_{33i}^{o}}{\sqrt{\epsilon_{33}^{s} c^{(i)}}} = \text{coupling coefficient} \tag{88}$$

$$e_{33i}^{o} = \sum_{j=1}^{3} \beta_j^{(i)} e_{33j} = \beta_1^{(i)} e_{331} + \beta_2^{(i)} e_{332} + \beta_3^{(i)} e_{333} \tag{46}$$

$2h$ = plate thickness

A = area of concern $\perp$ to thickness

ρ = plate material density

In expressions (94), (102), (88) and (46) the choice of x_3 in the thickness direction selects the coefficients; for an arbitrary direction m they become

$$C_o = A\,\epsilon_{mm}^{s}/2h \tag{94a}$$

$$n_i = Ae_{mmi}^{o}/2h \tag{102a}$$

$$k^{(i)} = A\,e_{mmi}^{o}/\sqrt{\epsilon_{mm}^{s} c^{(i)}} \tag{88a}$$

$$e_{mmi}^{o} = \beta_j^{(i)} e_{mmj} \text{ using the sign convention} \tag{46a}$$

A convenient expression for the turns ratio, n_i, can be obtained by using Eqs. (72), 76), (88), and (94);

$$(n_i)^2 = C_o Z_o (k^{(i)})^2 \frac{v^{(i)}}{2h} \;. \tag{150}$$

From Eq. (149) it is obvious that all the non-zero terms in the normal coordinate impedance matrix are frequency-dependent. Thus it is not practical to calculate the elements of this matrix as a separate identity, since it would have to be carried out for each frequency of interest.

However, in working with equivalent circuits of piezoelectric plates and describing material, it is usual to describe their piezoelectric properties in terms of coupling coefficients, velocities of propagation, dielectric constant and density. But, in order to use the normal coordinate matrix of Figure 3-13 in terms of already available constants, the properties must be specified in terms of the mode eigenvalves and eigenvectors as well as the appropriate tensor piezoelectric stress constants and dielectric constant.

These constants are available from the running of the previous programs, CROT and SYMEIG. Hence it is worthwhile, at this point, to accumulate the required information for the characterization of a plate, in the normal coordinate framework, and convert it to the more usual form of coupling coefficients and velocities. The program VCOUP, listed in Table 3-12, accomplishes this task. Again, the program has been written so that it is self-explanatory.

Line 160 is an index to keep track of the plate under discussion, since a multimode filter consists of several plates, which may or may not be identical.

Lines 165 through 290 are the input points for entering the output from the appropriate running of SYMEIG. Lines 295 through 330 are the input points for the output from the last part of the printout of CROT, for the material corresponding to the run of SYMEIG. Line 325 is the input point for the density of the plate under consideration.

All the program does is use Eqs. (46), (72), and (88) to make the appropriate calculations.

Table 3-13 shows the output of VCOUP for two plates. In the example the material in both cases was AT-cut quartz, with x_3 in the thickness direction, so the only difference in data is the plate label. The output consists of all the information about the plates under consideration for the multimode stacked filter required; so, at this point, it is possible to discard all previous data.

TABLE 3-12. LISTING OF PROGRAM VCØUP FOR THE CALCULATION OF NORMAL MODE VELOCITIES AND COUPLING COEFFICIENTS

```
100C PRØGRAM TØ CALCULATE THE VELØCITIES AND CØUPLING
101C CØEFFICIENTS FØR THE MØDES ØF A PLATE FØR USE
102C IN FØRMING THE NØRMAL MØDE MATRIX
110C    IT USES AS INPUT THE EIGENVALUES (EV) AND
111C    EIGENVECTØRS (B'S) WITH THE CØMPØNENTS ØF
112C    VECTØR STØRED BY CØLUMNS FRØM SYMEIG
120C    IT ALSØ USES THE PIEZØELECTRIC STRESS CØNSTANTS
121C    AND DIELECTRIC PERMITTIVITY APPRØPRIATE TØ THE
122C    DIRECTIØN ØF PRØPAGATIØN FRØM CRØT AS WELL
123C    AS THE DENSITY ØF THE PLATE UNDER CØNSIDERATIØN
140  DIMENSIØN EV(3),B(3,3),E(3)
150 DIMENSIØN EN(3),CT(3),XK(3)
155C ENTER PLATE NUMBER HERE I=1 TØ 9
160 I=1
165C EIGENVALUES EV(MØDE)
170 EV(1)=0.29239228E11
180 EV(2)=0.38256421E11
190 EV(3)=0.13012144E12
200C EIGENVECTØRS B(CØMPØNENT,MØDE) WITH THE CØMPØNENTS
201C FØR EACH MØDE STØRED BY CØLUMNS
210 B(1,1)=0.1E1
220 B(2,1)=0.0
230 B(3,1)=0.0
240 B(1,2)=0.0
250 B(2,2)=0.99806542
260 B(3,2)=0.62172451E-1
270 B(1,3)=0.0
280 B(2,3)=-0.62172451E-1
290 B(3,3)=0.99806542
295C PIEZØELECTRIC STRESS CØNSTANTS FØR THE APPRØPRIATE
296C PRØPAGATIØN DIRECTIØN J FRØM CRØT
297C E(1)=EEE(JJ1),E(2)=EEE(JJ2),E(3)=EEE(JJ3)
300 E(1)=-0.94904867E-1
310 E(2)=0.0
320 E(3)=0.0
325C DIELECTRIC CØNSTANT EPST(JJ) FRØM CRØT
330 EP=0.39816236E-10
335C DENSITY ØF THE PLATE MATERIAL
340 DT=2.649E3
355C CALCULATE NØRMAL MØDE PIEZØELECTRIC STRESS
356C CØNSTANTS EN(MØDE)
360 DØ 2 J=1,3
370 EN(J)=0.0
380 DØ 2 K=1,3
390 EN(J)=B(K,J)*E(K)+EN(J)
400 2 CØNTINUE
415C CALCULATE CØUPLING CØEFFICIENTS XK(MØDE) AND
416C VELØCITIES CT(MØDE)
420 DØ 3 J=1,3
430 XK(J)=SQRT(EN(J)*EN(J)/(EP*EV(J)))
440 CT(J)=SQRT(EV(J)/DT)
450 3 CØNTINUE
460 WRITE(6,100) I
470 WRITE(6,110)
480 WRITE(6,120) I,XK(1),I,XK(2),I,XK(3)
```

TABLE 3-12 (Cont'd)

```
490 WRITE(6,130)
500 WRITE(6,140) I,CT(1),I,CT(2),I,CT(3)
510 WRITE(6,150) I,DT
520 WRITE(6,160) I,EP
530 WRITE(6,170)
540 WRITE(6,180) I,B(1,1),I,B(1,2),I,B(1,3)
550 WRITE(6,190) I,B(2,1),I,B(2,2),I,B(2,3)
560 WRITE(6,200) I,B(3,1),I,B(3,2),I,B(3,3)
600 STOP
610 100 FØRMAT(20X,'FØR PLATE ',I1)
620 110 FØRMAT(2X,'THE CØUPLING CØEFFICIENTS ARE  XK(MØDE,PLATE)',//)
630 120 FØRMAT(6X,'XK1',I1,' = ',F13.9,//,6X,'XK2',I1,
631& ' =',F13.9,//,6X,'XK3',I1,' = ',F13.9)
640 130 FØRMAT(//,2X,'THE VELØCITIES ARE  CT(MØDE,PLATE)',//)
650 140 FØRMAT(6X,'CT1',I1,' = ',E15.8,//,6X,'CT2',I1,
651& ' = ',E15.8,//,6X,'CT3',I1,' = ',E15.8)
660 150 FØRMAT(//,2X,'THE DENSITY IS',//,6X,'DT',I1,
661& ' = ',E15.8)
670 160 FØRMAT(//,2X,'THE DIELECTRIC CØNSTANT IS',//,
671& 6X,'EP',I1,' = ',E15.8)
680 170 FØRMAT(//,2X,'THE EIGENVECTØRS FØR THIS PLATE ',
681&  'ARE   B(PLATE)(CØMPØNENT,MØDE)',//)
690 180 FØRMAT(1X,'B',I1,'(1,1)=',E15.8,1X,'B',I1,
691& '(1,2)=',E15.8,1X,'B',I1,'(1,3)=',E15.8,//)
700 190 FØRMAT(1X,'B',I1,'(2,1)=',E15.8,1X,'B',I1,
701& '(2,2)=',E15.8,1X,'B',I1,'(2,3)=',E15.8,//)
710 200 FØRMAT(1X,'B',I1,'(3,1)=',E15.8,1X,'B',I1,
711&'(3,2)=',E15.8,1X,'B',I1,'(3,3)=',E15.8)
750 END
```

TABLE 3.13. RESULTS OF VCØUP FOR 2 PLATES OF AT CUT QUARTZ WITH X_3 IN THE THICKNESS DIRECTION

```
*RUNM-01

7487T    02/23/77     13.437

                    FOR PLATE 1
 THE COUPLING COEFFICIENTS ARE   XK(MODE,PLATE)

     XK11 =      0.08795302

     XK21 =     0.

     XK31 =      0.

 THE VELOCITIES ARE  CT(MODE,PLATE)

     CT11 =  0.33223239E 04

     CT21 =  0.35002414E 04

     CT31 =  0.70063352E 04

 THE DENSITY IS

     DT1 =  0.26490000E 04

 THE DIELECTRIC CONSTANT IS

     EP1 =  0.39810238E-10

 THE EIGENVECTORS FOR THIS PLATE ARE    B(PLATE)(COMPONENT,MODE)
B1(1,1)= 0.10000000E 01 B1(1,2)= 0.                B1(1,3)= 0.
B1(2,1)= 0.             B1(2,2)= 0.99806542E 00 B1(2,3)=-0.62172451E-01
B1(3,1)= 0.             B1(3,2)= 0.62172451E-01 B1(3,3)= 0.99806542E 00
```

TABLE 3-13. (Cont'd)

```
*160 I=2
*RUNH

3198T  02/26/77    15.992

                FOR PLATE 2
 THE COUPLING COEFFICIENTS ARE   XK(MODE,PLATE)

     XK12 =     0.03795802

     XK22 =     0.

     XK32 =     0.

 THE VELOCITIES ARE  CT(MODE,PLATE)

     CT12 =  0.33223239E 04

     CT22 =  0.33002414E 04

     CT32 =  0.70036352E 04

 THE DENSITY IS

     DT2 =  0.26490000E 04

 THE DIELECTRIC CONSTANT IS

     EP2 =  0.39816236E-10

 THE EIGENVECTORS FOR THIS PLATE ARE   B(PLATE)(COMPONENT,MODE)
B2(1,1)= 0.10000000E 01 B2(1,2)= 0.                B2(1,3)= 0.
B2(2,1)= 0.             B2(2,2)= 0.99806542E 00 B2(2,3)=-0.62172451E-0
B2(3,1)= 0.             B2(3,2)= 0.62172451E-01 B2(3,3)= 0.99806542E 0
```

D. TRANSFORMATION TO ACTUAL PLATE COORDINATES FROM THE NORMAL COORDINATE SYSTEM

After the difficult trail in the previous section, to go from the actual plate coordinates to normal coordinates, we now return to actual plate coordinates.

The normal mode equivalent circuit of Figure 3-12 and the corresponding impedance matrix in Figure 3-13 have left the port variables expressed in terms of the normal coordinate stresses and displacement components. For practical use, an equivalent circuit and matrix, with the port variables expressed in terms of the actual stresses and displacement components applied to the plate, is needed.

Equations 44, 45, 47 and 48 provide the mechanism for carrying out this task.

The matrix equation pertinent to the normal coordinate impedance matrix of Figure 3-13 is shown in Figure 3-14 in symbolic form. In this representation the appropriate form of the normal coordinate impedance element can be determined by comparing it to Figure 3-13. In Figure 3-14 the correspondence between the normal coordinate equivalent circuit variables and normal coordinate plate variables expressed by Equations 111 and 112 is also shown, along with a symbolic representation of the matrix operation.

Figure 3-15 shows the matrix interpretation of the tensor equations for the Normal Coordinate transformation in Equations 44, 45, 47 and 48. In this figure $[\beta]_t$ represents the transpose of the matrix, $[\beta]$, which is obtained by interchanging rows and columns of the matrix. This terminology agrees with the way the eigenvectors from SYMEIG were stored in NORM and VCOUP.

Figure 3-16 shows how the augmented matrix of this transformation would look in terms of the Equivalent Circuit Port Voltages when the Actual Plate Voltage Coordinates are expressed in terms of the Normal Coordinate Plate Voltages. This transformation is carried out by evaluating Equation 47 twice, once at the right side (top of the plate) where $x_3 = +h$ and once at the left side (bottom of the plate) where $x_3 = -h$; then we apply the definitions in Equation 111 to the result. In carrying out this expression the obvious corollary to Equation 111 has been applied to the actual plate variables. After performing these two transformations they were written in a manner that yielded the desired 7×7 matrix. This resulted in the expression,

$$[V] = [B][V^o] , \tag{151}$$

where $[B]$ is related to $[\beta]$ as shown in Figure 16. Figure 3-16 also shows the relationship of the components of $[\beta]$ to the b_{ij} components of $[B]$.

Figure 3-17 shows how the augmented matrix, for expressing the normal coordinate equivalent circuit port currents in terms of the actual coordinate equivalent circuit port currents, would look. A comparison of this figure with Figure 3-16 shows that the matrix in Figure 3-17 is equal to the matrix of Figure 3-16, with the rows and columns interchanged. However, this is the definition of a transpose of a matrix; hence the symbol $[B]_t$ is used in

$$
\begin{bmatrix}
V_1^o = A\,T_{31}^o(-h) \\
V_2^o = A\,T_{32}^o(-h) \\
V_3^o = A\,T_{33}^o(-h) \\
V_4^o = A\,T_{31}^o(+h) \\
V_5^o = A\,T_{32}^o(+h) \\
V_6^o = A\,T_{33}^o(+h) \\
V_7^o = V_7^o
\end{bmatrix}
=
\left|\begin{array}{c|c|c|c|c|c|c}
Z_{11}^o & 0 & 0 & Z_{14}^o & 0 & 0 & Z_{17}^o \\
0 & Z_{22}^o & 0 & 0 & Z_{25}^o & 0 & Z_{27}^o \\
0 & 0 & Z_{33}^o & 0 & 0 & Z_{36}^o & Z_{37}^o \\
Z_{14}^o & 0 & 0 & Z_{11}^o & 0 & 0 & Z_{17}^o \\
0 & Z_{25}^o & 0 & 0 & Z_{22}^o & 0 & Z_{27}^o \\
0 & 0 & Z_{36}^o & 0 & 0 & Z_{33}^o & Z_{37}^o \\
Z_{17}^o & Z_{27}^o & Z_{37}^o & Z_{17}^o & Z_{27}^o & Z_{37}^o & Z_{77}^o
\end{array}\right|
\begin{bmatrix}
I_1^o = -j\omega u_1^o(-h) \\
I_2^o = -j\omega u_2^o(-h) \\
I_3^o = -j\omega u_3^o(-h) \\
I_4^o = +j\omega u_1^o(+h) \\
I_5^o = +j\omega u_2^o(+h) \\
I_6^o = +j\omega u_3^o(+h) \\
I_7^o = I_7^o
\end{bmatrix}
$$

$$\left[V^o\right] = \left[Z^o\right] \quad \left[I^o\right]$$

Figure 3-14. Matrix Equation of the Normal Coordinate System

$$\begin{bmatrix} T^o_{31} \\ T^o_{32} \\ T^o_{33} \end{bmatrix} = \begin{bmatrix} \beta_1^{(1)} & \beta_2^{(1)} & \beta_3^{(1)} \\ \beta_1^{(2)} & \beta_2^{(2)} & \beta_3^{(2)} \\ \beta_1^{(3)} & \beta_2^{(3)} & \beta_3^{(3)} \end{bmatrix} \begin{bmatrix} T_{31} \\ T_{32} \\ T_{33} \end{bmatrix} \qquad \begin{bmatrix} u^o_1 \\ u^o_2 \\ u^o_3 \end{bmatrix} = \begin{bmatrix} \beta_1^{(1)} & \beta_2^{(1)} & \beta_3^{(1)} \\ \beta_1^{(2)} & \beta_2^{(2)} & \beta_3^{(2)} \\ \beta_1^{(3)} & \beta_2^{(3)} & \beta_3^{(3)} \end{bmatrix} \begin{bmatrix} u_1 \\ u_2 \\ u_3 \end{bmatrix}$$

$$\begin{bmatrix} T_{31} \\ T_{32} \\ T_{33} \end{bmatrix} = \begin{bmatrix} \beta_1^{(1)} & \beta_1^{(2)} & \beta_1^{(3)} \\ \beta_2^{(1)} & \beta_2^{(2)} & \beta_2^{(3)} \\ \beta_3^{(1)} & \beta_3^{(2)} & \beta_3^{(3)} \end{bmatrix} \begin{bmatrix} T^o_{31} \\ T^o_{32} \\ T^o_{33} \end{bmatrix} \qquad \begin{bmatrix} u_1 \\ u_2 \\ u_3 \end{bmatrix} = \begin{bmatrix} \beta_1^{(1)} & \beta_1^{(2)} & \beta_1^{(3)} \\ \beta_2^{(1)} & \beta_2^{(2)} & \beta_2^{(3)} \\ \beta_3^{(1)} & \beta_3^{(2)} & \beta_3^{(3)} \end{bmatrix} \begin{bmatrix} u^o_1 \\ u^o_2 \\ u^o_3 \end{bmatrix}$$

$[T_3] = [\beta]\,[T^o_3]$ $\qquad$ $[u] = [\beta]\,[u^o]$

$[T^o_3] = [\beta]_t\,[T^o_3]$ $\qquad$ $[\beta]_t$ = transpose of $[\beta]$ $\qquad$ $[u^o] = [\beta]_t\,[u]$

Figure 3-15. Matrix Representation of Coordinate Transformation Equations

$$
\begin{bmatrix}
V_1 = AT_{31}(-h) \\
V_2 = AT_{32}(-h) \\
V_3 = AT_{33}(-h) \\
V_4 = AT_{31}(+h) \\
V_5 = AT_{32}(+h) \\
V_6 = AT_{33}(+h) \\
V_7 = V_7
\end{bmatrix}
=
\left[\begin{array}{ccc:ccc:c}
\beta_1^{(1)} = b_{11} & \beta_1^{(2)} = b_{12} & \beta_1^{(3)} = b_{13} & 0 & 0 & 0 & 0 \\
\beta_2^{(1)} = b_{21} & \beta_2^{(2)} = b_{22} & \beta_2^{(3)} = b_{23} & 0 & 0 & 0 & 0 \\
\beta_3^{(1)} = b_{31} & \beta_3^{(2)} = b_{32} & \beta_3^{(3)} = b_{33} & 0 & 0 & 0 & 0 \\
\hdashline
0 & 0 & 0 & \beta_1^{(1)} = b_{11} & \beta_1^{(2)} = b_{12} & \beta_1^{(3)} = b_{13} & 0 \\
0 & 0 & 0 & \beta_2^{(1)} = b_{21} & \beta_2^{(2)} = b_{22} & \beta_2^{(3)} = b_{23} & 0 \\
0 & 0 & 0 & \beta_3^{(1)} = b_{31} & \beta_3^{(2)} = b_{32} & \beta_3^{(3)} = b_{33} & 0 \\
\hdashline
0 & 0 & 0 & 0 & 0 & 0 & 1 = b_{77}
\end{array}\right]
\begin{bmatrix}
V_1^o = AT_{31}^o(-h) \\
V_2^o = AT_{32}^o(-h) \\
V_3^o = AT_{33}^o(-h) \\
V_4^o = AT_{31}^o(+h) \\
V_5^o = AT_{32}^o(+h) \\
V_6^o = AT_{33}^o(+h) \\
V_7^o = V_7^o
\end{bmatrix}
$$

$$[V] = [B]\,[V^o] \qquad [B] = \left[\begin{array}{c:c:c} \beta & 0 & 0 \\ \hdashline 0 & \beta & 0 \\ \hdashline 0 & 0 & 1 \end{array}\right]$$

Figure 3-16. Matrix Equation of Actual Coordinate Port Voltages in Terms of Normal Coordinate Port Voltages

$$
\begin{bmatrix}
I_1^o = -j\omega u_1^o(-h) \\
I_2^o = -j\omega u_2^o(-h) \\
I_3^o = -j\omega u_3^o(-h) \\
I_4^o = j\omega u_1^o(+h) \\
I_5^o = j\omega u_2^o(+h) \\
I_6^o = j\omega u_3^o(+h) \\
I_7^o = I_7^o
\end{bmatrix}
=
\left[\begin{array}{ccc|ccc|c}
\beta_1^{(1)} = b_{11} & \beta_2^{(1)} = b_{21} & \beta_3^{(1)} = b_{31} & 0 & 0 & 0 & 0 \\
\beta_1^{(2)} = b_{12} & \beta_2^{(2)} = b_{22} & \beta_3^{(2)} = b_{32} & 0 & 0 & 0 & 0 \\
\beta_1^{(3)} = b_{13} & \beta_2^{(3)} = b_{23} & \beta_3^{(3)} = b_{33} & 0 & 0 & 0 & 0 \\
\hline
0 & 0 & 0 & \beta_1^{(1)} = b_{11} & \beta_2^{(1)} = b_{21} & \beta_3^{(1)} = b_{31} & 0 \\
0 & 0 & 0 & \beta_1^{(2)} = b_{12} & \beta_2^{(2)} = b_{22} & \beta_3^{(2)} = b_{32} & 0 \\
0 & 0 & 0 & \beta_1^{(3)} = b_{13} & \beta_2^{(3)} = b_{23} & \beta_3^{(3)} = b_{33} & 0 \\
\hline
0 & 0 & 0 & 0 & 0 & 0 & I = b_{77}
\end{array}\right]
\begin{bmatrix}
I_1 = -j\omega u_1(-h) \\
I_2 = -j\omega u_2(-h) \\
I_3 = -j\omega u_3(-h) \\
I_4 = +j\omega u_1(+h) \\
I_5 = +j\omega u_2(+h) \\
I_6 = +j\omega u_3(+h) \\
I_7 = I_7
\end{bmatrix}
$$

$$
[I^o] = [B]_t \; [I] \qquad\qquad [B]_t = \left[\begin{array}{c|c|c} \beta_t & 0 & 0 \\ \hline 0 & \beta_t & 0 \\ \hline 0 & 0 & 1 \end{array}\right]
$$

Figure 3-17. Matrix Equation of the Normal Coordinate Port Currents in Terms of Actual Coordinate Port Currents

Figure 3-17. The operation shown in Figure 3-17 results in the expression,

$$[I^O] = [B]_t [I] \tag{152}$$

The matrix equation of Figure 3-14, for the Normal Coordinate Equivalent Circuit Port Variables, is

$$[V^O] = [Z^O] [I^O] . \tag{153}$$

If the actual coordinate equivalent circuit port variables are represented by the matrix relation in Equation 154,

$$[V] = [Z] [I] . \tag{154}$$

Equations 151, 152, and 153 can be used to find the relationship between the actual coordinate impedance matrix $[Z]$ of Equation 154 and the normal coordinate Impedance matrix $[Z^O]$ of Equation 153. Replacing $[I^O]$ of Equation 153 by its Equivalent in Equation 152, yields

$$[V^O] = [Z^O] [B]_t [I] . \tag{155}$$

If $[V^O]$ in Equation 155 is now pre multiplied by $[B]$ the result is

$$[V] = [B] [V^O] = [B] [Z^O] [B]_t [I] = [Z] [I] . \tag{156}$$

The identity in Equation 156 clearly establishes the relationship between the actual coordinate impedance matrix and the normal coordinate impedance matrix as

$$[Z] = [B] [Z^O] [B]_t . \tag{157}$$

The operation expressed in Equation 155 is shown in Figure 3-18, where the appropriate matrix multiplication technique has been employed. This figure shows the matrix elements expressed in terms of the eigenvector components and the b_{ij} elements of the $[B]$ matrix in Figure 3-16. Figure 3-19 shows the operation expressed in Equation 156, carried out in terms of the b_{ij} elements of the $[B]$ matrix.

The symmetry inherent in this Actual Coordinate Impedance matrix is shown in Figure 3-20. The variables here, may be identified by comparing them with the corresponding terms in the matrix of Figure 3-19.

After performing the operation of multiplying the matrices, it is relatively easy to write expressions for the elements in the actual coordinate impedance matrix in terms of the elements of the normal coordinate impedance matrix elements defined in Figure 3.13.

$$
\begin{bmatrix}
V_1^o = AT_{31}^o(-h) \\
V_2^o = AT_{32}^o(-h) \\
V_3^o = AT_{33}^o(\ h) \\
V_4^o = AT_{31}^o(+h) \\
V_5^o = AT_{32}^o(+h) \\
V_6^o = AT_{33}^o(+h) \\
\hline
V_7^o
\end{bmatrix}
=
\left[\begin{array}{c:c:c:c:c:c:c}
\begin{array}{l} Z_{11}^o\beta_1^{(1)} \\ = Z_{11}^o b_{11} \end{array} &
\begin{array}{l} Z_{11}^o\beta_2^{(1)} \\ = Z_{11}^o b_{21} \end{array} &
\begin{array}{l} Z_{11}^o\beta_3^{(1)} \\ = Z_{11}^o b_{31} \end{array} &
\begin{array}{l} Z_{14}^o\beta_1^{(1)} \\ = Z_{14}^o b_{11} \end{array} &
\begin{array}{l} Z_{14}^o\beta_2^{(1)} \\ = Z_{14}^o b_{21} \end{array} &
\begin{array}{l} Z_{14}^o\beta_3^{(1)} \\ = Z_{14}^o b_{31} \end{array} &
Z_{17}^o \\
\hdashline
\begin{array}{l} Z_{22}^o\beta_1^{(2)} \\ = Z_{22}^o b_{12} \end{array} &
\begin{array}{l} Z_{22}^o\beta_2^{(2)} \\ = Z_{22}^o b_{22} \end{array} &
\begin{array}{l} Z_{22}^o\beta_3^{(2)} \\ = Z_{22}^o b_{32} \end{array} &
\begin{array}{l} Z_{25}^o\beta_1^{(2)} \\ = Z_{25}^o b_{12} \end{array} &
\begin{array}{l} Z_{25}^o\beta_2^{(2)} \\ = Z_{25}^o b_{22} \end{array} &
\begin{array}{l} Z_{25}^o\beta_3^{(2)} \\ = Z_{25}^o b_{32} \end{array} &
Z_{27}^o \\
\hdashline
\begin{array}{l} Z_{33}^o\beta_1^{(3)} \\ = Z_{33}^o b_{13} \end{array} &
\begin{array}{l} Z_{33}^o\beta_2^{(3)} \\ = Z_{33}^o b_{23} \end{array} &
\begin{array}{l} Z_{33}^o\beta_3^{(3)} \\ = Z_{33}^o b_{33} \end{array} &
\begin{array}{l} Z_{36}^o\beta_1^{(3)} \\ = Z_{36}^o b_{13} \end{array} &
\begin{array}{l} Z_{36}^o\beta_2^{(3)} \\ = Z_{36}^o b_{23} \end{array} &
\begin{array}{l} Z_{36}^o\beta_3^{(3)} \\ = Z_{36}^o b_{33} \end{array} &
Z_{37}^o \\
\hdashline
\begin{array}{l} Z_{14}^o\beta_1^{(1)} \\ = Z_{14}^o b_{11} \end{array} &
\begin{array}{l} Z_{14}^o\beta_2^{(1)} \\ = Z_{14}^o b_{21} \end{array} &
\begin{array}{l} Z_{14}^o\beta_3^{(1)} \\ = Z_{14}^o b_{31} \end{array} &
\begin{array}{l} Z_{11}^o\beta_1^{(1)} \\ = Z_{11}^o b_{11} \end{array} &
\begin{array}{l} Z_{11}^o\beta_2^{(1)} \\ = Z_{11}^o b_{21} \end{array} &
\begin{array}{l} Z_{11}^o\beta_3^{(1)} \\ = Z_{11}^o b_{31} \end{array} &
Z_{17}^o \\
\hdashline
\begin{array}{l} Z_{25}^o\beta_1^{(2)} \\ = Z_{25}^o b_{12} \end{array} &
\begin{array}{l} Z_{25}^o\beta_2^{(2)} \\ = Z_{25}^o b_{22} \end{array} &
\begin{array}{l} Z_{25}^o\beta_1^{(2)} \\ = Z_{25}^o b_{32} \end{array} &
\begin{array}{l} Z_{22}^o\beta_1^{(2)} \\ = Z_{22}^o b_{12} \end{array} &
\begin{array}{l} Z_{22}^o\beta_2^{(2)} \\ = Z_{22}^o b_{22} \end{array} &
\begin{array}{l} Z_{22}^o\beta_3^{(2)} \\ = Z_{22}^o b_{32} \end{array} &
Z_{27}^o \\
\hdashline
\begin{array}{l} Z_{36}^o\beta_1^{(3)} \\ = Z_{36}^o b_{13} \end{array} &
\begin{array}{l} Z_{36}^o\beta_2^{(3)} \\ = Z_{36}^o b_{23} \end{array} &
\begin{array}{l} Z_{36}^o\beta_3^{(3)} \\ = Z_{36}^o b_{33} \end{array} &
\begin{array}{l} Z_{33}^o\beta_1^{(3)} \\ = Z_{33}^o b_{13} \end{array} &
\begin{array}{l} Z_{33}^o\beta_2^{(3)} \\ = Z_{33}^o b_{23} \end{array} &
\begin{array}{l} Z_{33}^o\beta_3^{(3)} \\ = Z_{33}^o b_{33} \end{array} &
Z_{37}^o \\
\hdashline
\begin{array}{l} Z_{17}^o\beta_1^{(1)} \\ +Z_{27}^o\beta_1^{(2)} \\ +Z_{37}^o\beta_1^{(3)} \\ = Z_{17}^o b_{11} \\ +Z_{27}^o b_{12} \\ +Z_{37}^o b_{13} \end{array} &
\begin{array}{l} Z_{17}^o\beta_2^{(1)} \\ +Z_{27}^o\beta_2^{(2)} \\ +Z_{37}^o\beta_2^{(3)} \\ = Z_{17}^o b_{21} \\ +Z_{27}^o b_{22} \\ +Z_{37}^o b_{23} \end{array} &
\begin{array}{l} Z_{17}^o\beta_3^{(1)} \\ +Z_{27}^o\beta_3^{(2)} \\ +Z_{37}^o\beta_3^{(3)} \\ = Z_{17}^o b_{31} \\ +Z_{27}^o b_{32} \\ +Z_{37}^o b_{33} \end{array} &
\begin{array}{l} Z_{17}^o\beta_1^{(1)} \\ +Z_{27}^o\beta_1^{(2)} \\ +Z_{37}^o\beta_1^{(3)} \\ = Z_{17}^o b_{11} \\ +Z_{27}^o b_{12} \\ +Z_{37}^o b_{13} \end{array} &
\begin{array}{l} Z_{17}^o\beta_2^{(1)} \\ +Z_{27}^o\beta_2^{(2)} \\ +Z_{37}^o\beta_2^{(3)} \\ = Z_{17}^o b_{21} \\ +Z_{27}^o b_{22} \\ +Z_{37}^o b_{23} \end{array} &
\begin{array}{l} Z_{17}^o\beta_3^{(1)} \\ +Z_{27}^o\beta_3^{(2)} \\ +Z_{37}^o\beta_3^{(3)} \\ = Z_{17}^o b_{31} \\ +Z_{27}^o b_{32} \\ +Z_{37}^o b_{33} \end{array} &
Z_{77}^o
\end{array}\right]
\begin{bmatrix}
I_1 = -j\omega u_1(-h) \\
I_2 = -j\omega u_2(-h) \\
I_3 = -j\omega u_3(-h) \\
I_4 = j\omega u_1(+h) \\
I_5 = j\omega u_2(+h) \\
I_6 = j\omega u_3(+h) \\
\hline
I_7
\end{bmatrix}
$$

Figure 3-18. Matrix Expressing Normal Coordinate Voltage Variables in Terms of Actual Coordinate Current Variables

$$
\begin{bmatrix}
V_1 = AT_{31}(-h) \\
V_2 = AT_{32}(-h) \\
V_3 = AT_{33}(-h) \\
V_4 = AT_{31}(+h) \\
V_5 = AT_{32}(+h) \\
V_6 = AT_{33}(+h) \\
V_7
\end{bmatrix}
=
\left[\begin{array}{c|c|c|c|c|c|c}
\begin{gathered} b_{11} Z^o_{11} b_{11} \\ +b_{12} Z^o_{22} b_{12} \\ +b_{13} Z^o_{33} b_{13} \end{gathered} &
\begin{gathered} b_{11} Z^o_{11} b_{21} \\ +b_{12} Z^o_{22} b_{22} \\ +b_{13} Z^o_{33} b_{23} \end{gathered} &
\begin{gathered} b_{11} Z^o_{11} b_{31} \\ +b_{12} Z^o_{22} b_{32} \\ +b_{13} Z^o_{33} b_{33} \end{gathered} &
\begin{gathered} b_{11} Z^o_{14} b_{11} \\ +b_{12} Z^o_{25} b_{12} \\ +b_{13} Z^o_{36} b_{13} \end{gathered} &
\begin{gathered} b_{11} Z^o_{14} b_{21} \\ +b_{12} Z^o_{25} b_{22} \\ +b_{13} Z^o_{36} b_{23} \end{gathered} &
\begin{gathered} b_{11} Z^o_{14} b_{31} \\ +b_{12} Z^o_{25} b_{32} \\ +b_{13} Z^o_{36} b_{33} \end{gathered} &
\begin{gathered} b_{11} Z^o_{17} \\ +b_{12} Z^o_{27} \\ +b_{13} Z^o_{37} \end{gathered} \\
\hline
\begin{gathered} b_{21} Z^o_{11} b_{11} \\ +b_{22} Z^o_{22} b_{12} \\ +b_{23} Z^o_{33} b_{13} \end{gathered} &
\begin{gathered} b_{21} Z^o_{11} b_{21} \\ +b_{22} Z^o_{22} b_{22} \\ +b_{23} Z^o_{33} b_{23} \end{gathered} &
\begin{gathered} b_{21} Z^o_{11} b_{31} \\ +b_{22} Z^o_{22} b_{32} \\ +b_{23} Z^o_{33} b_{33} \end{gathered} &
\begin{gathered} b_{21} Z^o_{14} b_{11} \\ +b_{22} Z^o_{25} b_{12} \\ +b_{23} Z^o_{36} b_{13} \end{gathered} &
\begin{gathered} b_{21} Z^o_{14} b_{21} \\ +b_{22} Z^o_{25} b_{22} \\ +b_{23} Z^o_{36} b_{23} \end{gathered} &
\begin{gathered} b_{21} Z^o_{14} b_{31} \\ +b_{22} Z^o_{25} b_{32} \\ +b_{23} Z^o_{36} b_{33} \end{gathered} &
\begin{gathered} b_{21} Z^o_{17} \\ +b_{22} Z^o_{27} \\ +b_{23} Z^o_{37} \end{gathered} \\
\hline
\begin{gathered} b_{31} Z^o_{11} b_{11} \\ +b_{32} Z^o_{22} b_{12} \\ +b_{33} Z^o_{33} b_{13} \end{gathered} &
\begin{gathered} b_{31} Z^o_{11} b_{21} \\ +b_{32} Z^o_{22} b_{22} \\ +b_{33} Z^o_{33} b_{23} \end{gathered} &
\begin{gathered} b_{31} Z^o_{11} b_{31} \\ +b_{32} Z^o_{22} b_{32} \\ +b_{33} Z^o_{33} b_{33} \end{gathered} &
\begin{gathered} b_{31} Z^o_{14} b_{11} \\ +b_{32} Z^o_{25} b_{12} \\ +b_{33} Z^o_{36} b_{13} \end{gathered} &
\begin{gathered} b_{31} Z^o_{14} b_{21} \\ +b_{32} Z^o_{25} b_{22} \\ +b_{33} Z^o_{36} b_{23} \end{gathered} &
\begin{gathered} b_{31} Z^o_{14} b_{31} \\ +b_{32} Z^o_{25} b_{32} \\ +b_{33} Z^o_{36} b_{33} \end{gathered} &
\begin{gathered} b_{31} Z^o_{17} \\ +b_{32} Z^o_{27} \\ +b_{33} Z^o_{37} \end{gathered} \\
\hline
\begin{gathered} b_{11} Z^o_{14} b_{11} \\ +b_{12} Z^o_{25} b_{12} \\ +b_{13} Z^o_{36} b_{13} \end{gathered} &
\begin{gathered} b_{11} Z^o_{14} b_{21} \\ +b_{12} Z^o_{25} b_{22} \\ +b_{13} Z^o_{36} b_{23} \end{gathered} &
\begin{gathered} b_{11} Z^o_{14} b_{31} \\ +b_{12} Z^o_{25} b_{32} \\ +b_{13} Z^o_{36} b_{33} \end{gathered} &
\begin{gathered} b_{11} Z^o_{11} b_{11} \\ +b_{12} Z^o_{22} b_{12} \\ +b_{13} Z^o_{33} b_{13} \end{gathered} &
\begin{gathered} b_{11} Z^o_{11} b_{21} \\ +b_{12} Z^o_{22} b_{22} \\ +b_{13} Z^o_{33} b_{23} \end{gathered} &
\begin{gathered} b_{11} Z^o_{11} b_{31} \\ +b_{12} Z^o_{22} b_{32} \\ +b_{13} Z^o_{33} b_{33} \end{gathered} &
\begin{gathered} b_{11} Z^o_{17} \\ +b_{12} Z^o_{27} \\ +b_{13} Z^o_{37} \end{gathered} \\
\hline
\begin{gathered} b_{21} Z^o_{14} b_{11} \\ +b_{22} Z^o_{25} b_{12} \\ +b_{23} Z^o_{36} b_{13} \end{gathered} &
\begin{gathered} b_{21} Z^o_{14} b_{21} \\ +b_{22} Z^o_{25} b_{22} \\ +b_{23} Z^o_{36} b_{23} \end{gathered} &
\begin{gathered} b_{21} Z^o_{14} b_{31} \\ +b_{22} Z^o_{25} b_{32} \\ +b_{23} Z^o_{36} b_{33} \end{gathered} &
\begin{gathered} b_{21} Z^o_{11} b_{11} \\ +b_{22} Z^o_{22} b_{12} \\ +b_{23} Z^o_{33} b_{13} \end{gathered} &
\begin{gathered} b_{21} Z^o_{11} b_{21} \\ +b_{22} Z^o_{22} b_{22} \\ +b_{23} Z^o_{33} b_{23} \end{gathered} &
\begin{gathered} b_{21} Z^o_{11} b_{31} \\ +b_{22} Z^o_{22} b_{32} \\ +b_{23} Z^o_{33} b_{33} \end{gathered} &
\begin{gathered} b_{21} Z^o_{17} \\ +b_{22} Z^o_{27} \\ +b_{23} Z^o_{37} \end{gathered} \\
\hline
\begin{gathered} b_{31} Z^o_{14} b_{11} \\ +b_{32} Z^o_{25} b_{12} \\ +b_{33} Z^o_{36} b_{13} \end{gathered} &
\begin{gathered} b_{31} Z^o_{14} b_{21} \\ +b_{32} Z^o_{25} b_{22} \\ +b_{33} Z^o_{36} b_{23} \end{gathered} &
\begin{gathered} b_{31} Z^o_{14} b_{31} \\ +b_{32} Z^o_{25} b_{32} \\ +b_{33} Z^o_{36} b_{33} \end{gathered} &
\begin{gathered} b_{31} Z^o_{11} b_{11} \\ +b_{32} Z^o_{22} b_{12} \\ +b_{33} Z^o_{33} b_{13} \end{gathered} &
\begin{gathered} b_{31} Z^o_{11} b_{21} \\ +b_{32} Z^o_{22} b_{22} \\ +b_{33} Z^o_{33} b_{23} \end{gathered} &
\begin{gathered} b_{31} Z^o_{11} b_{31} \\ +b_{32} Z^o_{22} b_{32} \\ +b_{33} Z^o_{33} b_{33} \end{gathered} &
\begin{gathered} b_{31} Z^o_{17} \\ +b_{32} Z^o_{27} \\ +b_{33} Z^o_{37} \end{gathered} \\
\hline
\begin{gathered} Z^o_{17} b_{11} \\ +Z^o_{27} b_{12} \\ +Z^o_{37} b_{13} \end{gathered} &
\begin{gathered} Z^o_{17} b_{21} \\ +Z^o_{27} b_{22} \\ +Z^o_{37} b_{23} \end{gathered} &
\begin{gathered} Z^o_{17} b_{31} \\ +Z^o_{27} b_{32} \\ +Z^o_{37} b_{33} \end{gathered} &
\begin{gathered} Z^o_{17} b_{11} \\ +Z^o_{27} b_{12} \\ +Z^o_{37} b_{13} \end{gathered} &
\begin{gathered} Z^o_{17} b_{21} \\ +Z^o_{27} b_{22} \\ +Z^o_{37} b_{23} \end{gathered} &
\begin{gathered} Z^o_{17} b_{31} \\ +Z^o_{27} b_{32} \\ +Z^o_{37} b_{33} \end{gathered} &
Z^o_{77}
\end{array}\right]
\begin{bmatrix}
I_1 = -j\omega u_1(-h) \\
I_2 = -j\omega u_2(-h) \\
I_3 = -j\omega u_3(-h) \\
I_4 = j\omega u_1(+h) \\
I_5 = j\omega u_2(+h) \\
I_6 = j\omega u_3(+h) \\
I_7
\end{bmatrix}
$$

Figure 3-19. Matrix Relating Actual Coordinate Voltage Variables to Actual Coordinate Current Variables

$$\begin{bmatrix} Z_{11} & Z_{12} & Z_{13} & Z_{14} & Z_{15} & Z_{16} & Z_{17} \\ Z_{12} & Z_{22} & Z_{23} & Z_{15} & Z_{25} & Z_{26} & Z_{27} \\ Z_{13} & Z_{23} & Z_{33} & Z_{16} & Z_{26} & Z_{36} & Z_{37} \\ Z_{14} & Z_{15} & Z_{16} & Z_{11} & Z_{12} & Z_{13} & Z_{17} \\ Z_{15} & Z_{25} & Z_{26} & Z_{12} & Z_{22} & Z_{23} & Z_{27} \\ Z_{16} & Z_{26} & Z_{36} & Z_{13} & Z_{23} & Z_{33} & Z_{37} \\ Z_{17} & Z_{27} & Z_{37} & Z_{17} & Z_{27} & Z_{37} & Z_{77} \end{bmatrix}$$

$$[Z] = [B] \, [Z^o] \, [B]_t$$

Figure 3-20. Actual Coordinate Impedance Matrix

For j and m ranging from 1 to 6 the appropriate expression is,

$$Z_{jm} = \sum_{p=1}^{3} b_{qp} Z^o_{pk} b_{\ell p} = \sum_{p=1}^{3} \beta_q^{(p)} Z^o_{pk} \beta_\ell^{(p)},$$

with $Z^o_{pk} = \dfrac{Z_o^{(p)}}{j \tan \theta_{(p)}}$ for $k = p$ (158)

and $Z^o_{pk} = \dfrac{Z_o^{(p)}}{j \sin \theta_{(p)}}$ for $k = p + 3$,

where the variables take the values shown below.

j	m	q	ℓ	k
1 to 3	1 to 3	j	m	p
	4 to 6	j	m - 3	p + 3
4 to 6	1 to 3	j - 3	m	p + 3
	4 to 6	j - 3	m - 3	p

For j or m equal to seven, the equation is,

$$Z_{jm} = \sum_{p=1}^{3} b_{qp} Z^{o}_{p7} = \sum_{p=1}^{3} \beta^{(p)}_{q} Z^{o}_{p7} , \tag{159}$$

with $$Z^{o}_{p7} = \frac{\beta^{(p)}}{C_o} ,$$

where the variables take the values shown below.

j	m	q	j	m	q
7	1 to 3	m	1 to 3	7	j
	4 to 6	m - 3	4 to 6		j - 3

For both j and m equal seven the equation is

$$Z_{77} = Z^{o}_{77} = \frac{1}{j\omega C_o} . \tag{160}$$

This impedance matrix is all that is required to specify the plate in the actual coordinate framework; however it would be nice to represent the normal coordinate equivalent circuit of Figure 3-12 as an Actual Coordinate Equivalent circuit. To do this, a network representation of the orthogonal transformation of Equations 44, 45, 47 and 48 is needed. Such a representation is available. Carlin and Giordano [18] show that a congruent transformation of a Z matrix ($C_t ZC$, where C is an $n \times n$ array of real values) can be represented as a multi-winding ideal transformer interconnection of the ports of the network. The orthogonal transformations of Equations 44, 45, 47 and 48 satisfy this condition since $\beta_t = \beta^{-1}$ and, incidentally, so does the coordinate rotation shown in Figure 3-2 and Equations 29 and 30. For the case of a 3 by 3 array this multi-winding ideal transformer is shown in Figure 3-21. This figure may be reversed, with the primary labeled with the superscripted variables upon interchanging sub and superscripts on the components of β (replace the components of β by the corresponding components of β_t) for the transformer turns ratios.

Applying this transformation to both plate surfaces of the crystal leads to the actual coordinate equivalent circuit shown in Figure 3-22.

Again, all the terms in the Impedance matrix of the actual coordinate Equivalent Circuit shown in Figure 3-20 are frequency dependent and, hence, there is no point in calculating them as a separate identity. Note, also, that in the general case every element is present in this Impedance matrix, whereas a large percentage of the elements of the normal mode impedance matrix of Figure 3-13 are zero.

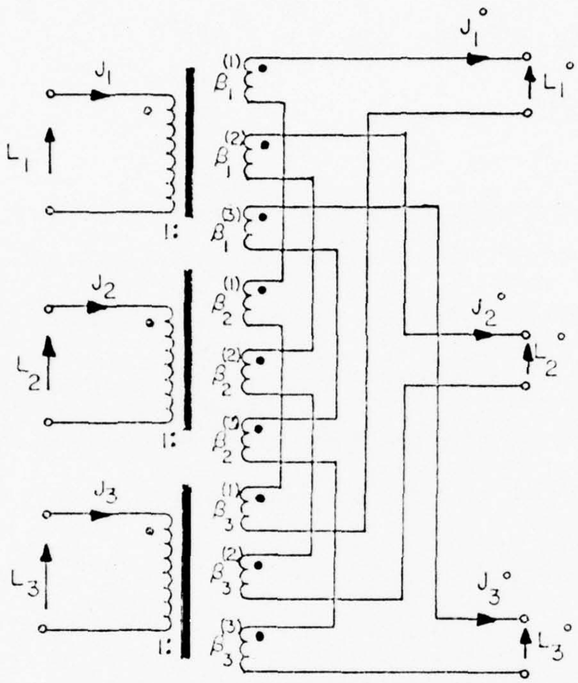

$$J = \beta J^{o}$$

$$L^{o} = \beta_{t} L$$

$$\beta = \begin{bmatrix} \beta_1^{(1)} & \beta_1^{(2)} & \beta_1^{(3)} \\ \beta_2^{(1)} & \beta_2^{(2)} & \beta_2^{(3)} \\ \beta_3^{(1)} & \beta_3^{(2)} & \beta_3^{(3)} \end{bmatrix}$$

Figure 3-21. Ideal Transformer Realization of an Orthogonal Transformation

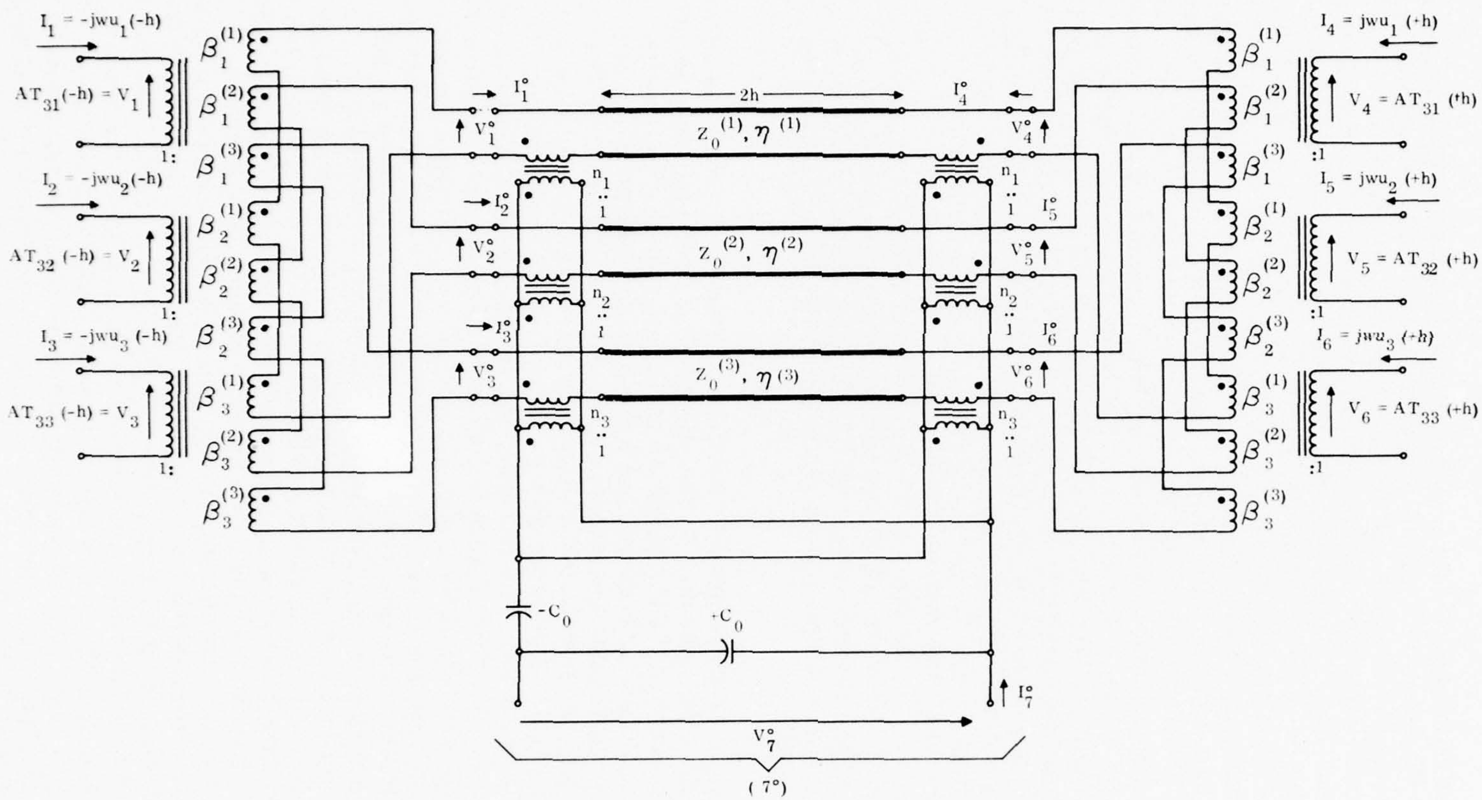

Figure 3-22. Seven Port Actual Coordinate Equivalent Circuit for a TETM Plate

E. MULTIMODE STACKED FILTERS AND MODE PROGRAMS

The actual coordinate impedance matrix for the TETM plate in Figure 3-20, or the equivalent circuit shown in Figure 3-22, are all that are required for an investigation of the multimode filters of concern in this program. Such a multimode filter consists of a group of such plates bonded together. If this is done with the actual coordinates of one plate, lined up with the actual coordinates of the preceding one, etc., the cascade consists of the equivalent circuit of Figure 3-22, where the ports 1, 2, 3 of the n^{th} plate (numbering left to right) are connected to ports 4, 5, 6, respectively, of the n-1 plate, with a prescribed network between them to account for the bond and to assure continuity of stress and displacement (velocity) across the boundary. The bond would be represented by a lumped constant T-version of the transmission line section shown in Figure 3-10. However, in general, bonds are lossy so that the j-multiplied trigonometric functions shown are replaced by hyperbolic functions and the propagation constant, θ, becomes complex. The values for $Z_0^{(i)}$ and θ_i also depend on the mode of propagation, so that a different circuit is required at each group of ports. The filter, in this case, is then completed by connecting, at least, one of the resulting electrical ports to a voltage generator with internal impedance, Z_g and, at least, one other of the ports to a load impedance, Z_ℓ. The other electrical ports are connected as desired. Of course, in the above description there is no requirement for the n^{th} plate parameters to bear any relationship to the plate parameters of any other plate. However, this description does require that the actual coordinates of each plate are lined up.

Even in the more general case the thickness coordinate of each plate in the stack must be lined up. In this discussion, each plate is assumed to have its x_3 coordinate in the thickness direction, so that this coordinate will be lined up; however, the only requirement for the x_1 and x_2 axes are that they form a right-hand rectangular coordinate system with the x_3 axis. So, in the general case, the lateral coordinates of one plate do not have to coincide with those of the next plate. This more general situation is illustrated for a two layer stack in Figure 3-23. The relationship between the axes shown in this figure can be determined from Figure 3-2 and are obtained from Equation 27. Since a coordinate rotation about a common origin is an orthogonal transformation[13] it can be represented by the ideal transformer network shown in Figure 3-21. In the particular case of coordinate rotation about a common x_3 axis, this general network reduces to the simpler one shown in Figure 3-24. Figure 3-25 shows the equivalent circuit for a two-layer stack, without a bond network between them, for two of the equivalent circuits for the plates shown in Figure 3-22, connected together with an arbitrary rotation about the assumed thickness direction. Figure 3-25 assumes that the coordinates of the plate on the left are the reference coordinates. In any multi-element structure of this type one plate must be used as the reference frame for the total system. If the structure is visualized as being built up in pieces, from left to right, it seems only logical to choose the first plate coordinates as the reference framework. The lack of a bond network in this figure assumes that the plates are in intimate contact with a rigid or welded contact between them, or that a lossless bond of negligible thickness has been used. One other observation should be made with regard to Figure 3-25. The electrical port variables have been turned around

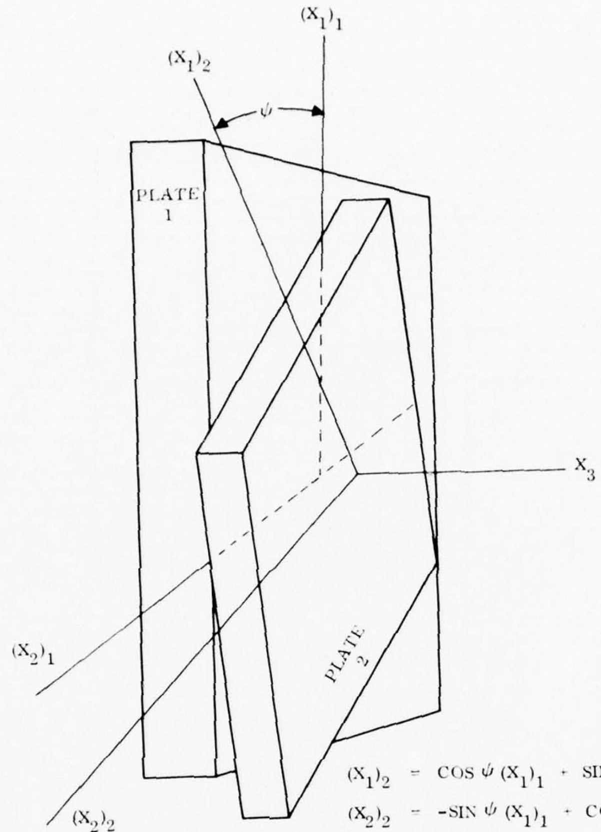

$$(X_1)_2 = \cos\psi\,(X_1)_1 + \sin\psi\,(X_2)_1$$
$$(X_2)_2 = -\sin\psi\,(X_1)_1 + \cos\psi\,(X_2)_1$$
$$(X_3)_2 = (X_3)_1$$

$$\begin{bmatrix}(X_1)_2\\(X_2)_2\\(X_3)_2\end{bmatrix} = \begin{bmatrix}a_{11} & a_{12} & a_{13}\\ a_{21} & a_{22} & a_{23}\\ a_{31} & a_{32} & a_{33}\end{bmatrix}\begin{bmatrix}(X_1)_1\\(X_2)_1\\(X_3)_1\end{bmatrix}$$

Figure 3-23. Two-Layer Stack of Crystal Plates Showing Relative Rotation About Common X_3 Axis

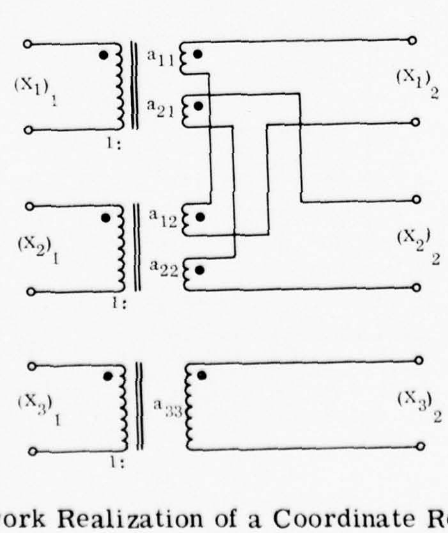

Figure 3-24. Network Realization of a Coordinate Rotation About X_3

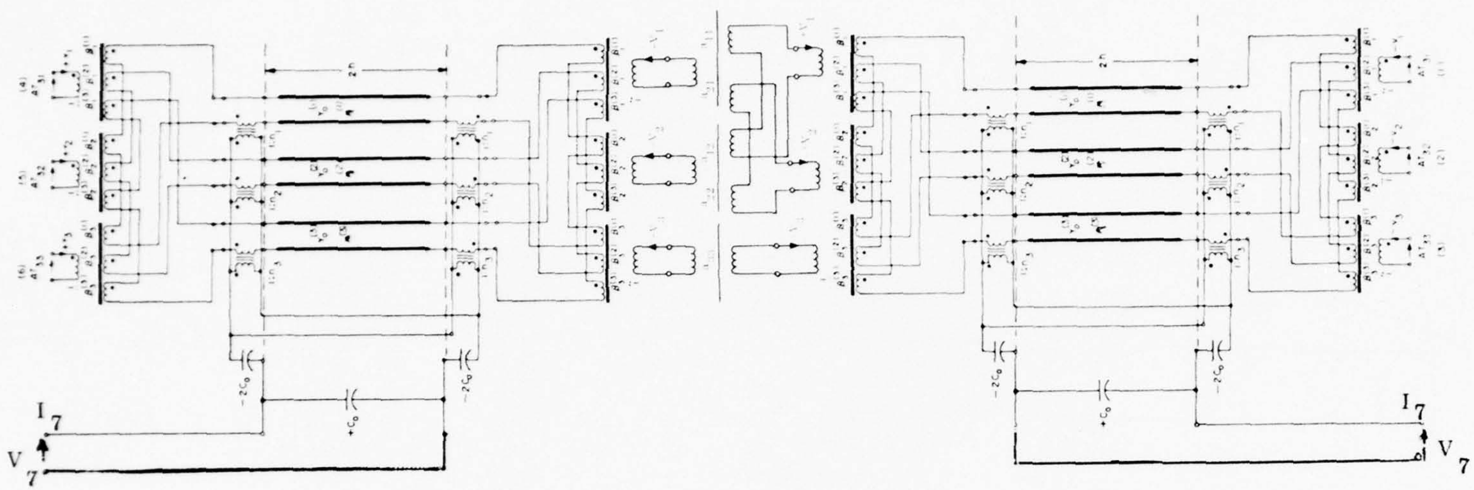

Figure 3-25. Equivalent Circuit of a Stacked Filter of Two Plates without Boundary Conditions Applied

between the two plates. This could be brought about in one of two ways: (1) either one plate could be reversed with respect to the other or, (2) if the port numbering system shown in Figure 3-25 is used, an ideal transformer with a 1 to 1 phase reversal would have to be inserted between the port variables shown and the plate connections, and then ignored.

In the work to follow it is this configuration in Figure 3-25 that is programmed, with the phase reversal transformer ignored and an intimate or rigid bond between plates assumed. As pointed out previously, conceptually, the inclusion of bonds is not a difficult task; however, they do complicate an already complicated circuit and tend to complicate the interpretation of the results. It, therefore, seems preferable to ignore them initially and concentrate on developing working programs. The programs are, likewise, limited to two plates but, again, procedures to include more are obvious.

In the course of this program three different two-plate, multimode programs were written, with varying assumptions. These are called MØDE1, MØDE2 and MØDE3.

MØDE1 assumes only one normal mode in each plate. This mode is either perpendicular or parallel to the plate direction and the plates in the filter stack are assumed to have their actual plate coordinates lined up. Thus, in essence, it is a transmission line representation of the lossless Mason Equivalent circuit. However, in arriving at the solution for this program, the same procedure was used, as in the MØDE2 and MØDE3 programs, instead of the common technique for the solution of a ladder network. It did not appear necessary to include plate rotation in this case since, unless the plates are oriented at right angles to each other (in which case no coupling between the mode in plate 1 and the mode in plate 2 takes place, so that the output is zero), the output will only be a reduced replica (more insertion loss) of the lined-up case.

MØDE2 allows for two normal modes to be present; these are assumed to be at right angles to the plate thickness so that there is no difference between normal coordinates and actual plate coordinates (x_1 and x_2). This program does allow for an arbitrary rotation to occur between plates.

MØDE3 is the program for the general case illustrated in Figure 3-25. All three normal modes are allowed and these may be at an angle to the actual plate coordinates; and one plate may be rotated with respect to the other.

In all three programs the two plates may have entirely different properties. In all the programs it is assumed that the electrodes for applying the fields are circular electrodes, on both the lateral surfaces of each plate. The area of these electrodes is also assumed to be the active area used in calculating the characteristic impedances. They also use the (common) convention of specifying a center frequency for each plate. In these programs the center frequency, f_0, is defined as "the frequency at which the plate thickness (2h in the previous discussion and TL in the programs) is a half wavelength thick at the velocity of propagation for model (CT1)". This center frequency is used as input data rather than the actual plate thickness,

$$f_o = F\phi = \frac{v^{(1)}}{2(2h)} = \frac{CT1}{2(TL)} \quad . \tag{161}$$

The frequency range of interest is specified in terms of the initial frequency, (FINIT), frequency increment between desired frequencies, (FINC) and number of frequencies in the range of interest, (IFREQ). If FFINAL is the last frequency of interest,

$$\text{IFREQ} = ((\text{FFINAL} - \text{FINIT})/\text{FINC}) + 1 \quad . \tag{162}$$

A listing of MØDE1 is shown in Table 3-14. The MØDE2 listing is given in Table 3-15.

These two programs do not, necessarily, require that information from CRØT, SYMEIG and VCØUP be supplied to them. They only require, as input, the coupling coefficients, velocities of the modes of interest, the plate densities, center frequencies, dielectric constants and electrode diameters for each plate, as well as the frequency range of interest. This information is inputted at lines 230 through 470.

Again, these programs were written for operation on the Honeywell Information Systems Series 6000/600 Computer, as installed at the General Electric ESD facility in Syracuse, in the YFØR mode of time-sharing operation. They also use a time-sharing plØt routine available at this facility in the permanent files. Lines 10, 130, 190, 200 and line 1960 all pertain to this particular plotting rØutine and, hence, do not apply to any other facility or mode of operation at this facility. However, it is relatively easy to convert or substitute other plotting programs for this particular one.

Most of the other statements are standard Fortran IV statements and should be adaptable to any other computing facility.

The free format statement at line 1810, in Mode 1 and 2 and at line 3020 in Mode 3, is a convenient way to write out the insertion loss versus frequency, and a great aid in trouble-shooting the programs. By inserting a write statement with this format reference at any appropriate place in the program, any desired variable can be printed out.

Again an attempt has been made to make the programs self-explanatory.

To aid in this Figure 3-26 shows the actual problem solved in the MØDE2 program and the assumed impedance matrix for each plate, obtained from the matrix in Figure 3-13 by eliminating rows and columns 3 and 6, corresponding to mode 3. The actual solution of this problem is shown in Table 3-16, using the nomenclature of the MØDE2 program. In general, for this case, the inherent symmetry of the plate matrices has been ignored, since this tends to make it easier to keep track of terms.

The IF conditions at lines 1675, 1677, 1707 and 1712 in the MØDE2 program allow for the handling of special cases. For example, if mode 2 is non-piezoelectrically coupled and the angle of plate rotation is zero, line 1712 is required. But this statement generally will not work at the resonant frequency of mode 2 in the case of identical plates; then line 1707 is required.

TABLE 3-14. LISTING OF PROGRAM MØDE1 STACKED FILTER OF TWO PLATES, ONE MODE IN EACH PLATE PERPENDICULAR TO THICKNESS DIRECTION (NO ROTATION BETWEEN PLATES)

```
10*#RUNH*;ADE576/RHYPLOT=(CØRE=28)
100C PRØGRAM TØ CALCULATE THE TRANSFER FUNCTIØN ØF A STACKED
101C FILTER ØF TWØ PLATES.
110C EACH PLATE HAS ØNLY ØNE PIEZØELECTRICALLY DRIVEN MØDE.
130 PARAMETER NPLTS=1
140 CØMPLEX ZL(5,5),ZR(5,5),ZLT(3,3),ZRT(3,3)
150 CØMPLEX ZRET(2,2)
160 CØMPLEX ZLE,ZG,EG,AMP1,AMP3
170 CØMPLEX AMP0,VIN,VØUT,ZIN
190 DIMENSIØN K1(NPLTS),PILØS(1000)
200 CHARACTER DA*1(NPLTS)/"*"/
210 K=0
220 PI=3.1415926
230C INPUT DATA
232C CENTER FREQUENCIES ØF PLATES 1 AND 2
240 F01=1.E7
250 F02=1.E7
255C DIAMETERS ØF PLATES 1 AND 2
260 D1=10.E-3
270 D2=10.E-3
280C PLATE CØNSTANTS
282C CØUPLING CØEFFICIENTS XK(MØDE,PLATE)
290 XK11=0.088
310 XK12=XK11
325C VELØCITIES CT(MØDE,PLATE)
330 CT11=3.32E3
350 CT12=CT11
365C DENSITIES ØF PLATES 1 AND 2
370 DT1=2.65E3
380 DT2=DT1
385C DIELECTRIC CØNSTANTS ØF PLATES 1 AND 2
390 EP1=4.58*8.85E-12
400 EP2=EP1
415C ELECTRICAL IMPEDANCES AND GENERATØR VØLTAGE
420 ZLE=CMPLX(1600.,0.)
430 ZG=ZLE
440 EG=CMPLX(1.,0.)
445C FREQUENCY RANGE ØF INTEREST
447C INITIAL FREQUENCY,FREQUENCY INTERVAL,NØ. ØF FREQUENCIES
448C IN RANGE
450 FINIT=9.7E6
460 FINC=0.025E6
470 IFREQ=69
490C AREAS ØF PLATES 1 AND 2
500 AREA1=PI*D1*D1/4.
510 AREA2=PI*D2*D2/4.
520C CHARACTERISTIC IMPEDANCES Z0(MØDE,PLATE)
530 Z011=AREA1*DT1*CT11
550 Z012=AREA2*DT2*CT12
570C THICKNESSES ØF PLATES 1 AND 2
580 TL1=CT11/(2.*F01)
590 TL2=CT12/(2.*F02)
600C CAPACITANCES C0 ØF PLATES 1 AND 2
610 C01=EP1*AREA1/TL1
620 C02=EP2*AREA2/TL2
```

TABLE 3-14 (Cont'd)

```
630C TURNS RATIØS XN(MØDE,PLATE)
640 XN11=XK11*SQRT(ZØ11*CØ1*2.*FØ1)
660 XN12=XK12*SQRT(ZØ12*CØ2*2.*FØ2)
680 FREQ=FINIT
690C LØØP THRØUGH FREQUENCIES
700 DØ1 I=1,IFREQ
710 K=K+1
720C PRØPAGATIØN CØNSTANTS THETA(MØDE,PLATE)
730 TH11=2.*PI*FREQ*TL1/CT11
750 TH12=2.*PI*FREQ*TL2/CT12
770C CØMPLEX IMPEDANCES
780 TGN11=SIN(TH11)/CØS(TH11)
800 TGN12=SIN(TH12)/CØS(TH12)
820 ZL(1,1)=CMPLX(0.,-ZØ11/TGN11)
830 ZL(1,2)=CMPLX(0.,0.)
840 ZL(1,3)=CMPLX(0.,-ZØ11/SIN(TH11))
850 ZL(1,4)=ZL(1,2)
860 ZL(1,5)=CMPLX(0.,-XN11/(2.*PI*FREQ*CØ1))
870 ZL(2,1)=ZL(1,2)
880 ZL(2,2)=ZL(1,2)
890 ZL(2,3)=ZL(1,2)
900 ZL(2,4)=ZL(1,2)
910 ZL(2,5)=ZL(1,2)
920 ZL(3,1)=ZL(1,3)
930 ZL(3,2)=ZL(1,2)
940 ZL(3,3)=ZL(1,1)
950 ZL(3,4)=ZL(1,2)
960 ZL(3,5)=ZL(1,5)
970 ZL(4,1)=ZL(1,2)
980 ZL(4,2)=ZL(2,4)
990 ZL(4,3)=ZL(1,2)
1000 ZL(4,4)=ZL(2,2)
1010 ZL(4,5)=ZL(2,5)
1020 ZL(5,1)=ZL(1,5)
1030 ZL(5,2)=ZL(2,5)
1040 ZL(5,3)=ZL(1,5)
1050 ZL(5,4)=ZL(2,5)
1060 ZL(5,5)=CMPLX(0.,-1./(2.*PI*FREQ*CØ1))
1070 ZR(1,1)=CMPLX(0.,-ZØ12/TGN12)
1080 ZR(1,2)=CMPLX(0.,0.)
1090 ZR(1,3)=CMPLX(0.,-ZØ12/SIN(TH12))
1100 ZR(1,4)=ZR(1,2)
1110 ZR(1,5)=CMPLX(0.,-XN12/(2.*PI*FREQ*CØ2))
1120 ZR(2,1)=ZR(1,2)
1130 ZR(2,2)=ZR(1,2)
1140 ZR(2,3)=ZR(1,2)
1150 ZR(2,4)=ZR(1,2)
1160 ZR(2,5)=ZR(1,2)
1170 ZR(3,1)=ZR(1,3)
1180 ZR(3,2)=ZR(1,2)
1190 ZR(3,3)=ZR(1,1)
1200 ZR(3,4)=ZR(1,2)
1210 ZR(3,5)=ZR(1,5)
1220 ZR(4,1)=ZR(1,2)
1230 ZR(4,2)=ZR(2,4)
1240 ZR(4,3)=ZR(1,2)
1250 ZR(4,4)=ZR(2,2)
1255 ZR(4,5)=ZR(2,5)
1260 ZR(5,1)=ZR(1,5)
1270 ZR(5,2)=ZR(2,5)
1280 ZR(5,3)=ZR(1,5)
```

TABLE 3-14. (Cont'd)

```
1290 ZR(5,4)=ZR(2,5)
1300 ZR(5,5)=CMPLX(0.,-1./(2.*PI*FREQ*C02))
1310C APPLY MECHANICAL BØUNDARY CØNDITIØNS TØ LEFT PLATE
1311C FØR PLATE 1 V1=0
1320 ZLT(1,1)=ZL(3,3)-ZL(3,1)*ZL(1,3)/ZL(1,1)
1330 ZLT(1,2)=CMPLX(0.,0.)
1340 ZLT(1,3)=ZL(3,5)-ZL(3,1)*ZL(1,5)/ZL(1,1)
1350 ZLT(2,1)=ZLT(1,2)
1360 ZLT(2,2)=ZLT(1,2)
1370 ZLT(2,3)=ZLT(1,2)
1380 ZLT(3,1)=ZL(5,3)-ZL(5,1)*ZL(1,3)/ZL(1,1)
1390 ZLT(3,2)=ZLT(1,2)
1400 ZLT(3,3)=ZL(5,5)-ZL(5,1)*ZL(1,5)/ZL(1,1)
1410C APPLY MECHANICAL BØUNDARY CØNDITIØNS TØ RIGHT PLATE
1411C FØR PLATE 2  V3=0
1420 ZRT(1,1)=ZR(1,1)-ZR(1,3)*ZR(3,1)/ZR(3,3)
1430 ZRT(1,2)=CMPLX(0.,0.)
1440 ZRT(1,3)=ZR(1,5)-ZR(1,3)*ZR(3,5)/ZR(3,3)
1450 ZRT(2,1)=ZRT(1,2)
1460 ZRT(2,2)=ZRT(1,2)
1470 ZRT(2,3)=ZRT(1,2)
1480 ZRT(3,1)=ZR(5,1)-ZR(5,3)*ZR(3,1)/ZR(3,3)
1490 ZRT(3,2)=ZRT(1,2)
1500 ZRT(3,3)=ZR(5,5)-ZR(5,3)*ZR(3,5)/ZR(3,3)
1510C TERMINATE PLATE 2 ØN RIGHT IN ZLE
1520 ZRET(1,1)=ZRT(1,1)-ZRT(1,3)*ZRT(3,1)/(ZLE+ZRT(3,3))
1530 ZRET(1,2)=CMPLX(0.,0.)
1540 ZRET(2,1)=ZRET(1,2)
1550 ZRET(2,2)=ZRET(1,2)
1660C AT THE JUNCTIØN ØF THE LEFT PLATE AND THE RIGHT
1661C PLATE,EQUATE VØLTAGES AND CURRENTS AND SØLVE FØR
1662C CURRENTS. V3(LEFT)=V1(RIGHT), I3(LEFT)=-I1(RIGHT)
1670C THIS GIVES I3 IN TERMS ØF IIN.
1671C WHEN THIS VALUE IS PUT IN THE EXPRESSIØN FØR V5(VIN)
1672C THE INPUT IMPEDANCE ZIN CAN BE ØBTAINED.
1680 ZIN=ZLT(3,3)-ZLT(3,1)*ZLT(1,3)/(ZLT(1,1)+ZRET(1,1))
1690 AMPI=EG/(ZG+ZIN)
1700 AMP3=-(ZLT(1,3)/(ZLT(1,1)+ZRET(1,1)))*AMPI
1720 VIN=ZLT(3,1)*AMP3+ZLT(3,3)*AMPI
1730 AMPØ=(ZRT(3,1)/(ZRT(3,3)+ZLE))*AMP3
1740 VØUT=-ZLE*AMPØ
1750C PØWER AND INSERTIØN LØSS
1760 PØ=REAL(VØUT*CØNJG(-AMPØ))
1770 PREF=REAL((EG*ZLE/(ZG+ZLE))*CØNJG(EG/(ZG+ZLE)))
1780 PILØS(K)=10.*ALØG10(PØ/PREF)
1785 WRITE(6,10) FREQ,PILØS(K)
1790 FREQ=FREQ+FINC
1800 1 CØNTINUE
1810 10 FØRMAT(V)
1900 YMAX=PILØS(1)
1910 YMIN=PILØS(1)
1920 DØ100 J=1,K
1930 IF(PILØS(J).GT.YMAX)  YMAX=PILØS(J)
1940 IF(PILØS(J).LT.YMIN)  YMIN=PILØS(J)
1950 100 CØNTINUE
1960 CALL YPLT(PILØS,FINIT,FINC,YMIN,YMAX,K,NPLTS,K1,DA,0)
1990 STØP
2000 END
```

TABLE 3-15. MØDE2 PROGRAM LISTING STACKED FILTER OF TWO PLATES, TWO NORMAL MODES IN EACH PLATE PERPENDICULAR TO THICKNESS DIRECTION (ROTATION BETWEEN PLATES ALLOWED)

```
10*#RUNH*;ADE576/RHYPLØT=(CØRE=28)
100C PRØGRAM TØ CALCULATE THE TRANSFER FUNCTIØN ØF A STACKED
101C FILTER ØF TWØ PLATES.
110C EACH PLATE HAS TWØ PIEZØELECTRICALLY DRIVEN MØDES.
120C PSI IS THE ANGLE ØF RØTATIØN BETWEEN PLATES
130 PARAMETER NPLTS=1
140 CØMPLEX ZL(5,5),ZR(5,5),ZLT(3,3),ZRT(3,3)
150 CØMPLEX ZRET(2,2),ZRETR(2,2)
160 CØMPLEX ZLE,ZG,EG,AMP1,AMP3,AMP4
170 CØMPLEX AMPØ,VIN,VØUT,ZIN
180 DIMENSIØN A(2,2)
190 DIMENSIØN K1(NPLTS),PILØS(1000)
200 CHARACTER DA*1(NPLTS)/"*"/
210 K=0
220 PI=3.1415926
230C INPUT DATA
232C CENTER FREQUENCIES ØF PLATES 1 AND 2
240 FØ1=1.E7
250 FØ2=1.E7
255C DIAMETER ØF PLATES 1 AND 2
260 D1=10.E-3
270 D2=10.E-3
280C PLATE CØNSTANTS
282C CØUPLING CØEFFICIENTS XK(MØDE,PLATE)
290 XK11=0.088
300 XK21=2.*XK11
310 XK12=XK11
320 XK22=2.*XK12
325C VELØCITIES CT(MØDE,PLATE)
330 CT11=3.32E3
340 CT21=1.1*CT11
350 CT12=CT11
360 CT22=1.1*CT12
365C DENSITIES ØF PLATES 1 AND 2
370 DT1=2.65E3
380 DT2=DT1
385C DIELECTRIC CØNSTANTS ØF PLATES 1 AND 2
390 EP1=4.58*8.85E-12
400 EP2=EP1
405C ANGLE ØF RØTATIØN PSI
407C PLATE 2 IS RØTATED BY PSI IN DEGREES IN RELATIØN TØ 1
410 PSI=5.0
415C ELECTRICAL IMPEDANCES AND GENERATØR VØLTAGE
420 ZLE=CMPLX(1600.,0.)
430 ZG=ZLE
440 EG=CMPLX(1.,0.)
445C FREQUENCY RANGE ØF INTEREST
447C INITIAL FREQUENCY,FREQUENCY INTERVAL,NØ. ØF FREQUENCIES
448C IN RANGE
450 FINIT=9.7E6
460 FINC=0.025E6
470 IFREQ=69
490C AREAS ØF PLATES 1 AND 2
500 AREA1=PI*D1*D1/4.
```

TABLE 3-15 (Cont'd)

```
510 AREA2=PI*D2*D2/4.
520C CHARACTERISTIC IMPEDANCES Z0(MØDE,PLATE)
530 Z011=AREA1*DT1*CT11
540 Z021=AREA1*DT1*CT21
550 Z012= AREA2*DT2*CT12
560 Z022=AREA2*DT2*CT22
570C THICKNESSES ØF PLATES 1 AND 2
580 TL1=CT11/(2.*F01)
590 TL2=CT12/(2.*F02)
600C CAPACITANCES C0 ØF PLATES 1 AND 2
610 C01=EP1*AREA1/TL1
620 C02=EP2*AREA2/TL2
630C TURNS RATIØS XN(MØDE,PLATE)
640 XN11=XK11*SQRT(Z011*C01*2.*F01)
650 XN21=XK21*SQRT(Z021*C01*CT21/TL1)
660 XN12=XK12*SQRT(Z012*C02*2.*F02)
670 XN22=XK22*SQRT(Z022*C02*CT22/TL2)
680 FREQ=FINIT
690C LØØP THRØUGH FREQUENCIES
700 DØ1 I=1,IFREQ
710 K=K+1
720C PRØPAGATIØN CØNSTANTS THETA(MØDE,PLATE)
730 TH11=2.*PI*FREQ*TL1/CT11
740 TH21=2.*PI*FREQ*TL1/CT21
750 TH12=2.*PI*FREQ*TL2/CT12
760 TH22=2.*PI*FREQ*TL2/CT22
770C CØMPLEX IMPEDANCES
780 TGN11=SIN(TH11)/CØS(TH11)
790 TGN21=SIN(TH21)/CØS(TH21)
800 TGN12=SIN(TH12)/CØS(TH12)
810 TGN22=SIN(TH22)/CØS(TH22)
820 ZL(1,1)=CMPLX(0.,-Z011/TGN11)
830 ZL(1,2)=CMPLX(0.,0.)
840 ZL(1,3)=CMPLX(0.,-Z011/SIN(TH11))
850 ZL(1,4)=ZL(1,2)
860 ZL(1,5)=CMPLX(0.,-XN11/(2.*PI*FREQ*C01))
870 ZL(2,1)=ZL(1,2)
880 ZL(2,2)=CMPLX(0.,-Z021/TGN21)
890 ZL(2,3)=ZL(1,2)
900 ZL(2,4)=CMPLX(0.,-Z021/SIN(TH21))
910 ZL(2,5)=CMPLX(0.,-XN21/(2.*PI*FREQ*C01))
920 ZL(3,1)=ZL(1,3)
930 ZL(3,2)=ZL(1,2)
940 ZL(3,3)=ZL(1,1)
950 ZL(3,4)=ZL(1,2)
960 ZL(3,5)=ZL(1,5)
970 ZL(4,1)=ZL(1,2)
980 ZL(4,2)=ZL(2,4)
990 ZL(4,3)=ZL(1,2)
1000 ZL(4,4)=ZL(2,2)
1010 ZL(4,5)=ZL(2,5)
1020 ZL(5,1)=ZL(1,5)
1030 ZL(5,2)=ZL(2,5)
1040 ZL(5,3)=ZL(1,5)
1050 ZL(5,4)=ZL(2,5)
1060 ZL(5,5)=CMPLX(0.,-1./(2.*PI*FREQ*C01))
1070 ZR(1,1)=CMPLX(0.,-Z012/TGN12)
1080 ZR(1,2)=CMPLX(0.,0.)
```

TABLE 3-15. (Cont'd)

```
1090 ZR(1,3)=CMPLX(0.,-ZØ12/SIN(TH12))
1100 ZR(1,4)=ZR(1,2)
1110 ZR(1,5)=CMPLX(0.,-XN12/(2.*PI*FREQ*CØ2))
1120 ZR(2,1)=ZR(1,2)
1130 ZR(2,2)=CMPLX(0.,-ZØ22/TGN22)
1140 ZR(2,3)=ZR(1,2)
1150 ZR(2,4)=CMPLX(0.,-ZØ22/SIN(TH22))
1160 ZR(2,5)=CMPLX(0.,-XN22/(2.*PI*FREQ*CØ2))
1170 ZR(3,1)=ZR(1,3)
1180 ZR(3,2)=ZR(1,2)
1190 ZR(3,3)=ZR(1,1)
1200 ZR(3,4)=ZR(1,2)
1210 ZR(3,5)=ZR(1,5)
1220 ZR(4,1)=ZR(1,2)
1230 ZR(4,2)=ZR(2,4)
1240 ZR(4,3)=ZR(1,2)
1250 ZR(4,4)=ZR(2,2)
1255 ZR(4,5)=ZR(2,5)
1260 ZR(5,1)=ZR(1,5)
1270 ZR(5,2)=ZR(2,5)
1280 ZR(5,3)=ZR(1,5)
1290 ZR(5,4)=ZR(2,5)
1300 ZR(5,5)=CMPLX(0.,-1./(2.*PI*FREQ*CØ2))
1310C APPLY MECHANICAL BØUNDARY CØNDITIØNS TØ LEFT PLATE
1311C FØR PLATE 1  V1=V2=0
1320 ZLT(1,1)=ZL(3,3)-ZL(3,1)*ZL(1,3)/ZL(1,1)
1330 ZLT(1,2)=CMPLX(0.,0.)
1340 ZLT(1,3)=ZL(3,5)-ZL(3,1)*ZL(1,5)/ZL(1,1)
1350 ZLT(2,1)=ZLT(1,2)
1360 ZLT(2,2)=ZL(4,4)-ZL(4,2)*ZL(2,4)/ZL(2,2)
1370 ZLT(2,3)=ZL(4,5)-ZL(4,2)*ZL(2,5)/ZL(2,2)
1380 ZLT(3,1)=ZL(5,3)-ZL(5,1)*ZL(1,3)/ZL(1,1)
1390 ZLT(3,2)=ZL(5,4)-ZL(5,2)*ZL(2,4)/ZL(2,2)
1400 ZLT(3,3)=ZL(5,5)-(ZL(5,1)*ZL(1,5)/ZL(1,1))
1401& -(ZL(5,2)*ZL(2,5)/ZL(2,2))
1410C APPLY MECHANICAL BØUNDARY CØNDITIØNS TØ RIGHT PLATE
1411C FØR PLATE 2   V3=V4=0
1420 ZRT(1,1)=ZR(1,1)-ZR(1,3)*ZR(3,1)/ZR(3,3)
1430 ZRT(1,2)=CMPLX(0.,0.)
1440 ZRT(1,3)=ZR(1,5)-ZR(1,3)*ZR(3,5)/ZR(3,3)
1450 ZRT(2,1)=ZRT(1,2)
1460 ZRT(2,2)=ZR(2,2)-ZR(2,4)*ZR(4,2)/ZR(4,4)
1470 ZRT(2,3)=ZR(2,5)-ZR(2,4)*ZR(4,5)/ZR(4,4)
1480 ZRT(3,1)=ZR(5,1)-ZR(5,3)*ZR(3,1)/ZR(3,3)
1490 ZRT(3,2)=ZR(5,2)-ZR(5,4)*ZR(4,2)/ZR(4,4)
1500 ZRT(3,3)=ZR(5,5)-(ZR(5,3)*ZR(3,5)/ZR(3,3))
1501& -(ZR(5,4)*ZR(4,5)/ZR(4,4))
1510C TERMINATE PLATE 2 ØN RIGHT IN ZLE
1520 ZRET(1,1)=ZRT(1,1)-ZRT(1,3)*ZRT(3,1)/(ZLE+ZRT(3,3))
1530 ZRET(1,2)=-(ZRT(1,3)*ZRT(3,2))/(ZLE+ZRT(3,3))
1540 ZRET(2,1)=-(ZRT(2,3)*ZRT(3,1))/(ZLE+ZRT(3,3))
1550 ZRET(2,2)=ZRT(2,2)-ZRT(2,3)*ZRT(3,2)/(ZLE+ZRT(3,3))
1560C PLATE 2 IS RØTATED ABØUT THE THICKNESS BY THE ANGLE
1561C PSI IN DEGREES IN RELATIØN TØ PLATE 1
1562C THE DIRECTIØN CØSINES BETWEEN THE NEW AND ØLD AXIS
1563C ØF PLATE 2 ARE
1570 A(1,1)=CØS(PSI*PI/180.)
1580 A(1,2)=SIN(PSI*PI/180.)
```

TABLE 3-15. (Cont'd)

```
1590 A(2,1)=-A(1,2)
1600 A(2,2)=A(1,1)
1610C THE IMPEDANCES ØF THE PLATE ØN THE RIGHT AFTER
1611C RØTATIØN ARE
1620 ZRETR(1,1)=A(1,1)*A(1,1)*ZRET(1,1)
1621& +A(2,1)*A(1,1)*ZRET(2,1)+A(2,1)*A(1,1)*ZRET(1,2)
1622& +A(2,1)*A(2,1)*ZRET(2,2)
1630 ZRETR(1,2)=A(1,2)*A(1,1)*ZRET(1,1)
1631& +A(1,2)*A(2,1)*ZRET(2,1)+A(2,2)*A(1,1)*ZRET(1,2)
1632& +A(2,2)*A(2,1)*ZRET(2,2)
1640 ZRETR(2,1)=A(1,1)*A(1,2)*ZRET(1,1)
1641& +A(1,1)*A(2,2)*ZRET(2,1)+A(2,1)*A(1,2)*ZRET(1,2)
1642& +A(2,1)*A(2,2)*ZRET(2,2)
1650 ZRETR(2,2)=A(1,2)*A(1,2)*ZRET(1,1)
1651& +A(1,2)*A(2,2)*ZRET(2,1)+A(2,2)*A(1,2)*ZRET(1,2)
1652& +A(2,2)*A(2,2)*ZRET(2,2)
1660C AT THE JUNCTIØN ØF THE LEFT PLATE AND THE RØTATED RIGHT
1661C PLATE,EQUATE VØLTAGES AND CURRENTS AND SØLVE FØR
1662C CURRENTS.  V3=V1T,V4=V2T,I3=-I1T,I4=-I2T
1670C THIS GIVES I3 AND I4 IN TERMS ØF IIN.
1671C WHEN THESE VALUES ARE PUT IN EXPRESSIØN FØR V5(VIN)
1672C THE INPUT IMPEDANCE ZIN CAN BE ØBTAINED
1675 IF(ZRETR(2,2)+ZLT(2,2).EQ.(0.0,0.0).AND.ZRETR(1,2)
1676& .EQ.(0.0,0.0)) ZRETR(2,2)=(0.0,0.5)
1677 IF(ZRETR(2,2)+ZLT(2,2).EQ.(0.0,0.0).AND.ZRETR(1,2)
1678& .EQ.(0.0,0.0))  ZLT(2,2)=(0.0,0.5)
1680 ZIN=(ZLT(3,1)*(ZLT(2,3)*ZRETR(1,2)-ZLT(1,3)*(ZRETR(2,2)
1681& +ZLT(2,2)))+ZLT(3,2)*(ZRETR(2,1)*ZLT(1,3)-ZLT(2,3)
1682& *(ZRETR(1,1)+ZLT(1,1))))/((ZRETR(1,1)+ZLT(1,1))
1683& *(ZRETR(2,2)+ZLT(2,2))-ZRETR(2,1)*ZRETR(1,2))+ZLT(3,3
1690 AMPI=EG/(ZG+ZIN)
1700 AMP3=((ZLT(2,3)*ZRETR(1,2)-ZLT(1,3)*(ZRETR(2,2)+ZLT(2,2)))
1701& /((ZRETR(1,1)+ZLT(1,1))*(ZRETR(2,2)+ZLT(2,2))
1702& -ZRETR(2,1)*ZRETR(1,2)))*AMPI
1707 IF(ZRETR(1,2).NE.(0.0,0.0)) AMP4=-(ZLT(1,3)/ZRETR(1,2)
1708& )*AMPI-((ZLT(1,1)+ZRETR(1,1))/ZRETR(1,2))*AMP3
1712 IF(ZRETR(1,2).EQ.(0.0,0.0)) AMP4=-(ZLT(2,3)/(ZRETR(2,2)
1713& +ZLT(2,2)))*AMPI-(ZRETR(2,1)/(ZRETR(2,2)+ZLT(2,2)))
1714& *AMP3
1720 VIN=ZLT(3,1)*AMP3+ZLT(3,2)*AMP4+ZLT(3,3)*AMPI
1730 AMPØ=((A(1,1)*ZRT(3,1)+A(2,1)*ZRT(3,2))/(ZLE+ZRT(3,3)))
1731& *AMP3+((A(1,2)*ZRT(3,1)+A(2,2)*ZRT(3,2))/(ZLE+
1732& ZRT(3,3)))*AMP4
1740 VØUT=-ZLE*AMPØ
1750C PØWER AND INSERTIØN LØSS
1760 PØ=REAL(VØUT*CØNJG(-AMPØ))
1770 PREF=REAL((EG*ZLE/(ZG+ZLE))*CØNJG(EG/(ZG+ZLE)))
1780 PILØS(K)=10.*ALØG10(PØ/PREF)
1785 WRITE(6,10) FREQ,PILØS(K)
1790 FREQ=FREQ+FINC
1800 1 CØNTINUE
1810 10 FØRMAT(V)
1900 YMAX=PILØS(1)
1910 YMIN=PILØS(1)
1920 DØ100 J=1,K
1930 IF(PILØS(J).GT.YMAX)  YMAX=PILØS(J)
1940 IF(PILØS(J).LT.YMIN)  YMIN=PILØS(J)
1950 100 CØNTINUE
1960 CALL YPLT(PILØS,FINIT,FINC,YMIN,YMAX,K,NPLTS,K1,DA,0)
1990 STØP
2000 END
```

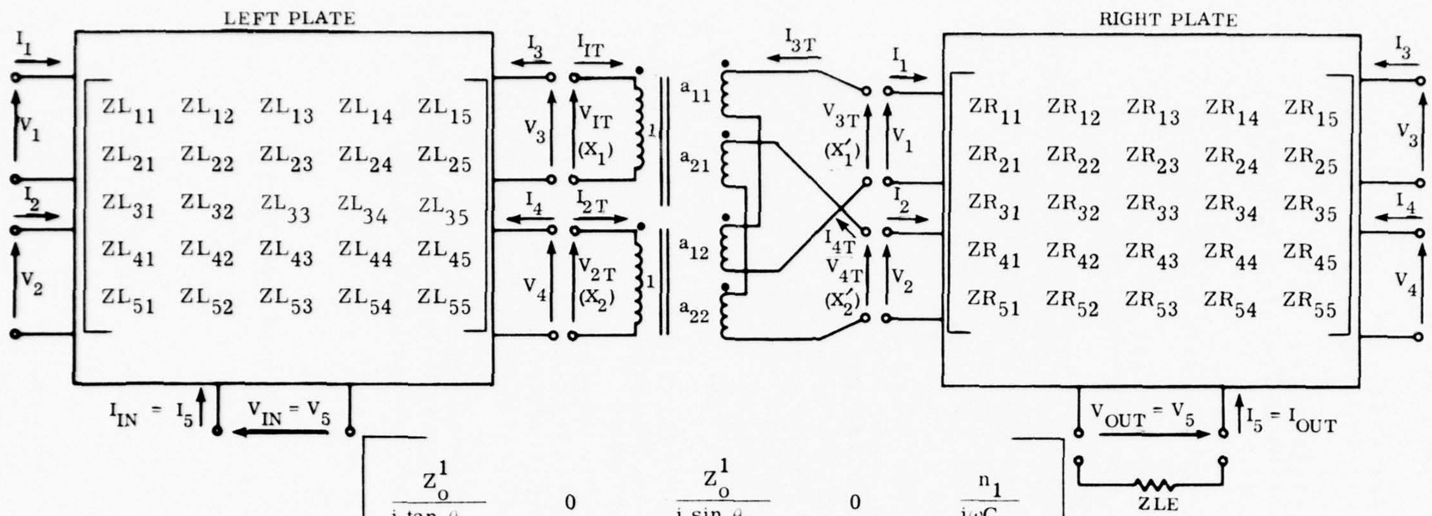

$$[Z] = \begin{bmatrix} \frac{Z_o^1}{j\tan\theta_1} & 0 & \frac{Z_o^1}{j\sin\theta_1} & 0 & \frac{n_1}{j\omega C_0} \\ 0 & \frac{Z_o^2}{j\sin\theta_2} & 0 & \frac{Z_o^2}{j\sin\theta_2} & \frac{n_2}{j\omega C_0} \\ \frac{Z_o^1}{j\sin\theta_1} & 0 & \frac{Z_o^1}{j\tan\theta_1} & 0 & \frac{n_1}{j\omega C_0} \\ 0 & \frac{Z_o^2}{j\sin\theta_2} & 0 & \frac{Z_o^2}{j\tan\theta_2} & \frac{n_2}{j\omega C_0} \\ \frac{n_1}{j\omega C_0} & \frac{n_2}{j\omega C_0} & \frac{n_1}{j\omega C_0} & \frac{n_2}{j\omega C_0} & \frac{1}{j\omega C_0} \end{bmatrix}$$

Figure 3-26. Mode-2 Problem

TABLE 3-16. SOLUTION OF MØDE 2 PROBLEM

Apply mechanical boundary conditions to left plate $V_1 = V_2 = 0$

$$V_1 = ZL_{11}I_1 + ZL_{13}I_3 + ZL_{15}I_5 = 0$$

$$I_1 = -\frac{ZL_{13}}{ZL_{11}} I_3 - \frac{ZL_{15}}{ZL_{11}} I_5$$

$$V_2 = ZL_{22}I_2 + ZL_{24}I_4 + ZL_{25}I_5 = 0$$

$$I_2 = \frac{-ZL_{24}}{ZL_{22}} I_4 - \frac{ZL_{25}}{ZL_{22}} I_5$$

$$V_3 = ZL_{31}I_1 + ZL_{33}I_3 + ZL_{35}I_5$$

$$V_4 = ZL_{42}I_2 + ZL_{44}I_4 + ZL_{45}I_5$$

$$V_5 = ZL_{51}I_1 + ZL_{52}I_2 + ZL_{53}I_3 + ZL_{54}I_4 + ZL_{55}I_5$$

$$V_3 = \left\{ZL_{33} - \frac{ZL_{31}ZL_{13}}{ZL_{11}}\right\} I_3 + \left\{ZL_{35} - \frac{ZL_{31}ZL_{15}}{ZL_{11}}\right\} I_5$$

$$V_4 = \left\{ZL_{44} - \frac{ZL_{42}ZL_{24}}{ZL_{22}}\right\} I_4 + \left\{ZL_{45} - \frac{ZL_{42}ZL_{25}}{ZL_{22}}\right\} I_5$$

$$V_5 = \left\{ZL_{53} - \frac{ZL_{51}ZL_{13}}{ZL_{11}}\right\} I_3 + \left\{ZL_{54} - \frac{ZL_{52}ZL_{24}}{ZL_{22}}\right\} I_4$$

$$+ \left\{ZL_{55} - \frac{ZL_{51}ZL_{15}}{ZL_{11}} - \frac{ZL_{52}ZL_{25}}{ZL_{22}}\right\} I_5$$

$$V_3 = ZLT_{11}I_3 + ZLT_{13}I_5$$

$$V_4 = + ZLT_{22}I_4 + ZLT_{23}I_5$$

$$V_5 = ZLT_{31}I_3 + ZLT_{32}I_4 + ZLT_{33}I_5$$

$$I_5 = I_{IN} \quad , \quad V_5 = V_{IN}$$

TABLE 3-16. (CONT'D).

Apply mechanical boundary conditions to right plate $V_3 = V_4 = 0$

$$V_3 = ZR_{31}I_1 + ZR_{33}I_3 + ZR_{35}I_5 = 0$$

$$I_3 = -\frac{ZR_{31}}{ZR_{33}} I_1 - \frac{ZR_{35}}{ZR_{33}} I_5$$

$$V_4 = ZR_{42}I_2 + ZR_{44}I_4 + ZR_{45}I_5 = 0$$

$$I_4 = -\frac{ZR_{42}}{ZR_{44}} I_2 - \frac{ZR_{45}}{ZR_{44}} I_5$$

$$V_1 = ZR_{11}I_1 + ZR_{13}I_3 + ZR_{15}I_5$$

$$V_2 = ZR_{22}I_2 + ZR_{24}I_4 + ZR_{25}I_5$$

$$V_5 = ZR_{51}I_1 + ZR_{52}I_2 + ZR_{53}I_3 + ZR_{54}I_4 + ZR_{55}I_5$$

$$V_1 = \left\{ZR_{11} - \frac{ZR_{13}ZR_{31}}{ZR_{33}}\right\} I_1 + \left\{ZR_{15} - \frac{ZR_{13}ZR_{35}}{ZR_{33}}\right\} I_5$$

$$V_2 = \left\{ZR_{22} - \frac{ZR_{24}ZR_{42}}{ZR_{44}}\right\} I_2 + \left\{ZR_{25} - \frac{ZR_{24}ZR_{45}}{ZR_{44}}\right\} I_5$$

$$V_5 = \left\{ZR_{51} - \frac{ZR_{53}ZR_{31}}{ZR_{33}}\right\} I_1 + \left\{ZR_{52} - \frac{ZR_{54}ZR_{42}}{ZR_{44}}\right\} I_2$$

$$+ \left\{ZR_{55} - \frac{ZR_{53}ZR_{35}}{ZR_{33}} - \frac{ZR_{54}ZR_{45}}{ZR_{44}}\right\} I_5$$

$$V_1 = ZRT_{11}I_1 \qquad\qquad + ZRT_{13}I_5$$

$$V_2 = \qquad\qquad + ZRT_{22}I_2 + ZRT_{23}I_5$$

$$V_5 = ZRT_{31}I_1 + ZRT_{32}I_2 + ZRT_{33}I_5$$

$$V_5 = V_{out} \quad , \quad I_5 = I_{out}$$

Terminate plate on right electrically in ZLE

$$V_{out} = -\ ZLE\ I_{out}$$

TABLE 3-16. (CONT'D).

$$V_{out} = ZRT_{31}I_1 + ZRT_{32}I_2 + ZRT_{33}I_{out} = -ZLE\,I_{out}$$

$$I_{out} = -\frac{ZRT_{31}}{ZLE + ZRT_{33}} I_1 - \frac{ZRT_{32}}{ZLE + ZRT_{33}} I_2$$

$$V_1 = \left\{ZRT_{11} - \frac{ZRT_{13}ZRT_{31}}{ZLE + ZRT_{33}}\right\} I_1 - \left\{\frac{ZRT_{13}ZRT_{32}}{ZLE + ZRT_{33}}\right\} I_2$$

$$V_2 = -\left\{\frac{ZRT_{23}ZRT_{31}}{ZLE + ZRT_{33}}\right\} I_1 + \left\{ZRT_{22} - \frac{ZRT_{23}ZRT_{32}}{ZLE + ZRT_{33}}\right\} I_2$$

$$V_1 = ZRET_{11}I_1 + ZRET_{12}I_2$$

$$V_2 = ZRET_{21}I_1 + ZRET_{22}I_2$$

Coordinates of plate on right are rotated about $\mathbf{X}_3$ by the angle ψ in comparison to left plate coordinates (reference coordinates) to account for this

$$V_{3T} = a_{11}V_{1T} + a_{12}V_{2T} \qquad -I_{1T} = a_{11}I_{3T} + a_{21}I_{4T}$$

$$V_{4T} = a_{21}V_{1T} + a_{22}V_{2T} \qquad -I_{2T} = a_{12}I_{3T} + a_{22}I_{4T}$$

This is an orthogonal transformation so that

$$V_{1T} = a_{11}V_{3T} + a_{21}V_{4T} \qquad -I_{3T} = a_{11}I_{1T} + a_{12}I_{2T}$$

$$V_{2T} = a_{12}V_{3T} + a_{22}V_{4T} \qquad -I_{4T} = a_{21}I_{1T} + a_{22}I_{2T}$$

From Figure 3-26

$$V_{3T} = V_1 \qquad I_{3T} = -I_1$$

$$V_{4T} = V_2 \qquad I_{4T} = -I_2$$

$$V_{3T} = V_1 = ZRET_{11}(-I_{3T}) + ZRET_{12}(-I_{4T})$$

$$V_{4T} = V_2 = ZRET_{21}(-I_{3T}) + ZRET_{22}(-I_{4T})$$

$$V_{1T} = \left\{a_{11}ZRET_{11} + a_{21}ZRET_{21}\right\}(-I_{3T}) + \left\{a_{11}ZRET_{12} + a_{21}ZRET_{22}\right\}(-I_{4T})$$

TABLE 3-16. (CONT'D).

$$V_{2T} = \left\{ a_{12}ZRET_{11} + a_{22}ZRET_{21} \right\} (-I_{3T})$$

$$+ \left\{ a_{12}ZRET_{12} + a_{22}ZRET_{22} \right\} (-I_{4T})$$

$$V_{1T} = \left\{ a_{11}a_{11}ZRET_{11} + a_{21}a_{11}ZRET_{21} + a_{11}a_{21}ZRET_{12} + a_{21}a_{21}ZRET_{22} \right\} (I_{1T})$$

$$+ \left\{ a_{11}a_{12}ZRET_{11} + a_{21}a_{12}ZRET_{21} + a_{11}a_{22}ZRET_{12} + a_{21}a_{22}ZRET_{22} \right\} (I_{2T})$$

$$V_{2T} = \left\{ a_{12}a_{11}ZRET_{11} + a_{22}a_{11}ZRET_{21} + a_{22}a_{21}ZRET_{22} + a_{12}a_{21}ZRET_{12} \right\} (I_{1T})$$

$$+ \left\{ a_{12}a_{12}ZRET_{11} + a_{22}a_{12}ZRET_{21} + a_{22}a_{22}ZRET_{22} + a_{12}a_{22}ZRET_{12} \right\} (I_{2T})$$

$$V_{1T} = ZRETR_{11}I_{1T} + ZRETR_{12}I_{2T}$$

$$V_{2T} = ZRETR_{21}I_{1T} + ZRETR_{22}I_{2T}$$

but from Figure 3-26

$$V_3 = V_{1T} \qquad I_3 = -I_{1T}$$

$$V_4 = V_{2T} \qquad I_4 = -I_{2T}$$

$$V_3 = -ZRETR_{11}I_3 - ZRETR_{12}I_4$$

$$V_4 = -ZRETR_{21}I_3 - ZRETR_{22}I_4$$

$$V_3 = ZLT_{11}I_3 + ZLT_{13}I_{IN} = -ZRETR_{11}I_3 - ZRETR_{12}I_4$$

$$* \ - I_4 = \left\{ \frac{ZLT_{11} + ZRETR_{11}}{ZRETR_{12}} \right\} I_3 + \left\{ \frac{ZLT_{13}}{ZRETR_{12}} \right\} I_{IN}$$

$$V_4 = ZLT_{22}I_4 + ZLT_{23}I_{IN} = -ZRETR_{21}I_3 - ZRETR_{22}I_4$$

$$- I_4 = \left\{ \frac{ZRETR_{21}}{ZRETR_{22} + ZLT_{22}} \right\} I_3 + \left\{ \frac{ZLT_{23}}{ZRETR_{22} + ZLT_{22}} \right\} I_{IN}$$

$$\therefore \left\{ \frac{ZLT_{11} + ZRETR_{11}}{ZRETR_{12}} \right\} I_3 + \left\{ \frac{ZLT_{13}}{ZRETR_{12}} \right\} I_{IN}$$

$$= \left\{ \frac{ZRETR_{21}}{ZRETR_{22} + ZLT_{22}} \right\} I_3 + \left\{ \frac{ZLT_{23}}{ZRETR_{22} + ZLT_{22}} \right\} I_{IN}$$

TABLE 3-16. (CONT'D).

$$* \; I_3 = \left\{ \frac{ZLT_{23}ZRETR_{12} - ZLT_{13}\,(ZRETR_{22} + ZLT_{22})}{(ZLT_{11} + ZRETR_{11})\,(ZRETR_{22} + ZLT_{22}) - ZRETR_{21}ZRETR_{12}} \right\} I_{IN}$$

From

$$V_3 = - ZRETR_{11}I_3 - ZRETR_{12}I_4 = ZLT_{11}I_3 + ZLT_{13}I_{IN}$$

$$-I_3 = \left\{ \frac{ZRETR_{12}}{ZLT_{11} + ZRETR_{11}} \right\} I_4 + \left\{ \frac{ZLT_{13}}{ZLT_{11} + ZRETR_{11}} \right\} I_{IN}$$

$$V_4 = -ZRETR_{21}I_3 - ZRETR_{22}I_4 = ZLT_{22}I_4 + ZLT_{23}I_{IN}$$

$$-I_3 = \left(\frac{ZLT_{22} + ZRETR_{22}}{ZRETR_{21}} \right) I_4 + \left(\frac{ZLT_{23}}{ZRETR_{21}} \right) I_{IN}$$

$$I_4 = \left\{ \frac{ZLT_{13}ZRETR_{21} - ZLT_{23}\quad(ZLT_{11} + ZRETR_{11})}{(ZLT_{11} + ZRETR_{11})\,(ZLT_{22} + ZRETR_{22}) - ZRETR_{12}ZRETR_{21}} \right\} I_{IN}$$

$$* \; V_{IN} = ZLT_{31}I_3 + ZLT_{32}I_4 + ZLT_{33}I_{IN}$$

$$* \; Z_{IN} = ZLT_{31} \left\{ \frac{ZLT_{23}ZRETR_{12} - ZLT_{13}\,(ZRETR_{22} + ZLT_{22})}{(ZLT_{11} + ZRETR_{11})\,(ZRETR_{22} + ZLT_{22}) - ZRETR_{21}ZRETR_{12}} \right\}$$

$$+ ZLT_{32} \left\{ \frac{ZLT_{13}ZRETR_{21} - ZLT_{23}\quad(ZLT_{11} + ZRETR_{11})}{(ZLT_{11} + ZRETR_{11})\,(ZLT_{22} + ZRETR_{22}) - ZRETR_{21}ZRETR_{12}} \right\}$$

$$+ ZLT_{33}$$

For a generator with Impedance Z_G and voltage E_g

$$* \; I_{IN} = E_g/(Z_G + Z_{IN})$$

$$I_{out} = \frac{- ZRT_{31}}{ZLE + ZRT_{33}} \quad I_1 - \frac{ZRT_{32}}{ZLE + ZRT_{33}} I_2$$

Retracing steps leads to

$$-I_1 = a_{11}I_3 + a_{12}I_4$$

$$-I_2 = a_{21}I_3 + a_{22}I_4$$

TABLE 3-16. (CONT'D).

$$* \; I_{out} = \left\{ \frac{a_{11}ZRT_{31} + a_{21}ZRT_{32}}{ZLE + ZRT_{33}} \right\} I_3$$

$$+ \left\{ \frac{a_{12}ZRT_{31} + a_{22}ZRT_{32}}{ZLE + ZRT_{33}} \right\} I_3$$

$$* \; V_{out} = - ZLE \; I_{out}$$

By the sign convention of Figure 3-26

$$* \; P_{ower\ out} = V_{out} \cdot (-I_{out})\ \text{conjugate}$$

Equations with asterix are those used in MØDE 2 program.

The statements at lines 1675 and 1677 are one-way, to handle the behavior of identical plates, except that mode 2 in the left-hand plate is piezoelectrically coupled, while mode 2 in the right-hand plate is not. Time has not permitted a complete evaluation of these programs under all possible conditions, so there are probably other circumstances that also will not operate. Those that were corrected are those encountered in running the programs up to this time.

The listing for the MØDE3 program is shown in Table 3-17. The method of solution employed in the program follows that shown in Figure 3-26 and Table 3-16, where, in place of the normal mode matrix shown, the full actual coordinate matrix of Figure 3-19 is employed and the nomenclature is extended to allow for the inclusion of the additional terms. In writing this program the symmetry of the actual plate coordinate matrix has been employed, or neglected, depending on whether a simpler calculation could be done. The input data include all the data required for the MØDE2 program, extended to three modes as well as the eigenvectors for each plate. The general case of the MØDE3 program requires two runs, each, of CRØT, SYMEIG and VCØUP, one of each for each plate. The comments about the MØDE1 and MØDE2 programs, in general, apply to this program as well. Again, an attempt was made to make the program self-explanatory. Time did not permit a complete evaluation of this program so there are probably conditions that will not run. The IF at line 1950 handles the case of AT-cut quartz with no rotation between plates. For AT-cut quartz at the resonant frequency of mode 1, an exponential overflow, which has not been corrected, occurs; however, the results appear correct.

TABLE 3-17. LISTING OF MØDE3 PROGRAM STACKED FILTER OF TWO PLATES; THREE NORMAL MODES ALLOWED IN EACH PLATE AT ARBITRARY ANGLES TO ACTUAL PLATE COORDINATES (ROTATION BETWEEN PLATES ALSO ALLOWED)

```
10*#RUNH*;ADE576/RHYPLØT=(CØRE=28)
100C     PRØGRAM TØ CALCULATE THE TRANSFER FUNCTIØN
101C     ØF A STACKED FILTER ØF TWØ PLATES
110C      EACH PLATE CAN HAVE THREE PIEZØELECTRICALLY DRIVEN MØDES
120C      PSI IS THE ANGLE ØF RØTATIØN BETWEEN PLATES
130 PARAMETER NPLTS=1
140 CØMPLEX ZNL(7,7),ZNR(7,7),ZL(7,7),ZR(7,7)
150 CØMPLEX ZLT(4,4),ZRT(4,4),ZRET(3,3),ZRETR(3,3)
160 CØMPLEX D(36),R(36),PL1,PL2,PL3,PL4,PL5
170 CØMPLEX PR1,PR2,PR3,PR4,PR5,  ZS(3,3),ZSS,ZSS3
180 CØMPLEX ZLE,ZG,EG
190 CØMPLEX AMP1,AMP4,AMP5,AMP6,AMPØ
200 CØMPLEX VIN,VØUT,ZIN
210 DIMENSIØN B1(3,3),B2(3,3),A(3,3)
220 DIMENSIØN K1(NPLTS),PILØS(1000)
230 CHARACTER DA*1(NPLTS)/"*"/
240 K=0
250 PI=3.1415926
255 PI2=2.*PI
260C         ****** INPUT DATA ******
262C       PLATE 1 IS ØN THE LEFT AND PLATE 2 IS ØN THE RIGHT
265C     CENTER FREQUENCIES ØF PLATES 1 AND 2
270 FØ1=1.E7
280 FØ2=1.E7
285C     DIAMETER ØF PLATES 1 AND 2
290 DIA1=10.E-3
295 DIA2=10.E-3
300C            *** PLATE CØNSTANTS ***
305C     CØUPLING CØEFFICIENTS XK(MØDE,PLATE)
310 XK11=0.08795802
312 XK21=0.0
314 XK31=0.0
320 XK12=0.08795802
322 XK22=0.0
324 XK32=0.0
329C     VELØCITIES CT(MØDE,PLATE)
330 CT11=3.3223239E3
332 CT21=3.8002414E3
334 CT31=7.0086352E3
340 CT12=3.3223239E3
342 CT22=3.8002414E3
344 CT32=7.0086352E3
349C     DENSITIES ØF PLATES DT(PLATE)
350 DT1=2649.0
355 DT2=2649.0
359C     DIELECTRIC CØNSTANTS ØF PLATES EP(PLATE)
360 EP1=0.39816236E-10
365 EP2=0.39816236E-10
370C          *** EIGENVECTØRS ***
371C     THE CØMPØNENTS ØF A MØDE ARE STØRED BY CØLUMNS IN
372C     ARRAY B   B-PLATE-(CØMPØNENT,MØDE)
380 B1(1,1)=1.0
381 B1(2,1)=0.0
382 B1(3,1)=0.0
```

TABLE 3-17. (Cont'd)

```
383 B1(1,2)=0.0
384 B1(2,2)=0.99806542
385 B1(3,2)=0.62172451E-1
386 B1(1,3)=0.0
387 B1(2,3)=-0.62172451E-1
388 B1(3,3)=0.99806542
400 B2(1,1)=1.0
401 B2(2,1)=0.0
402 B2(3,1)=0.0
403 B2(1,2)=0.0
404 B2(2,2)=0.99806542
405 B2(3,2)=0.62172451E-1
406 B2(1,3)=0.0
407 B2(2,3)=-0.62172451E-1
408 B2(3,3)=0.99806542
415C       *** ANGLE ØF RØTATIØN PSI ***
416C    PLATE 2 IS RØTATED BY PSI DEGREES IN RELATIØN TØ PLATE 1
420 PSI=5.0
428C    *** ELECTRICAL IMPEDANCES  GENERATØR(ZG)  LØAD(ZLE) ***
429C    *** GENERATØR VØLTAGE(EG) ***
430 ZLE=(1600.,0.)
434 ZG=ZLE
438 EG=(1.0,0.)
440C    ******* FREQUENCY RANGE ØF INTEREST *******
441C    INITIAL FREQUENCY  FINIT
442C    FREQUENCY SPACING  FINC
443C    NØ. ØF FREQUENCIES IN RANGE  IFREQ=(FFINAL-FINIT)/FINC + 1
450 FINIT=9.7E6
454 FINC=0.025E6
458 IFREQ=69
460C       ****** CALCULATED DATA ******
469C    AREAS ØF PLATES  AREA(PLATE)
470 AREA1=PI*DIA1*DIA1/4.
475 AREA2=PI*DIA2*DIA2/4.
479C    CHARACTERISTIC IMPEDANCES  ZØ(MØDE,PLATE)
480 Z011=AREA1*DT1*CT11
484 Z021=AREA1*DT1*CT21
488 Z031=AREA1*DT1*CT31
500 Z012=AREA2*DT2*CT12
504 Z022=AREA2*DT2*CT22
508 Z032=AREA2*DT2*CT32
519C    THICKNESSES ØF PLATES TL(PLATE)
520 TL1=CT11/(2.*FØ1)
525 TL2=CT12/(2.*FØ2)
529C CAPACITANCES ØF PLATES  CØ(PLATE)
530 CØ1=EP1*AREA1/TL1
535 CØ2=EP2*AREA2/TL2
539C    TURNS RATIØS  XN(MØDE,PLATE)
540 XN11=SQRT(XK11*XK11*Z011*CØ1*CT11/TL1)
544 XN21=SQRT(XK21*XK21*Z021*CØ1*CT21/TL1)
548 XN31=SQRT(XK31*XK31*Z031*CØ1*CT31/TL1)
560 XN12=SQRT(XK12*XK12*Z012*CØ2*CT12/TL2)
564 XN22=SQRT(XK22*XK22*Z022*CØ2*CT22/TL2)
568 XN32=SQRT(XK32*XK32*Z032*CØ2*CT32/TL2)
570C       *** FRØM NØW ØN TERMS ARE FREQUENCY DEPENDENT ***
575 FREQ=FINIT
579C    LØØP THRØUGH FREQUENCIES
580 DØ 100 I=1,IFREQ
```

TABLE 3-17. (Cont'd)

```
585 K=K+1
588C     PROPAGATION CONSTANTS   TH(MØDE,PLATE)=THETA(MØDE,PLATE)
589 W=PI2*FREQ
590 TH11=W*TL1/CT11
594 TH21=W*TL1/CT21
598 TH31=W*TL1/CT31
610 TH12=W*TL2/CT12
614 TH22=W*TL2/CT22
618 TH32=W*TL2/CT32
629C     NORMAL MØDE MATRIX FØR PLATE 1   ZNL
630 TGN11=SIN(TH11)/CØS(TH11)
634 TGN21=SIN(TH21)/CØS(TH21)
636 TGN31=SIN(TH31)/CØS(TH31)
640 ZNL(1,1)=CMPLX(0.,-Z011/TGN11)
641 ZNL(1,2)=(0.,0.)
642 ZNL(1,3)=(0.,0.)
643 ZNL(1,4)=CMPLX(0.,-Z011/SIN(TH11))
644 ZNL(1,5)=(0.,0.)
645 ZNL(1,6)=(0.,0.)
646 ZNL(1,7)=CMPLX(0.,-XN11/(W*C01))
650 ZNL(2,1)=(0.,0.)
651 ZNL(2,2)=CMPLX(0.,-Z021/TGN21)
652 ZNL(2,3)=(0.,0.)
653 ZNL(2,4)=(0.,0.)
654 ZNL(2,5)=CMPLX(0.,-Z021/SIN(TH21))
655 ZNL(2,6)=(0.,0.)
656 ZNL(2,7)=CMPLX(0.,-XN21/(W*C01))
660 ZNL(3,1)=(0.,0.)
661 ZNL(3,2)=(0.,0.)
662 ZNL(3,3)=CMPLX(0.,-Z031/TGN31)
663 ZNL(3,4)=(0.,0.)
664 ZNL(3,5)=(0.,0.)
665 ZNL(3,6)=CMPLX(0.,-Z031/SIN(TH31))
666 ZNL(3,7)=CMPLX(0.,-XN31/(W*C01))
670 ZNL(4,1)=ZNL(1,4)
671 ZNL(4,2)=ZNL(2,4)
672 ZNL(4,3)=ZNL(3,4)
673 ZNL(4,4)=ZNL(1,1)
674 ZNL(4,5)=(0.,0.)
675 ZNL(4,6)=(0.,0.)
676 ZNL(4,7)=ZNL(1,7)
680 ZNL(5,1)=ZNL(1,5)
681 ZNL(5,2)=ZNL(2,5)
682 ZNL(5,3)=ZNL(3,5)
683 ZNL(5,4)=ZNL(4,5)
684 ZNL(5,5)=ZNL(2,2)
685 ZNL(5,6)=(0.,0.)
686 ZNL(5,7)=ZNL(2,7)
690 ZNL(6,1)=ZNL(1,6)
691 ZNL(6,2)=ZNL(2,6)
692 ZNL(6,3)=ZNL(3,6)
693 ZNL(6,4)=ZNL(4,6)
694 ZNL(6,5)=ZNL(5,6)
695 ZNL(6,6)=ZNL(3,3)
696 ZNL(6,7)=ZNL(3,7)
700 ZNL(7,1)=ZNL(1,7)
701 ZNL(7,2)=ZNL(2,7)
702 ZNL(7,3)=ZNL(3,7)
703 ZNL(7,4)=ZNL(4,7)
```

TABLE 3-17. (Cont'd)

```
704 ZNL(7,5)=ZNL(5,7)
705 ZNL(7,6)=ZNL(6,7)
706 ZNL(7,7)=CMPLX(0.,-1./(W*C01))
799C    NØRMAL MØDE MATRIX FØR PLATE 2  ZNR
800 TGN12=SIN(TH12)/CØS(TH12)
804 TGN22=SIN(TH22)/CØS(TH22)
808 TGN32=SIN(TH32)/CØS(TH32)
810 ZNR(1,1)=CMPLX(0.,-Z012/TGN12)
811 ZNR(1,2)=(0.,0.)
812 ZNR(1,3)=(0.,0.)
813 ZNR(1,4)=CMPLX(0.,-Z012/SIN(TH12))
814 ZNR(1,5)=(0.,0.)
815 ZNR(1,6)=(0.,0.)
816 ZNR(1,7)=CMPLX(0.,-XN12/(W*C02))
820 ZNR(2,1)=ZNR(1,2)
821 ZNR(2,2)=CMPLX(0.,-Z022/TGN22)
822 ZNR(2,3)=(0.,0.)
823 ZNR(2,4)=(0.,0.)
824 ZNR(2,5)=CMPLX(0.,-Z022/SIN(TH22))
825 ZNR(2,6)=(0.,0.)
826 ZNR(2,7)=CMPLX(0.,-XN22/(W*C02))
830 ZNR(3,1)=ZNR(1,3)
831 ZNR(3,2)=ZNR(2,3)
832 ZNR(3,3)=CMPLX(0.,-Z032/TGN32)
833 ZNR(3,4)=(0.,0.)
834 ZNR(3,5)=(0.,0.)
835 ZNR(3,6)=CMPLX(0.,-Z032/SIN(TH32))
836 ZNR(3,7)=CMPLX(0.,-XN32/(W*C02))
840 ZNR(4,1)=ZNR(1,4)
841 ZNR(4,2)=ZNR(2,4)
842 ZNR(4,3)=ZNR(3,4)
843 ZNR(4,4)=ZNR(1,1)
844 ZNR(4,5)=(0.,0.)
845 ZNR(4,6)=(0.,0.)
846 ZNR(4,7)=ZNR(1,7)
850 ZNR(5,1)=ZNR(1,5)
851 ZNR(5,2)=ZNR(2,5)
852 ZNR(5,3)=ZNR(3,5)
853 ZNR(5,4)=ZNR(4,5)
854 ZNR(5,5)=ZNR(2,2)
855 ZNR(5,6)=(0.,0.)
856 ZNR(5,7)=ZNR(2,7)
860 ZNR(6,1)=ZNR(1,6)
861 ZNR(6,2)=ZNR(2,6)
862 ZNR(6,3)=ZNR(3,6)
863 ZNR(6,4)=ZNR(4,6)
864 ZNR(6,5)=ZNR(5,6)
865 ZNR(6,6)=ZNR(3,3)
866 ZNR(6,7)=ZNR(3,7)
870 ZNR(7,1)=ZNR(1,7)
871 ZNR(7,2)=ZNR(2,7)
872 ZNR(7,3)=ZNR(3,7)
873 ZNR(7,4)=ZNR(4,7)
874 ZNR(7,5)=ZNR(5,7)
875 ZNR(7,6)=ZNR(6,7)
876 ZNR(7,7)=CMPLX(0.,-1./(W*C02))
997C    CØNVERT FRØM NØRMAL MØDE CØØRDINATES TØ ACTUAL
998C    PLATE CØØRDINATES FØR BØTH PLATES 1 AND 2
```

TABLE 3-17. (Cont'd)

```
999C        ZL=(BB1)*ZNL*(BB1)T    ZR=(BB2)*ZNR*(BB2)T
1000 DØ 20 M=1,7
1004 DØ 20 N=1,7
1006 ZL(M,N)=(0.,0.)
1007 ZR(M,N)=(0.,0.)
1008 20 CØNTINUE
1010 DØ 30 M=1,3
1012 DØ 30 N=1,3
1014 DØ 30 J=1,3
1020 ZL(M,N)=B1(M,J)*ZNL(J,J)*B1(N,J)+ZL(M,N)
1022 ZL(M,N+3)=B1(M,J)*ZNL(J,J+3)*B1(N,J)+ZL(M,N+3)
1024 ZL(M+3,N)=ZL(M,N+3)
1026 ZL(M+3,N+3)=ZL(M,N)
1028 ZL(N,7)=B1(N,J)*ZNL(J,7)+ZL(N,7)
1030 ZL(N+3,7)=ZL(N,7)
1032 ZL(7,N)=ZL(N,7)
1034 ZL(7,N+3)=ZL(N,7)
1040 ZR(M,N)=B2(M,J)*ZNR(J,J)*B2(N,J)+ZR(M,N)
1042 ZR(M,N+3)=B2(M,J)*ZNR(J,J+3)*B2(N,J)+ZR(M,N+3)
1044 ZR(M+3,N)=ZR(M,N+3)
1046 ZR(M+3,N+3)=ZR(M,N)
1048 ZR(N,7)=B2(N,J)*ZNR(J,7)+ZR(N,7)
1050 ZR(N+3,7)=ZR(N,7)
1052 ZR(7,N)=ZR(N,7)
1054 ZR(7,N+3)=ZR(N,7)
1060 30 CØNTINUE
1062 ZL(7,7)=ZNL(7,7)
1064 ZR(7,7)=ZNR(7,7)
1100C     APPLY MECHANICAL BØUNDARY CØNDITIØNS TØ LEFT PLATE
1101C     FØR PLATE 1  V1=V2=V3=0
1102C     THIS CØNVERSIØN IS MØST EASILY CARRIED ØUT BY
1103C     DEFINING THE FØLLØWING PRØDUCTS
1109 M=0
1110 DØ 40 N=2,7
1112 DØ 40 J=2,7
1114 M=M+1
1116 D(M)=ZL(1,1)*ZL(N,J)-ZL(N,1)*ZL(1,J)
1119 40 CØNTINUE
1120C     IT IS ALSØ CØNVENIENT TØ DEFINE THESE PRØDUCTS
1130 PL1=ZL(1,1)*D(1)
1132 PL2=D(8)*D(1)-D(7)*D(2)
1134 PL3=D(14)*D(1)-D(13)*D(2)
1136 PL4=D(20)*D(1)-D(19)*D(2)
1138 PL5=D(26)*D(1)-D(25)*D(2)
1140 ZLT(1,1)=((D(15)*D(1)-D(13)*D(3))/PL1)
1141& -(PL3*(D(9)*D(1)-D(7)*D(3))/(PL1*PL2))
1150 ZLT(1,2)=((D(16)*D(1)-D(13)*D(4))/PL1)
1151& -(PL3*(D(10)*D(1)-D(7)*D(4))/(PL1*PL2))
1160 ZLT(1,3)=((D(17)*D(1)-D(13)*D(6))/PL1)
1161& -(PL3*(D(11)*D(1)-D(7)*D(5))/(PL1*PL2))
1170 ZLT(1,4)=((D(18)*D(1)-D(13)*D(6))/PL1)
1171& -(PL3*(D(12)*D(1)-D(7)*D(6))/(PL1*PL2))
1180 ZLT(2,1)=ZLT(1,2)
1190 ZLT(2,2)=((D(22)*D(1)-D(19)*D(4))/PL1)
1191& -(PL4*(D(10)*D(1)-D(7)*D(4))/(PL1*PL2))
1200 ZLT(2,3)=((D(23)*D(1)-D(19)*D(5))/PL1)
1201& -(PL4*(D(11)*D(1)-D(7)*D(5))/(PL1*PL2))
1210 ZLT(2,4)=((D(24)*D(1)-D(19)*D(6))/PL1)
```

TABLE 3-17. (Cont'd)

```
1211& -(PL4*(D(12)*D(1)-D(7)*D(6))/(PL1*PL2))
1220 ZLT(3,1)=ZLT(1,3)
1230 ZLT(3,2)=ZLT(2,3)
1240 ZLT(3,3)=((D(29)*D(1)-D(25)*D(5))/PL1)
1241& -(PL5*(D(11)*D(1)-D(7)*D(5))/(PL1*PL2))
1250 ZLT(3,4)=((D(30)*D(1)-D(25)*D(6))/PL1)
1251& -(PL5*(D(12)*D(1)-D(7)*D(6))/(PL1*PL2))
1260 ZLT(4,1)=ZLT(1,4)
1270 ZLT(4,2)=ZLT(2,4)
1280 ZLT(4,3)=ZLT(3,4)
1290 ZLT(4,4)=((D(36)*D(1)-D(31)*D(6))/PL1)
1291& -((D(32)*D(1)-D(31)*D(2))*(D(12)*D(1)-D(7)*D(6))/(PL1*PL2))
1300C     APPLY MECHANICAL BØUNDARY CØNDITIØNS TØ RIGHT PLATE
1301C     FØR PLATE 2   V4=V5=V6=0
1302C     THIS CØNVERSIØN IS MØST EASILY CARRIED ØUT BY
1303C     DEFINING THE FØLLØWING PRØDUCTS
1304C     THE SYMMETRY ØF ZR IS MADE USE ØF IN THESE PRØDUCTS
1309 M=0
1310 DØ 60 N=2,7
1312 DØ 60 J=2,7
1314 M=M+1
1316 R(M)=ZR(4,4)*ZR(N,J)-ZR(N,1)*ZR(1,J)
1319 60 CØNTINUE
1320C     IT IS ALSØ CØNVENIENT TØ DEFINE THESE PRØDUCTS
1330 PR1=ZR(4,4)*R(1)
1332 PR2=R(8)*R(1)-R(7)*R(2)
1334 PR3=R(14)*R(1)-R(13)*R(2)
1336 PR4=R(20)*R(1)-R(19)*R(2)
1338 PR5=R(26)*R(1)-R(25)*R(2)
1340 ZRT(1,1)=((R(15)*R(1)-R(13)*R(3))/PR1)
1341& -(PR3*(R(9)*R(1)-R(7)*R(3))/(PR1*PR2))
1350 ZRT(1,2)=((R(16)*R(1)-R(13)*R(4))/PR1)
1351& -(PR3*(R(10)*R(1)-R(7)*R(4))/(PR1*PR2))
1360 ZRT(1,3)=((R(17)*R(1)-R(13)*R(5))/PR1)
1361& -(PR3*(R(11)*R(1)-R(7)*R(5))/(PR1*PR2))
1370 ZRT(1,4)=((R(18)*R(1)-R(13)*R(6))/PR1)
1371& -(PR3*(R(12)*R(1)-R(7)*R(6))/(PR1*PR2))
1380 ZRT(2,1)=ZRT(1,2)
1390 ZRT(2,2)=((R(22)*R(1)-R(19)*R(4))/PR1)
1391& -(PR4*(R(10)*R(1)-R(7)*R(4))/(PR1*PR2))
1400 ZRT(2,3)=((R(23)*R(1)-R(19)*R(5))/PR1)
1401& -(PR4*(R(11)*R(1)-R(7)*R(5))/(PR1*PR2))
1410 ZRT(2,4)=((R(24)*R(1)-R(19)*R(6))/PR1)
1411& -(PR4*(R(12)*R(1)-R(7)*R(6))/(PR1*PR2))
1420 ZRT(3,1)=ZRT(1,3)
1430 ZRT(3,2)=ZRT(2,3)
1440 ZRT(3,3)=((R(29)*R(1)-R(25)*R(5))/PR1)
1441& -(PR5*(R(11)*R(1)-R(7)*R(5))/(PR1*PR2))
1450 ZRT(3,4)=((R(30)*R(1)-R(25)*R(6))/PR1)
1451& -(PR5*(R(12)*R(1)-R(7)*R(6))/(PR1*PR2))
1460 ZRT(4,1)=ZRT(1,4)
1470 ZRT(4,2)=ZRT(2,4)
1480 ZRT(4,3)=ZRT(3,4)
1490 ZRT(4,4)=((R(36)*R(1)-R(31)*R(6))/PR1)
1491& -((R(32)*R(1)-R(31)*R(2))*(R(12)*R(1)-R(7)*R(6))/(PR1*PR2))
1500C     TERMINATE PLATE 2 ØN RIGHT IN ZLE
1501C     THIS RESULTS IN VØUT=-ZLE*AMPØ
1510 ZRET(1,1)=ZRT(1,1)-ZRT(1,4)*ZRT(4,1)/(ZLE+ZRT(4,4))
```

TABLE 3-17. (Cont'd)

```
1520 ZRET(1,2)=ZRT(1,2)-ZRT(1,4)*ZRT(4,2)/(ZLE+ZRT(4,4))
1530 ZRET(1,3)=ZRT(1,3)-ZRT(1,4)*ZRT(4,3)/(ZLE+ZRT(4,4))
1540 ZRET(2,1)=ZRT(2,1)-ZRT(2,4)*ZRT(4,1)/(ZLE+ZRT(4,4))
1550 ZRET(2,2)=ZRT(2,2)-ZRT(2,4)*ZRT(4,2)/(ZLE+ZRT(4,4))
1560 ZRET(2,3)=ZRT(2,3)-ZRT(2,4)*ZRT(4,3)/(ZLE+ZRT(4,4))
1570 ZRET(3,1)=ZRT(3,1)-ZRT(3,4)*ZRT(4,1)/(ZLE+ZRT(4,4))
1580 ZRET(3,2)=ZRT(3,2)-ZRT(3,4)*ZRT(4,2)/(ZLE+ZRT(4,4))
1590 ZRET(3,3)=ZRT(3,3)-ZRT(3,4)*ZRT(4,3)/(ZLE+ZRT(4,4))
1620C     PLATE 2 IS ROTATED ABOUT THE THICKNESS BY THE ANGLE
1621C     PSI IN DEGREES IN RELATION TO PLATE 1
1622C     THE DIRECTION COSINES BETWEEN THE NEW AXES AND OLD AXES
1623C     OF PLATE 2 ( OR BETWEEN AXES OF PLATE 2 AND AXES
1624C     OF PLATE 1 ) ARE
1630 A(1,1)=COS(PSI*PI/180.)
1634 A(1,2)=SIN(PSI*PI/180.)
1638 A(1,3)=0.0
1640 A(2,1)=-A(1,2)
1644 A(2,2)=A(1,1)
1648 A(2,3)=0.0
1650 A(3,1)=0.0
1654 A(3,2)=0.0
1658 A(3,3)=1.0
1670C     THE IMPEDANCES OF THE PLATE ON THE RIGHT ( PLATE 2 )
1671C     AFTER ROTATION ARE    ZRETR=(A)T*ZRET*(A)
1680 DO 80 L=1,3
1682 DO 80 M=1,3
1684 ZRETR(L,M)=(0.,0.)
1686 DO 80 J=1,3
1688 DO 80 N=1,3
1690 ZRETR(L,M)=A(N,L)*ZRET(N,J)*A(J,M)+ZRETR(L,M)
1700 80 CONTINUE
1800C     AT THE JUNCTIO OF THE LEFT PLATE AND THE ROTATED
1801C     RIGHT PLATE ,EQUATE VOLTAGES AND CURRENTS AND
1802C     SOLVE FOR CURRENTS
1803C       V4=V1T,V5=V2T,V6=V3T,   I4=I1T,I5=I2T,I6=I3T
1804C     THIS GIVES I4,I5,AND I6 IN TERMS OF IIN
1806C     WHEN THESE VALUES ARE PUT IN THE EXPRESSION
1807C     FOR V7(VIN) OF LEFT PLATE THE INPUT IMPEDANCE
1808C     ZIN CAN BE OBTAINED
1810C     IN CARRYING OUT THIS POCEDURE IT IS CONVENIENT
1811C     TO USE THE FOLLOWING VARIABLES
1820 ZS(1,1)=ZLT(1,1)+ZRETR(1,1)
1830 ZS(1,2)=ZLT(1,2)+ZRETR(1,2)
1840 ZS(1,3)=ZLT(1,3)+ZRETR(1,3)
1850 ZS(2,1)=ZLT(2,1)+ZRETR(2,1)
1860 ZS(2,2)=ZLT(2,2)+ZRETR(2,2)
1870 ZS(2,3)=ZLT(2,3)+ZRETR(2,3)
1880 ZS(3,1)=ZLT(3,1)+ZRETR(3,1)
1890 ZS(3,2)=ZLT(3,2)+ZRETR(3,2)
1900 ZS(3,3)=ZLT(3,3)+ZRETR(3,3)
1910 ZSS=ZS(1,1)*ZS(2,2)-ZS(2,1)*ZS(1,2)
1920 ZSS3= ZS(1,1)*ZS(3,2)-ZS(3,1)*ZS(1,2)
1950 IF(ZRETR(1,2).EQ.(0.0,0.0)) GO TO 85
2000 ZIN=(((ZLT(4,1)*ZS(1,2)-ZLT(4,2)*ZS(1,1))*(ZS(2,3)*ZS(1,2)
2001& -ZS(1,3)*ZS(2,2))+(ZLT(4,3)*ZS(1,2)-ZLT(4,2)*ZS(1,3))*ZSS)
2002& *((ZLT(3,4)*ZS(1,2)-ZLT(1,4)*ZS(3,2))*ZSS-(ZLT(2,4)*ZS(1,2)
2003& )))/((ZS(1,2)*ZSS)*((ZS(2,3)*ZS(1,2)-ZS(1,3)*ZS(2,2))*
2004& (ZS(1,1)*ZS(3,2)-ZS(3,1)*ZS(1,2))-(ZS(3,3)*ZS(1,2)-ZS(1,3)
```

TABLE 3-17. (Cont'd)

```
2005& *ZS(3,2))*ZSS))+(((ZLT(4,1)*ZS(1,2)-ZLT(4,2)*ZS(1,1))
2006& *(ZLT(2,4)*ZS(1,2)-ZLT(1,4)*ZS(2,2))+(ZLT(4,4)*ZS(1,2)
2007& -ZLT(4,2)*ZLT(4,4))*ZSS)/(ZS(1,2)*ZSS))
2100 AMPI=EG/(ZG+ZIN)
2200 AMP6=(((ZLT(3,4)*ZS(1,2)-ZLT(1,4)*ZS(3,2))*ZSS
2201& -(ZLT(2,4)*ZS(1,2)-ZLT(1,4)*ZS(2,2))*ZSS3)
2202& /((ZS(2,3)*ZS(1,2)-ZS(1,3)*ZS(2,2))*ZSS3
2203& -(ZS(3,3)*ZS(1,2)-ZS(1,3)*ZS(3,2))*ZSS))*AMPI
2300 AMP4=((ZS(2,3)*ZS(1,2)-ZS(1,3)*ZS(2,2))/ZSS)*AMP6
2301& +((ZLT(2,4)*ZS(1,2)-ZLT(1,4)*ZS(2,2))/ZSS)*AMPI
2400 AMP5=-(ZS(1,1)/ZS(1,2))*AMP4-(ZS(1,3)/ZS(1,2))*AMP6
2401& -(ZLT(1,4)/ZS(1,2))*AMPI
2410 G0 T0 90
2420 85 ZIN=((((ZLT(4,1)*ZS(2,2)-ZLT(4,2)*ZS(2,1))
2421& *(ZS(2,3)*ZS(1,2)-ZS(1,3)*ZS(2,2))
2422& +(ZLT(4,4)*ZS(2,2)-ZLT(4,2)*ZS(2,1))*ZSS)
2423& *((ZLT(2,4)*ZS(3,2)-ZLT(3,4)*ZS(2,2))*ZSS3
2424& -(ZLT(3,4)*ZS(1,2)-ZLT(1,4)*ZS(3,2))
2425& *(ZS(3,1)*ZS(2,2)-ZS(2,1)*ZS(3,2))))
2426& /(ZSS*ZS(2,2)*((ZS(3,3)*ZS(1,2)-ZS(1,3)*ZS(3,2))
2427& *(ZS(3,1)*ZS(2,2)-ZS(2,1)*ZS(3,2))
2428& -(ZS(2,3)*ZS(3,2)-ZS(3,3)*ZS(2,2))*ZSS3)))
2429& +(((ZLT(4,1)*ZS(2,2)-ZLT(4,2)*ZS(2,1))
2430& *(ZLT(2,4)*ZS(1,2)-ZLT(1,4)*ZS(2,2))
2431& +(ZLT(4,4)*ZS(2,2)-ZLT(4,2)*ZLT(2,4))*ZSS)
2432& /(ZSS*ZS(2,2)))
2440 AMPI=EG/(ZG+ZIN)
2450 AMP6=(((ZLT(2,4)*ZS(3,2)-ZLT(3,4)*ZS(2,2))*ZSS3
2451& -(ZLT(3,4)*ZS(1,2)-ZLT(1,4)*ZS(3,2))
2452& *(ZS(3,1)*ZS(2,2)-ZS(2,1)*ZS(3,2)))
2453& /((ZS(3,3)*ZS(1,2)-ZS(1,3)*ZS(3,2))
2454& *(ZS(3,1)*ZS(2,2)-ZS(2,1)*ZS(3,2))
2455& -(ZS(2,3)*ZS(3,2)-ZS(3,3)*ZS(2,2))*ZSS3))*AMPI
2460 AMP4=((ZS(3,3)*ZS(1,2)-ZS(1,3)*ZS(3,2))/ZSS3)*AMP6
2461& +((ZLT(3,4)*ZS(1,2)-ZLT(1,4)*ZS(3,2))/ZSS3)*AMPI
2470 AMP5=-(ZS(3,1)/ZS(3,2))*AMP4-(ZS(3,3)/ZS(3,2))*AMP6
2471& -(ZLT(3,4)/ZS(3,2))*AMPI
2500 90 VIN=ZLT(4,1)*AMP4+ZLT(4,2)*AMP5
2501& +ZLT(4,3)*AMP6+ZLT(4,4)*AMPI
2600 AMP0=((A(1,1)*ZRT(4,1)+A(2,1)*ZRT(4,2)+A(3,1)*ZRT(4,3))
2601& /(ZLE+ZRT(4,4)))*AMP4
2602& +((A(1,2)*ZRT(4,1)+A(2,2)*ZRT(4,2)+A(3,2)*ZRT(4,3))
2603& /(ZLE+ZRT(4,4)))*AMP5
2604& +((A(1,3)*ZRT(4,1)+A(2,3)*ZRT(4,2)+A(3,3)*ZRT(4,3))
2605& /(ZLE+ZRT(4,4)))*AMP6
2700 V0UT=-ZLE*AMP0
```

TABLE 3-17. (Cont'd)

```
C        **** PØWER AND INSERTIØN LØSS ****
      PØ=REAL(VØUT*CØNJG(-AMPØ))
      PREF=REAL((EG*ZLE/(ZG+ZLE))*CØNJG(EG/(ZLE+ZG)))
      PILØS(K)=10.*ALØG10(PØ/PREF)
      WRITE(6,200) FREQ,PILØS(K)
      FREQ=FREQ+FINC
  100 CØNTINUE
  200 FØRMAT(V)
      YMAX=PILØS(1)
      YMIN=PILØS(1)
      DØ 300 J=1,K
      IF(PILØS(J).GT.YMAX) YMAX=PILØS(J)
      IF(PILØS(J).LT.YMIN) YMIN=PILØS(J)
  300 CØNTINUE
      CALL YPLT(PILØS,FINIT,FINC,YMIN,YMAX,K,NPLTS,K1,DA,0)
      STØP
      END
```

F. COMPUTER GRAPHS OF TYPICAL MODE PROGRAM RESULTS

This section presents some of the results obtained to date from the MØDE programs of the previous section. Obviously, in the time allowed, it has been impossible to completely evaluate these programs since the number of variables involved, and the number of possible combinations, are so enormous. Of these programs MØDE2 is probably the most interesting from an experimental point of view, since it is relatively easy to generate sets of compatible variables for different cases (which may or may not be realizable in practice). However, in actual filter construction, MØDE3 is more appropriate.

Figures 3-27 and 3-28 show two runs of the MØDE1 program. The first is for two identical plates, each with a single mode called mode 1, with a coupling coefficient, XK1 = .088 velocity CT1 = 3.32×10^3 meters/sec, density DT1 = 2.65×10^3 kg/m^3, dielectric constant EP = $4.58 \times 8.85 \times 10^{-12}$ F/m, and electrode diameter = 1×10^{-2}m. Each plate is assumed to be a half wavelength thick at a center frequency of 10 MHz at this velocity of propagation. The filter, constructed of two of these plates, is driven from a generator of 1V and a resistance of 1600 ohms. The output voltage is also measured across a load resistor of 1600 ohms. These material parameters are appropriate for AT-cut quartz, as shown in Table 3-13.

The power insertion loss axis of these curves is in dB and the frequency axis is in hertz. These time sharing curves are crude but convenient for examining cases.

The curve of Figure 3-28 is called mode 2 and is characterized by a coupling coefficient that is twice that of mode 1 XK2 = 2XK1 and a velocity, CT2 = 1.1 CT1. Calculations for the response shown in Figure 3-28 were done for a half wavelength plate thickness at 10 MHz, determined by the velocity of propagation for mode 1 rather than mode 2. These curves, taken together, show the individual responses of the two modes most often used in the MØDE2 program.

Figure 3-29 shows the response obtained when Modes 1 and 2 are combined in one plate, and two of these identical plates are bonded together with zero rotation between them. When the two modes are combined together in a single plate, and two of these plates are operated as a stacked filter, the most obvious change is the dip in the response curve, following the mode-1 response, over that obtained by just adding the two response curves shown previously. There is also a slight decrease in the frequency of peak response for mode 2 as compared to only having mode 2 alone.

Figure 3-30 shows the response of this same filter for a rotation angle of 5° between plates. Nothing much happens to the response except for a slight decrease in insertion loss at the peak response.

Figures 3-31, 3-32 and 3-33 show the response of this 5°-rotated stack of two 10 MHz plates about 5, 15 and 20 MHz. In all cases these curves are compatible with the type of response expected for a stacked filter of single-mode elements using Mason's equivalent circuit.

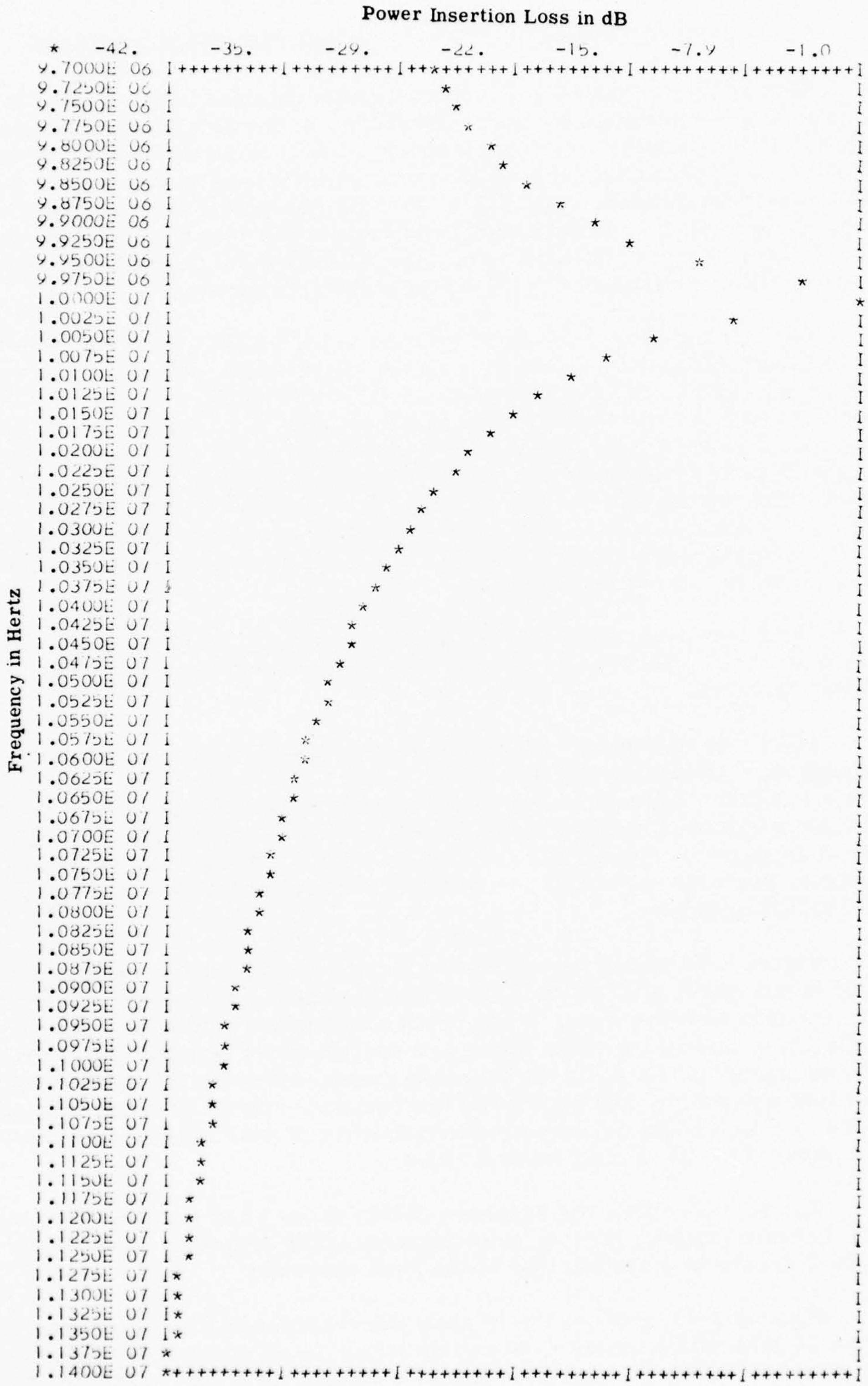

Figure 3-27. Mode 1 Response from MØDE 1 Program

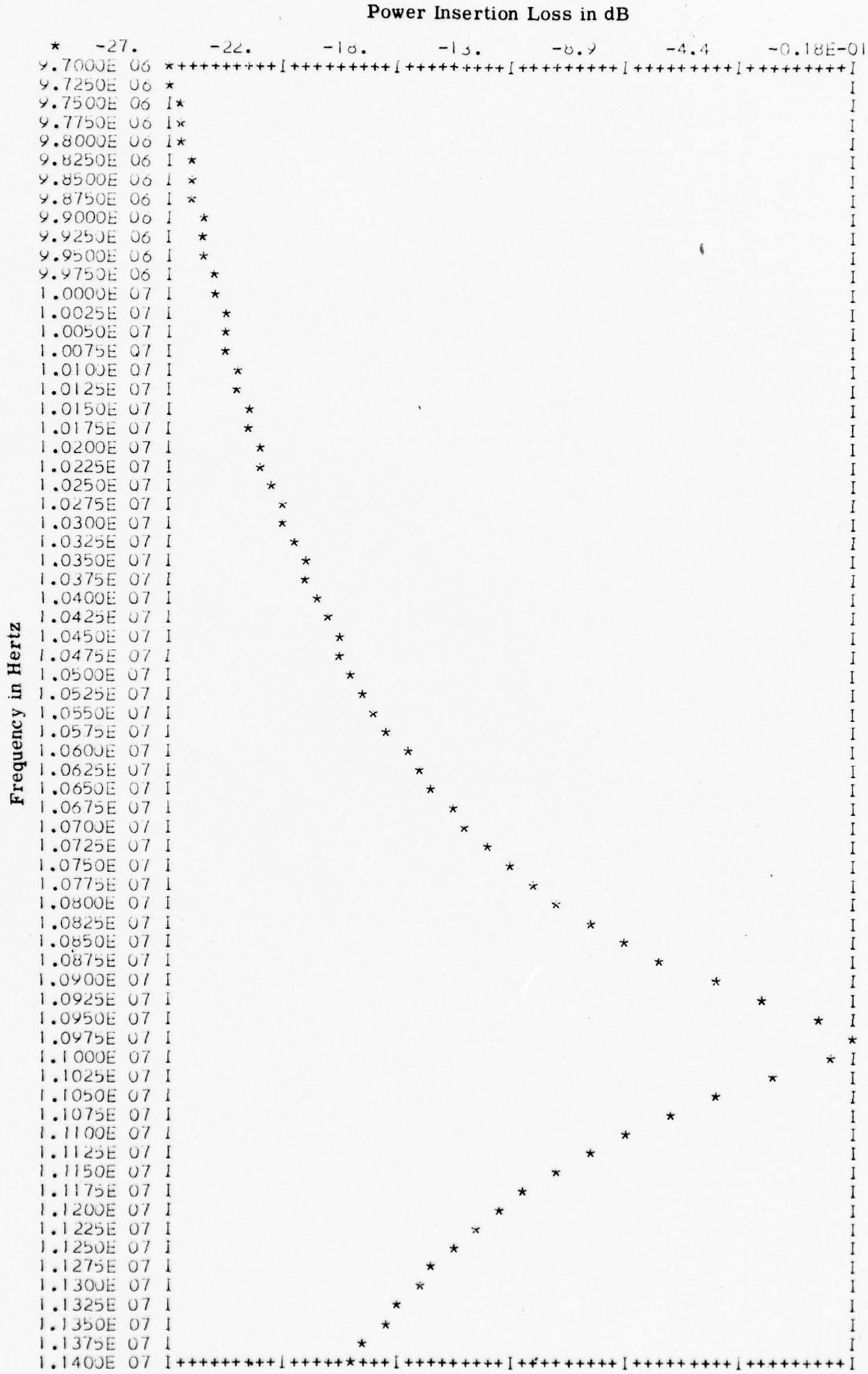

Figure 3-28. Mode 2 Response from MØDE 1 Program

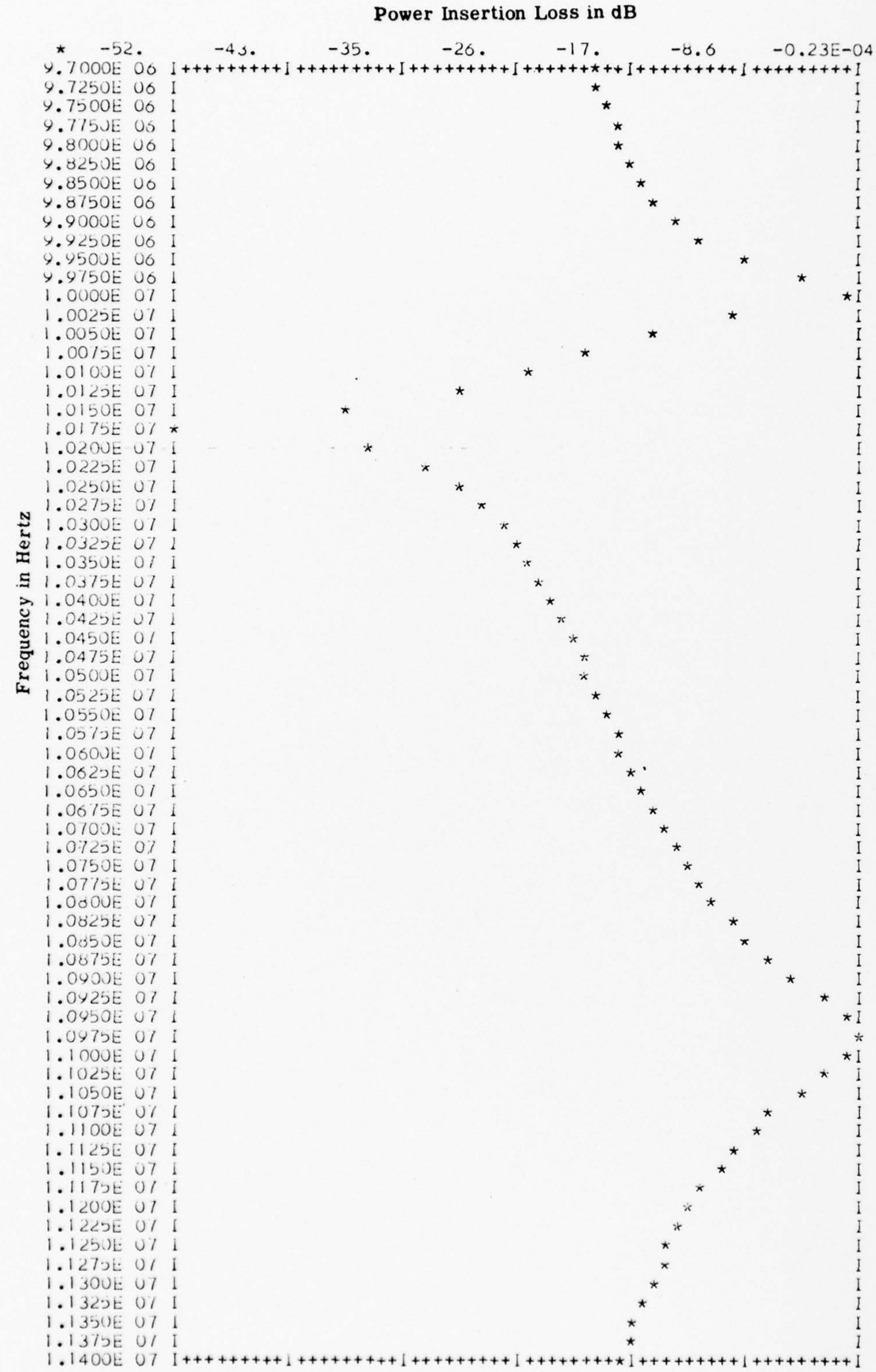

Figure 3-29. Two Element Stacked Filter (Mode 1 and Mode 2 in each plate)
0° rotation between plates

Each	XK1 = 0.088	CT1 = 3.32×10^3
Plate	XK2 = 2XK1	CT2 = 1.1 CT1

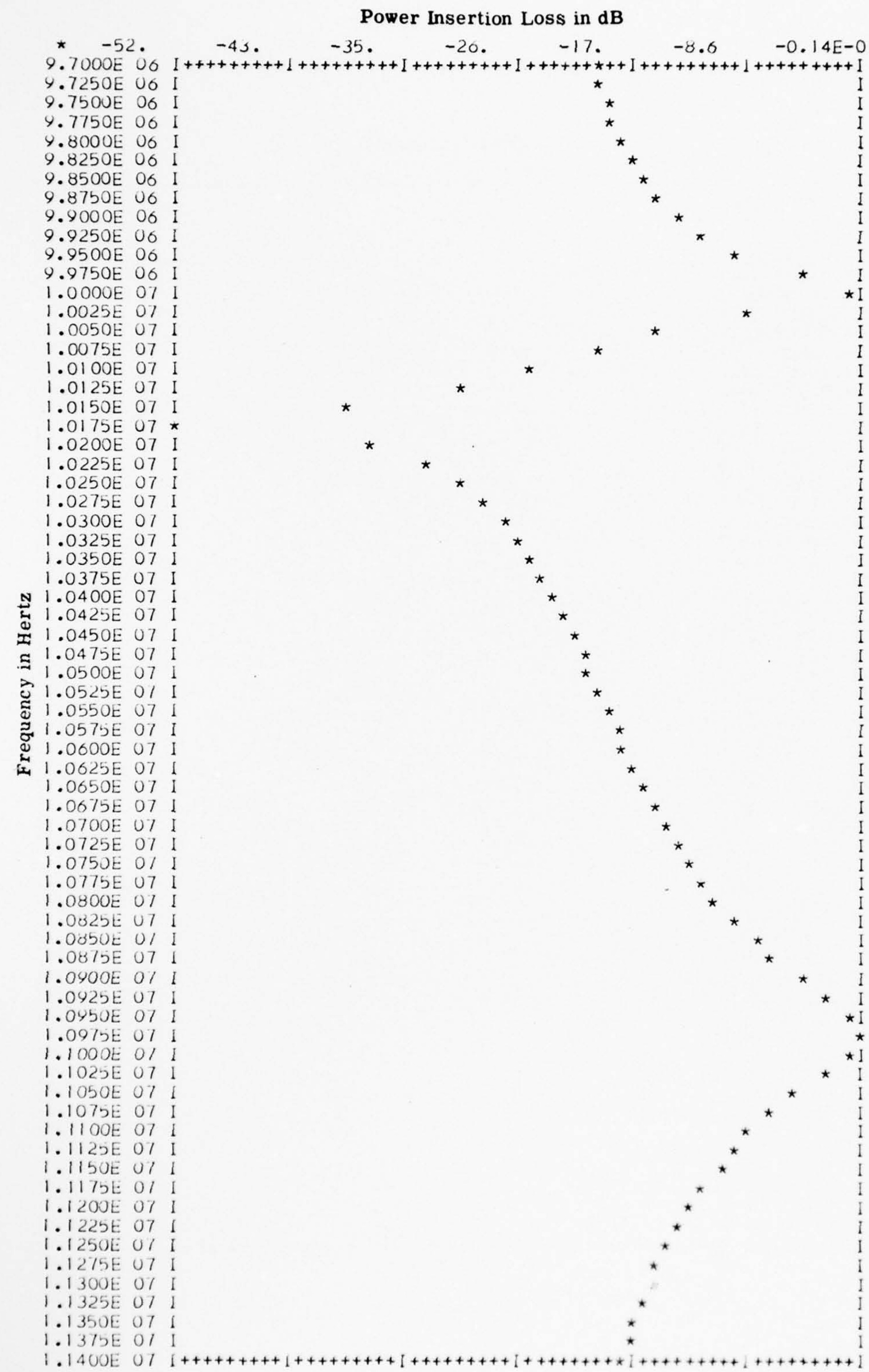

Figure 3-30. Two Element Stack $+5^{\circ}$ Rotation Between Plates Response at 10 Megahertz

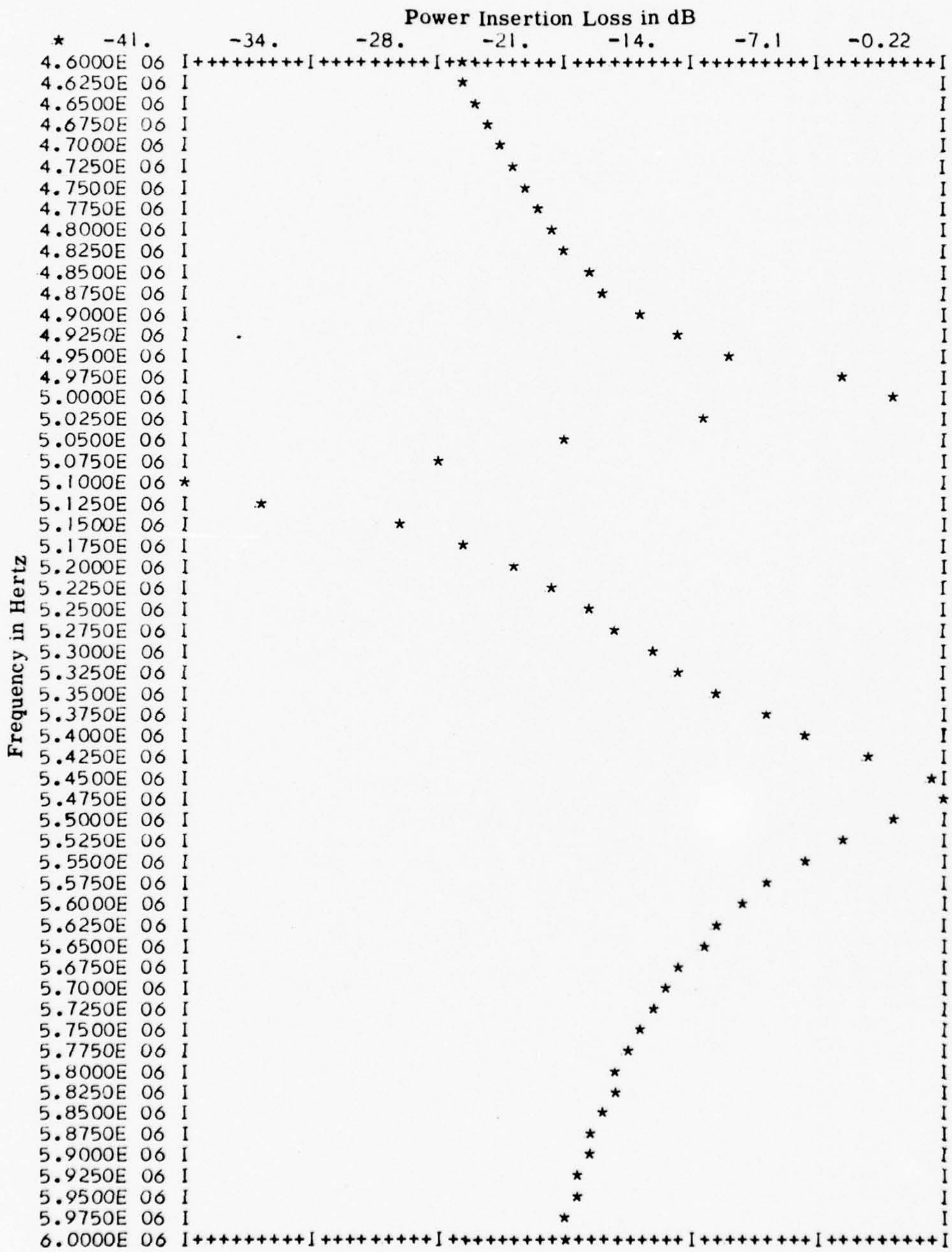

Figure 3-31. Two Element Stack $+5^{\circ}$ Rotation Between Plates Response at 5 Megahertz

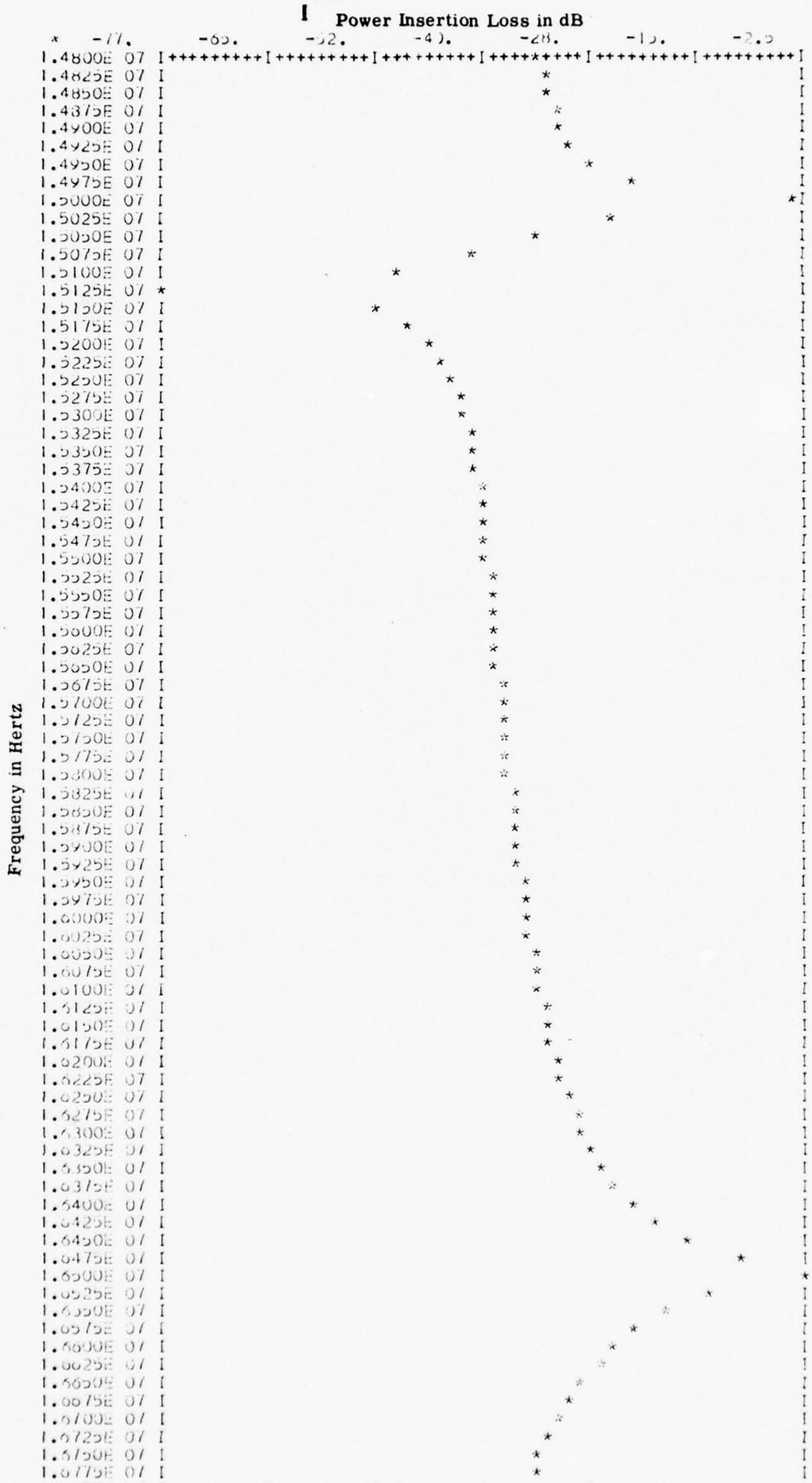

Figure 3-32. Two Element Stack $+5^{o}$ Rotation Between Plates Response at 15 Megahertz

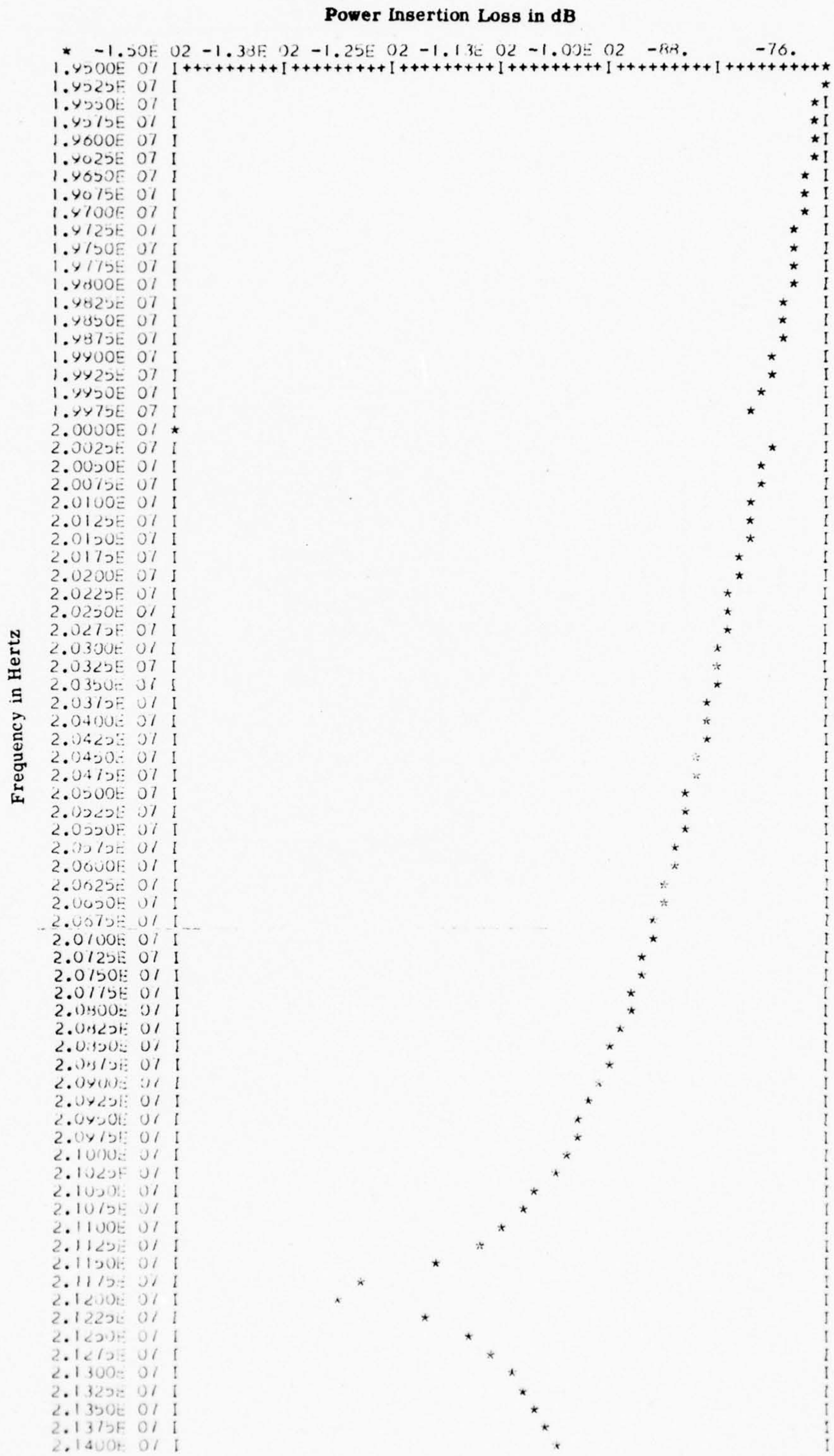

Figure 3-33. Two Element Stack $+5^{\circ}$ Rotation Response at 20 Megahertz

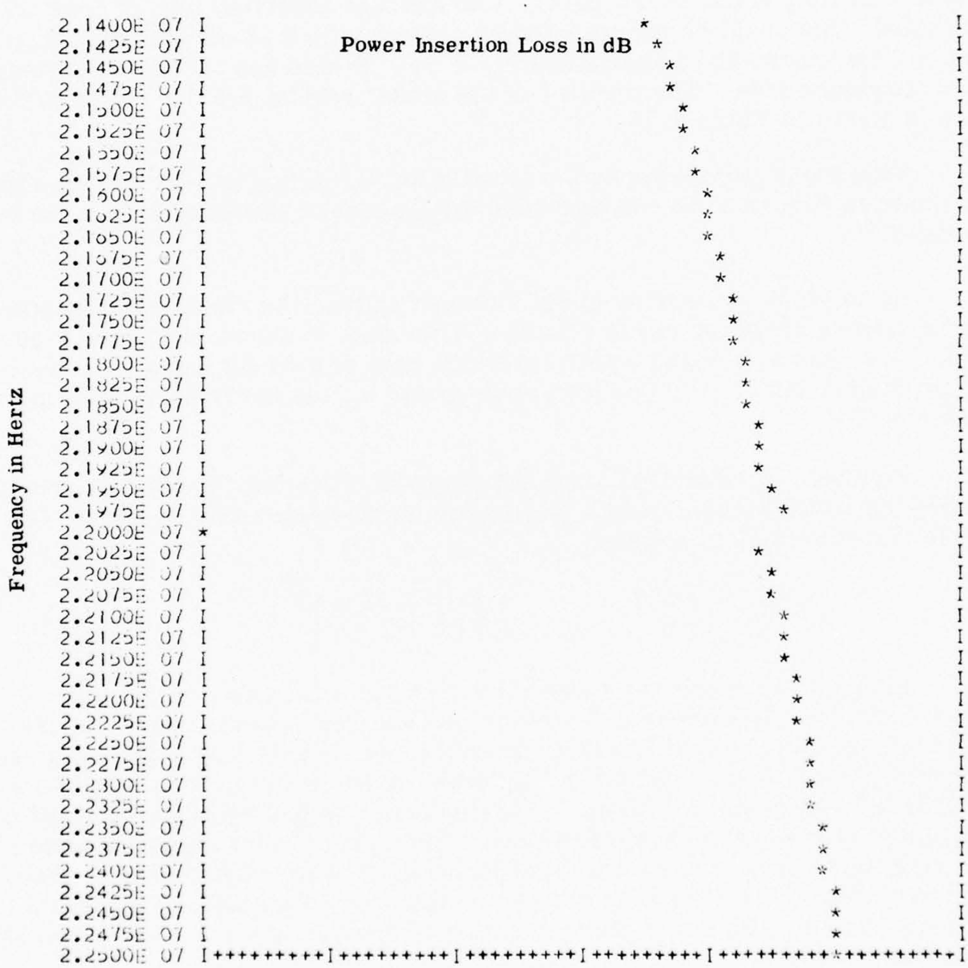

Figure 3-33. (Continued)

Figure 3-34 shows the response obtained with a -20° rotation between plates. Even at this angle of rotation, for these particular plates, nothing much happens. The response at a plate rotation angle of 45° is shown in Figure 3-35. Here, the response of mode 1 has decreased considerably and the notch following the mode 1 response has become shallower.

Figure 3-36 show the affect of rotating the two plates by 70°. A double-humped configuration occurs around the mode 2 response (actually a shifted down mode 2 response from that of Figure 3-29), and mode 1 has completely disappeared. Figure 3-37 continues the rotation of the two plates to 80°. The response now has a 5.73 dB peak at 10.4 MHz, a 7.1 dB dip at 10.475 MHz, and a 3.14 dB peak at 10.55 MHz. If an average insertion loss of 5 dB is assumed, this could be represented as a filter with a ± 2 dB passband ripple and a 3 dB bandwidth of approximately 2.5%. It also has a relatively steep low-frequency side. The printout of the actual results for this angle of rotation is shown in Table 3.18.

This looks promising so the results for a rotation of -82° between plates is shown in Figure 3-38. In this case the amount of passband ripple has been reduced.

At an angle of rotation of 85° between plates, the ripple has disappeared and a smooth response curve results. This case is shown in Figure 3-39. This curve has a midband power insertion loss of 3.67 dB and a 3 dB bandwidth of approximately 1.5%. The data appropriate to this curve are shown in Table 3-19.

Figures 3-40 and 3-41 show the effect of operating the MØDE2 program, where the second mode in each plate is not piezoelectrically coupled. For these two curves in each plate,

$$XK1 = 0.088 \qquad CT1 = 3.32 \times 10^{3}$$
$$XK2 = 0.0 \qquad CT2 = 1.1\,CT1$$

Figure 3-40 shows the response curve for this case at a 0° angle of plate rotation. As expected, this curve is identical to the curve of Figure 3-27 for, in this case, there is no possible way to couple into the non piezoelectric second mode. Figure 3-41 shows the same case, but with plate 2 rotated 5° with respect to plate 1. In this case the plate boundary condition coupling to the non-piezoelectric mode, takes place, showing up as a dip in the response curve at the location of mode 2, shown in Figure 3-28. Incidentally, due to the method of solution employed in this MØDE2 program, it will not operate with a non-piezoelectrically coupled mode 1. Mode 1 is always assumed present.

The case of two non-identical plates is illustrated in Figures 3-42 and 3-43. For these two curves the values for each plate are:

Plate 1		For Plate 2	
$XK1 = 0.088$	$CT1 = 3.32 \times 10^{3}$	$XK1 = 0.088$	$CT1 = 3.32 \times 10^{3}$
$XK2 = 2XK1$	$CT2 = 1.1\,CT1$	$XK2 = 0$	$CT2 = 1.1\,CT1$

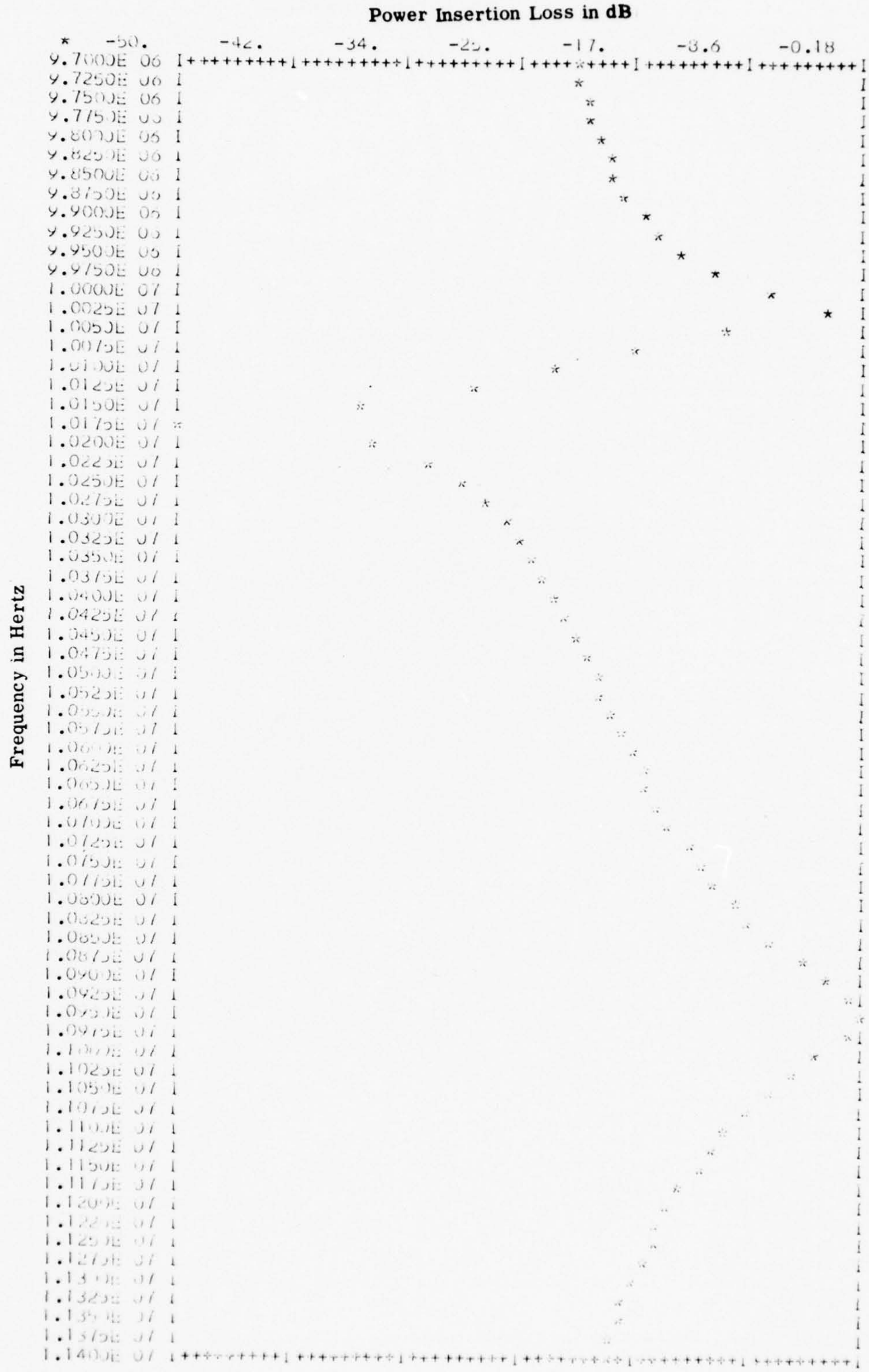

Figure 3-34. Two Element Stack -20° Rotation Between Plates

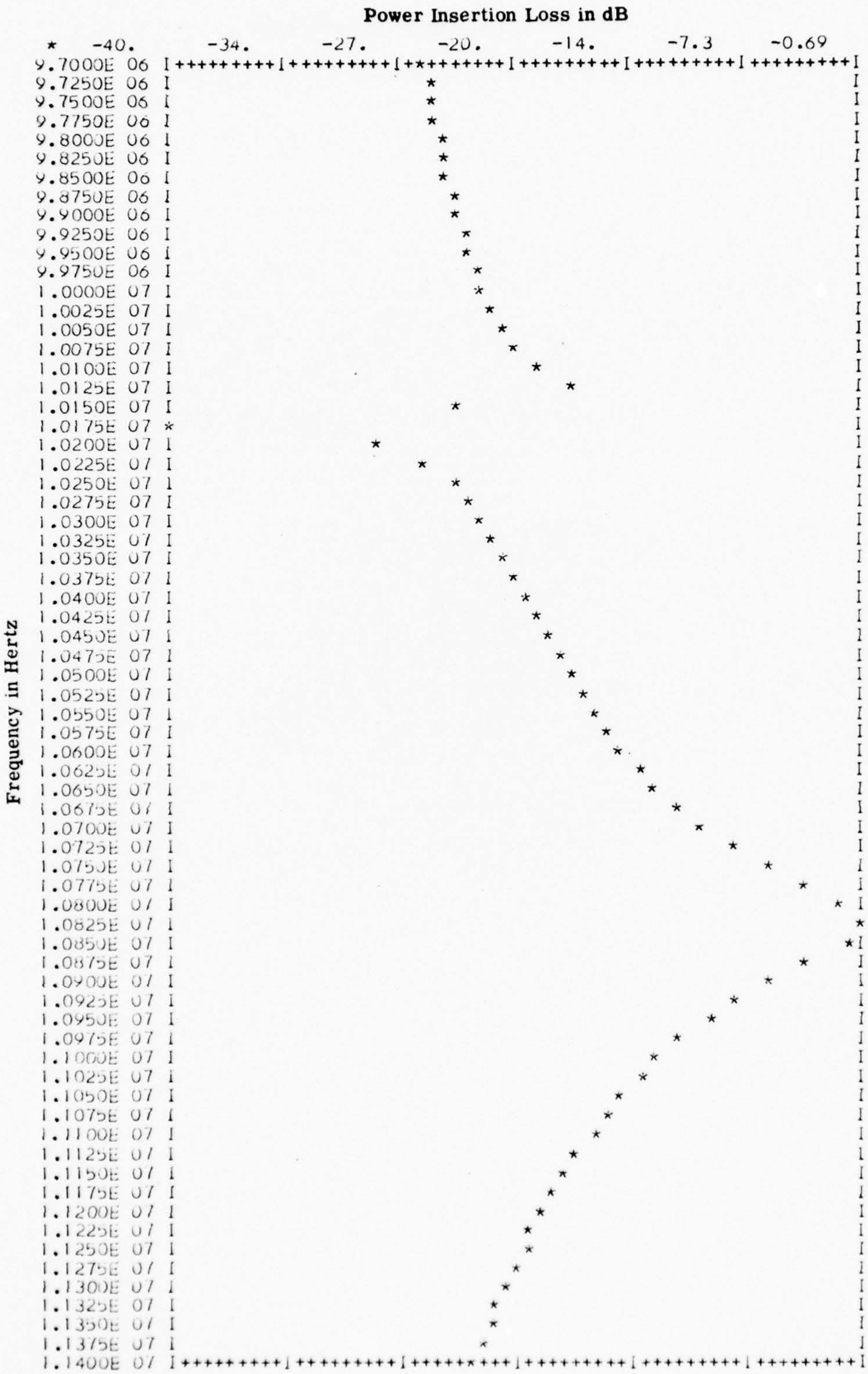

Figure 3-35. Two Element Stack 45° Rotation Between Plates

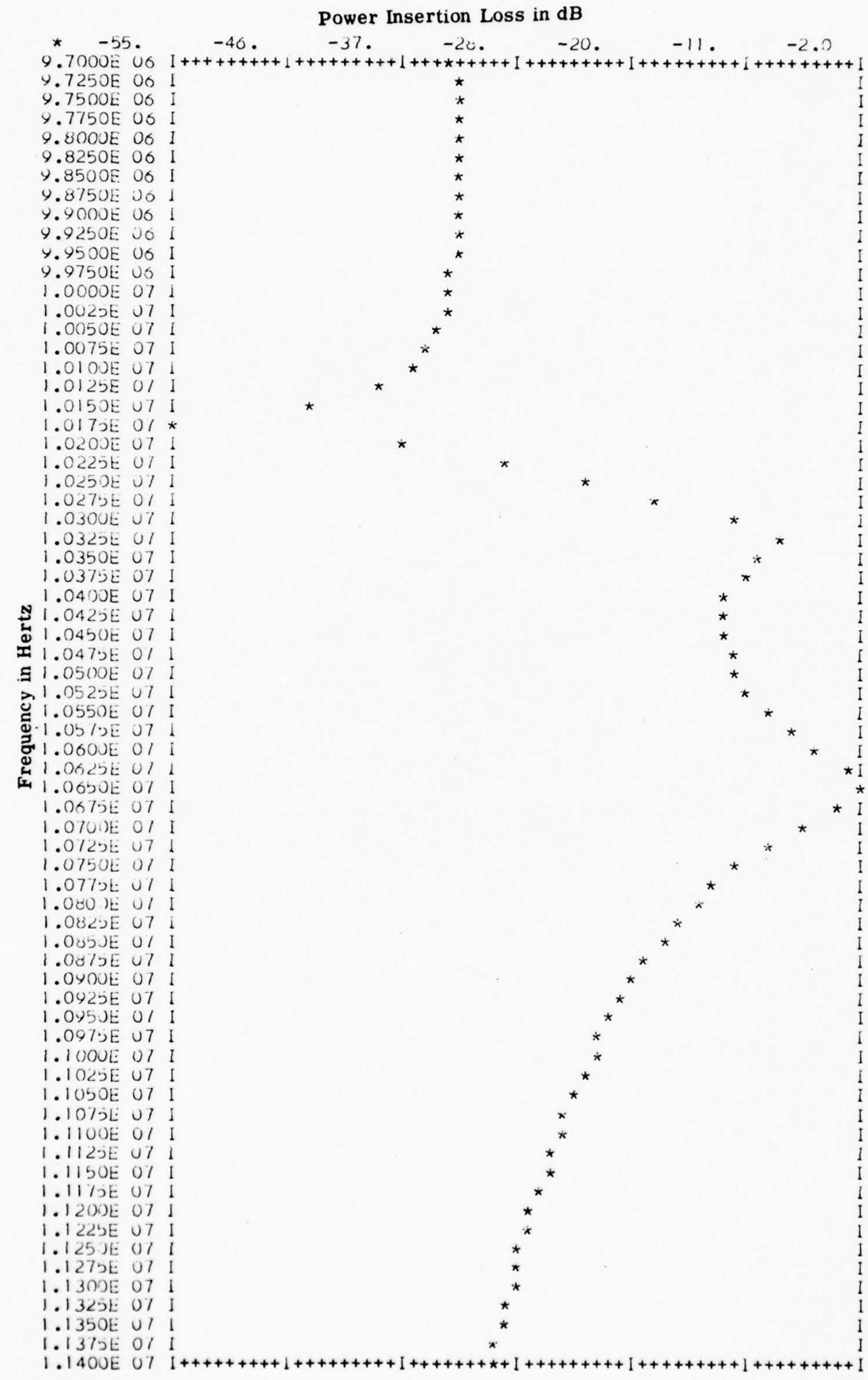

Figure 3-36. Two Element Stack 70^{O} Rotation Between Plates

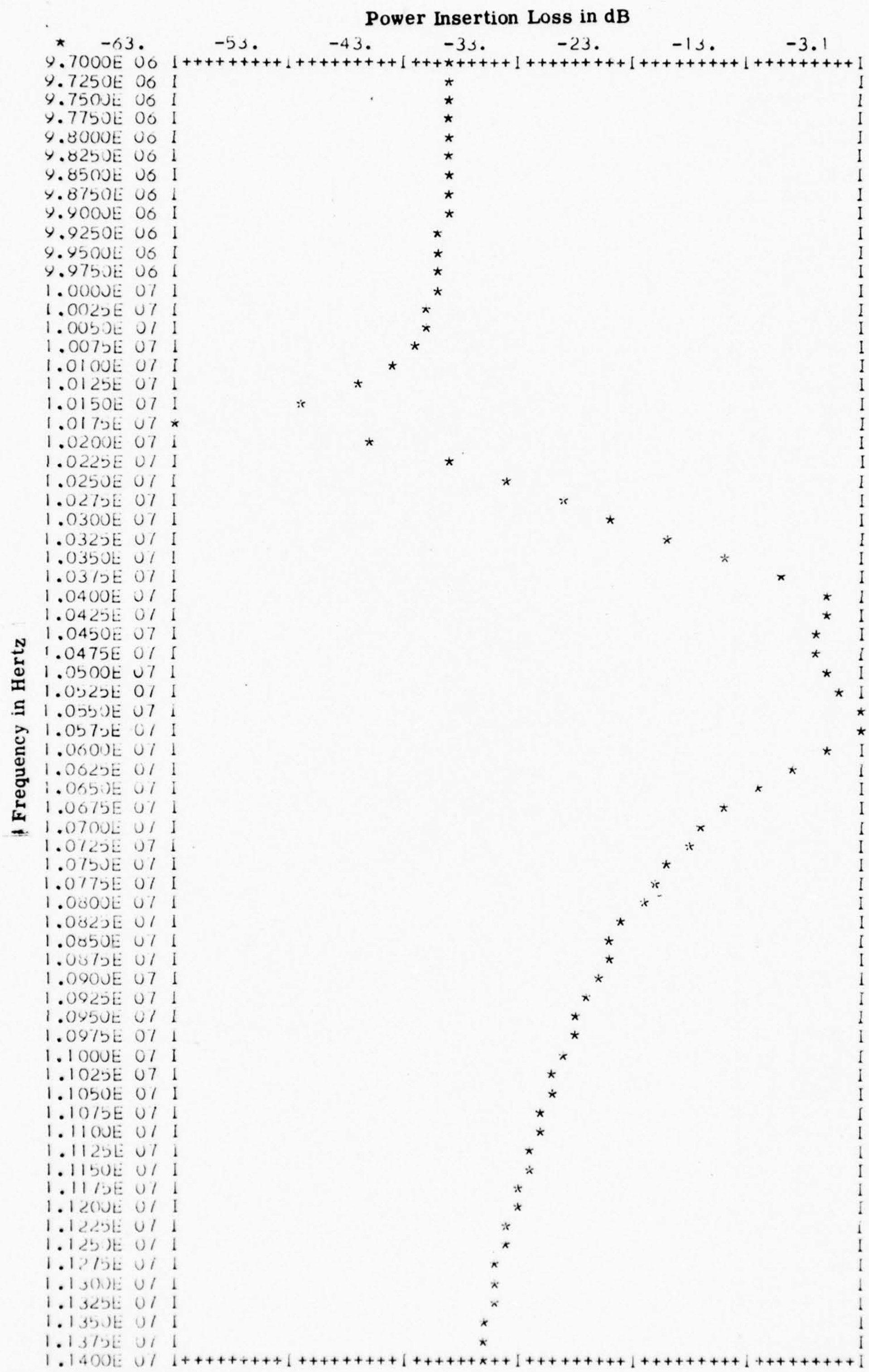

Figure 3-37. Two Element Stack 80° Rotation Between Plates

TABLE 3-18. DATA FOR STACKED FILTER OF TWO IDENTICAL PLATES OF FIGURE 37

Each Plate	CT1 = 3.32×10^3	Angle of Plate
XK1 = 0.088	CT2 = 1.1 CT1	Rotation
XK2 = 2XK2		80^O

```
SOURCE LINE   2000
<W>1470 EQUALITY OR NON-EQUALITY COMPARISON MAY NOT BE MEANINGFUL I
N LOGICAL IF EXPRESSIONS
   0.97000000E 07 -0.39546316E 02
   0.97250000E 07 -0.39493949E 02
   0.97500000E 07 -0.39449318E 02
   0.97750000E 07 -0.39414415E 02
   0.98000000E 07 -0.39391693E 02
   0.98250000E 07 -0.39384327E 02
   0.98500000E 07 -0.39396351E 02
   0.98750000E 07 -0.39432996E 02
   0.99000000E 07 -0.39501232E 02
   0.99250000E 07 -0.39610388E 02
   0.99500000E 07 -0.39773354E 02
   0.99750000E 07 -0.40008307E 02
   0.10000000E 08 -0.40342085E 02
   0.10025000E 08 -0.40815485E 02
   0.10050000E 08 -0.41494490E 02
   0.10075000E 08 -0.42495325E 02
   0.10100000E 08 -0.44047886E 02
   0.10125000E 08 -0.46703523E 02
   0.10150000E 08 -0.52477751E 02
   0.10175000E 08 -0.63001627E 02
   0.10200000E 08 -0.45983184E 02
   0.10225000E 08 -0.39022934E 02
   0.10250000E 08 -0.33859016E 02
   0.10275000E 08 -0.29317022E 02
   0.10300000E 08 -0.24923980E 02
   0.10325000E 08 -0.20367315E 02
   0.10350000E 08 -0.15366761E 02
   0.10375000E 08 -0.98611822E 01
   0.10400000E 08 -0.57309360E 01
   0.10425000E 08 -0.58422754E 01
   0.10450000E 08 -0.68777331E 01
   0.10475000E 08 -0.70871861E 01
   0.10500000E 08 -0.63929900E 01
   0.10525000E 08 -0.43941731E 01
   0.10550000E 08 -0.31440103E 01
   0.10575000E 08 -0.33192564E 01
   0.10600000E 08 -0.62390100E 01
   0.10625000E 08 -0.95754723E 01
   0.10650000E 08 -0.12433500E 02
   0.10675000E 08 -0.14808603E 02
   0.10700000E 08 -0.16810252E 02
   0.10725000E 08 -0.18529768E 02
   0.10750000E 08 -0.20032231E 02
   0.10775000E 08 -0.21364023E 02
   0.10800000E 08 -0.22558673E 02
   0.10825000E 08 -0.23640826E 02
   0.10850000E 08 -0.24629232E 02
   0.10875000E 08 -0.25538499E 02
   0.10900000E 08 -0.26379982E 02
   0.10925000E 08 -0.27163029E 02
   0.10950000E 08 -0.27894739E 02
   0.10975000E 08 -0.28581625E 02
```

TABLE 3-18. (Cont'd)

0.11000000E 08	-0.29228710E 02
0.11025000E 08	-0.29840316E 02
0.11050000E 08	-0.30419816E 02
0.11075000E 08	-0.30970744E 02
0.11100000E 08	-0.31495515E 02
0.11125000E 08	-0.31996601E 02
0.11150000E 08	-0.32476065E 02
0.11175000E 08	-0.32935607E 02
0.11200000E 08	-0.33376869E 02
0.11225000E 08	-0.33801254E 02
0.11250000E 08	-0.34209992E 02
0.11275000E 08	-0.34604214E 02
0.11300000E 08	-0.34984924E 02
0.11325000E 08	-0.35353002E 02
0.11350000E 08	-0.35709313E 02
0.11375000E 08	-0.36054554E 02
0.11400000E 08	-0.36389422E 02

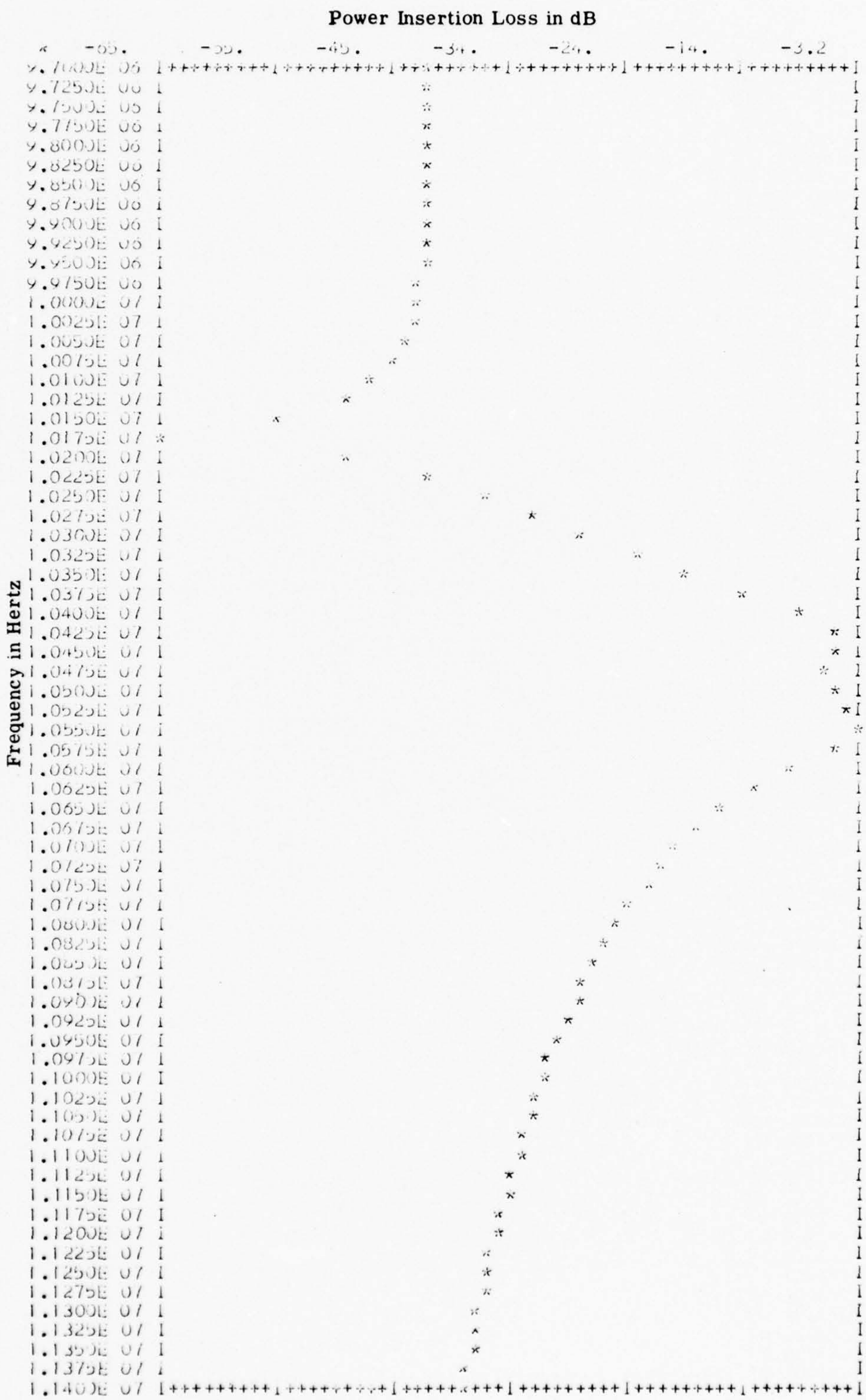

Figure 3-38. Two Element Stack -82° Rotation Between Plates

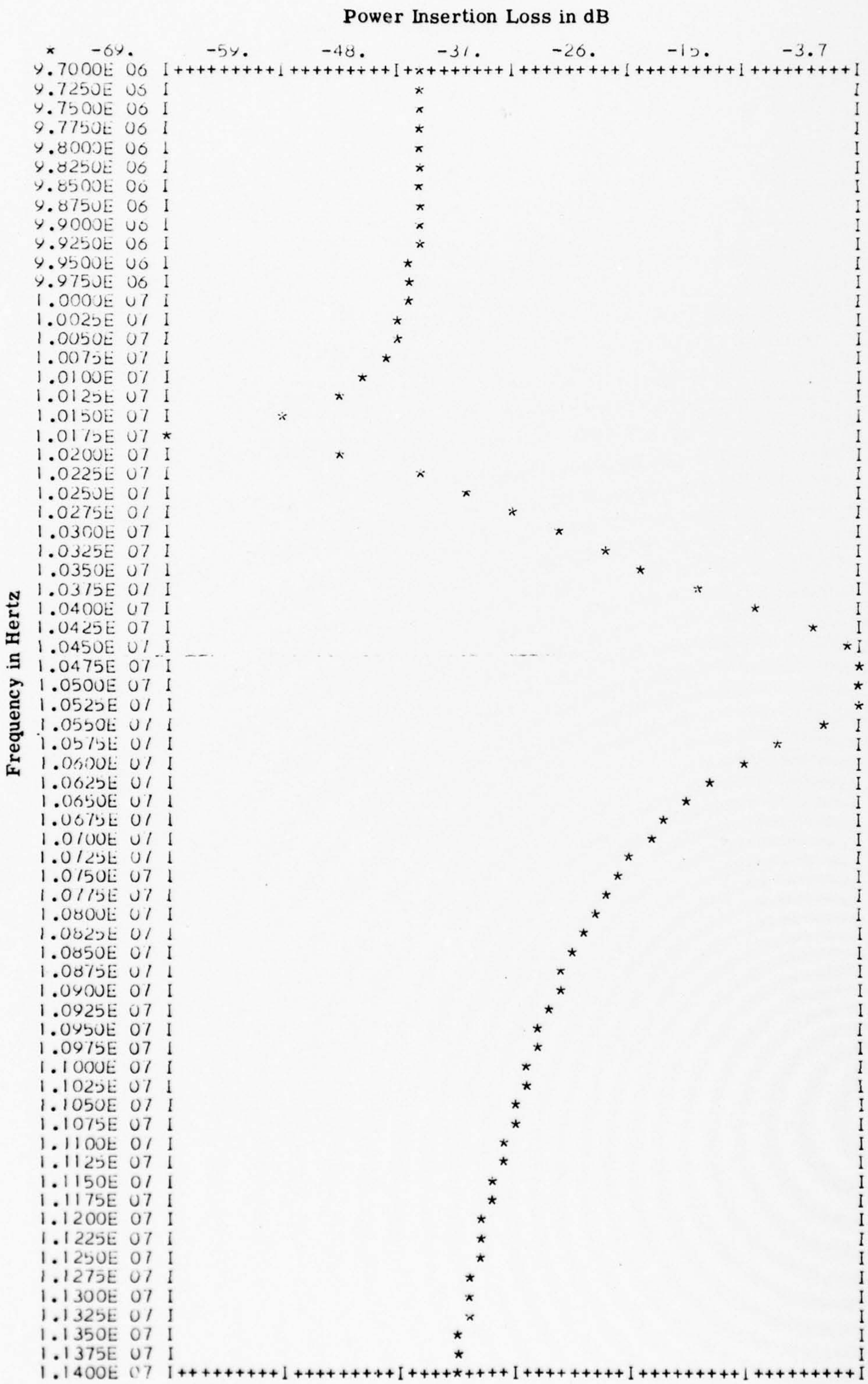

Figure 3-39. Two Element Stack 85^{O} Rotation Between Plates

Table 3-19. Data for Stacked Filter of Two Identical Plates of Figure 39

Each Plate

XK1 = 0.088 CT1 = 3.32×10^5 Angle of Plate Rotation

XK2 = 2XK1 CT2 = 1.1CT1 85°

```
SOURCE LINE   2000
<A>1470 EQUALITY OR NON-EQUALITY COMPARISON MAY NOT BE MEANINGFUL I
N LOGICAL IF EXPRESSIONS
  0.97000000E 07 -0.45613794E 02
  0.97250000E 07 -0.45566490E 02
  0.97500000E 07 -0.45527452E 02
  0.97750000E 07 -0.45498733E 02
  0.98000000E 07 -0.45482907E 02
  0.98250000E 07 -0.45483247E 02
  0.98500000E 07 -0.45503904E 02
  0.98750000E 07 -0.45550284E 02
  0.99000000E 07 -0.45629547E 02
  0.99250000E 07 -0.45751264E 02
  0.99500000E 07 -0.45928622E 02
  0.99750000E 07 -0.46180148E 02
  0.10000000E 08 -0.46533184E 02
  0.10025000E 08 -0.47029113E 02
  0.10050000E 08 -0.47734707E 02
  0.10075000E 08 -0.48767248E 02
  0.10100000E 08 -0.50358026E 02
  0.10125000E 08 -0.53060284E 02
  0.10150000E 08 -0.58892118E 02
  0.10175000E 08 -0.69488659E 02
  0.10200000E 08 -0.52563060E 02
  0.10225000E 08 -0.45724549E 02
  0.10250000E 08 -0.40724295E 02
  0.10275000E 08 -0.36408985E 02
  0.10300000E 08 -0.32340657E 02
  0.10325000E 08 -0.28263915E 02
  0.10350000E 08 -0.23969077E 02
  0.10375000E 08 -0.19234704E 02
  0.10400000E 08 -0.13842220E 02
  0.10425000E 08 -0.80800430E 01
  0.10450000E 08 -0.46146222E 01
  0.10475000E 08 -0.41721899E 01
  0.10500000E 08 -0.36707944E 01
  0.10525000E 08 -0.38846952E 01
  0.10550000E 08 -0.70461994E 01
  0.10575000E 08 -0.11140528E 02
  0.10600000E 08 -0.14669787E 02
  0.10625000E 08 -0.17560205E 02
  0.10650000E 08 -0.19959005E 02
  0.10675000E 08 -0.21991750E 02
  0.10700000E 08 -0.23747145E 02
  0.10725000E 08 -0.25287279E 02
  0.10750000E 08 -0.26656160E 02
  0.10775000E 08 -0.27886198E 02
  0.10800000E 08 -0.29001707E 02
  0.10825000E 08 -0.30021171E 02
  0.10850000E 08 -0.30959112E 02
  0.10875000E 08 -0.31827167E 02
  0.10900000E 08 -0.32634569E 02
  0.10925000E 08 -0.33389111E 02
  0.10950000E 08 -0.34096759E 02
  0.10975000E 08 -0.34763133E 02
```

TABLE 3-19. (Cont'd)

0.11000000E 08	-0.35392596E 02
0.11025000E 08	-0.35988952E 02
0.11050000E 08	-0.36555177E 02
0.11075000E 08	-0.37094472E 02
0.11100000E 08	-0.37608992E 02
0.11125000E 08	-0.38100995E 02
0.11150000E 08	-0.38572382E 02
0.11175000E 08	-0.39024711E 02
0.11200000E 08	-0.39459499E 02
0.11225000E 08	-0.39878054E 02
0.11250000E 08	-0.40281532E 02
0.11275000E 08	-0.40670977E 02
0.11300000E 08	-0.41047351E 02
0.11325000E 08	-0.41411469E 02
0.11350000E 08	-0.41764166E 02
0.11375000E 08	-0.42106088E 02
0.11400000E 08	-0.42437910E 02

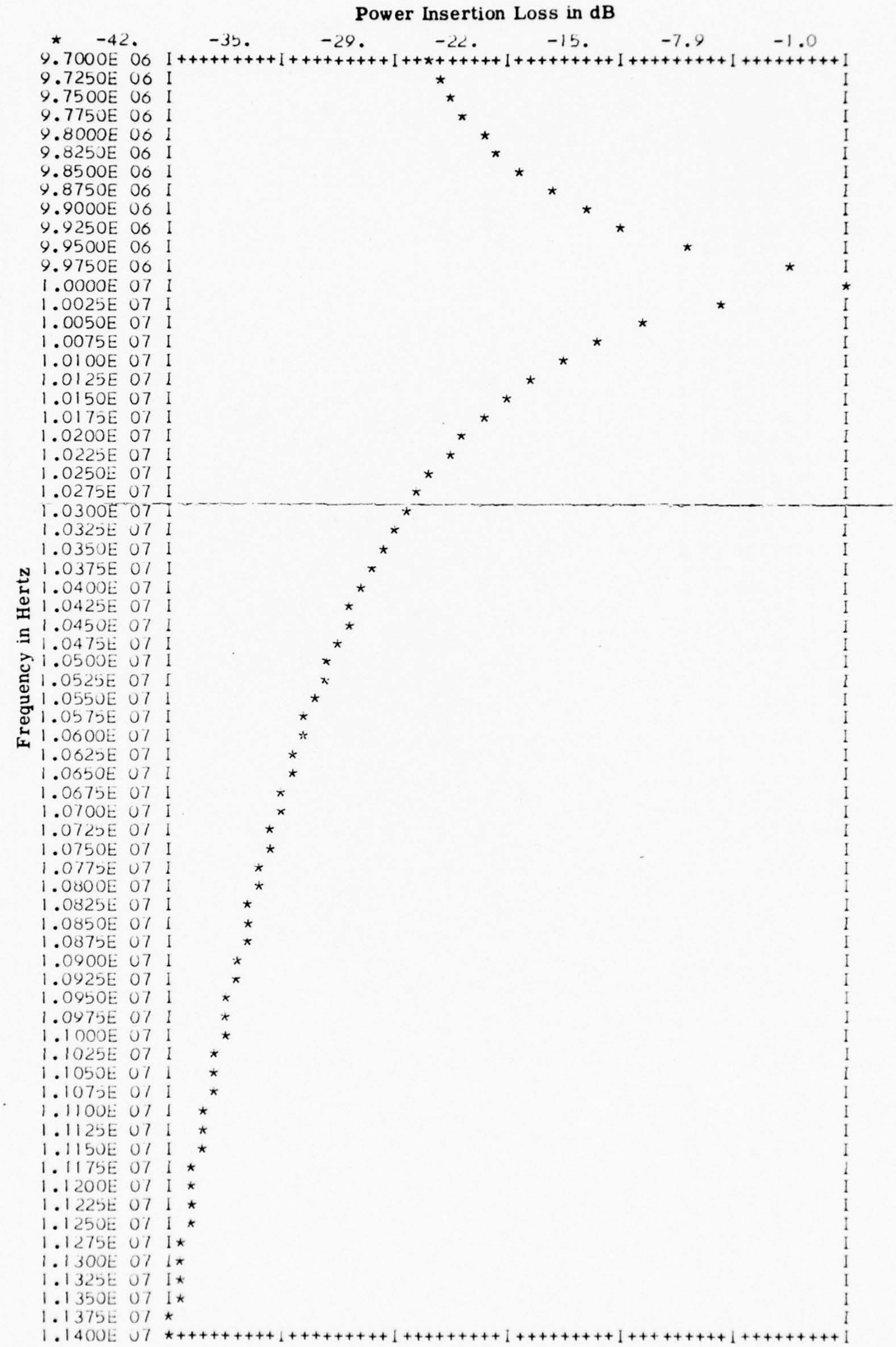

Figure 3-40. Two Element Identical Plate Stack Nonpiezoelectrically Coupled
2nd Mode
0^{o} Rotation Between Plates
Each Plate
XK1 = 0.088 CT1 = 3.32×10^{3}
XK2 = 0.0 CT2 = 1.1 CT1

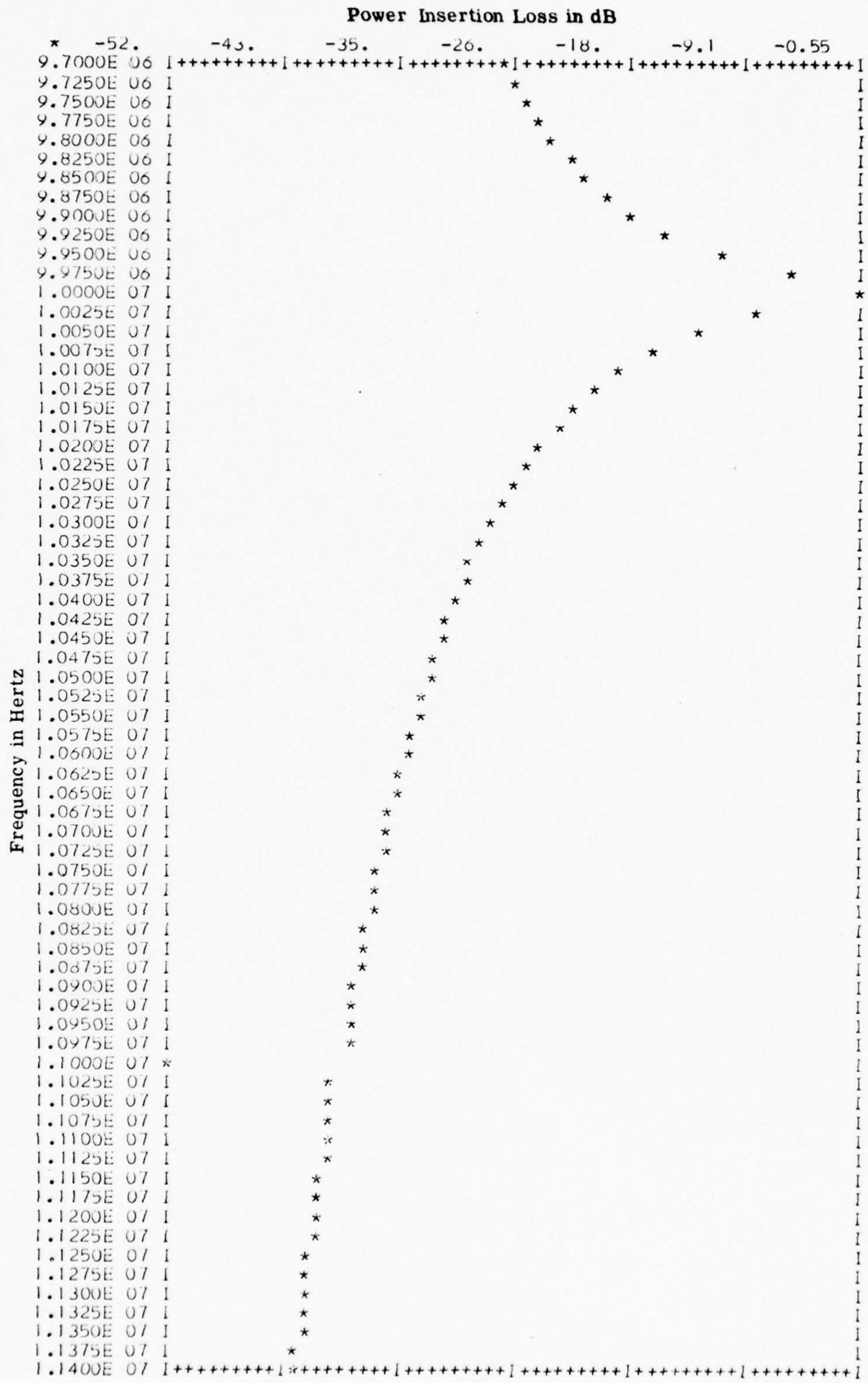

Figure 3-41. Two Element Identical Plate Stack Nonpiezoelectrically Coupled 2nd Mode 5^{O} Rotation Between Plates

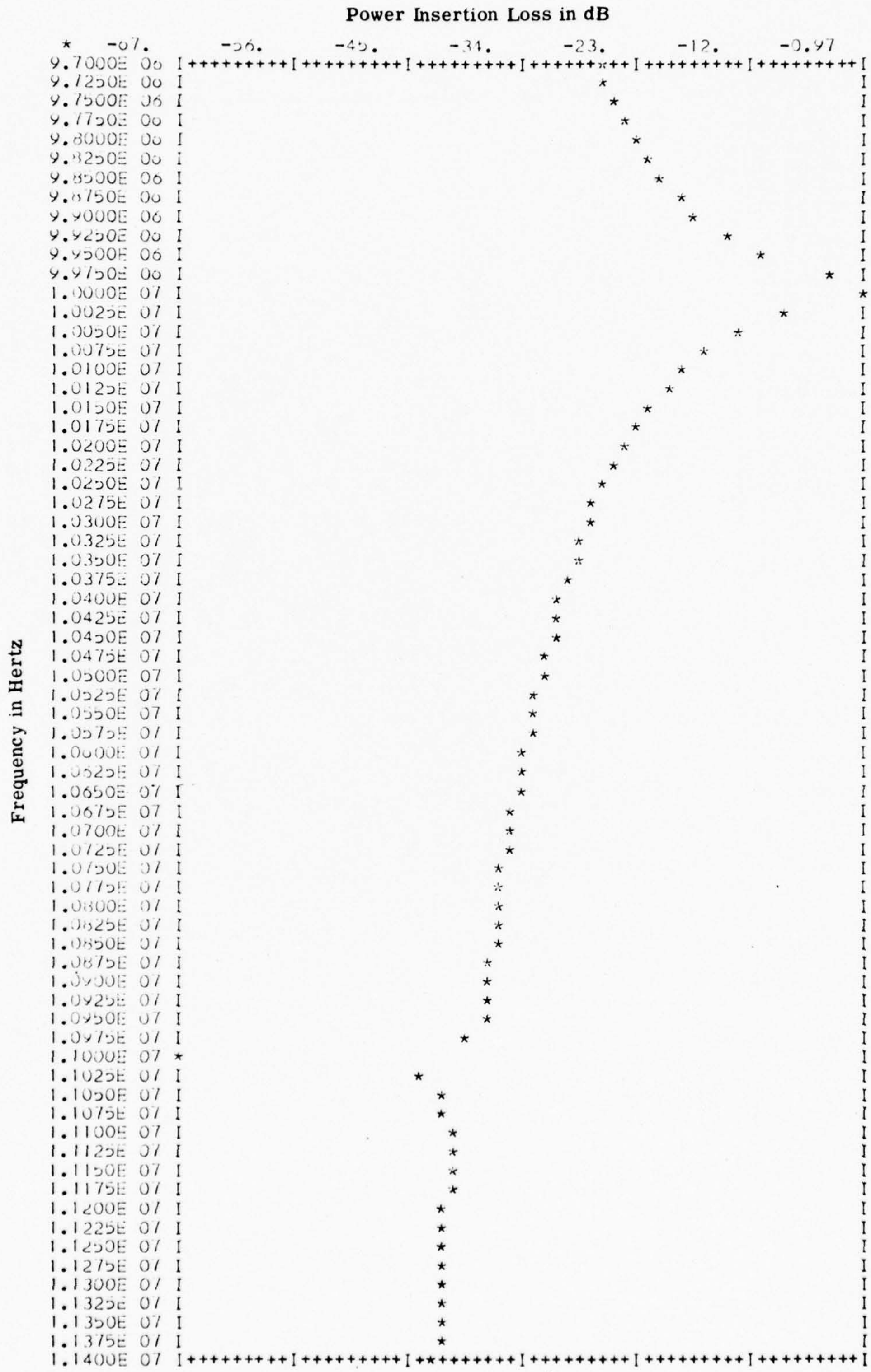

Figure 3-42. Two Element Non-Identical Plate Stack 0^{o} Rotation Between Plates

Plate 1		Plate 2	
XK1 = 0.088	CT1 = 3.32×10^{3}	XK1 = 0.088	CT1 = 3.32×10^{3}
XK2 = 2XK1	CT2 = 1.1 CT1	XK2 = 0	CT2 = 1.1 CT1

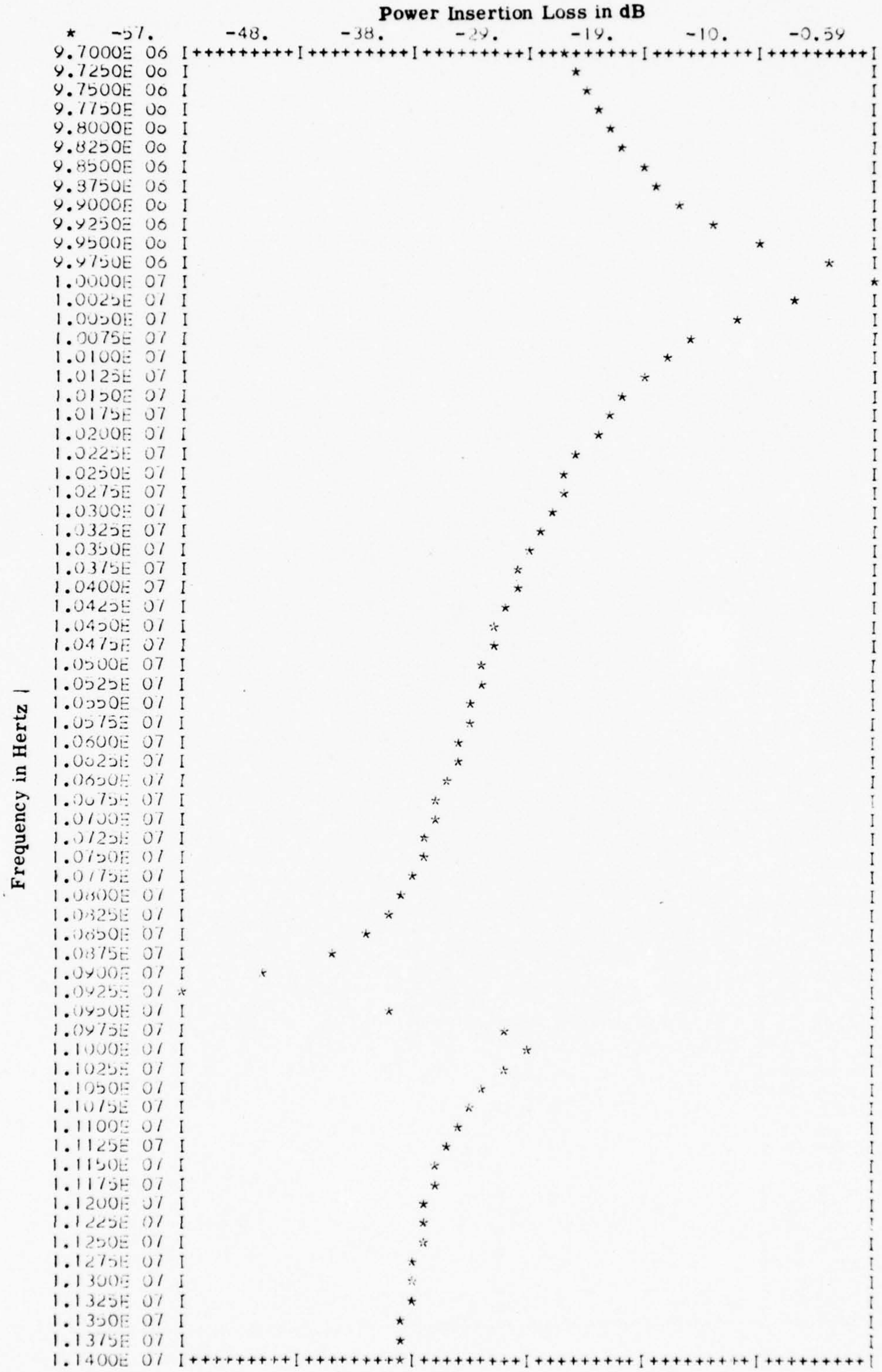

Figure 3-43. Two Element Non-Identical Plate Stack of Figure 3-42 with 5^{o} Rotation Between Plates

Thus, in plate 2, the second mode is not piezoelectrically coupled. Except for this, the plate parameters are identical. Figure 3.42 shows the response of these plates when they are lined up. The response, in this case, will exhibit a notch at the mode-2 frequency, in contrast to Figure 3-41, since energy is coupled into this mode by plate 1, but is not available as output energy because of the lack of piezoelectric coupling to this mode in plate 2. Figure 3.43 shows the same two plates with a 5^{o} rotation between them. In this case a small resonance is observed at mode 2, in contrast to Figure 3-42 since, now, due to plate boundary coupling, some of the piezoelectrically excited energy of plate 1 in mode 2 can be coupled to the output.

Figure 3-44 shows the response at 5^{o} of plate rotation of a two-plate stack of identical elements similar to those shown in Figure 3-30 at a 5^{o} rotation between the plates. However, for these plates,

$$XK1 = 0.088 \qquad CT1 = 3.32 \times 10^{3}$$
$$XK2 = 2XK1 \qquad CT2 = 1.15\ CT1,$$

so that here the velocity of mode 2 is faster than that shown earlier. Besides the obvious fact of making the mode 2 response occur at a higher frequency, this change also causes the notch following the mode-1 response to occur at a higher frequency. This means that the null in the response is due to the phase shift between the mode-1 and mode-2 responses. It also suggests that, in multi element stacked cascades, plates with different mode properties can be used to control stop-band rejection.

Figures 3-45, 3-46 and 3-47 show the effects on the frequency response of two identical element stacks, when the velocity of the second mode is slower than that of the first mode. For these plates

$$XK1 = 0.088 \qquad CT1 = 3.32 \times 10^{3}$$
$$XK2 = 1.1XK1 \qquad CT2 = 0.95\ CT11$$

Again, except for the change in velocity of the second mode, the plates are identical to those shown earlier. This change in velocity of mode 2 obviously makes the mode-2 response occur at a lower frequency than that of mode 1. (The plate is still one half wavelength thick at a frequency of 10 MHz and a velocity of propagation corresponding to CT1.)

Figure 3-45 shows the response for this case at a plate rotation angle of 5^{o}. In this figure the lower-frequency response is the mode-2 response, and the higher-frequency response is the mode-1 response. Contrasting this figure to that shown in Figure 3-30 shows that the notch frequency now occurs below the mode-1 response.

Figure 3-46 shows the frequency response for this case at a plate rotation angle of 70^{o}, similar to that shown in Figure 3-36. Again, a double-humped response begins to appear but, in this case, the notch is on the high side while, in Figure 3-36, it is on the low side.

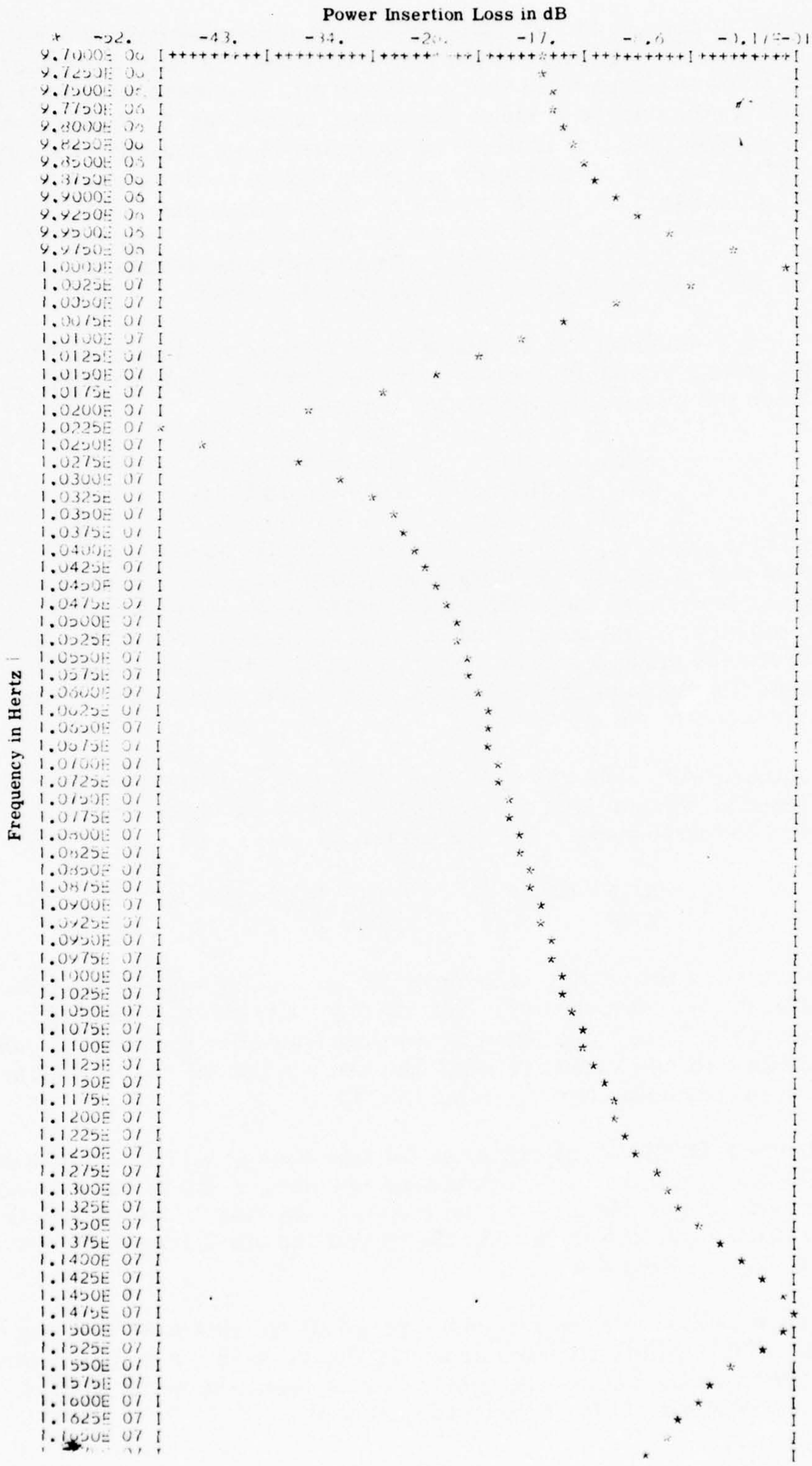

Figure 3-44. Two Element Identical Plate Stack 5^{o} Rotation Between Plates Each Plate (Faster Mode2 Velocity)

XK1 = 0.088 CT1 = 3.32×10^{3}

XK2 = 2XK1 CT2 = 1.15 CT1

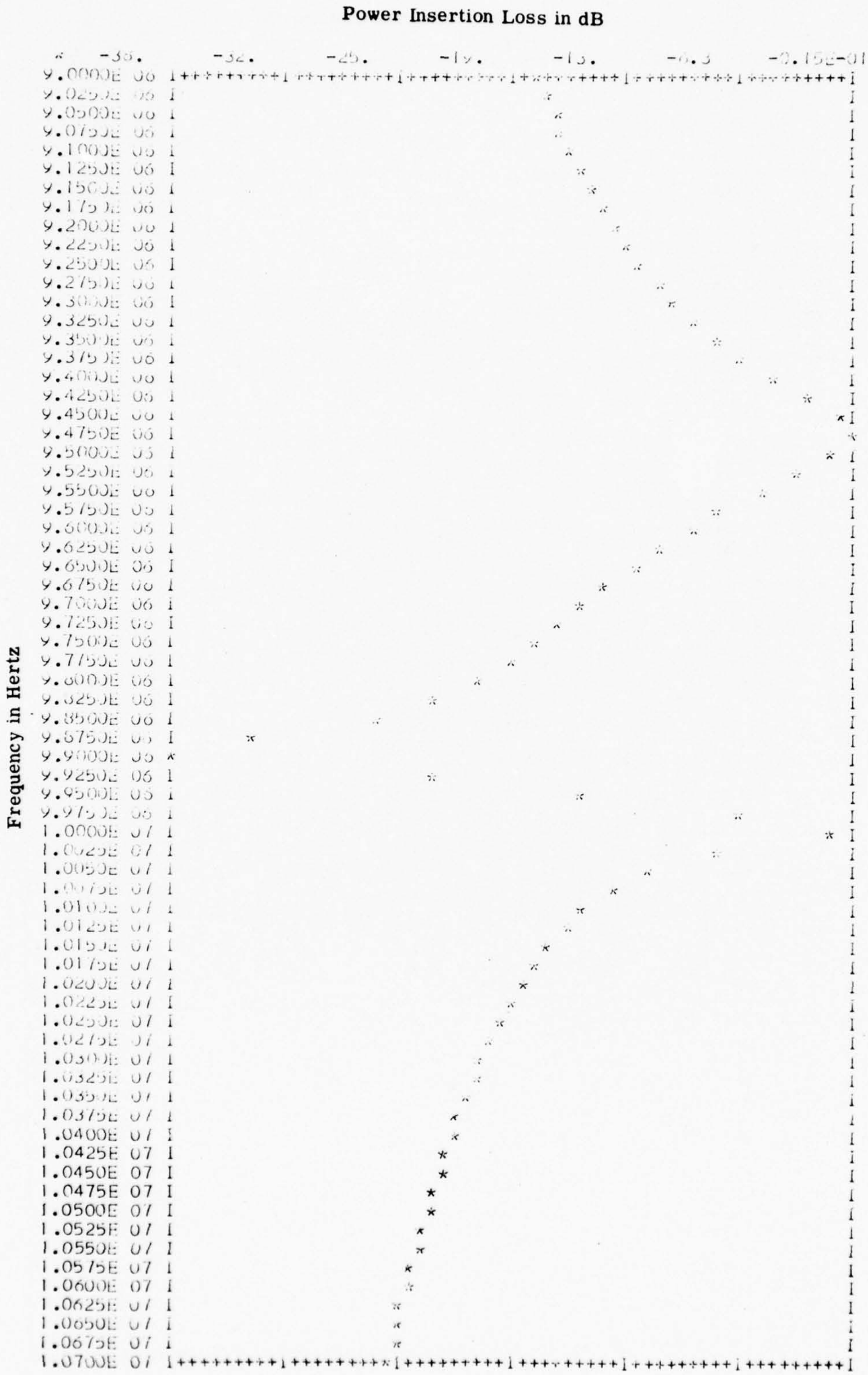

Figure 3-45. Two Element Identical Plate Stack 5^{O} Rotation Between Plates Each Plate (Slower Mode 2 Velocity)

XK1 = 0.088 CT1 = 3.32×10^{3}

XK2 = 2XK1 CT2 = 0.95 CT1

Figure 3-46. Two Element Identical Plate Stack Slower Mode 2 Velocity
70^{O} Rotation Between Plates

Figure 3-47 shows a continuation of the plate rotation for this case to an angle of 83^o. A single-peaked response curve, similar to that shown for the first case at an angle of 85^o (shown in Figure 3-39), has occurred but, again, the notch occurs above the main response. This suggests the possibility of cascading, electrically, two (or more) element stacks of multimode filters to tailor the overall response. An electrical cascade of an element of the type shown in Figure 3-47, with that shown in Figure 3-39, after appropriately adjusting the plate thicknesses to make the main responses in each stack coincide, would yield an overall response curve with notches both above and below the main response.

Figures 3-48, 3-49, 3-50 and 3-51 show the response obtained from the MØDE3 program for AT-cut quartz. Input values for both plates are shown in Table 3-13, as the output of the VCØUP program. A sketch of the relationship of the normal modes of each plate to the plate axes are shown in Figure 3-3. For this crystal cut, mode 2 and mode 3 (those modes lying in the $\beta^{(2)}$ and $\beta^{(3)}$ directions of Figure 3-3) are non-piezoelectrically coupled.

Figure 3-48 shows the filter response of this two-plate stack of AT-cut quartz elements with the two plates lined up. A nice smooth response curve results (as expected from the mode-2 program results discussed in connection with Figure 3-40). Figure 3-49 shows the effects of rotating plate 2 by 5^o with respect to plate 1. Again, similar to the discussion in connection with Figure 3-41, plate boundary condition coupling takes place and the response curve shows nulls and peaks due to the three modes.

Figure 3-50 shows the effects of continuing the plate rotation to 45^o. Here an interchange of energy, from mode 1 to mode 2 occurs. The resonant effects of mode 2 appear, and are coupled back to the output through mode 1.

Figure 3-51 demonstrates the effects of continuing the plate rotation to 75^o.

While not illustrated, the 3-mode equivalent of the MØDE2 program with the normal mode axes, lined up with the plate axes, can be achieved by setting $\beta_1^{(1)} = \beta_2^{(2)} = \beta_{(3)}^{3} = 1.0$, and the other components of the eigenvectors equal to zero in the MØDE3 program.

Also, while most of the results employed identical plates, the programs work equally well, if not better, for plates with non-identical parameters (since then many of the problems associated with impedance terms in both plates going to zero, at the same time, are avoided).

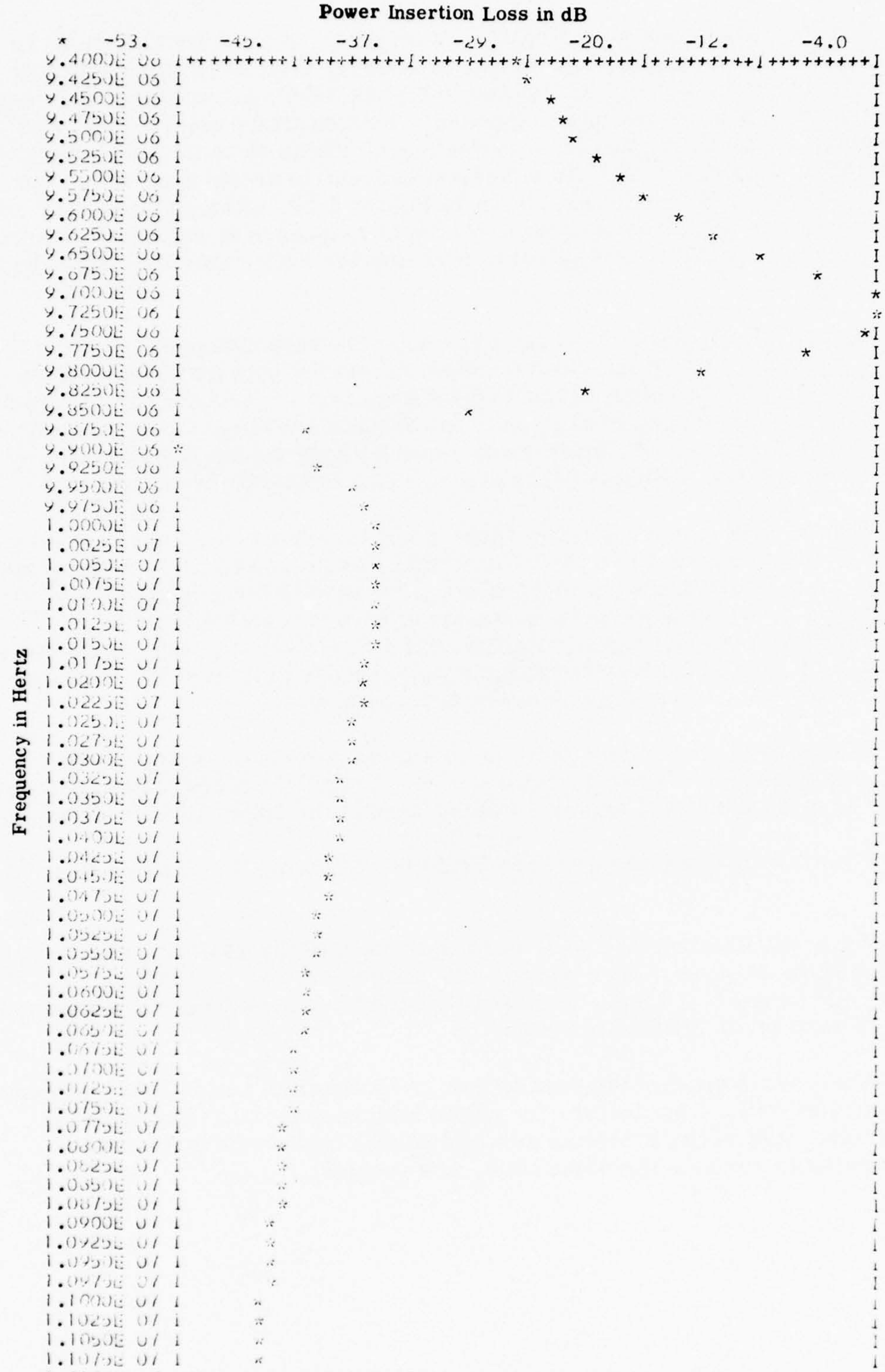

Figure 3-47. Two Element Identical Plate Stack Slower Mode 2 Velocity 83° Rotation Between Plates

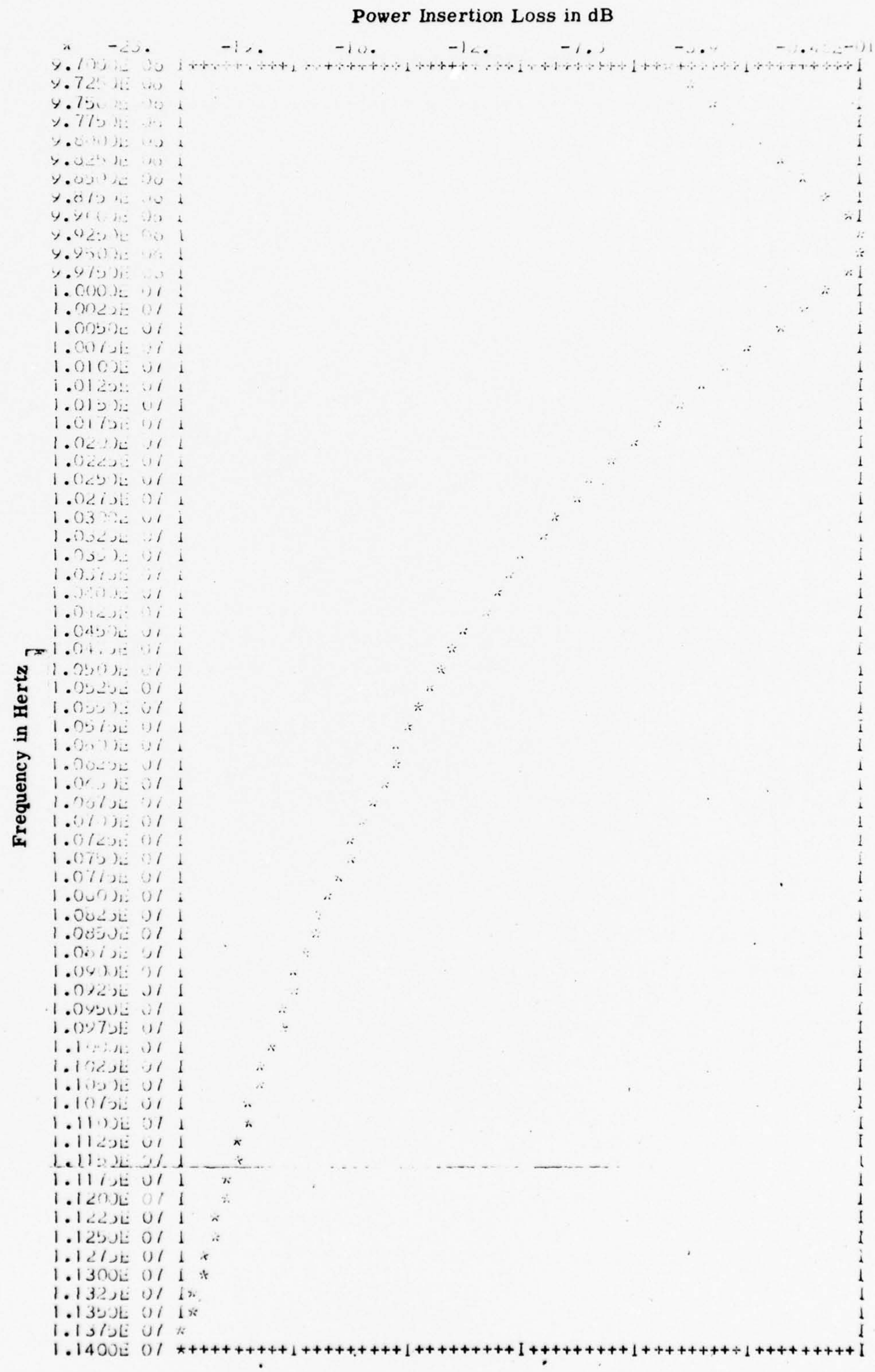

Figure 3-48. Two Element Identical Plate Stack of AT Cut-Quartz Plates 0^{o} Rotation Between Plates

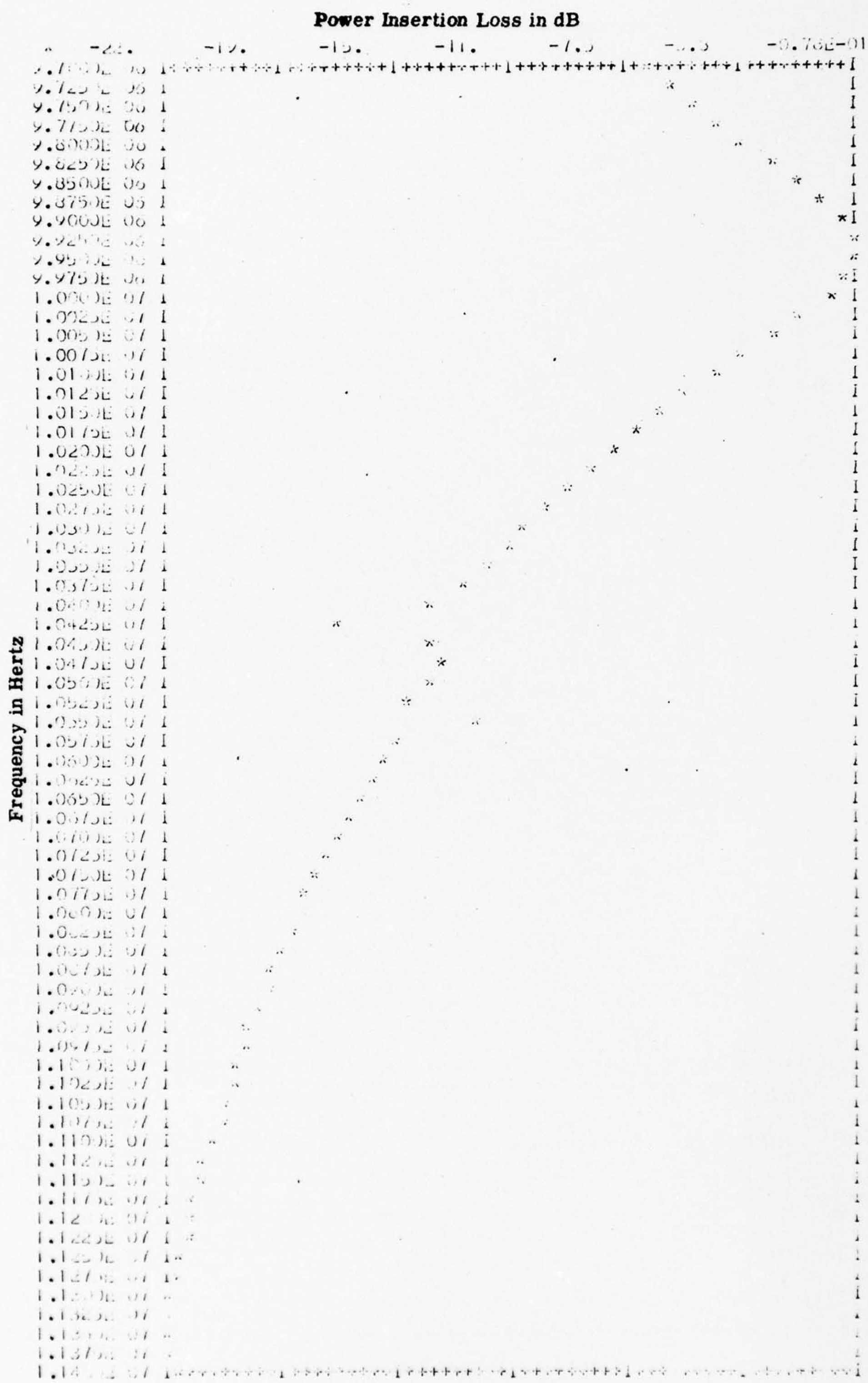

Figure 3-49. Two Element AT Cut Quartz Stack 5° Rotation Between Plates

Figure 3-50. Two Element AT Cut Quartz Stack 45° Rotation Between Plates

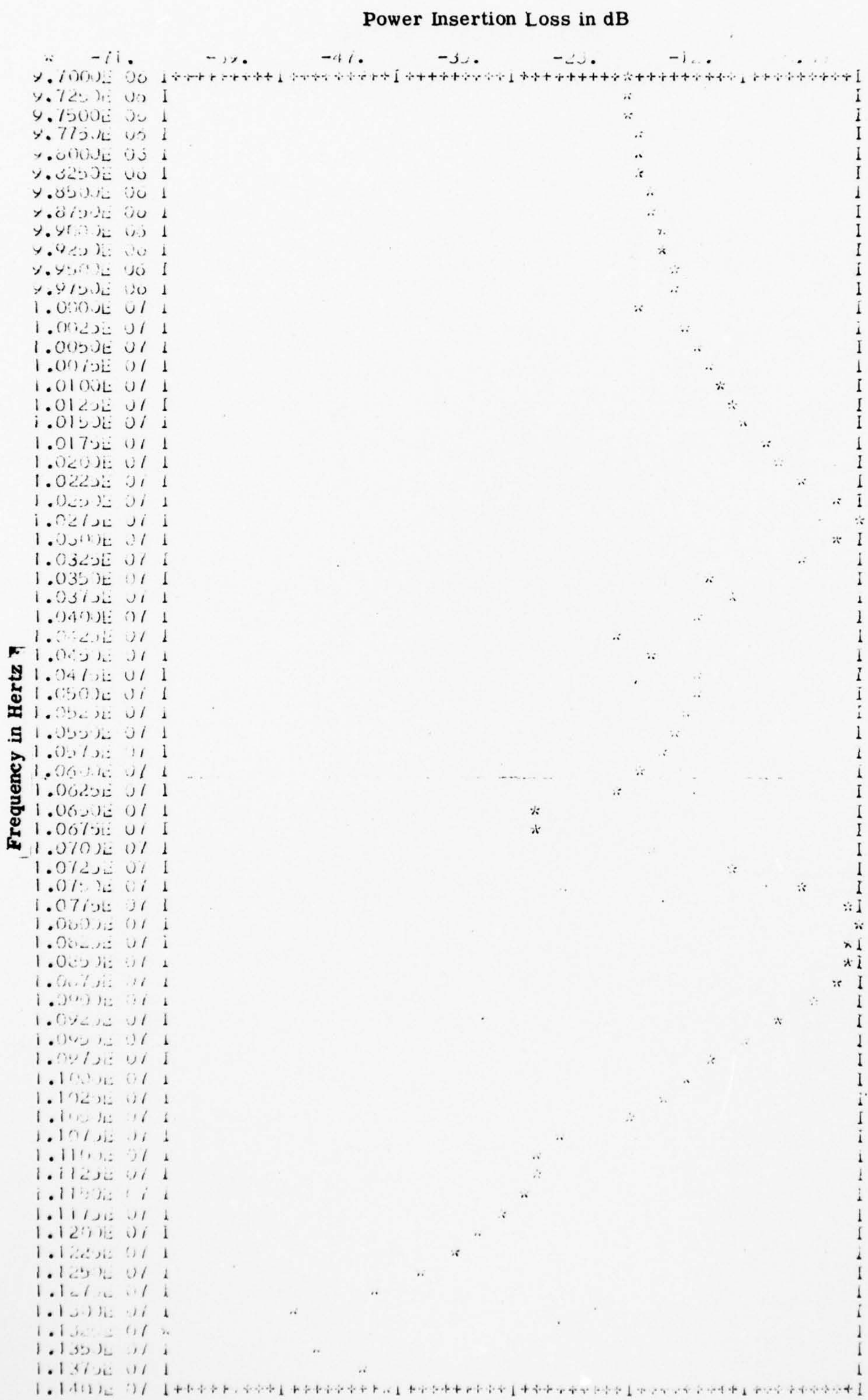

Figure 3-51. Two Element AT Cut Quartz Stack 75° Rotation Between Plates

REFERENCES FOR SECTION 3

1. A.D. Ballato, "Transmission-Line Analogs for Piezoelectric Layered Structures", Ph.D. Dissertation, Polytechnic Institute of Brooklyn, 1972; also U.S. Army Electronics Command Report ECOM-4413, May, 1976.

2. H.F. Tiersten, "Thickness Vibrations of Piezoelectric Plates", J. Acoust. Soc. Amer.,Vol 35, No. 1, Jan. 1963, pp 53-58.

3. H.F. Tiersten, "Linear Piezoelectric Plate Vibrations", Plenum Press, N.Y. 1969.

4. J.F. Nye, "Physical Properties of Crystals", Oxford University Press, London, 1957.

5. "Standards on Piezoelectric Crystals, 1949", Proc. IRE, Vol. 37, No. 12, Dec. 1949, pp 1378-1395.

6. W.P. Mason, "Piezoelectric Crystals and Their Application to Ultrasonics", D. Van Nostrand Co., Inc. N.Y., 1950.

7. R. Bechmann, "Elastic and Piezoelectric Constants of Alpha Quartz", Phys Rev., Vol.,110, No. 5, June 1958, pp 1060-1061.

8. A.J. Slobodnik, Jr. and J.V. OBrien, "Complete Theory of Acoustic Bulk Wave Propagation in Anisotropic Piezoelectric Media", AirForce Systems Command Report AFCRL-71-0601, November 1971.

9. F.B. Hildebrand, "Methods of Applied Mathematics", Prentice Hall, Inc, Engelwood Cliffs, N.J., 1952.

10. E.A. Guillemin, "The Mathematics of Circuit Analysis", John Wiley & Sons, Inc, New York, N.Y., 1949.

11. E.A. Guillemin, "Theory of Linear Physical Systems", John Wiley & Sons, Inc, New York, N.Y., 1963.

12. J.L. Powell, "Quantum Mechanics", Addison Wesley Publishing Co., Inc, Reading, Mass, 1961.

13. H. Goldstein, "Classical Mechanics", Addison Wesley Publishing Co., Reading, Mass, 1959.

14. R.C. Weast, "Handbook of Tables for Mathematics", 3rd Ed., The Chemical Rubber Co., Cleveland, Ohio, 1964.

REFERENCES FOR SECTION 3 (CONT'D)

15. T. Yamada and N.Niizeki, "Admittance of Piezoelectric Plates Vibrating Under the Perpendicular Field Excitation", Proc IEEE,Vol. 58, No. 6, June 1970, pp 941-942.

16. S.A. Basri, "A Method for the Dynamical Determination of the Elastic, Dielectric and Piezoelectric Constants of Quartz", National Bureau of Standards Monograph 9, U.S. Department of Commerce, June 1960.

17. R.B. Adler, L.J. Chu and R.M. Fano, "Electromagnetic Energy Transmission and Radiation", John Wiley & Sons, Inc, New York, N.Y., 1960.

18. H.J. Carlin and A.B. Giordano, "Network Theory: An Introduction to Reciprocal and Nonreciprocal Circuits", Prentice Hall Inc, Englewood Cliffs, N.J., 1964.

4. DEVICE FABRICATION AND TEST

A. RESONATOR MATERIALS

The dominant material in the fabrication of crystal resonators has been single-crystal quartz. It has many advantages, including the very significant one of being relatively inexpensive. The low cost is well supported by the large number of commercially available source suppliers and their ability to process it with great accuracy. Quartz has excellent mechanical properties; it can be sawed, ground, lapped and highly optically polished in both small and large quantities. Crystalline quartz occurs in natural and in synthetic form. The latter can be grown with properties similar to and sometimes superior to that of the natural form. The orientations of quartz, for the application considered here, are the Y-cut, AC-cuts and the AT-cuts. All rotated Y-cut plates vibrate in pure thickness shear modes. The uniqueness of quartz for frequency control and filter applications results from the zero value of the first and second-order temperature coefficients for the AT-cut at room temperature. The AT-cut has a k value of about .088 compared to .14 for the Y-cut. However, the Y-cut has a temperature coefficient of +90 ppm/^{o}C. The slightly smaller k value for the AT does not, therefore, detract from its value for resonators and filters. Quartz, itself, has a relatively high mechanical Q, both in the natural and synthetic form.

Although quartz has been the mainstay for frequency control and wave filters, several new crystals with high piezoelectric coupling and favorable mechanical properties are now available. Some of the more successful of these are the ferroelectrics, lithium niobate ($LiNbO_3$), lithium tantalate ($LiTaO_3$) and barium sodium niobate ($Ba_2NaNb_5O_{15}$), sometimes dubbed "banana". All three exhibit strong piezoelectric effects.

$LiNbO_3$ and $LiTaO_3$ have strong thickness shear mode X and Y-plates, but they are not pure. The Z-cuts contain pure extensional modes.

$LiNbO_3$ has several utilized rotated-Y-cuts, but the particle motion does not lie ideally for pure-mode orientation. Some of the cuts may have undesired mode coupling that is still low enough for some applications but, generally, they are second choices. The Z-cut is the only pure mode, its coupling being of the order of .17. The X-cut plate exhibits a large value of k, about .68. However, coupling exists to two shear modes — one strong and one weak.

$LiTaO_3$ is of the same crystal class, 3m, as $LiNbO_3$. The basic difference lies in values of coupling coefficient and temperature coefficient. $LiTaO_3$ has a cut [1] with a low temperature coefficient that may be useful for resonator applications. The X-cut has a parabolic frequency versus temperature characteristic.

$Ba_2NaNb_5O_{15}$ belongs to the crystal class, mm 2; it differs considerably from $LiNbO_3$ and $LiTaO_3$. The X- and Y-cut plates have pure thickness shear modes and the Z-cut plate has a pure thickness extensional mode. The Z-cut has a very high coupling factor, k = .57, which remains constant over a wide temperature range. This material has not been utilized as extensively as quartz, $LiNbO_3$ and $LiTaO_3$, and its present cost is relatively high.

Table 4-1 summarizes the various orientations and physical parameters of the crystals discussed here.

There are other materials that could qualify for use in multimode filter applications. $LiGaO_2$ and other new materials should be considered, but first a careful evaluation of their potential as crystal filter plates must be made. The often-used AT-cut quartz, along with some of the cuts from the various materials listed in Table 4-1. merit investigation. In particular, the recently measured material berlinite shows promise as a future useful crystal for filter applications. This material has very similar properties to crystalline quartz (including temperature-stable orientations) but has the added feature of a higher electromechanical coupling coefficient. As soon as a good quality supply of this material becomes available it will find application in various types of crystal filter configurations.

Other candidates for consideration in multimode filters, would be the doubly-rotated orientations of crystals as described by Ballato. (2) The doubly-rotated crystal plate has the advantage of two degrees of freedom with two selected angle cuts. As an example, this would lead to temperature stability and higher electromechanical coupling that cannot be achieved by some of the single-oriented crystal cuts.

B. BONDING TECHNIQUES

Bonding techniques can be divided in two general categories — 1) transparent organic materials that are used to form thin adhesive bonding layers and 2) metal surface films that are joined together to form a single bond.

The epoxy or polymer adhesive bonds have relatively low mechanical impedances and, therefore, layers (of such materials) of any appreciable thickness could have a significant effect on the shape of the frequency/response curves. Although these bonds possess good stability over wide temperature ranges, the low mechanical impedance has, in most applications, required that the thickness of the bonding layer be very thin — of the order of a few hundredths of an acoustic wavelength.

TABLE 4-1. PROPERTIES OF SOME FILTER MATERIALS.

Material	Cut	Mode	k	Temp. Coeff. $\times 10^{-6}/^{o}C$	Vel. $\times 10^{3}$ m/s	Density kg/m^3
Quartz	X	TE	.10	-20	5.70	2.65
Quartz	Y	TS	.14	+90	3.85	2.65
Quartz	AT	TS	.088	0	3.32	2.65
$LiNbO_3$	X	TS	.68		4.75	4.7
$LiNbO_3$	Z	E	.17		7.33	4.7
$LiNbO_3$	$36^{o}Y$	E	.49		7.37	4.7
$LiNbO_3$	$163^{o}Y$	S	.62		4.56	4.7
$LiTaO_3$	X		.44		4.2	5.3
$LiTaO_3$	Z		.19		6.08	5.3
$LiTaO_3$	$47^{o}Y$		.29		7.40	5.3
$LiTaO_3$	$165^{o}Y$		.41		4.56	5.3
$BaNaNb_5O_{15}$	X	S	.21		1.82	5.3
	Y	S	.25		1.83	5.3
	Z	E	.57		3.07	5.3

Although the organic bonds are insulating, they can be used in very thin layers, provided no problems are encountered due to the ground surface layers of the resonators being separated by this thin layer. One advantage in using some of the organic materials is that the bond may be dissolved and the resonator discs recovered for additional experimental testing of other bonds or reso tor configurations.

Table 4-2 is a tabulation of some of the materials (and their characteristics) that may be considered for use in bonding tasks. The bonds themselves could include one or more of the materials shown depending on the substrate and type of layer being attempted.

TABLE 2. PROPERTIES OF BONDING MATERIALS

Material	Velocity $\times 10^5$ m/s		$Z \cdot 10^6$ kg/s m^2	
Epoxy	2.60 Ext	1.22 Shear	2.86 Ext	1.34 Shear
Phenyl Benzoate			3.38	0.48
Indium	2.30	1.44	17.0	10.5
Gold	3.24	1.20	62.5	23.2
Silver	3.65	1.61	38.0	16.7
Copper	5.01	2.11	40.6	18.3
Aluminum	6.42	3.04	17.3	8.2
Quartz	5.70	3.32	15.1	8.8
$LiNbO_3$	6.55	4.76	30.8	22.4
$LiTaO_3$	5.55	4.21	29.4	22.3
$BaNaNb_5O_5$	3.07	1.82	16.3	9.65

Most metallic bonds have been achieved using thermocompression bonding of indium or lead, singly or together with combinations of other metallic layers. The metallic bonds have larger characteristic mechanical impedances that more closely match that of the resonator material. Another advantage of using metallic-layer bonding is the resultant electrical conduction layer. While early techniques of metallic bonding involved only layers of indium or lead, these have been largely replaced by combinations of layers of several types of metals. Typical bonds consist of a flash of chromium, a thick layer of gold for adhesion and electrical conduction, and then the two surfaces to be bonded are plated with thin layers of indium. The two pieces are then thermocompression bonded together, so that the indium and gold alloy forms a good electrical and bond layer.

Various metallic-bonding techniques, have been used [3,4,5] which incorporate the evaporation of thin metallic layers to optically polished surfaces and are then welded by compression. These compression techniques involve the use of both thermocompression and room temperature compression in vacuum, air and inert gases.

The bonds themselves, fall into two categories, thin and thick. The thin films generally include organic, inorganic and metallic films. The thick film bonds will generally be metallic films. For precise thick bond layers, properly dimensioned glass or metal balls, wire or shims may be inserted together with the metallic films to obtain a specific bond thickness.

Since the main objective of the present study (Phase I) was the analytical modelling and programming of multimode stacked crystal filters, it was decided to use an organic lens bond for the preliminary studies of an experimental model. The lens bond has several advantages, the main one being that it can be dissolved and the resonator plates recovered for experimental testing of other bonds or resonators. A disadvantage is that it is insulating and can cause contact problems if the ground surface layers of the crystal stacks are separated by the thin insulating layer. The problem can be eliminated by some selective plating and offsetting of the crystal stack elements. These polymer bonds generally have low mechanical impedances.

Glass slide samples were first bonded together using the lens bond resin under pressure at room temperature. The bonds adhered well and did not separate when heated to $90^{o}C$. The test samples were successfully separated without damage using a decementing reagent. This lens bond was therefore selected for use in our initial studies of the stacked crystal filter elements.

Metallic bonds have large characteristic mechanical impedances that match the resonator impedances more closely. Bonds using expoxy and gold films were used in our analytical studies of two and three stacked crystal filters. In the past, indium was used as a metallic thermal compression bond. This method suffered in that the entire bonding operation, i.e., plating and pressure-bonding, had to be done in one pumpdown in a vacuum system using complicated fixtures and manipulators. Since bonding is a major consideration in the SCF, various procedures of thin metallic film bonds were studied. Some of these will be utilized in phase II of this program, which deals mainly with the fabrication of a variety of SCF representative models.

The bonding procedures include a wide variety of methods, including:

1. Cold-weld bonding of metallic films such as indium both in air and in vacuum.
2. Elevated temperature bonding of metallic films in both air and vacuum.
3. Room temperature non-indium metallic bond welding.
4. Ultrasonically welded layers using gold-aluminum and/or other metallic layers.
5. Field-assisted bonding of layers at low temperatures.

These metallic film techniques offer a well-matched bonding layer and some of these methods will be utilized as a permanently fixed bond for use in the Phase II study of experimental models of SCF's.

C. ELECTRODE CONSIDERATIONS

The characteristics of the electrodes, which have an effect on the electrical properties of the quartz resonator plate, depend on the surface finish of the plate, the electrode material, the geometry of the plate and the orientation of the electrodes with respect to the quartz plate. The electrodes are also affected by the size, shape, position and material properties of the connecting leads and the characteristics of the filter mounting supports. For purposes of orientation and rotation our electrode configurations were circular discs, with tabs extending from the active electrode area as shown in Figure 4-1 (Commonly referred to as a keyhole geometry). The latter can serve to locate the principal axis and act as a connector for external leads.

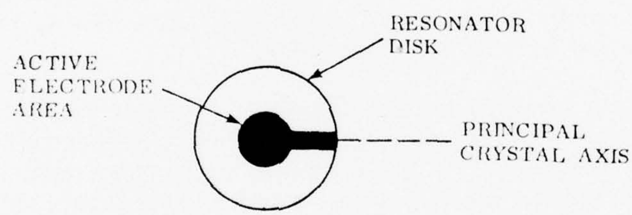

Figure 4-1. Electrode Configuration.

D. EXPERIMENTAL RESULTS

In order to verify some of the computer calculated results of Section 3.0 some cultured quartz crystal blanks were obtained from the J.K. Miller Co. These blanks were AT-cut with a 12 1/2 micron finish. Each blank was approximately 0.45" square and .011" thick. Gold electrodes of a keyhole design approximately 400 mils in diameter were then deposited on each of the broad faces of these crystals. A typical response curve for one of these electroded resonators is shown in Figure 4-2. This response curve was obtained by connecting the resonator in series with the input and output terminals of a 50 ohm H.P. Network Analyzer. The trace in 4-2a shows the plate response from 0 to 10 megahertz and indicates that the resonator is free of interfering modes in this region. Figure 4-2b shows a blown up version of the main plate response at the expected 6 MHz frequency, based on the velocity of AT-cut quartz and the plate thickness, and again exhibits a reasonably clean response.

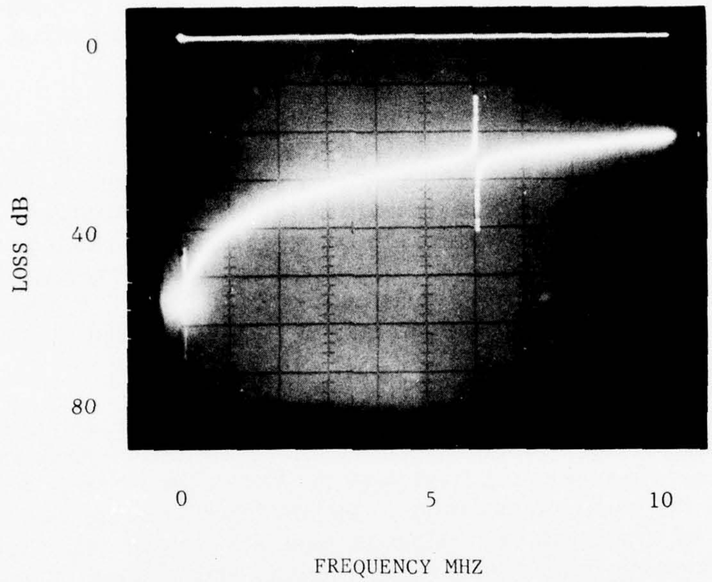

(a)

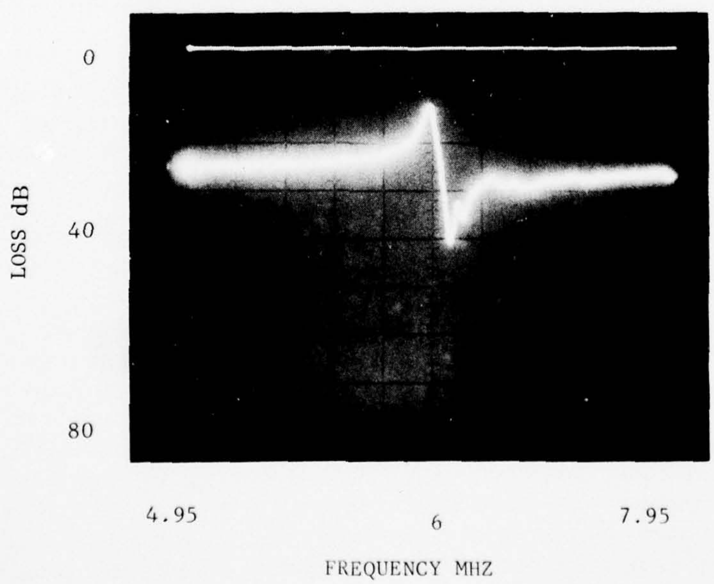

(b)

Figure 4-2. Typical Response Curve for Range AT-Cut Quartz.

Two of these electroded plates were then bonded together with the crystallgraphic axes or actual plate axes lined up. For this experiment a lens bond from Summers Laboratories, Inc. of Port Washington, Pennsylvania was used. This bonding material is a synthetic polyester adhesive that has worked well for applying transducers to acousto-optic delay lines. Using this bonding material and a pressure of approximately 80 lbs/sq inch,good adhering bonds with thicknesses in the order of 0.05 mils were achieved.

Figure 4-3 shows the Network Analyzer curves of this two-element stack of AT-cut quartz plates with zero degrees relative rotation between the plates of the stack. These traces were obtained by connecting the electrical terminals of one plate in the stack to the input terminals of the Network Analyzer and the electrical terminals of the other plate to the output terminals. Based on calculations of the clamped capacitances of the plates, the best termination impedance for these plates at 6 MHz is approximately 2000 ohms. However, the traces shown were measured in a 50 ohm circuit with no attempt at impedance matching.

Figure 4-3a shows the response from 0 to 110 MHz. The major peaks on this trace are the overtone responses of a single plate in the stack at 6, 18, 30, 42, and 54 MHz. However, the first peak visible on the trace is the fundamental response of the two-element stack. As discussed in conjunction with Figure 2-4 a stack of two crystals in intimate (welded) contact, each of which has a fundamental resonance at 6 MHz should display stack resonances at 3, 6 and 9 MHz.

Figure 4-3b shows an expanded view of the response of this stack from 0 to 40 MHz; Figure 4-3c shows a further expansion and covers only the range from 0 to 10 MHz.

It is obvious from this last curve that the stack bond departs from the ideal welded bond used in the computer simulation. Even allowing for the impedance mismatch between the optimum stack impedance and the 50 ohm measuring circuit impedance, it is obvious that the bond is not functioning well when it is located at a high stress point such as that required for resonances at half-wavelength and three-halves wavelength of the full stack. The two small responses visible in Figure 4-3c correspond to these resonances. The larger response is for the full stack, when it is wavelength thick. A comparison of this full wavelength resonance with the computer-generated response (Figure 3-48) for a two-element stack of AT-cut quartz plates, with 0° rotation between plates, shows that the measured response exhibits the predicted clean resonance.

This two-element stack was then disassembled. As stated earlier the ability of a lens bond to be dissolved with a heated solution of lens bond decementing fluid is an advantage in this type of investigation. The same set of stacked crystal elements can be used repeatedly to study the effect of plate rotation on the frequency response without introducing effects due to different crystals.

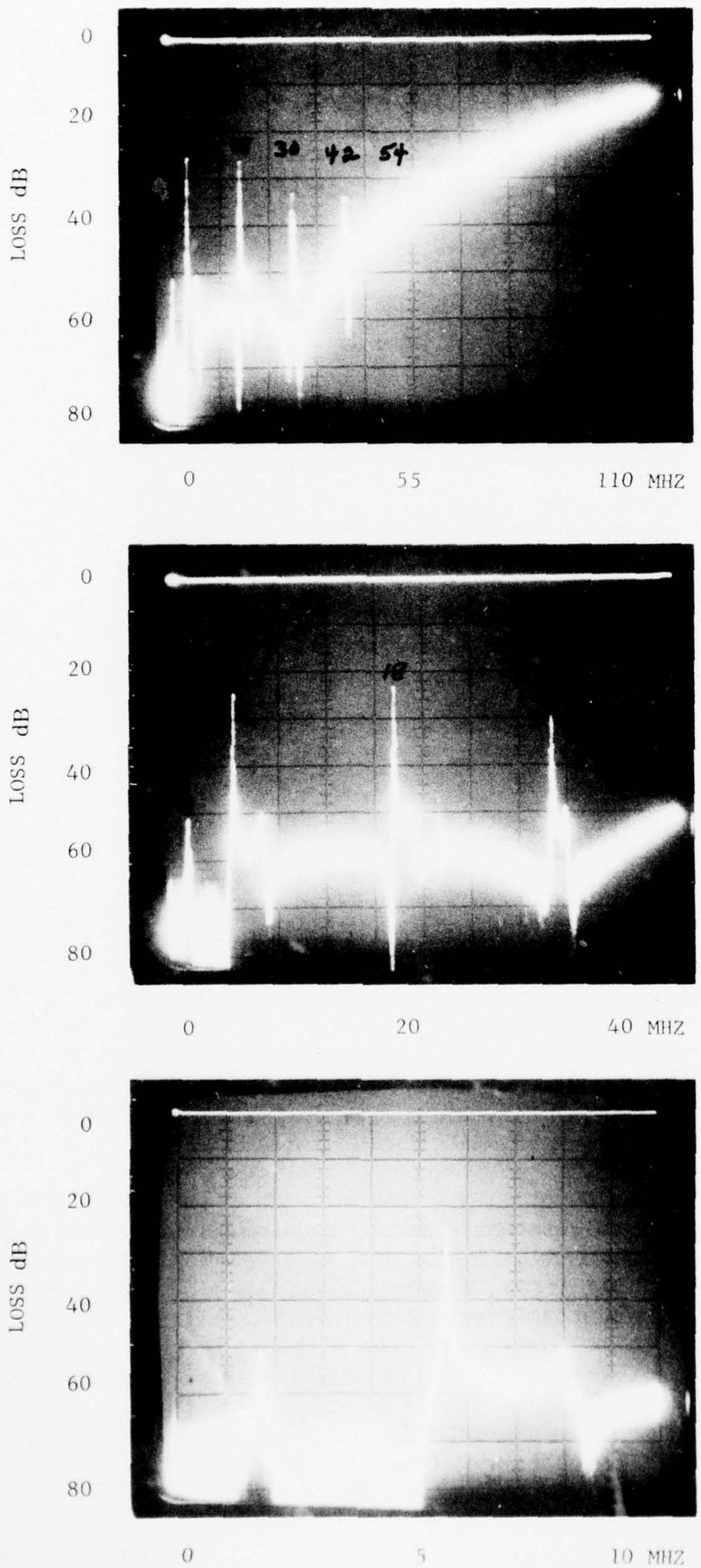

(a)

(b)

(c)

Figure 4-3. 2-Stack AT-Cut Crystals, 0° Rotation

The two elements were then reassembled with a relative plate rotation of approximately 45^o. Figure 4-4 shows the H.P. Network Analyzer response of this configuration in a 50 ohm system about the full wavelength resonant frequency of the stack. Each horizontal scale division on this trace represents approximately 0.3 MHz and the left peak is centered at approximately 6 MHz.

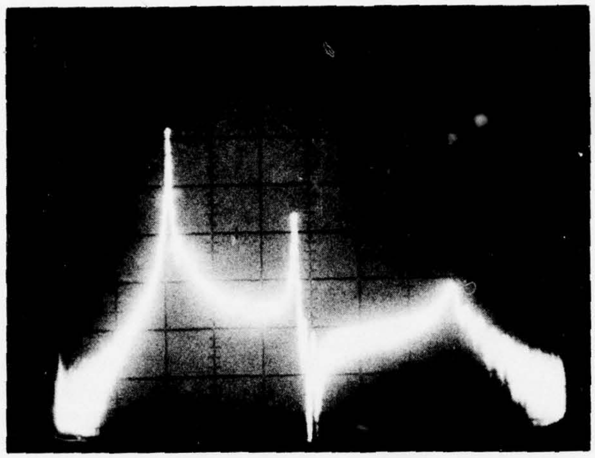

Figure 4-4. 2-Stack AT-Cut Crystals 45^o Rotation.

The theoretical result for this case is shown in Figure 3-50. Scaling the frequencies shown there, from the assumed 10 MHz single-plate resonance to the 6 MHz used in the experimental crystals, places the first peak at 6 MHz, the center peak at 6.36 MHz and the right peak at 6.72 MHz in Figure 3-50. Comparison of this theoretical response with the experimental response of Figure 4-4, reveals a visible dip and peak in the vicinity of 6.36 MHz in the experimentally fabricated stacked response. The only responses visible in the trace are those at 6, 6.8 and 7.8 MHz. The latter response corresponds to the three-halves wavelength resonance of a filter stack and, again, shows that a satisfactory welded bond has not been totally achieved.

Without having an opportunity to examine either the theoretical response or the experimental configuration in detail, to conclusively establish whether the discrepancy between results is due to a plate rotation discrepancy, a calculation error, or a bond error, it is suggested that a better bond in the experimental device would bring the results into closer agreement. However, it might be necessary to include a lossy bond in the computer calculations to achieve satisfactory agreement at this particular angle of relative plate rotation.

The last configuration examined in this preliminary attempt to obtain a correlation between the experimental and theoretical results was a two-element stack of AT-cut quartz plates with approximately 75^o of relative plate rotation between elements in the stack. The H.P. Network analyzer traces for this configuration are shown in Figure 4-5. Again, no attempt was made at impedance matching to the 2000 ohm impedance of the filter stack. Instead, the curves were measured in a 50-ohm circuit.

AD-A046 091 GENERAL ELECTRIC CO SYRACUSE N Y ELECTRONICS LAB F/G 9/5
MULTIMODE FILTERS.(U)
OCT 77 S WANUGA, C M STEARNS, A L KACHELMYER DAAB07-76-C-1337
UNCLASSIFIED ECOM-76-1337-F NL

3 OF 3
ADA046091

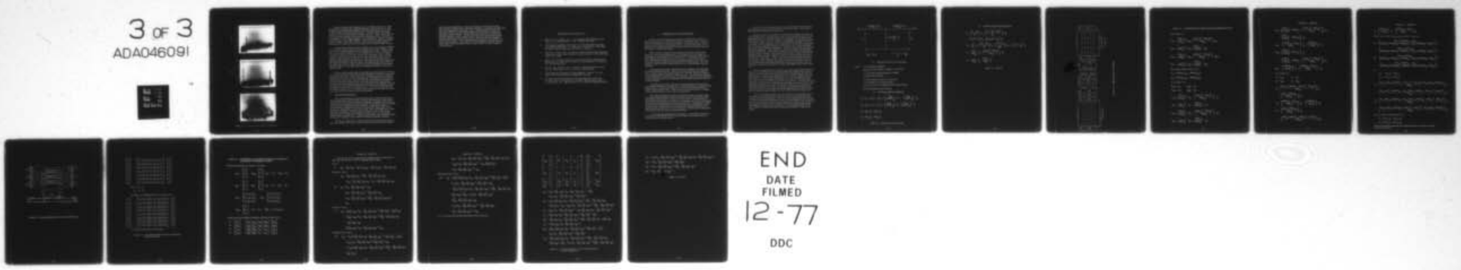

END
DATE
FILMED
12-77
DDC

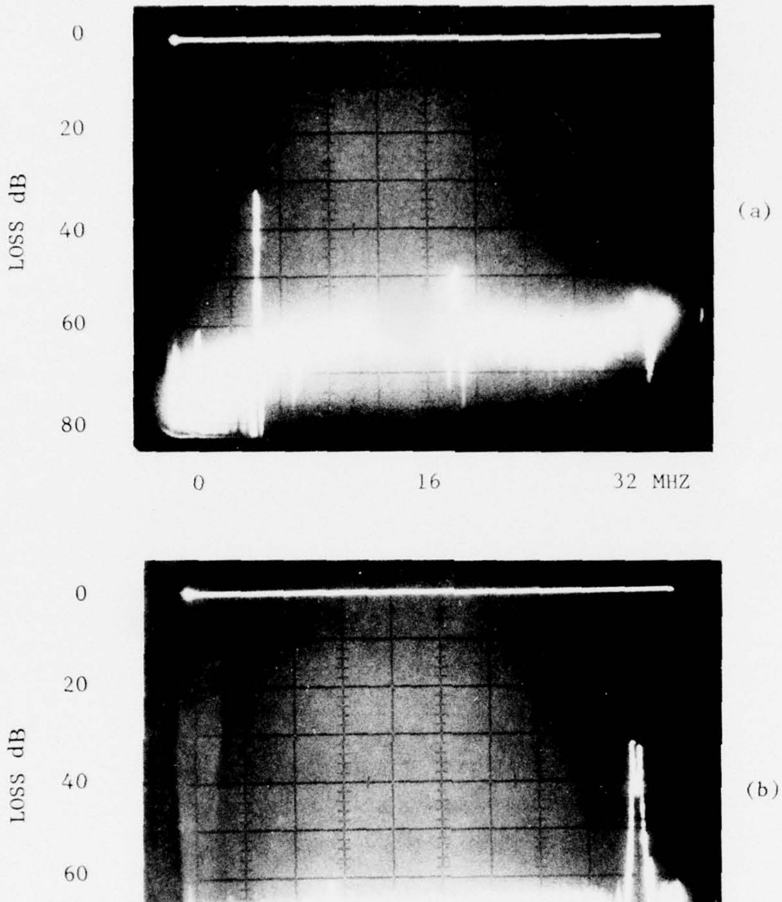

Figure 4-5. 2-Stack AT-Cut Crystal 75° Rotation.

Figure 4-5a shows the response from 0 to 32 MHz of the stack. Again, the overtone responses of the individual elements in the stack at 6, 18, and 30 MHz are the predominant responses with the half and three-halves wavelength responses of the stack barely visible. The half and full-wavelength responses of the stack are shown in Figure 4-5b trace. Here, again, the bond is not functioning properly when located at a high stress point. The double-humped nature of the 6 MHz response is also visible here. Figure 4-5c shows two expansions of this 6 MHz response. Both of these are centered at approximately 6.3 MHz. The lower of these two traces has a horizontal scale of approximately 1 MHz per division; the upper trace is about 0.3 MHz/division.

A comparison of these curves with Figure 3-51, for a computer response of a welded two-element stack of AT-cut quartz plates at 75° of relative rotation, shows excellent agreement in the response curve shapes. When the frequency scale shown in Figure 3-51 is multiplied by 0.6, the factor required to scale the frequency to the experimental filter frequency, there is almost complete agreement between this curve and the experimental curve over the frequency interval plotted in Figure 3-51. The two curves exhibit almost identical shapes with the dips and peaks at approximately the same frequencies. The major discrepancy is that the relative loss between peaks and valleys on the experimental curve is approximately one-half that predicted theoretically. This discrepancy is most likely due to the impedance mismatch of the experimental circuit.

This preliminary experimental investigation has demonstrated that there is a close correlation between the computer-generated response curves and the actual response curves. This means that it is realistic to use the simulation procedure to search for element configurations that exhibit the best response characteristics and, then, to fabricate only the most desirable configurations. It has been stressed throughout this section that the present experimental elements using lens bond to bond the elements together lack coupling of the half and three-halves wavelength resonances of the stack, and this condition must be equated to a poor bond. In actual practice, if a low-loss bond at the full wavelength resonance of a two-element stack is achieved, the lack of the other resonances would be immaterial and even desirable.

E. PROGRAM SIGNIFICANCE

The combined analytical results and preliminary experimental data obtained during Phase I of this program indicate that multimode crystal filters can be utilized in an effective manner to shape filter response characteristics. Together with recent advances in packaging[(6)(7)], the SCF (which is compatible with integrated circuits) can yield a reasonably rugged device capable of achieving filter responses that cannot be achieved with single-plate crystal resonators. Whereas the various filter types, such as the single plate, monolithic and SAW devices, utilize a single orientation or cut for the crystal response, the SCF offers the advantage of a wide variety of crystal plates bonded together mechanically, so that both piezoelectric and mechanical effects can be used to achieve a great multitude of desired frequency responses.

The two-port SCF offers a wider bandwidth potential than other types of bulk-mode filters. SCF plates of different materials and unequal thicknesses

also offer narrowband filters. One main advantage of the stacked crystal filter should be in applications requiring a minimum of modulation and distortion effects for moderate-to-high signal levels. Nonlinear effects in front-end and output filtering can cause major problems in proximity to transmitters operating in adjacent bands. The SCF bulk-wave device with its high power-handling capability, greater selectivity and small size employs bulk acoustic waves and should have low nonlinear effects, thereby preserving frequency stability. Many types of filter responses are also required for frequency division multiplex systems. The SCF has the wide flexibility to deliver many different types of filter topologies that are useful in these and other frequency-control systems.

REFERENCES FOR SECTION 4.0

1. Warner, A.W., Ballman, A.A., "Low Temperature Coefficient of Frequency in a $LiTaO_3$ Resonator", Proc. IEEE, 55, 450 (1967).

2. "The Angular Dependence of Piezoelectric Plate Frequencies and Their Temperature Coefficients", A. Ballato and J. Iafrate; Proc. 30th Annual Frequency Control Symposium, June 1976, pp. 141-156.

3. Sittig, E.K., Cook, H.D., "A Method for Preparing and Bonding Ultrasonic Transducers Used in High Frequency Digital Delay Lines", Proc. IEEE, 56, (1375) - Aug. 1968.

4. Knox, J.D., "A Room Temperature Non-Indium Metallic Bond Tested by Welding Acoustic Shear-Wave Transducers to Paratellurite", RCA Review, Vol. 34, (369) June 1973.

5. Larson, J.D., Winslow, D.K., "Ultrasonic Welded Piezoelectric Transducers", IEEE Trans. on SU, Vol. SU-18, (142) July 1971.

6. "Packaging Precision Quartz Crystal Resonators", John R. Vig, Eric Hafner, R&D Technical Report, ECOM 4134, July 1973.

7. "Ceramic Flat Pack Enclosures for Precision Quartz Crystal Units", R. Donald Peters, General Electric Company, Neutron Devices Dept., St. Petersburg, Fla., ERDA Contract No. E-(29-2)-656, September 1976.

5. SUGGESTIONS FOR FURTHER WORK

With any work encompassing the number of independent variables employed in this project it is almost impossible to examine all cases. Hence the obvious recommendation is that the programs written during the nine month course of this project be exercised more fully. A catalog of results, for considerably more cases than time permitted examination of during the course of this contract, should be developed.

There is also no claim that the programs as presently listed in this report are in the best possible format. As written they are convenient for operating in a time sharing mode of operation where a limited number of complete changes in input data are to be carried out. In this mode of operation a few changes in input data can be conveniently carried out on-line, and the results of these changes are available almost instantaneously. For more extensive changes in data off-line preparation of an input data paper tape was employed.

This input data procedure probably should be changed to one employing Namelist and Data Statements. While the time-sharing programs presented here are convenient for the rapid examination of program changes the quality of the resulting graphs produced as output are poor. For better documentation of the results batch versions of these time-sharing programs should be developed so that the higher quality result obtainable with plotting routines like CalComp could be obtained.

In conjunction with this conversion to batch programs the use of Namelist and Data statements would also allow for the development of program object decks,so that it would not be necessary to compile the programs each time before execution of each case. This would result in some saving on computer costs if a large number of cases were to be examined.

Even with the programs as they now stand the special cases that result in programming difficulties or aborts should be examined more closely than was possible within the time framework of the project. The easiest way to discover these difficulties is to exercise the programs with various combination of variables until an unexpected result is encountered. The equations are then examined to determine the source of the difficulty and the appropriate course of action taken. With problems of the degree of complexity inherent in the multimode stacked filters it is almost impossible to determine in advance what these special cases are without encountering them.

A more thorough experimental confirmation of multimode stacked filter theoretical results should also be carried out than was possible within the time limits of the present project.

So far, most of the suggestions made have dealt with matters pertaining to the programs as they were presented in the present report. Extensions to these programs should also be carried out.

The first of these is accounting for bonding layers between the plates in the multimode stack. As pointed out earlier, it is the authors' opinion that the appropriate time to incorporate bonds in the calculations is after fully operational thin bond cases have been obtained. Conceptually, the addition of bonds is relatively simple. Figure 5-1 shows the appropriate equivalent circuit of a lossy bond. In this equivalent circuit the parameters of the bond will depend on the type of wave propagating through the bond (shear waves and longitudinal waves will in general behave differently). Figure 5-1 also shows the Impedance Equations appropriate to this equivalent circuit along with the Transmission Equations of the bond. These latter equations are probably more appropriate for the inclusion of bonds in the multimode filter stack. Figure 5-2 shows the MØDE2 problem of Figure 3-26 with a bond layer inserted between the plates in equivalent circuit form. Table 5-1 carries out the procedure required in this case for a determination of the output currents of the left plates in terms of the input current. Once this determination has been made these currents are then followed back through the equivalent circuit in a manner similar to that shown in Table 3-16 to obtain the comparable MØDE2 solution with a bond layer.

The present programs are also limited to stacks of two multimode plates. While this is probably the most commonly employed configuration of stacked filters, it does not allow for an examination of the full potential of multimode stacked filters. Further work should, therefore, involve extending the multimode stack to a larger number of elements. It is again the authors' opinion that if this is to be carried out it should be done in terms of the augmented equivalent circuit of a TETM plate as shown in Figure 5-3. The use of this augmented circuit will allow for considerable flexibility in how the electrical input and output terminals in the stack are formed in relation to the electrical terminals of each plate in the stack. The augmented impedance matrix of this equivalent circuit is easily obtained from the impedance matrix for the actual plate coordinates shown in Figures 3-19 and 3-20, as shown in Figure 5-4.

It is also the authors' opinion that the problem of a multimode stack of more than two elements should be carried out in terms of the transmission matrix for this augmented plate. Table 5-2 shows schematically how this conversion of the augmented impedance matrix to the augmented transmission matrix can be carried out in terms of the submatrices of Figures 5-4. Figure 5-5 shows again schematically the transmission matrix associated with the augmented plate equivalent circuit of Figure 5-3. In this approach the stack of filter elements is built up and then the appropriate boundary conditions are applied.

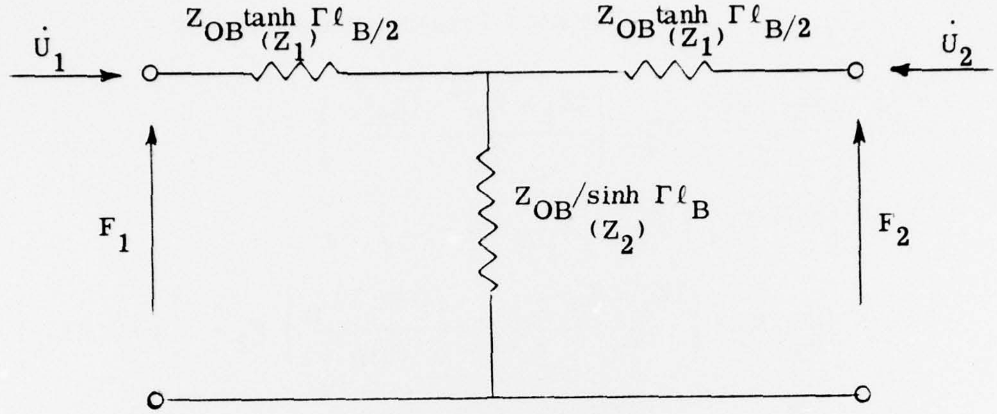

$Z_{OB} = A \rho c_B$ $\qquad$ $\Gamma = \frac{\omega}{c_B} \left(1 + \frac{j}{2Q}\right)$

a) Equivalent Circuit of a Lossy Bond.

where ω is the angular frequency

Z_{OB} is the characteristic impedance of the bond

Γ is the bond complex propagation constant

ℓ_B is the bond thickness

A is the cross sectional area of the bond

ρ is the density of the bond material

c_B is the velocity of propagation in the bond material

Q is the mechanical Q of the bond

b) The Bond Impedance Equations

$$F_1 = (Z_1 + Z_2)\dot{U}_1 + Z_2\dot{U}_2 = \left\{\frac{Z_{OB}}{\tanh \Gamma \ell_B}\right\}\dot{U}_1 + \left\{\frac{Z_{OB}}{\sinh \Gamma \ell_B}\right\}\dot{U}_2$$

$$F_2 = Z_2\dot{U}_1 + (Z_1 + Z_2)\dot{U}_2 = \left\{\frac{Z_{OB}}{\sinh \Gamma \ell_B}\right\}\dot{U}_1 + \left\{\frac{Z_{OB}}{\tanh \Gamma \ell_B}\right\}\dot{U}_2$$

$$F_1 = ZB_{11}\dot{U}_1 + ZB_{12}\dot{U}_2$$

$$F_2 = ZB_{12}\dot{U}_1 + ZB_{11}\dot{U}_2$$

Figure 5-1. Equivalent Circuit of Bond.

c) The Bond Transmission Equations

$$F_1 = \left\{ \frac{Z_1 + Z_2}{Z_2} \right\} F_2 - \left\{ \frac{(Z_1 + Z_2)^2 - (Z_2)^2}{Z_2} \right\} \dot{U}_2$$

$$= \left\{ \cosh \Gamma \ell_B \right\} F_2 - \left\{ Z_{OB} \sin \Gamma \ell_B \right\} \dot{U}_2$$

$$\dot{U}_1 = \left(\frac{1}{Z_2}\right) F_2 - \left\{ \frac{(Z_1 + Z_2)}{Z_2} \right\} \dot{U}_2 = \left\{ \frac{\sinh \Gamma \ell_B}{Z_{OB}} \right\} F_2 - \left\{ \cosh \Gamma \ell_B \right\} \dot{U}_2$$

$$F_1 = \left(\frac{ZB_{11}}{ZB_{12}}\right) F_2 - \left\{ \frac{(ZB_{11})^2 - (ZB_{12})^2}{ZB_{12}} \right\} \dot{U}_2$$

$$\dot{U}_1 = \left(\frac{1}{ZB_{12}}\right) F_2 - \left(\frac{ZB_{11}}{ZB_{12}}\right) \dot{U}_2$$

Figure 5-1. (Cont'd).

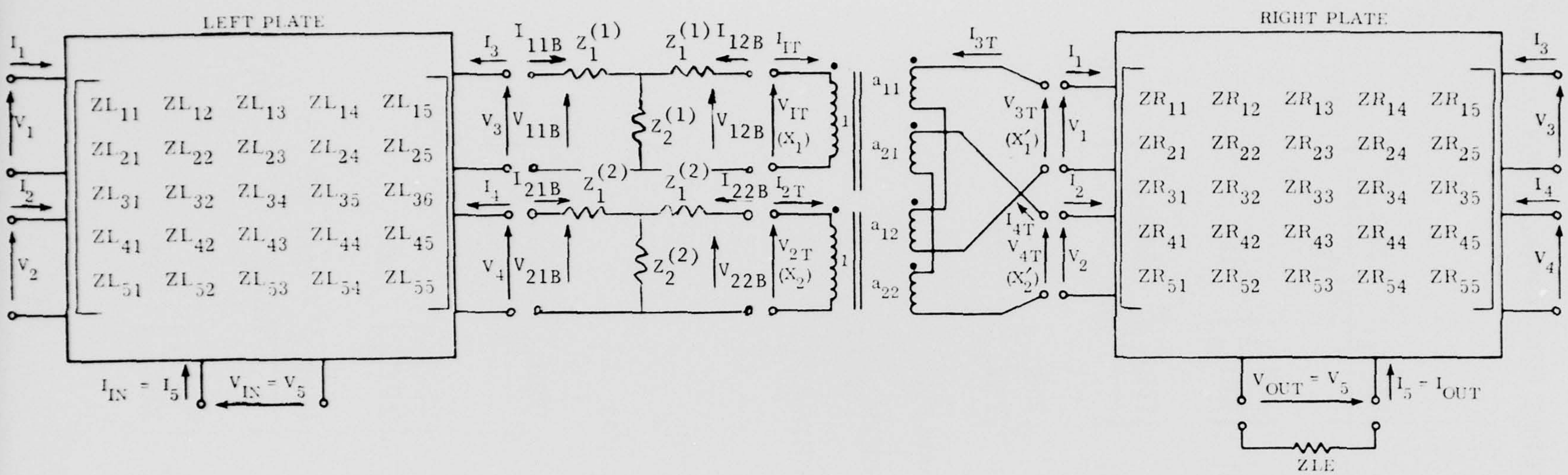

Figure 5-2. MØDE2 Problem with Bonds

TABLE 5-1. PROCEDURE FOR ADDING BONDS TO MØDE2 SOLUTION

From Figure 5.1

$$V_{11B} = \left\{ \frac{ZB1_{11}}{ZB1_{12}} \right\} V_{12B} - \left\{ \frac{(ZB1_{11})^2 - (ZB1_{12})^2}{ZB1_{12}} \right\} I_{12B}$$

$$I_{11B} = \left\{ \frac{1}{ZB1_{12}} \right\} V_{12B} - \left\{ \frac{ZB1_{11}}{ZB1_{12}} \right\} I_{12B}$$

$$V_{21B} = \left\{ \frac{ZB2_{11}}{ZB2_{12}} \right\} V_{22B} - \left\{ \frac{(ZB2_{11})^2 - (ZB2_{12})^2}{ZB2_{12}} \right\} I_{22B}$$

$$I_{21B} = \left\{ \frac{1}{ZB2_{12}} \right\} V_{22B} - \left\{ \frac{ZB2_{11}}{ZB2_{12}} \right\} I_{22B}$$

From Mode 2 solution Table 3-16

$$V_{1T} = ZRETR_{11}\, I_{1T} + ZRETR_{12}\, I_{2T}$$

$$V_{2T} = ZRETR_{21}\, I_{1T} + ZRETR_{22}\, I_{2T}$$

From Figure 5.2

$$V_{12B} = V_{1T} \qquad I_{12B} = -I_{1T}$$

$$V_{22B} = V_{2T} \qquad I_{22B} = -I_{2T}$$

$$V_{11B} = \left\{ \frac{ZB1_{11}}{ZB1_{12}} \right\} V_{1T} + \left\{ \frac{(ZB1_{11})^2 - (ZB1_{12})^2}{ZB1_{12}} \right\} I_{1T}$$

$$I_{11B} = \left\{ \frac{1}{ZB1_{12}} \right\} V_{1T} + \left\{ \frac{ZB1_{11}}{ZB1_{12}} \right\} I_{1T}$$

$$V_{21B} = \left\{ \frac{ZB2_{11}}{ZB2_{12}} \right\} V_{2T} - \left\{ \frac{(ZB2_{11})^2 - (ZB2_{12})^2}{ZB2_{12}} \right\} I_{2T}$$

$$I_{21B} = \left\{ \frac{1}{ZB2_{12}} \right\} V_{2T} + \left\{ \frac{ZB2_{11}}{ZB2_{12}} \right\} I_{2T}$$

TABLE 5-1. (CONT'D).

$$V_{11B} = \left\{ \left(\frac{ZB1_{11}}{ZB1_{12}} \right) ZRETR_{11} + \left[\frac{(ZB1_{11})^2 - (ZB1_{12})^2}{ZB1_{12}} \right] \right\} I_{1T}$$

$$+ \left\{ \left(\frac{ZB1_{11}}{ZB1_{12}} \right) ZRETR_{12} \right\} I_{2T}$$

$$I_{11B} = \left\{ \frac{ZRETR_{11} + ZB1_{11}}{ZB1_{12}} \right\} I_{1T} + \left\{ \frac{ZRETR_{12}}{ZB1_{12}} \right\} I_{2T}$$

$$V_{21B} = \left\{ \left(\frac{ZB2_{11}}{ZB2_{12}} \right) ZRETR_{21} \right\} I_{1T}$$

$$+ \left\{ \left(\frac{ZB2_{11}}{ZB2_{12}} \right) ZRETR_{22} + \left[\frac{(ZB2_{11})^2 - (ZB2_{12})^2}{ZB2_{12}} \right] \right\} I_{2T}$$

$$I_{21B} = \left\{ \frac{ZRETR_{21}}{ZB2_{12}} \right\} I_{1T} + \left\{ \frac{ZRETR_{22} + ZB2_{11}}{ZB2_{12}} \right\} I_{2T}$$

From Figure 5.2

$V_3 = V_{11B}$ $\quad I_3 = -I_{11B}$

$V_4 = V_{21B}$ $\quad I_4 = -I_{21B}$

$$V_3 = \left\{ \frac{(ZB1_{11})\ ZRETR_{11} + (ZB1_{11})^2 - (ZB1_{12})^2}{ZB1_{12}} \right\} I_{1T}$$

$$+ \left\{ \frac{(ZB1_{11})\ ZRETR_{12}}{ZB1_{12}} \right\} I_{2T}$$

$$-I_3 = \left\{ \frac{ZRETR_{11} + ZB1_{11}}{ZB1_{12}} \right\} I_{1T} + \left\{ \frac{ZRETR_{12}}{ZB1_{12}} \right\} I_{2T}$$

$$V_4 = \left\{ \frac{(ZB2_{11})\ ZRETR_{21}}{ZB2_{12}} \right\} I_{1T}$$

$$+ \left\{ \frac{(ZB2_{11})\ ZRETR_{22} + (ZB2_{11})^2 - (ZB2_{12})^2}{ZB2_{12}} \right\} I_{2T}$$

TABLE 5-1. (CONT'D).

$$-I_4 = \left\{ \frac{ZRETR_{21}}{ZB2_{12}} \right\} I_{1T} + \left\{ \frac{ZRETR_{22} + ZB2_{11}}{ZB2_{12}} \right\} I_{2T}$$

These can be solved for I_{1T} and I_{2T} in terms of I_3 and I_4

$$I_{1T} = \left\{ \frac{(ZB1_{12})\,(ZRETR_{22} + ZB2_{11})}{(ZRETR_{12})\,(ZRETR_{21}) - (ZRETR_{11} + ZB1_{11})\,(ZRETR_{22} + ZB2_{11})} \right\} I_3$$

$$- \left\{ \frac{(ZB2_{12})\,(ZRETR_{12})}{(ZRETR_{12})\,(ZRETR_{21}) - (ZRETR_{11} + ZB1_{11})\,(ZRETR_{22} + ZB2_{11})} \right\} I_4$$

$$I_{2T} = - \left\{ \frac{(ZB1_{12})\,ZRETR_{21}}{(ZRETR_{12})\,(ZRETR_{21}) - (ZRETR_{11} + ZB1_{11})\,(ZRETR_{22} + ZB2_{11})} \right\} I_3$$

$$+ \left\{ \frac{(ZB2_{12})\,(ZRETR_{11} + ZB1_{11})}{(ZRETR_{12})\,(ZRETR_{21}) - (ZRETR_{11} + ZB1_{11})\,(ZRETR_{22} + ZB2_{11})} \right\} I_4$$

Let

$$I_{1T} = BF_{11}\, I_3 - BF_{12}\, I_4$$

$$I_{2T} = -BF_{21}\, I_3 + BF_{22}\, I_4$$

$$V_3 = \left[\frac{BF_{11} \left\{ (ZB1_{11})\,(ZRETR_{11}) + (ZB1_{11})^2 - (ZB1_{12})^2 \right\} - BF_{12}\,(ZB1_{11})\,(ZRETR_{12})}{ZB1_{12}} \right] I_3$$

$$+ \left[\frac{BF_{22}\,(ZB1_{11})\,(ZRETR_{12}) - BF_{12} \left\{ (ZB1_{11})\,ZRETR_{11} + (ZB1_{11})^2 - (ZB1_{12})^2 \right\}}{ZB1_{12}} \right] I_4$$

$$V_4 = \left[\frac{BF_{11}\,(ZB2_{11})\,(ZRETR_{21}) - BF_{21} \left\{ (ZB2_{11})\,(ZRETR_{22}) + (ZB2_{11})^2 - (ZB2_{12})^2 \right\}}{ZB2_{12}} \right] I_3$$

$$+ \left[\frac{BF_{22} \left\{ (ZB2_{11})\,(ZRETR_{22}) + (ZB2_{11})^2 - (ZB2_{12})^2 \right\} - BF_{12}\,(ZB2_{11})\,(ZRETR_{21})}{ZB2_{12}} \right] I_4$$

but from Mode 2 solution Table 3-16

$$V_3 = ZLT_{11}\, I_3 + ZLT_{13}\, I_{IN}$$

$$V_4 = ZLT_{22}\, I_4 + ZLT_{23}\, I_{IN}$$

Solution then follows along the same pattern as shown for Mode 2 with additional steps involved.

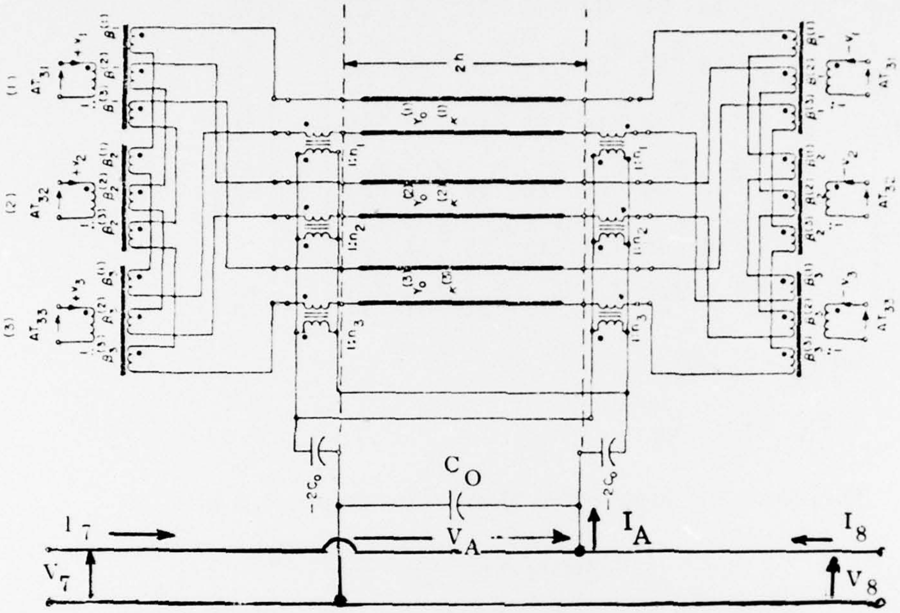

Figure 5-3. Augmented Equivalent Circuit of a TETM Plate.

$$
\begin{bmatrix} V_1 \\ V_2 \\ V_3 \\ V_4 \\ V_5 \\ V_6 \\ V_A \end{bmatrix}
=
\begin{bmatrix}
Z_{11} & Z_{12} & Z_{13} & Z_{14} & Z_{15} & Z_{16} & Z_{17} \\
Z_{12} & Z_{22} & Z_{23} & Z_{15} & Z_{25} & Z_{26} & Z_{27} \\
Z_{13} & Z_{23} & Z_{33} & Z_{16} & Z_{26} & Z_{36} & Z_{37} \\
Z_{14} & Z_{15} & Z_{16} & Z_{11} & Z_{12} & Z_{13} & Z_{17} \\
Z_{15} & Z_{25} & Z_{26} & Z_{12} & Z_{22} & Z_{23} & Z_{27} \\
Z_{16} & Z_{26} & Z_{36} & Z_{13} & Z_{23} & Z_{33} & Z_{37} \\
Z_{17} & Z_{27} & Z_{37} & Z_{17} & Z_{27} & Z_{37} & Z_{77}
\end{bmatrix}
\begin{bmatrix} I_1 \\ I_2 \\ I_3 \\ I_4 \\ I_5 \\ I_6 \\ I_A \end{bmatrix}
$$

but $I_A = I_7 + I_8$

$V_A = V_7 = V_8$

Therefore the Augmented Matrix for Figure 5.3 is

$$
\left[\begin{array}{c} V_1 \\ V_2 \\ V_3 \\ \hline V_4 \\ V_5 \\ V_6 \\ \hline V_7 \\ \hline V_8 \end{array}\right]
=
\left[\begin{array}{ccc|ccc|c|c}
Z_{11} & Z_{12} & Z_{13} & Z_{14} & Z_{15} & Z_{16} & Z_{17} & Z_{17} \\
Z_{12} & Z_{22} & Z_{23} & Z_{15} & Z_{25} & Z_{26} & Z_{27} & Z_{27} \\
Z_{13} & Z_{23} & Z_{33} & Z_{16} & Z_{26} & Z_{36} & Z_{37} & Z_{37} \\
\hline
Z_{14} & Z_{15} & Z_{16} & Z_{11} & Z_{12} & Z_{13} & Z_{17} & Z_{17} \\
Z_{15} & Z_{25} & Z_{26} & Z_{12} & Z_{22} & Z_{23} & Z_{27} & Z_{27} \\
Z_{16} & Z_{26} & Z_{36} & Z_{13} & Z_{23} & Z_{33} & Z_{37} & Z_{37} \\
\hline
Z_{17} & Z_{27} & Z_{37} & Z_{17} & Z_{27} & Z_{37} & Z_{77} & Z_{77} \\
\hline
Z_{17} & Z_{27} & Z_{37} & Z_{17} & Z_{27} & Z_{37} & Z_{77} & Z_{77}
\end{array}\right]
\left[\begin{array}{c} I_1 \\ I_2 \\ I_3 \\ \hline I_4 \\ I_5 \\ I_6 \\ \hline I_7 \\ \hline I_8 \end{array}\right]
$$

For later use subdivide as shown above

Figure 5-4. Augmented Impedance Matrix of Augmented Equivalent Circuit.

TABLE 5-2. CONVERSION OF AUGMENTED IMPEDANCE MATRIX TO AUGMENTED TRANSMISSION MATRIX

Define the subdivisions in Figure 5.4 as shown

$$V_{MI} = \begin{bmatrix} V_1 \\ V_2 \\ V_3 \end{bmatrix} \qquad V_{MO} = \begin{bmatrix} V_4 \\ V_5 \\ V_6 \end{bmatrix} \qquad V_{EI} = [\,V_7\,] \qquad V_{EO} = [\,V_8\,]$$

$$I_{MI} = \begin{bmatrix} I_1 \\ I_2 \\ I_3 \end{bmatrix} \qquad I_{MO} = \begin{bmatrix} I_4 \\ I_5 \\ I_6 \end{bmatrix} \qquad I_{EI} = [\,I_7\,] \qquad I_{EO} = [\,I_8\,]$$

$$Z_{MI} = \begin{bmatrix} Z_{11} & Z_{12} & Z_{13} \\ Z_{12} & Z_{22} & Z_{23} \\ Z_{13} & Z_{23} & Z_{33} \end{bmatrix} \qquad Z_{MT} = \begin{bmatrix} Z_{14} & Z_{15} & Z_{16} \\ Z_{15} & Z_{25} & Z_{26} \\ Z_{16} & Z_{26} & Z_{36} \end{bmatrix}$$

$$Z_{ME} = \begin{bmatrix} Z_{17} \\ Z_{27} \\ Z_{37} \end{bmatrix} \qquad Z_{EI} = [\,Z_{77}\,] \qquad Z_{ME}^T = [\,Z_{17}\ Z_{27}\ Z_{37}\,]$$

In these terms the augmented Impedance Matrix of Figure 5.4 is

$$\begin{array}{c} (1) \\ (2) \\ (3) \\ (4) \end{array} \quad \left[\begin{array}{c} V_{MI} \\ \hline V_{MO} \\ \hline V_{EI} \\ \hline V_{EO} \end{array}\right] = \left[\begin{array}{c:c:c:c} Z_{MI} & Z_{MT} & Z_{ME} & Z_{ME} \\ \hdashline Z_{MT} & Z_{MI} & Z_{ME} & Z_{ME} \\ \hdashline Z_{ME}^T & Z_{ME}^T & Z_{EI} & Z_{EI} \\ \hdashline Z_{ME}^T & Z_{ME}^T & Z_{EI} & Z_{EI} \end{array}\right] \left[\begin{array}{c} I_{MI} \\ \hline I_{MO} \\ \hline I_{EI} \\ \hline I_{EO} \end{array}\right]$$

TABLE 5-2. (CONT'D).

Solve this set of four equations using algebraic matrix techniques for V_{MI}, I_{MI}, V_{EI} and I_{EI} in terms of V_{MO}, I_{MO}, V_{EO}, and I_{EO}

From 2

$$(5) \qquad I_{MI} = Z_{MT}^{-1} V_{MO} - Z_{MT}^{-1} Z_{MI} I_{MO} - Z_{MT}^{-1} Z_{ME} I_{EI} - Z_{MT}^{-1} Z_{ME} I_{EO}$$

Substitute 5 into 4

$$V_{EO} = Z_{ME}^{T} Z_{MT}^{-1} V_{MO} + (Z_{ME}^{T} - Z_{ME}^{T} Z_{MT}^{-1} Z_{MI}) I_{MO}$$

$$+ (Z_{EI} - Z_{ME}^{T} Z_{MT}^{-1} Z_{ME}) I_{EI} + (Z_{EI} - Z_{ME}^{T} Z_{MT}^{-1} Z_{ME}) I_{EO}$$

$$(6)^{*} \qquad I_{EI} = (Z_{EI} - Z_{ME}^{T} Z_{MT}^{-1} Z_{ME})^{-1} V_{EO}$$

$$- (Z_{EI} - Z_{ME}^{T} Z_{MT}^{-1} Z_{ME})^{-1} (Z_{ME}^{T} Z_{MT}^{-1}) V_{MO}$$

$$- (Z_{EI} - Z_{ME}^{T} Z_{MT}^{-1} Z_{ME})^{-1} (Z_{ME}^{T} - Z_{ME}^{T} Z_{MT}^{-1} Z_{MI}) I_{MO}$$

$$- I_{EO}$$

Substitute 6 into 5

$$(7)^{*} \qquad I_{MI} = \left\{ (Z_{MT}^{-1} Z_{ME}) (Z_{EI} - Z_{ME}^{T} Z_{MT}^{-1} Z_{ME})^{-1} (Z_{ME}^{T} Z_{MT}^{-1}) + Z_{MT}^{-1} \right\} V_{MO}$$

$$+ \left\{ (Z_{MT}^{-1} Z_{ME}) (Z_{EI} - Z_{ME}^{T} Z_{MT}^{-1} Z_{ME})^{-1} (Z_{ME}^{T} - Z_{ME}^{T} Z_{MT}^{-1} Z_{MI}) \right.$$

$$\left. - \; Z_{MT}^{-1} Z_{MI} \right\} I_{MO}$$

$$- \left\{ (Z_{MT}^{-1} Z_{ME}) (Z_{EI} - Z_{ME}^{T} Z_{MT}^{-1} Z_{ME})^{-1} \right. V_{EO}$$

Substitute 6 and 7 into 1

$$(8)^{*} \qquad V_{MI} = [\, Z_{MI} \left\{ (Z_{MT}^{-1} Z_{ME}) (Z_{EI} - Z_{ME}^{T} Z_{MT}^{-1} Z_{ME})^{-1} (Z_{ME}^{T} Z_{MT}^{-1}) + Z_{MT}^{-1} \right\}$$

$$- Z_{ME} (Z_{EI} - Z_{ME}^{T} Z_{MT}^{-1} Z_{ME})^{-1} (Z_{ME}^{T} Z_{MT}^{-1})] \; V_{MO}$$

$$+ [\, Z_{MI} \left\{ (Z_{MT}^{-1} Z_{ME}) (Z_{EI} - Z_{ME}^{T} Z_{MT}^{-1} Z_{ME})^{-1} (Z_{ME}^{T} - Z_{ME}^{T} Z_{MT}^{-1} Z_{MI}) \right.$$

$$\left. - Z_{MT}^{-1} Z_{MI} \right\}$$

TABLE 5-2. (CONT'D).

$$+ Z_{MT} - Z_{ME} (Z_{EI} - Z_{ME}^{T} Z_{MT}^{-1} Z_{ME})^{-1} (Z_{ME}^{T} - Z_{ME}^{T} Z_{MT}^{-1} Z_{MI})] I_{MO}$$

$$+ [Z_{ME} (Z_{EI} - Z_{ME}^{T} Z_{MT}^{-1} Z_{ME})^{-1} - Z_{MI} \{ (Z_{MT}^{-1} Z_{ME})$$

$$(Z_{EI} - Z_{ME}^{T} Z_{MT}^{-1} Z_{ME})^{-1}] V_{EO}$$

Substituting 6 and 7 into 3

(9)* $$V_{EI} = [Z_{ME}^{T} \left\{ (Z_{MT}^{-1} Z_{ME}) (Z_{EI} - Z_{ME}^{T} Z_{MT}^{-1} Z_{ME})^{-1} (Z_{ME}^{T} Z_{MT}^{-1}) + Z_{MT}^{-1} \right\}$$

$$- Z_{EI} (Z_{EI} - Z_{ME}^{T} Z_{MT}^{-1} Z_{ME})^{-1} (Z_{ME}^{T} Z_{MT}^{-1})] V_{MO}$$

$$+ [Z_{ME}^{T} \left\{ (Z_{MT}^{-1} Z_{ME}) (Z_{EI} - Z_{ME}^{T} Z_{MT}^{-1} Z_{ME})^{-1} (Z_{ME}^{T} - Z_{ME}^{T} Z_{MT}^{-1} Z_{MI}) \right.$$

$$\left. - Z_{MT}^{-1} Z_{MI} \right\} + Z_{ME}^{T} - Z_{EI} (Z_{EI} - Z_{ME}^{T} Z_{MT}^{-1} Z_{ME})^{-1}$$

$$(Z_{ME}^{T} - Z_{ME}^{T} Z_{MT}^{-1} Z_{MI})] I_{MO}$$

$$+ [Z_{EI} (Z_{EI} - Z_{ME}^{T} Z_{MT}^{-1} Z_{ME})^{-1} - Z_{ME}^{T} (Z_{MT}^{-1} Z_{ME})$$

$$(Z_{EI} - Z_{ME}^{T} Z_{MT}^{-1} Z_{ME})^{-1}] V_{EO}$$

6, 7, 8 and 9 are the desired transmission matrix equations.

$$\left[\begin{array}{cc} & V_1 \\ V_{MI} & V_2 \\ & V_3 \\ \hline & I_1 \\ I_{MI} & I_2 \\ & I_3 \\ \hline V_{EI} & V_7 \\ \hline I_{EI} & I_7 \end{array}\right] = \left[\begin{array}{c|c|c|c} & & & 0 \\ AM & B_M & A_E & 0 \\ & & & 0 \\ \hline & & & 0 \\ C_M & D_M & C_E & 0 \\ & & & 0 \\ \hline E_M & F_M & E_E & 0 \\ \hline G_M & H_M & G_E & -1 \end{array}\right] \left[\begin{array}{cc} V_4 & \\ V_5 & V_{MO} \\ V_6 & \\ \hline I_4 & \\ I_5 & I_{MO} \\ I_6 & \\ \hline V_8 & V_{EO} \\ \hline I_8 & I_{EO} \end{array}\right]$$

$$A_M = [\, Z_{MI} \left\{ Z_{MT}^{-1} Z_{ME} (Z_{EI} - Z_{ME}^T Z_{MT}^{-1} Z_{ME})^{-1} + Z_{MT}^{-1} \right\}$$
$$- Z_{ME} (Z_{EI} - Z_{ME}^T Z_{MT}^{-1} Z_{ME})^{-1} (Z_{ME}^T Z_{MT}^{-1})\,]$$

$$B_M = [\, Z_{MI} \left\{ Z_{MT}^{-1} Z_{ME} (Z_{EI} - Z_{ME}^T Z_{MT}^{-1} Z_{ME})^{-1} (Z_{ME}^T - Z_{ME}^T Z_{MT}^{-1} Z_{MI}) \right.$$
$$\left. - Z_{MT}^{-1} Z_{MI} \right\} + Z_{MT} - Z_{ME} (Z_{EI} - Z_{ME}^T Z_{MT}^{-1} Z_{ME})^{-1} (Z_{ME}^T - Z_{ME}^T Z_{MT}^{-1} Z_{MI})\,]$$

$$A_E = [\, Z_{ME} (Z_{EI} - Z_{ME}^T Z_{MT}^{-1} Z_{ME})^{-1} - Z_{MI} Z_{MT}^{-1} Z_{ME} (Z_{EI} - Z_{ME}^T Z_{MT}^{-1} Z_{ME})^{-1}\,]$$

$$C_M = [\, Z_{MT}^{-1} Z_{ME} (Z_{EI} - Z_{ME}^T Z_{MT}^{-1} Z_{ME})^{-1} (Z_{ME}^T Z_{MT}^{-1}) + Z_{MT}^{-1}\,]$$

$$D_M = [\, Z_{MT}^{-1} Z_{ME} (Z_{EI} - Z_{ME}^T Z_{MT}^{-1} Z_{ME})^{-1} (Z_{ME}^T - Z_{ME}^T Z_{MT}^{-1} Z_{MI}) - Z_{MT}^{-1} Z_{MI}\,]$$

$$C_E = -[\, Z_{MT}^{-1} Z_{ME} (Z_{EI} - Z_{ME}^T Z_{MT}^{-1} Z_{ME})^{-1}\,]$$

$$E_M = [\, Z_{ME}^T \left\{ Z_{MT}^{-1} Z_{ME} (Z_{EI} - Z_{ME}^T Z_{MT}^{-1} Z_{ME})^{-1} (Z_{ME}^T Z_{MT}^{-1}) + Z_{MT}^{-1} \right\}$$
$$- Z_{EI} (Z_{EI} - Z_{ME}^T Z_{MT}^{-1} Z_{ME})^{-1} (Z_{ME}^T Z_{MT}^{-1})\,]$$

$$F_M = [\, Z_{ME}^T \left\{ Z_{MT}^{-1} Z_{ME} (Z_{EI} - Z_{ME}^T Z_{MT}^{-1} Z_{ME})^{-1} (Z_{ME}^T - Z_{ME}^T (Z_{MT}^{-1} Z_{MI})) \right.$$
$$\left. - Z_{MT}^{-1} Z_{MI} \right\} + Z_{ME}^T - Z_{EI} (Z_{EI} - Z_{ME}^T Z_{MT}^{-1} Z_{ME})^{-1} (Z_{ME}^T - Z_{ME}^T Z_{MT}^{-1} Z_{MI})\,]$$

Figure 5-5. Transmission Matrix of the Augmented Plate Circuit of Figure 5-3.

$$E_E = [\, Z_{EI} (Z_{EI} - Z_{ME}^T Z_{MT}^{-1} Z_{ME})^{-1} - Z_{ME}^T Z_{MT}^{-1} Z_{ME} (Z_{EI} - Z_{ME}^T Z_{MT}^{-1} Z_{ME})^{-1}]$$

$$G_M = -[\, (Z_{EI} - Z_{ME}^T Z_{MT}^{-1} Z_{ME})^{-1} (Z_{ME}^T Z_{MT}^{-1})]$$

$$H_M = -[\, (Z_{EI} - Z_{ME}^T Z_{MT}^{-1} Z_{ME})^{-1} (Z_{ME}^T - Z_{ME}^T Z_{MT}^{-1} Z_{MI})]$$

$$G_E = [\, (Z_{EI} - Z_{ME}^T Z_{MT}^{-1} Z_{ME})^{-1}]$$

Figure 5-5. (Cont'd)